TAMPEREEN TEKNILLINEN YLIOPISTO
TAMPERE UNIVERSITY OF TECHNOLOGY

Ville Ellä

Effects of Processing Parameters on P(L/D)LA 96/4 Fibers and Fibrous Products for Medical Applications

Julkaisu 1039 • Publication 1039

Tampere 2012

Tampereen teknillinen yliopisto. Julkaisu 1039
Tampere University of Technology. Publication 1039

Ville Ellä

Effects of Processing Parameters on P(L/D)LA 96/4 Fibers and Fibrous Products for Medical Applications

Thesis for the degree of Doctor of Science in Technology to be presented with due permission for public examination and criticism in Rakennustalo Building, Auditorium RG202, at Tampere University of Technology, on the 4th of May 2012, at 12 noon.

Tampereen teknillinen yliopisto - Tampere University of Technology
Tampere 2012

ISBN 978-952-15-2811-8 (printed)
ISBN 978-952-15-2848-4 (PDF)
ISSN 1459-2045

Abstract

Tissue engineering is expected to fulfill its promises to produce knowledge, methods, and products that would benefit the health care sector. The need of a degradable construct is a necessity when trying to grow a living tissue inside a porous structure. The fibers offer a unique approach to this, since the porosity can easily be altered with different methods especially using the textile methods. Textile industry on the other hand offers a broad and variable archive of methods to manufacture products and preforms. These preforms can be further used together with the composite technology to further increase the number of applications to which they can be used. When combining different fields of sciences it is possible to manufacture a living tissue, based on fibrous degradable constructs. Thus fibers and fibrous products are versatile preforms that can be shaped and designed to fulfill many of the demands in the field of tissue engineering.

The main objective of this thesis was to study the biodegradable medical grade P(L/D)LA 96/4 polymer fibers and the fibrous products manufactured from them. The thermal degradation behavior of this polymer in single screw extruder environment in melt spinning process was studied. The online hot-drawing was used for fiber orientation. The information based on those studies was analyzed and gathered for future optimization of such melt spinning processes. Different batches and fiber diameters were produced using different processing parameters. Textile methods were further introduced to the melt-spun fibers. The effect of the knitting parameters on fiber properties were studied during the hydrolytic degradation and long term storage. These knits were studied as in vivo soft tissue implant preforms, in vitro spinal fusion cage composite preforms, and in vivo temporomandibular jaw implant preforms. Non-woven fabrics were produced from the melt-spun fibers manufactured by hot-drawing and high-speed drawing. These non-woven felts were used for plasma and solvent based wetting enhancement tests accompanied by cell seeding tests. The felts were also used as a component for temporomandibular jaw implant preforms.

The results showed increasing degradation in the extruder barrel in regards to the P(L/D)LA 96/4 polymer molecular weight and viscosity. Lactide monomer was induced into the polymer during the melt spinning process due to the temperature and shear. Monomer content also varied according to the polymer residence time. Fiber showed

different hydrolytical degradation behavior depending on the monomer amount. Higher monomer content caused rapid degradation of the mechanical properties and molecular weight. We acquired three different degradation profiles for the fibers that were related to the monomer content. The knitted soft tissue implants degraded faster during the hydrolysis than in in vivo. These knitted soft tissue implants acted as real tissue engineered implants; the cells grew and filled in the scaffolds. While the tissue matured in the scaffolds, the measured mechanical properties of the scaffolds improved despite the loss of mechanical strength of an empty scaffold. Non-woven scaffolds increased their wetting capability due to the oxygen plasma treatment. This also enhanced the cell attachment and proliferation.

Acknowledgements

The experimental work of this thesis was carried out at the Department of Biomedical Engineering, Tampere University of Technology and at 3B's research group, University of Minho, Portugal, during the 7 month visiting researcher period in 2004-2005.

I wish to express my deepest gratitude to my supervisor and mentor Professor Dr Tech. Minna Kellomäki. Her guidance and belief in me as a researcher made all this possible. I would also like to thank Professor Emeritus Pertti Törmälä, Ph.D. M.D. Sci.h.c., for giving me an opportunity to start the work in the field of biomedical materials.

I express my thanks to my co-authors for their contribution and help in publishing the papers especially Kaarlo Paakinaho M.Sc., Tuija Annala M.Sc. and Satu Länsman M.D. Special thanks go to all the colleagues and staff at the Department of Biomedical Engineering, without your support, help and humor this would have not happened. I am most grateful to the Eira Lehtinen for all the work and help I received from her while she was working at the department.

The financial support from the Graduate School of Processing of Polymers and Polymer-based Multimaterials (POPROK) is gratefully appreciated. Further funding from Finnish Technology Agency (TEKES) and the European Union (EU) for different projects to which I was let to contribute is gratefully acknowledged.

I would like to thank all my family and friends for their support. Thanks to Riku Suomela Dr Tech., you always knew how to encourage me during this process.

Miia my wonderful wife, thank you for being there.

Eemil, you are the light of my life.

Finally the two persons who could not make it this far but would have liked to be here and see this. I remember you, my dearest uncle Markku Ellä and colleague Raija Reinikainen.

Pirkkala, March, 2012 Ville Ellä

Thesis outline

This thesis consists of literature review and the experimental part which summarizes the work performed in the publications listed below.

I. Pirhonen, E. & **Ellä, V**. 2008. Melt spinning. In: Wnek, G.E. & Bowlin, G.L. (eds.). Encyclopedia of Biomaterials and Biomedical Engineering. New York, NY. Informa Health Care. 2nd ed., 3. pp. 1816-1823.

II. **Ellä, V**., Nikkola, L. & Kellomäki, M. 2011. Process-induced monomer on a medical-grade polymer and its effect on short-term hydrolytic degradation. Journal of Applied Polymer Science, vol. 119, no. 5, pp. 2996-3003.

III. Paakinaho, K**., Ellä, V**., Syrjälä, S. & Kellomäki, M. 2009. Melt spinning of poly(L/D)lactide 96/4: Effects of molecular weight and melt processing on hydrolytic degradation. Polymer Degradation and Stability, vol. 94, no. 3, pp. 438-442.

IV. **Ellä, V**., Annala, T., Länsman, S., Nurminen, M., Kellomäki, M. 2011 Knitted polylactide 96/4 L/D structures and scaffolds for tissue engineering: Shelf life, in vitro and in vivo studies. Biomatter, vol. 1, no.1, pp. 102-113.

V. **Ellä, V**., Gomes, M.E., Reis, R.L., Törmälä, P. & Kellomäki, M. 2007. Studies of P(L/D)LA 96/4 non-woven scaffolds and fibres; properties, wettability and cell spreading before and after intrusive treatment methods. Journal of Materials Science: Materials in Medicine vol.18, pp. 1253-1261.

VI. **Ellä, V**., Kellomäki, M. & Törmälä, P. 2005. In vitro properties of PLLA screws and novel bioabsorbable implant with elastic nucleus to replace intervertebral disc. Journal of Materials Science: Materials in Medicine, vol 16, pp. 655-662.

VII. **Ellä, V**., Sjölund, A., Kellomäki, M. & Mauno, J. 2006. Manufacturing of temporomandibular joint scaffolds. In: Salonen, R. (ed.). FiberMed06, Fibrous Products in Medical and Health Care, Proceedings, June7-9, 2006 Tampere Hall, Finland 6 p.

Author's contribution

The author's contribution considering each of the publications is the following.

I. Author was responsible for all the writing in the paper regarding the melt spinning of polymers and their use/applications.

II. Author was responsible for writing the paper, planning, processing and analyzing the data for this work. Second author carried out the tests according to the main author's planning.

III. Author was responsible for planning the work for this paper. The processing of polymers was carried out together with the first author. Author took part to the writing process as a co-author.

IV. Author was responsible for writing this paper. Author manufactured all the polymer fibers used in these studies and manufactured most of the used samples. Author also analyzed most of the data acquired during the test periods.

V. Author was responsible for writing the paper, planning, processing and analyzing the data for this work, excluding parts of the cell culturing and seeding process which were done by the second author.

VI. Author was responsible for writing the paper, manufacturing the implants (excluding the screws), and analyzing the data. Materials were processed together with the second author.

VII. Author was responsible all the work related to this publication besides the implant outlook, which was designed by the third author.

Abbreviations & symbols

Ø	Diameter
ΔH_f	Melting enthalpy
ΔH_c	Recrystallization enthalpy
β–TCP	βeta Tricalsium Phosphate
PEOT70PBT30	Segmented block copolymer of poly(ethylene oxide terephthalate)/ Poly(butylene terephthalate) with PEOT/PBT ratio being 70/30
ACL	Anterior cruciate ligament
BG	Bioactive glass
DSC	Differential scanning calorimetry
dr / DR	Draw ratio
FTIR	Fourier transform infrared microscopy
GPC	Gel permeation chromatography
hMSCs	Human derived mesenchymal stem cells
i.v.	Inherent viscosity
IVD	Intervertebral disc
MCP	Metacarpophalangeal
M_n	Number average molecular weight
M_w	Weight average moleculat weight
M_v	Viscosity average molecular weight
P4HB	Poly-4-hydroxy butyrate
PACT	Polyactive (trade name) = PEOT70PBT30
PBS	Phosphate buffered saline
PGA	Polyglycolic acid, polyglycolide
PCL	Polycaprolactone
PD	Polydispersity
PDS	Polydioxanone
PLGA	50/50 copolymer of lactide and glycolide
PLGA X/Y	X/Y copolymer of lactide and glycolide
PLA	Family of polylactide polymers
PLA 50	Polylactide with 50 L and 50 D monomer
PLA X	Polylactide with X L and 100-X D monomer
PLLA	Poly-L-lactide
PLCL	Copolymer of lactide and caprolactone
PLDLA	Polylactide with 50 L and 50 D monomer
P(L/DL)LA 70/30	Polylactide with 70 L and 30 DL monomer
P(L/D)LA 96/4	Polylactide with 96 L and 4 D monomer
ROP	Ring opening polymerization
SBF	Simulated body fluid
SEC	Size exclusion chromatography
SEM	Scanning electron microscopy
SR-	Self reinforced
TE	Tissue engineering
T_g	Glass transition temperature
T_m	Melting temperature
TMJ	Temporomandibular joint
TGA	Thermogravimetric analysis
UHMWPE	Ultra high molecular weight polyethylene
UTS	Ultimate tensile strength
UV	Ultraviolet
X_c	Crystallinity

Definitions

Branching
Polymer chain that contains other or similar polymeric chains in more than one direction.

Catgut
Suture material made of intestines of sheep or horse.

Catalyst
A substance that enables the chemical reaction or speeds up the reaction.

Dura
The tough outermost membrane enveloping the brain and spinal cord.

Godet
A heated roll that heats up the fiber and transfers it further.

Intracardiac
Inside the heart.

Intramedullary
Inside the bone cavity, the place containing the bone marrow.

Intervertebral disc
A layer of cartilage separating adjacent vertebrae in the spine.

Lumbar
The lower back, part of the spine comprising 5 vertebrae.

Metacarpophalangeal joint
Joint between the palm and the finger.

Osteosynthesis
Attaching to the bone.

Paraspinal
Adjacent to the spinal column.

Subcutaneous
Under the skin.

Temporomandibular joint
The hinge joint between the temporal bone and the lower jaw.

Quenching
Rapid cooling.

1. Introduction

The history of bioabsorbable fibers can be dated back to the late 16th century when the word catgut was introduced. The definition of the word according to the Oxford Dictionary is

"A material used for the strings of musical instruments and for surgical sutures, made of the dried twisted intestines of sheep or horses, but not cats. The association with cat remains unexplained."

The catgut was the very first biodegradable medical fiber that was used for the internal fixation of humans. Catgut, made from purified connective tissue and the chromic catgut, chromium salt treated catgut (for a prolonged absorption), are still used although it has been shown that they cause infections and sustain them (Lindeque 2007). The ethical matters, concerning the questions why, this writer will skip, but still wants to point out that some of the ethical issues even nowadays are set aside due to the economic reasons.

Since the catgut, the biomedical material industry has produced fibers from several bioabsorbable materials both natural and synthetic ones. The first commercial biodegradable fiber related device, and probably the most referred product ever produced in the medical material field, was the PGA poly(glycolic acid) suture that was patented in 1967 (Schmitt & Polistina 1967) and commercialized by the name of the Dexon® suture. The first implications to use PLLA poly(L-lactic acid) for medical purposes came when the non-toxic effects of the material were noticed in the in vivo testing by Kulkarni et al. (1966). The fibrous format of this polymer was for the first time used as sutures in 1971 (Cutright & Hunsuck 1971).

The one thing that makes the fibrous format far more interesting than just the suture is that it can be used as a preform for different versatile structures. Now almost all the possibilities that we already have from the textile technology is in our grasp, only alterations or modifications to the machinery is needed. This has enabled the development of the biodegradable felts, knits, meshes, and stents. When moving

forward with the technology it is now practical to use these fibrous products as a part of a composite when further technology is put into the device for tailored purposes or desired properties.

Using these technologies we are thriving for the optimal outcome bearing in mind that the optimal for in vitro is not necessary optimal for the in vivo purposes. When using fibrous format instead of a solid material we can increase the surface area of the material thus decreasing the amount of the material put in to the body. The elasticity factor can be altered with different fibrous structures whereas for the solid structures and materials this is a material property. The porosity can be easily handled in the fibrous format. This allows the penetration of the cells and bodily fluids into the structure. Now the behavior of the cells from the material point of view is mainly regulated by the free volume, pore size, pore size distribution and the fiber thickness. In the matrix, the cells attach on to the fiber and/or attach into the pores, or they do nothing. To this we must influence using our knowledge and skills. So engineers must work together with biologists who have the knowledge of the cells.

This thesis presents the studies on bioabsorbable polymer fibers for medical applications. The fibers were produced by means of melt spinning. The production and the properties of those fibers were studied. The produced fibers were further processed as a textile or composite scaffolds to be used as a support structures or implants. The properties of those scaffolds and composites were studied.

2. Bioabsorbable polymers

Bioabsorbability of polymers refers to their properties where the polymer is degraded to smaller particles and absorbed into the body or by the body. Therefore these polymers should not evoke sustained inflammatory response nor release toxic degradation products, and they should fully metabolize in the body. These bioabsorbable polymers can be classified by dividing them into natural or synthetic ones. These both can further be classified on the basis of degradability as hydrolytically or enzymatically degradable polymers. (Nair & Laurencin 2007)

The bioabsorbability of synthetic materials suitable for biomedical operations were investigated already at the 1960s (Kulkarni et al. 1966). There are two key interest areas towards the bioabsorbable polymers. For one, in most of the cases the damaged tissue only needs temporary support during the time of healing. When using a bioabsorbable support there is no need for a removal operation (Törmälä et al. 1998). During the fixation the material should sustain its supportive properties and gradually release those properties to the healing tissue which eventually takes over (Middleton & Tipton 2000, Hutmacher 2000). The second reason is that for TE purposes the tissue is grown into/onto the scaffold making the removal operations of non-absorbable polymers impossible, thus they would be permanently a part of the newly formed tissue. For some cases this is maybe tolerable but for the most, not (Ikada 2006). Although for TE purposes the natural degradable polymers have suitable properties but for the fixation purposes yet most of the natural polymers are not mechanically suitable therefore the synthetic polymers are used instead (Nair & Laurencin 2007).

The synthetic polymers as a group is a versatile one and the properties of the polymers are mostly given while synthesizing them. There are several factors that affect the process such as monomer, initiator, and processing conditions and by altering these it is possible to alter the polymer structure and the properties. So it is possible to synthesize a polymer targeted for a required TE purpose and action (Nair & Laurencin 2007). There are at the moment several synthetic biodegradable polymers available and some of them are more widely used and commercialized than others. The use of synthetic polymers has extensively been increasing in the medical field and the study amongst those materials and new ones is strong (Woodruff & Hutmacher 2010, Tian et al. 2011).

The widely studied group of synthetic bioabsorbable polymers are the aliphatic polyesters such as poly(ε-caprolactone), polydioxanone, poly(hydroxy butyrate), and poly(trimethylene carbonate). The most used polymers in this group are the poly(α-hydroxy acids) such as polyglycolide, polylactides and poly(lactide-*co*-glycolide) polymers (Vert et al. 1984, Vert 2005, Middleton & Tipton 2000, Nair & Laurencin 2007).

2.1. Poly (α-hydroxy acids)

Poly(α-hydroxy acids) are a widely used and studied group of biodegradable polymers. To this group belong the polymers such as polyglycolide (PGA), polylactides (PLA) and the poly(lactide-*co*-glycolide) copolymer (PLGA). In this work I concentrate on the PLA polymers. The repeating unit in the structure of polylactides is based on the chiral monomer molecule lactic acid that exist either in L-form (naturally occurring) or D-form. The two enantiomers are optically active and thus they should be referred as L(+)-lactic acid (S) or the D(-) lactic acid (R). The PLLA can be synthesized using polycondensation process but this leads to low molecular weight polymers. When the ring opening polymerization (ROP) of lactides was introduced (Carothers et al. 1932) the high molecular weight polylactides could be produced. In ROP method the lactic acid is first polycondensated to a prepolymer and then depolymerized to cyclic lactide ring of either L-lactide, D-lactide or *meso*-lactide (DL-lactide) (Figure 1). The fourth lactide is an equimolar mixture of L-lactide and D-lactide and that is called a rasemic lactide. In the ring opening polymerization the lactide rings are opened with a suitable catalyst and the polymer is formed (Figure 2) (Gruber et al. 1992, Södergård & Stolt 2002, Groot et al. 2010).

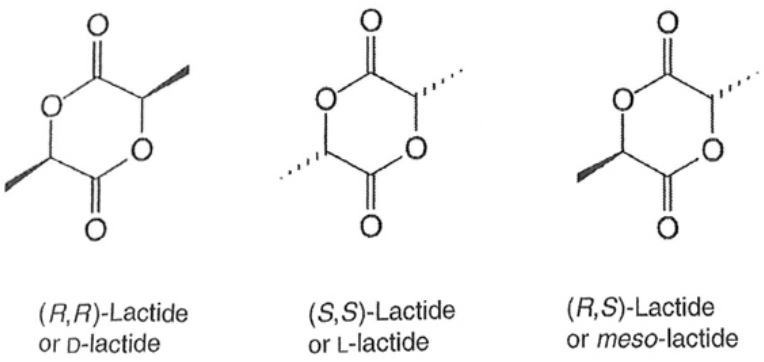

Figure 1. Lactide stereo isomers (Groot et al. 2010).

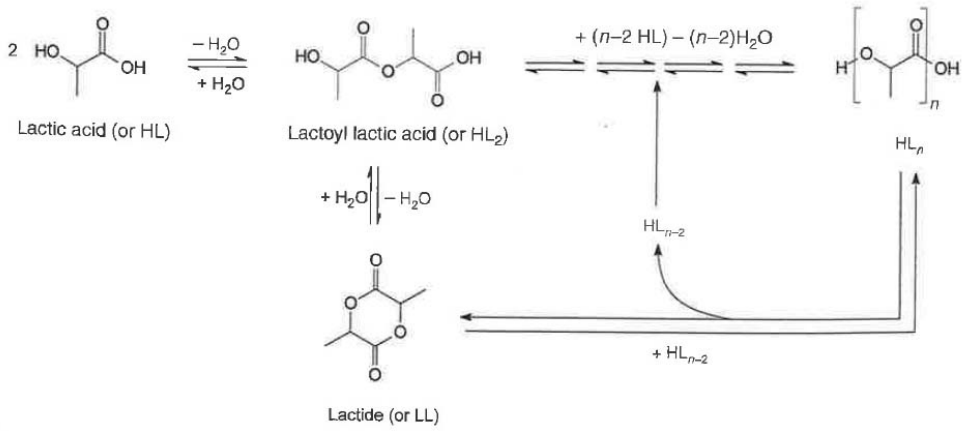

Figure 2. Lactic acid condensation, interchange to lactide, and ROP to polylactide (Groot et al. 2010).

It is possible to obtain different ratios of L and D for high molecular weight lactide polymers through the ROP, whereas only PLLA can be achieved through polycondensation. The different ratios of L and D affect the properties of the polylactides. Homopolymers polymerized from L- or D- lactide, PLLA and PDLA, are semi crystalline polymers (Urayama et al. 2003). Chabot et al. (1983) stated that crystallinity limit corresponds to the rule PLA X where X < 87.5. Thus if the amount of L is less that 87.5 % the polymer is amorphous. In their study the PLA 87.5 was polymerized from 75 % of L-lactide and 25% of rasemic (DL)-lactide and it was amorphous. Sarasua et al. (1998) noticed that it is possible to crystallize PLA polymers with optical purity as low as 40 %. Instead of using the most common initiators they studied polylactides with multiblock microstructure polymerized using a Salen-Al-OCH_3 initiator. As for the biomedical industry, the most common PLA polymers used in the medical industry at the moment are the PLLA (semi crystalline), PLDLA (amorphous), P(L/DL)LA 70/30 (amorphous) and P(L/D)LA 96/4 (semi crystalline).

The thermal characteristics of the PLA polymers are influenced by the crystalline/amorphous regions of the polymer. The glass transition temperature (T_g) is affected by many factors such as crystallinity, morphology, aging and impurities (Migliaresi et al. 1991, Jiang et al. 2010). Thermal properties of pure PLLA raw material also changes according to the molecular weight. For example, three different M_w PLLAs (2, 30, and 200 kDa) were measured (Fambri & Migliaresi 2010) in DSC

and the T_g was 43, 55 and 64°C respectively. The melting peak temperature of those were 147, 171, 192°C and crystallinity 51, 73 and 72 % respectively. In the studies of PLLA Fisher et al. (1973) showed that the theoretical value for the heat of fusion of 100% pure PLLA was 93.7 J/g.

The thermal characteristics of the PLA stereocopolymers are different from the pure PLLA. The melting point of the semicrystalline polylactide changes when the amount of D unit changes. As the amount of D-unit in the stereocopolymer increases, the melting point decreases (Chabot et al. 1983). Figure 3 clearly shows this dependency.

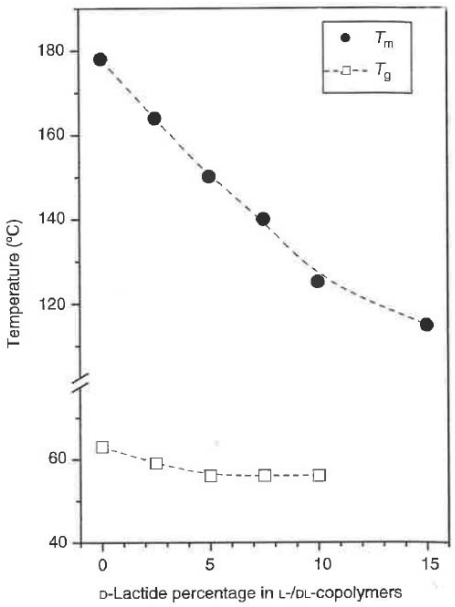

Figure 3. The T_g and T_m of poly(L/DL)lactide as a function of D in L/DL copolymers (Jamshidi et al. 1988, Fambri & Migliaresi 2010).

2.2. Degradation processes of bioabsorbable polymers

The degradation of bioabsorbable polymers can occur through different mediators and in different phases during the life cycle of a bioabsorbable material. The polymer can degrade during the processing stage, sterilization stage, storing stage, and finally after implantation to a living organism. The polymer further degrades during the hydrolysis studies where the in vivo degradation is trying to be mimicked. All these have to be taken into account and understood when working with and studying the degradable polymers.

2.2.1. Thermal degradation of polylactides

The random main-chain scission and unzipping are the two dominant depolymerization reactions during the thermal degradation of polylactides. The random scission is due to the hydrolysis, oxidative degradation, intra/intermolecular transesterification, or *cis*-elimination (Abe et al. 2004, Nishida 2010).

According to Gupta & Deshmukh (1982) the polyesters have three possible linkages where it can be broken and these are the C-O ether linkage, carbonyl carbon-carbon linkage and carbonyl carbon-oxygen linkage. They heated the PLLA powder from 70 to 105^{o}C in air and noticed the degradation behavior. They concluded that the isothermal degradation happens as a random chain scission, where two kinetically independent units take part in the degradation. The initial time it took to start the degradation suggested to them that the weak chain links randomly initiate the degradation. What Gupta & Deshmukh (1982) did not consider in their study was the PLLA end groups and the effects of the residual catalysts and monomers. Moreover, the PLLA used was solution polymerized low molecular weight PLLA.

The dominant PLLA thermal degradation process was proposed by McNeill & Leiper (1985) (Figure 4) to be a non–radical, backbiting ester interchange reaction involving the OH chain ends. This is also called an intramolecular transesterification from the chain end. This was also suggested by Jamshidi et al. (1988). According to Wachsen et al. (1997a) the thermal degradation is mostly due to intramolecular transesterification. It can also occur from the middle of the chain (Wachsen et al. 1997b). Now it depends on the place in the chain end whether the molecule is a lactide (1), an oligomeric ring with more than two repeating units (2), or an acetaldehyde and carbon monoxide (3). Kopinke et al. (1996) added the fourth possibility (4) where another type of cyclic transition state leads to an olefinic double bond plus a carboxyl group.

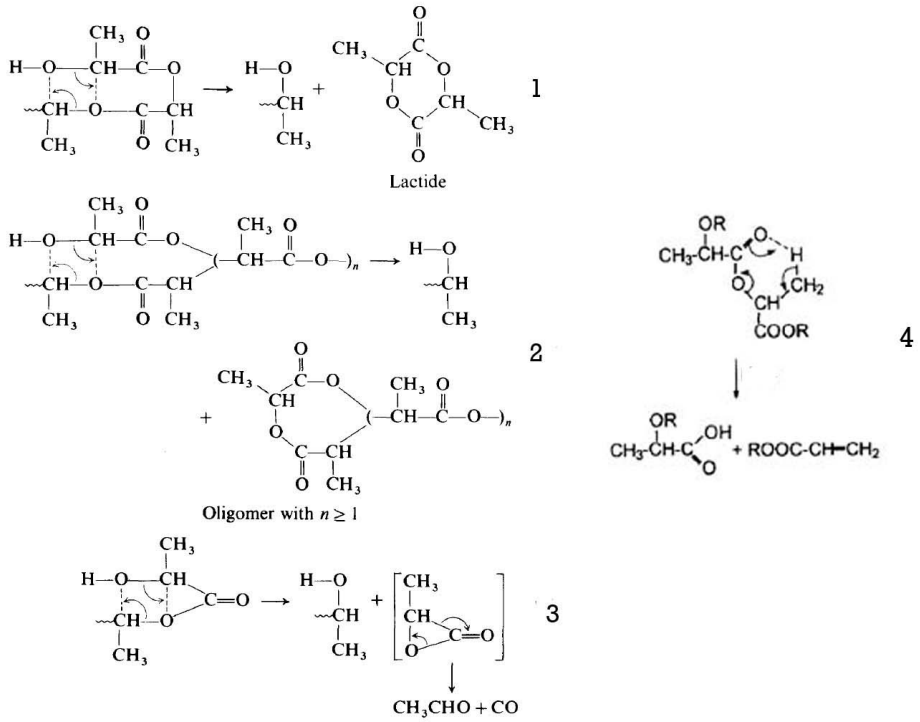

Figure 4. Non-radical reactions in thermal decomposition of PLA (modified from Kopinke et al. 1996, and Mcneill and Leiper 1985).

Jamshidi et al. (1988) showed that PLLA is relatively sensitive to the thermal degradation. The heating under N_2 atmosphere decreased the molecular weight of as-polymerized non-purified PLLA. Already after 10 minutes of heating at the temperatures of 180, 190, 200, 210, and 220^{o}C the molecular weight dropped 0, 0, 8, 33, and 75 % respectively. The 180^{o}C heating temperature had no effect on the M_w during 30 minute experiment, whereas in 190^{o}C the thermal degradation started to occur after 15 minutes of heating. The effect of the hydrolysis on main-chain ester bonds was uncertain although conventionally dried and carefully dried samples showed no difference. To study the effect of the monomer and residual catalyst, the PLLA was purified by means of repeated precipitation method. This resulted to better thermal stability at 200^{o}C, where purified PLLA still had 50% higher M_n after 10 minute heating compared to the non-purified PLLA. It was shown that the presence of the catalyst clearly affects the thermal stability (Jamshidi et al. 1988, Cam & Marucci 1997). Jamshidi et al. (1988) suggested that the transesterification reactions will lead to M_w reduction where the catalysts induce the monomer and cyclic oligomer formation. The role of the monomer was left uncertain since it was not measured in that study. Other studies also report the accelerating effect of the catalyst on the thermal degradation

(Kopinke et al. 1996, Wachsen et al. 1997) and the effect of purification on melt degradation (Södergård & Näsman 1996). Liu et al. (2006) showed that especially low molecular oligomers and air should be removed during the molten state to avoid thermal degradation. They stated that the degradation of PLLA in processing temperatures proceeds in a random chain scission mechanism and that there were from two to three stages. The first stage was dominated by hydroxyl and carboxylic acid containing oligomers. When these were consumed, the second stage started and was governed by the thermo-oxidation promoted by the presence of oxygen. At the third stage the polymer was degraded over 200^{o}C in N_2 due to the carboxylic acid substance. Paakinaho et al. (2011) showed that melt processing induces thermal degradation that further induces a lactide monomer accumulation into the purified PLGA 85L/15G polymer. This lactide monomer amount of ≤ 0.2 wt-% already effects the mechanical properties during the hydrolysis.

Zou et al. (2009) measured PLLA thermal degradation products by means of TGA coupled to the FTIR and noticed that when heating the PLLA 20^{o}C/min in N_2 atmosphere the peak decomposition temperature was 372^{o}C. The FTIR measured from different temperatures but mainly from 372^{o}C showed gaseous cyclic oligomers, lactide, acetaldehyde, carbon monoxide and carbon dioxide. They concluded that this is related to the hydroxyl end-initiated ester interchange and chain homolysis.

2.2.2. Radiation degradation

Why the radiation may be used, is to purify, kill bacteria, and sterilize the polymeric products for medical use. The conventional methods like heat and chemicals might not be suitable for polymer sterilization so other methods, like irradiation is used. The radiation sterilization is based on gamma rays from a cobalt-60 isotope source or machine generated accelerated electrons. The latter is also called as “e-beam sterilization” method (Kowalski & Morrissey 1996). The polymers undergo certain deterioration due to the radiation sterilization. The effect of high energy radiation such as γ-irradiation is intense and can ionize molecules unselectively through strong interactions affecting molecules nucleus or electron clouds. The secondary electrons that are produced have enough energy to trigger further ionizations and energy

excitations of those molecules surrounding the target molecule. The cascade continues further when the new active species induce homolytic cleavage, ionic scission, electron transition and energy transition. (Sakai & Tsutsumi 2010). Babalbandi et al. (1995) studied the PLLA and PLDLA with electron spin resonance spectroscopy under liquid nitrogen and suggested that there are three possible different radicals forming from the main chain scission. One radical from the hydrogen abstraction from the methine groups located on the backbone of the polylactic acid chain and two radicals from chain scission at the ester groups of the polymer macromolecule.

Birkinshaw et al. (1992) showed the dose dependent degradation when they studied the irradiation degradation on compression molded plaques made from commercial PLLA, molecular weight of 100 kDa. They used dosages of 0, 2.5, 5.0, and 10 Mrad. They noticed that the tensile strength dropped 15 % by the 2.5 Mrad dose. The 5.0 Mrad dose influenced a drop of 40% and 42 % in tensile strength and elongation at break respectively. The molecular weight dropped 24, 38, and 53 % from the zero dose with 2.5, 5.0, and 10.0 Mrad doses respectively. The different irradiation doses had no effect on the mechanical properties during storage either in 336 or 504 days follow-up. From this they assumed that radiation did not form metastable peroxy or hydroperoxy groups. This was also indicated by hydrolysis tests. Indications lead to assume that the primary function of irradiation is only in molecular weight decrease. Nuutinen et al. (2002a) studied the effects of the gamma irradiation on SR-PLLA fibers. The 25 kGy dose during the gamma irradiation introduced a drop of ~ 62 % in viscosity and a ~ 31 % increase in crystallinity. The irradiation caused a 12 to 17 % decrease in UTS and a 3 to 29 % increase in elastic modulus.

2.2.3. Hydrolytic degradation

Polymers from lactic acid, have an ester group and through this group they are hydrolytically degradable. This leads to a molecular fragmentation of the polymer chain according to following reaction: $–COO- + H_2O \rightarrow -COOH + HO-$. There are two main pathways to degradation, the surface erosion and bulk erosion. The surface erosion occurs when the surface degradation rate (water diffusion rate to the molecules) is higher in the surface than within the material. In the bulk erosion, the phenomenon

occurs simultaneously in the surface and within the material core. Thus the degradation is homogenous throughout the material. There is also a degradation pathway that originates from the sample size. This is called a "large object degradation" or core accelerated degradation where the slowly degrading surface entraps the degrading molecules. The degradation of the inner part and the ester bond cleavage leads to formation of new carboxyl and hydroxyl end groups, these further catalyze the hydrolysis of the material. This catalysis phenomenon is also called autocatalysis. (Li et al. 1990, Grizzi et al. 1995, Tsuji et al. 2000, Burkersroda et al. 2002, Tsuji 2010).

According to Weir et al. (2004a) the morphology and molecular weight play an important role in the degradation profile. Besides these there are several other factors that affect the degradation. It has been shown that there are correlations between the in vivo degradation and in vitro degradation and although there are a lot of factors governing this, to some extent they can be estimated and predicted. Tsuji (2008, 2010) listed the material and media-related factors that affect the degradation of PLA based materials (Table 1).

Table 1. Material and media-related factors that affect the degradation of PLA based materials Tsuji (2008, 2010).

Material factors	**Media-related factors**
Molecular structures	Temperature
Molecular weight and distribution	pH
Optical purity and distribution	Solutes (kinds and concentrations)
Comonomer structure, content, and distribution	Enzymes (kinds and concentrations)
Terminal groups	Microbes (kinds, number, and culture conditions)
Branching	Stress or strain
Cross-links	
Highly ordered structures	
Crystallinity	
Crystalline structure	
Spherulitic size and morphology	
Orientation	
Hybridization (blends and composites)	
Material morphology	
Material shape and dimensions	
Porosity and pore size	
Surface treatment	
Coating	
Alkaline treatment	

When the PLA polymers degrade there are three main stages to be noticed. First, there is the water absorbing into the materials. Second, there is the molecular weight loss

without the mass loss. Third, there is the weight loss when the water soluble oligomers and monomers are formed and further dissolute. At the beginning of hydrolytic degradation of semi crystalline PLA polymers the amorphous regions are degraded first. Tsuji & Ikada (2000) noticed also that the increase in initial crystallinity seemed to increase the degradation by increased defects in the amorphous regions that take up the water. The degradation took mainly place in the amorphous region between the crystalline regions. The rate of degradation in this region was also higher than that of the free amorphous regions (Pohjonen & Törmälä 1994, Tsuji & Ikada 2000, Tsuji et al. 2000). The crystalline phase is more resistant to degradation due to the rigid structure of crystallites. This prohibits the water penetration into the crystalline regions. After the amorphous regions have degraded the crystalline regions called crystalline residues remain. The growth of these crystalline regions took place during the hydrolysis at elevated temperatures (Tsuji et al. 2004). Tsuji et al. (2008) also explained the method for hydrolytical degradation in elevated temperatures under a saturated water pressures. They noticed that the yield of lactic acid from PLLA was higher than the 1 % at temperatures of 120, 140, 160, and 180^{o}C after 360, 180, 60, and 25 minutes respectively. The formation of oligomers during the hydrolytic degradation was mentioned above and Hakkarainen et al. (2000) studied the effect of low molecular weight lactic acid derivatives on degradation. They noticed that these derivatives in the films enhanced the degradability of polylactide in biotic medium.

Li (1999) reviewed the materials used and proposed the degradation PLLA-PGA-PDLA triangle chart where different regions form during the hydrolysis depending on the starting composition. He found out that some compositions in this triangle form hollow structures during the hydrolytic degradation in PBS at 37^{o}C. No such behavior was noticed for the PLLA, PLA 96 or PLA 87.5. The PLA 96 polymer belongs to the semicrystalline part of this triangle together with the PLLA. The PLA 96 has 4 % of D-lactide in the structure and by making amorphous PLA 96a and PLA 100a he found out that PLA 96a crystallizes faster than the PLA 100a in PBS 37^{o}C. He stated that the crystallization (the increase in crystallinity) during the hydrolysis resulted from degradation by products or short chains of the faster degrading PLA 96a. Opposite results to this were reported (Mainil-Varlet et al. 1997). Li (1999) also presented degradation half-life times (50 % of initial material lost) for the selected compression molded polymer plates (10 x 15 x 2 mm). For the PLLA, PLA 96, PLA 87.5, PLA 75,

PLA 62.5, and PLA 50 the half-life times were 110, 90, 80, 22, 23 and 10 weeks respectively in PBS at 37^{o}C at pH 7.4. No monomers or residual catalysts were measured or reported therefore it can be argued whether the autocatalytic behavior, where predominant, was influenced by these factors.

2.2.4. In vivo degradation

The complete degradation in the body will follow when the lactic acid is formed. This polymer residue will finally be metabolized by the body. But prior to last lactic acid monomer removal there are obstacles in the way when considering the semicrystalline PLA materials. The crystalline residues that form during the degradation of PLLA reported by Tsuji et al. (2004) can be problematic since the molecular weight of those can remain unchanged for several years although supportive function has been lost much earlier (Suuronen et al. 1998). These implications are backed up by other studies that have reported long in vivo degradation. Although to the cytotoxicity of PLLA the crystallinity seems to have no effect. This was noticed in the cell studies by Sarasua et al. (2011). Böstman & Pihlajamäki (2000) did a review on the clinical biocompatibility of orthopedic implants and found out that the foreign body reactions due to PLLA will start as late as 4 to 5 years after surgery. This was mainly due to the poorly vascularized bone sections, the use of a polymer dye and implant geometry.

The in vivo degradation of PLA 96 polymer has shown that the material is biodegradable and retains its properties for various time periods depending on the form of device, the implantation site, and the species (Bonnichon et al. 1996, Saikku-Bäckström et al. 1999, Saikku-Bäckström et al. 2004, and Hietala et al. 2001). Cordewener et al. (1995) reported a loss in mechanical properties and mild foreign body reactions in 7 weeks for PLA 96 polymer but they used the as-polymerized PLA 96, the material that was stated not to use as osteosynthesis material (Bergsma et al. 1995). Cordewener at al. (2000) proposed that the degradation products of the as-polymerized PLA 96 will not be a problem during the in vivo rather the accumulation of those and the following pH decrease. They proposed that the further tissue reactions are triggered by the time M_w is in the range of 5000-6000 Da. For the injection molded P(L/DL)LA 95/5 it was noticed that 95 % from the M_w had already gone by the week 12 (Mainil-Varlet et al. 1997). To this rapid degradation the monomer content of 0.7 % and residual

catalyst content of 520 ppm might have played a part. The SR-PLA 96 intramedullary nail showed good in vivo results although mild histological reactions were seen at 6-18 months. The material was still somewhat present although almost disintegrated after three years (Saikku-Bäckström et al. 2004). Lazennec et al. (2003) studied the injection molded amorphous P(L/DL)LA 96/4 for lumbar interbody fusion. They noticed that after 36 months in vivo (sheep) there was a low potential for foreign body reaction. They showed a promising balance between the fusion and degradation. The implant degradation time was in their scale moderate after 6 months, marked after 24 months and complete after 36 months. The group suggests that the good results might have been due to the amorphous material compared to the semi crystalline one. As for the long term effects in the intravascular stents in vivo, Hietala et al. (2001) showed a fragmentation of PLA 96 stents in 24 months and only minimal tissue reactions due to degradation.

The in vivo behavior of degradable polymers has been evaluated with in vitro testing for practical, economical and ethical reasons. Due to the complex nature of human body and tissues there is only some information that can be achieved with in vitro testing. By comparing the two it may be possible to model a specific tissue type and its behavior on degradation. The in vitro and in vivo (subcutaneously in rats) was compared by Weir et al. (2004b) as they studied PLLA rods. They noticed that there is a delayed degradation with the in vivo implants. The in vivo implants had higher shear strengths after 32 weeks of implantation compared to the in vitro reference rods. This point can be observed from the molecular weight results as well since the 26-week in vivo implant had a higher M_w and M_n than the in vitro implant. As for the gamma irradiated PLA 96 monofilament sutures, Kangas et al. (2001) did not see any difference in degradation between the in vitro or in vivo sutures after 6 weeks. In both groups the tensile strength decreased from ~ 420 to ~ 310 MPa. When comparing the PLA 96 polymer in vitro and in vivo (rabbit knee) Daculsi et al. (2011) found that the crystallinity after 76 weeks in vitro was 73 ± 7 % in in vitro and 60 ± 7 % in in vivo. The molecular weight decreased from 56 k to 10 k in 48 weeks whereas in vivo it took 38 weeks to do the same. No foreign body reactions were noticed but the bone contact was no longer maintained at week 76 for the pure PLA 96. Then again by adding a 24 wt-% of β–TCP into the PLA 96 polymer resulted in bone growth and mineralization.

2.2.5. Storage degradation

As previously mentioned Birkinshaw et al. (1992) studied the influence of the radiation to storage time from 0 to 336 days and up to 504 days for some doses. These results present also the data that there is no considerable degradation when studying the M_w but there is a decrease in number average molecular weight (M_n) for the non-irradiated plaques. Pluta et al. (2008) also studied the effect of storing. They noticed no change in molecular weight after one year aging of compression molded PLLA.

3. Biodegradable fibers and composites

The processing methods for biodegradable polymers mainly include melt processing or solvent based methods (Figure 5). In the case of fibers, melt spinning, wet spinning, dry spinning, and electro spinning processing methods, are the most common. When the scaffold manufacturing is the goal then further processing is needed. For fibers the textile methods are a one route from fiber to a scaffold. Other commonly used scaffolding techniques for biodegradable polymers include particulate leaching, thermally induced phase separation, 3-D printing, stereolithography, selective laser sintering, and direct writing (Woodruff & Hutmacher 2010). In this work we focus on the melt spinning regarding the fibers and on textile methods regarding the preforms, scaffolds, and composites.

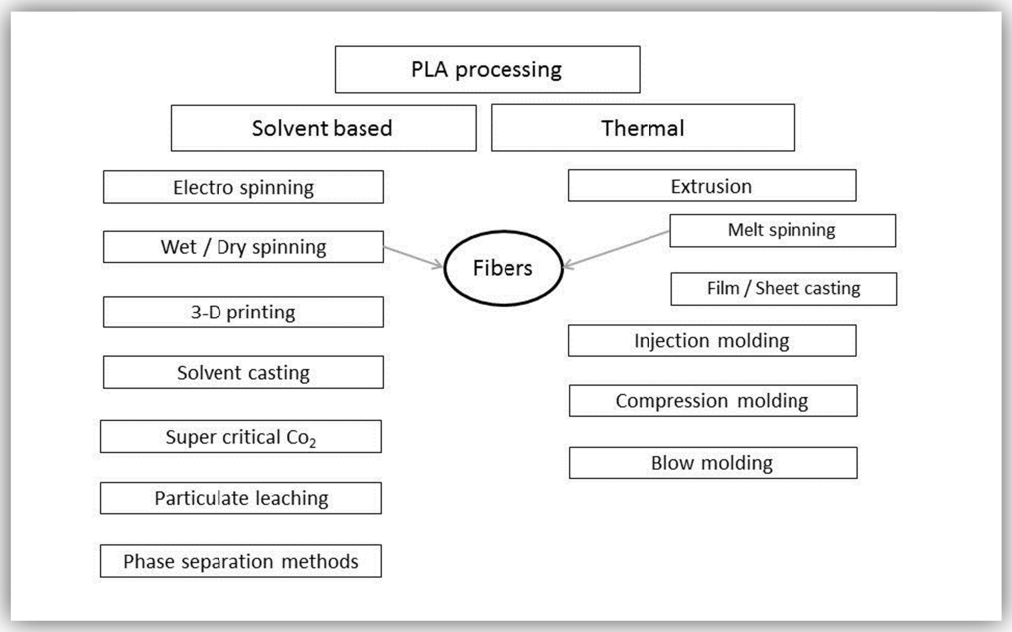

Figure 5. The most common PLA processing methods. The processing methods that are suitable for continuous fiber formation and further textile processing are shown with arrows.

3.1. Melt processing

For the PLA polymers the melt processing is one of the most common processing methods, especially melt extrusion and injection molding. In the melt processing the raw polymer is heated above its melting point, melt is formed to a desired shape and then cooled down to stabilize the shape and dimensions. The PLA polymers must be dried prior to melt processing to minimize the hydrolytic degradation during the processing. (von Oepen & Michaeli 1992, Tsuji et al. 2008, Taubner & Shisoo 2001). When processing PLLA Taubner & Shishoo (2001) observed a higher M_w loss for the PLLA with moisture content of 0.3 wt-% when compared to the dried PLLA. Earlier reports with similar results, where residual moisture resulted in increased degradation, were also reported by von Oepen & Michaeli (1992) for polycondensated polyesters. The polymer producers have worked on the materials and they have guidelines for their use. According to a "sheet extrusion processing guide", given by commercial polymer manufacturer for plastics industry (NatureWorks LCC, USA), if temperatures higher than 240^{o}C are used the PLA polymer should be dried to below 50 ppm of water (0.005 % w/w).

When processing the biodegradable polymers such as PLA-based polymers, another important factors that should be considered are the temperature and the residence time. Ramkumar & Bhattacharya (1998) studied the rheology of the commercial PLAs and noticed that PLLA is susceptible to degradation and suggested that the temperatures should be kept low to avoid the thermal degradation. Taubner & Shishoo (2001) melt processed PLLA (start M_n of 40,000 g/mol) in twin-screw extruder and noticed that when the residence time increased from 1 min 45 s to 7 min the number average molecular weight after extrusion dropped from 33,660 to 30,200 g/mol at 210^{o}C and from 25,600 to 13,600 g/mol at 240^{o}C. From this they concluded that effect of the increase in processing temperature on the molecular weight decrease is noticeable. The degradation behavior was also shown during the melt spinning process by several publications (Table 2). Despite the spinning method the degradation of the PLA polymer was high. In some studies it stayed at the level from 13 to 40 % but on average it was higher being closer to the level from 50 to 60 %.

Table 2. Degradation of the PLA polymers during melt-spinning.

Polymer	Purified	Fiber	Nozzle temp (^{o}C)	Raw material M_w / Viscosity	After processing M_w / Viscosity	Melt degradation (%) of M_w / Viscosity	Reference
PLLA	NA	Mono fil	240	330000	105900	**68**	Pegoretti et al. 1997
PLLA	NA	Mono fil	240	330000	107200	**68**	Pegoretti et al. 1997
PLLA	NA	Mono fil	240	330000	118000	**64**	Fambri et al. 1997
PLLA	NA	Mono fil	240	330000	121600	**63**	Fambri et al. 1997
PLLA	NA	Mono fil	240	330000	122400	**63**	Fambri et al. 1997
PLLA	NA	Mono fil	240	330000	101900	**69**	Fambri et al. 1997
PLLA	NA	Mono fil	240	398400 (a	123600	**69**	Yuan et al. 2000
PLLA	NA	Mono fil	230	264700 (a	112200	**57**	Yuan et al. 2000
PLLA	NA	Mono fil	230	221400 (a	105900	**52**	Yuan et al. 2000
PLLA	Yes	Mono fil	295	/ 9.52	/ 3.7 - 4.3	**/ 54 - 61**	Nuutinen et al. 2002a
PLLA	Yes	Mono fil		648 000 / 9.52	164 000	**75**	Nuutinen et al. 2002b
P(L/D)LA 85/15	NA	Mono fil	135	510000 / 3.0	/ 1.2	**/ 60**	Andriano et al. 1994
P(L/D)LA 90/10	NA	Mono fil	146	948000 / 4.5	/ 1.7	**/ 62**	Andriano et al. 1994
PLA 92 + meso 8	NA	Multi fil 12	185	207000 / 1.01	180000 / 0.91	**13 / 10**	Schmack et al. 2001
P(L/D)LA 92/08	NA	Mono fil		98500	71300 - 61700	**28 - 37**	Cicero & Dorgan 2001
P(L/D)LA 95.7/4.3	No	Multi fil 400		74500 (b / 3.96	41500 (b	**44** (b	Solarski et al. 2007
P(L/D)LA 96/4	Yes	Mono fil		413 000 / 6.85	177 000	**57**	Nuutinen et al. 2002b
P(L/D)LA 96/4	Yes	Multi fil 4	260	/ 6.80	/ 1.28	**81**	Honkanen et al. 2003

(a after milling of the raw material
(b M_n
NA Not available

Palade et al. (2001) studied the rheological properties of semi-commercial PLA polymers with high L-content (higher than 96 %). They showed that these polymers can be drawn to large strains in dynamic testing and they showed considerable strain hardening. They suggested that this hardening was due to the high molecular weight tail present in the polymer. They suggested that this combination of rheological properties for the polylactides should be advantageous for spinning, casting and blowing.

3.2. Melt spinning

Almost all synthetic fibers are manufactured by means of spinning. Here only the melt spinning is discussed. Melt spinning is a method where the polymer is melted and from the melt the fibers are formed by extruding the melt through the plate, nozzle, or spinneret with small holes. The fibers that are drawn from the melt and have not undergone further processing are called as-spun fibers. The orientation of fibers can be

done separately for the as-spun fibers or fibers can be continuously drawn from the melt and oriented using a suitable orientation method. The post die treatment includes the melt stretching, cooling and hot or cold drawing. (Tadmor & Zehev 2006)

The melt spinning method starts from the extrusion of the melt. The polymer is melted in the extruder. There are two types of extruders, a single screw and a twin-screw extruder. For a typical single screw extruder there are three zones in the screw: feeding zone, compression zone, and metering section. In the compression zone the polymer is compressed as the flight depth of the screw decreases. In this zone the polymer is melted. In the metering section the polymer melt is homogenized. The most important parameters are the temperature of the extruder zones and the screw speed that affects the residence time, shear, and the output volume. When the polymer exits the spinneret, it is melt drawn to achieve a proper pre-orientation. This solidification from molten to solid is one of the most important factors in melt spinning (Ziabicki 1976, Ward 1997, Fourné 1999) The quality of the fiber is important for any industrial and medical purpose therefore it is essential that the fiber dimensions are stable. Therefore the resonance of the fiber (variable change in fiber diameter) should be controlled. The resonance is due to the fiber stretching near the take up roll. This leads to a thicker fiber formation at the die exit, which in turn, when it reaches the take up roll will go faster through, again thinning the fiber. This leads to uneven fiber diameter at the end product. Kase (1974) noticed that if the solidification of the melt occurs before the take up rolls there is no resonance detected. Therefore the proper cooling, quenching of the fiber, is essential. During the quenching the speed and the control of cooling down affects, not only to the pre-oriented fiber itself, but to the orientation parameters that are used. This solidification state sets the amount and a format of crystallites that form into the pre oriented semi-crystalline polymeric fiber, thus setting the molecular basis for the further orientation. With rapid cooling the rate of crystallite forming and the size can be minimized. (Ziabicki 1976, Ward 1997).

The actual drawing of the fibers starts from the pre-oriented as-spun fibers. In the drawing process the fiber will be either fully or partly oriented. When the heat is applied to the drawing process it is called a hot drawing and if not, it is called cold drawing. In this thesis we discuss about the hot drawing of the polymer fibers. In hot drawing the pre-oriented fiber is subjected to temperatures higher than their glass transition temperature but lower than their melting temperature. In drawing the fiber is pulled

onward and simultaneously heated. The fiber draw-ratio increases and the fiber diameter decreases. As the diameter decreases the filament length increases and the orientation is further affecting the crystallites by closely packing and orientating the lamellar structure. This on the other hand affects the tensile modulus and tensile properties by increasing strength on the account of elasticity, thus the elongation (strain, stretching capacity) decreases. The further the drawing continues, the more closely packed are the chains and crystalline regions. (Ziabicki 1976, Ward 1997, Fourné 1999). The melt spinning of PLA fibers and results from those studies are further discussed in the next chapter.

3.3. Fibers

The melt spinning processes, as methods for fiber manufacturing, have been studied by several groups. These melt spinning studies, materials and properties are reviewed in Table 3. The processes can be divided into three groups based on the orientation or fiber collection process. They are the melt spinning with continuous hot drawing process, two-step hot drawing process from as-spun fibers, and high speed spinning. The latter can also be divided in two sub groups based on the orientation process; as-spun fibers and spin-drawn fibers.

3.3.1. Continuous melt spinning hot drawing

The first reported fibers for implant manufacturing were reported by Andriano et al. (1994). They produced melt-spun fibers with melt spinning and continuous hot drawing. They used fairly low nozzle temperatures from 135 to 146^{o}C. They produced fairly thick monofilaments with diameters from 250 to 500 μm. Kellomäki & Honkanen (Kellomäki et al. 2000, Kellomäki 2000, Honkanen et al. 2003, Kellomäki & Törmälä 2004) melt-spun P(L/D)LA 96/4 4-filament yarns with single yarn diameters from 70 to 120 μm. They used nozzle temperature of 260^{o}C. Similar P(L/D)LA 96/4 4-filament yarns, with the same methodology, were also melt-spun by Huttunen et al. (2006) and Viinikainen et al. (2006, 2009). Nuutinen et al. (2002a-b, 2003a-b) melt-spun PLLA and P(L/D)LA 96/4 monofilaments with diameters from 210 to 320 μm. They used nozzle temperature of 295^{o}C in the PLLA monofilament spinning. All the filaments were

produced using a single screw extruder. We can observe that with these methods, at least at the time of making, it is not possible to produce really fine fibers since the minimum produced fiber thickness was 70 μm. The draw ratios varied from 4.5 to 8.9. The highest ratios were obtained with the machinery where only one orientation stage was used whereas for the other studies there was several orientation stages with separate heating units, feed rolls, and take-off rolls. The breaking strength of the fibers varies yet we can observe similar properties for mono- and multifilaments. The average breaking strength was from 300 to 400 MPa. The maximum breaking strength obtained for mono- and multifilaments was ~ 600 MPa. The tensile modulus varied from 5.8 to 7.4 GPa. By adding x-ray positive filler into the monofilaments, the mechanical properties were decreased according to the filler content. The degradation behavior of the fibers by Andriano et al. (1994) showed very rapid loss of mechanical strength and molecular properties. This may be due to the impurity of the raw material since the processing temperatures were fairly low.

The gamma irradiated PLLA monofilaments lost 50 % of their mechanical strength in 8 to 20 weeks and 50 % of molecular weight in 18 weeks (Nuutinen et al. 2002a-b, 2003b). The effect of the 25 kGy gamma irradiation sterilization was noticeable. At 6-week time point the un-sterilized fiber had lost 30 % of its ultimate tensile strength whereas the sterilized had lost 50 %. This difference remained until the week 18 after which the UTS was the same for both of the fibers, average 15 % left at week 22. During the hydrolysis the both fibers lost 50 % of their intrinsic viscosity at week 12. (Nuutinen et al 2002a). The P(L/D)LA 96/4 monofilaments lost 50 % of their mechanical strength in 22 weeks and 50 % of molecular weight in 15 weeks (Nuutinen et al. 2003a). The multifilament P(L/D)LA 96/4 yarns lost 50 % of their mechanical strength either in 13 weeks or in 42 weeks. This difference is probably related to the machinery properties (Kellomäki 2000, Honkanen et al 2003). The multifilament P(L/D)LA 96/4 yarns lost 50 % of M_w in 36 weeks during the hydrolysis (Kellomäki 2000). The same drop in in vivo for M_w was seen between the weeks 10 and 20 (Kellomäki et al. 2000). The effect of aging on fiber degradation was not found on the literature, yet for the PLA 96 injection molded samples, stretching (orientation) at 90^{o}C increased the enzymatic degradation stability compared to the 60^{o}C or non-stretched samples (Cai et al. 1996).

Table 3. The melt-spun-fibers from PLA and their properties. (Fibers in hydrolysis studies were gamma irradiated except the ones marked with *)

Polymer	Purified	Fiber	Nozzle temp (°C)	Nozzle Ø (mm)	Orientation temp (°C)	Draw ratio / high speed (m/min)	Filament Ø (µm)	Crystallinity %, hot drawn	Breaking strength (MPa)	Young's modulus (GPa)	In vitro 50 % Mol weight / viscosity left (Weeks)	In vitro 50 % UTS left (Weeks)	Ref.
Continuous melt spinning hot drawing													
P(L/D)LA 90/10	?	Mono fil	146	1.5	80-90	3.3-7.5	250-500		max. 387 ± 41	max 6.5 ± 0.4	/ 8*	4*	Andriano et al. 1994
P(L/D)LA 85/15	?	Mono fil	135	1.5	80-84	3.0-8.9	250-500		max 430 ± 59	max 6.7 ± 1.0	/ 12*	2*	Andriano et al. 1994
PLLA	Yes	Mono fil			95 - 138	7	280-420		knot 291 ± 36			> 12	Heino et al. 1996
P(L/D)LA 96/4	Yes	Multi fil 4	260	0.4		4.8	80-120				In vivo > 10 < 20		Kellomäki et al. 2000
P(L/D)LA 96/4	Yes	Multi fil 4				4.8	80-120				36	42	Kellomäki 2000
P(L/D)LA 96/4	Yes	Multi fil 4	260	0.5		4.5	70 - 80		345 ± 41			13	Honkanen et al. 2003
PLLA	Yes	Mono fil	295	1.0	150-180	6.0	300 ± 20	47 - 57	599 ± 33	7.4 ± 0.5	/ 12	8 and 13	Nuutinen et al. 2002a
PLLA	Yes	Mono fil		1.0		6.5	210		260 ± 15	6.7 ± 0.4	18	20	Nuutinen et al. 2002b
P(L/D)LA 96/4	Yes	Mono fil		1.0		5.0	270		231 ± 16	5.8 ± 0.2	15	22	Nuutinen et al. 2002b
P(L/D)LA 96/4	Yes	Mono fil				5.0	270		231 ± 16	5.8 ± 0.2	/ 22	22	Nuutinen et al. 2003a
P(L/D)LA 96/4 + BaSo4 15-30	Yes	Mono fil				5.4 - 6.5	300 - 320		136 ± 56 - 373 ± 49	5.6 ± 0.7 - 6.4 ± 0.8	/ 18 - 45	12 - 42	Nuutinen et al. 2003a
PLLA	Yes	Mono fil		1.0		6.2	310				18	8	Nuutinen et al. 2003b
P(L/D)LA 96/4	Yes	Multi fil 4	260	0.4		4.0 - 4.8	70-120		450 - 600	6.5 - 8.5			Kellomäki & Törmälä 2004
P(L/D)LA 96/4	Yes	Multi fil 4		0.4									Huttunen et al. 2006
P(L/D)LA 96/4	Yes	Multi Fil	270										Viinikainen et al. 2006, 2009
Two-step hot drawing from as-spun fibers													
PLLA	?	As-spun Mono, hot drawn	240	1.0	160	7.3 - 20.5	48 - 106	53.1 - 65.0	410 ± 80 - 870 ± 11	7.0 ± 0.9 - 9.2 ± 1.7			Fambri et al. 1997
PLLA	?	As-spun Mono, hot drawn	240	1.0	160		120 ± 10	66.5	890 ± 96	10.4 ± 0.4	7*	4*	Pegoretti et al. 1997
PLLA	?	As-spun Mono, hot drawn	240	1.0	160		72 ± 7	66.6	968 ± 105	8.3 ± 0.6	2 - 3*	8*	Pegoretti et al. 1997
PLLA	?	As-spun Mono, hot drawn	230 - 240	1.0	120	4.77 - 5.89	134 ± 8 - 146 ± 11	61.0 - 61.8	332 ± 34 - 500 ± 50	3.88 ± 0.3 - 5.1 ± 0.5	32*, >35 *	> 35*	Yuan et al. 2001, 2002
P(L/D)LA 92/08	?	As-spun Mono, hot drawn			71-93	1-8		0 - 51	max. 380	max 3.1		Cicero & Dorgan 2001, Cicero et al. 2002	
P(L/D)LA 96/4	?	As-spun Mono, hot drawn						0 - 35	80 - 380	1.4 -3.1			Cicero et al. 2002a
High speed spinning													
PLLA	?	Multi fil 4 (high speed as-spun)	233			/ 100- 4700		0 - 45	90 - 385	3.6 - 6.0			Mezghani et al. 1998
PLA 92 + meso 8	?	Multi fil 12 (high speed spin drawn)	185	0.3	65-110	4.0 - 6.0 / 800 - 1200		18.6 - 23.9	211 - 460	4.3 - 6.3			Schmack et al. 2001
PLA 92 + meso 8	?	Multi fil 12 (high speed as-spun)	185	0.3	65-110	/ 1000 - 5000		0.0 - 11.0	205 - 317	3.2 - 4.1			Schmack et al. 2001
PLA 98.5	?	Mono fil (High speed as-spun)	230	0.5		/ 1000 - 9000	35 -480	8 - 48	100 - 560	2.1 - 5.8			Takasaki et al. 2003a
PLA 91.9	?	Mono fil (High speed as-spun)	220	0.5		/ 1000 - 8000	35 -480	0 - 18	100 - 420	2.2 - 5.9			Takasaki et al. 2003a
PLA 83.6	?	Mono fil (High speed as-spun)	220	0.5		/ 1000 - 7000	30 -500		110 - 330	3.1 - 4.2			Takasaki et al. 2003a
Racemic PLDA	?	Mono fil (High speed as-spun)	230	0.5		/ 1000 - 6000	22-500	5 - 38	100 - 400	2.5 - 4-8			Takasaki et al 2003b
PLA 98.5	?	Mono fil (High speed as-spun)	230	0.5		/ 1000 - 9000	22 - 390	6 - 28	100 - 560	2.1 - 5.8			Takasaki et al 2003b
PLA 99 - PLA 92	?	Multi fil 12 (high speed as-spun)	185	0.3		/ 2000 - 5000		0 - 40		3 - 6			Schmack et al. 2004
PLA 95.7	No	Multi fil 400 (High speed spin drawn)		0.4	70-120	2-3.5 / 200-400	43- 56	18-38	210 - 442	4.0-6.5			Solarski et al. 2007
Manufacturing method not known													
PLLA		Multi fil 30	Manufactured by Albany international , Mansfield MA				fil 12 ± 0.6 µm, yarn 295 ± 44 µm						Freeman et al. 2007
PLLA		Multi fil 30	Manufactured by Albany international , Mansfield MA										Lu et al. 2005

3.3.2. Two-step hot drawing from as-spun fibers

All the as-spun fibers that were hot drawn were monofilaments. The multifilament type as-spun fibers by Ekevall et al.(2004) were not hot drawn. Fambri et al. (1997) and Pegoretti et al. (1997) studied the melt-spun PLLA fibers in a two-step process. The extruder nozzle temperature was 240^{o}C and the drawing temperature was 160^{o}C used. After the hot drawing the fiber diameters were 72 and 120 μm by Pegoretti and from 48 to 106 μm by Fambri. Yuan et al. (2001, 2002) studied the monofilament PLLA. They used extruder nozzle temperature from 230 to 240^{o}C. They produced fibers with diameters ~ 110 to 150 μm. In PBS saline the hydrolytic degradation decreased the viscosity average molecular weight by 40 to 60 % in 35 weeks. The fiber tensile strength was ~ 450 - 500 MPa and it did not significantly change during the 35-week follow-up. Cicero et al. (Cicero et al. 2002a-b, Cicero & Dorgan 2002) studied the effect of polymer branching and cold-drawing on fiber properties. The maximum breaking strengths obtained for the as-spun hot drawn were from 870 to 970 MPa. The maximum tensile modulus varied from 9 to 10 GPa. Based on these studies it can be noted that with the as-spun hot drawn fibers it is possible achieve higher strength and modulus properties when compared to the two other methods.

3.3.3. High speed spinning

Mezghani et al. (1998) used high speed spinning with non-medical grade PLLA. They used a spinning pump (233^{o}C) and a nozzle with 4 holes (single orifice diameter 0.762 mm). The fibers were drawn directly from the melt with speeds from 100 to 4700 m/min to produce as-spun fibers with diameters from 14 to 73 μm. Maximum properties obtained were tensile modulus of 6 GPa and break stress 385 MPa. The continuous melt spinning hot drawing process was used on amorphous 92 (wt-%) PLLA + 8 (wt-%) meso-lactide, by Schmack et al. (1999, 2001). The molecular weight of the raw polymer was 207 000 g/mol and viscosity 1.01 dl/g. They used the extruder with the spinning pump, multifilament nozzle with 12 holes, (single hole 0.3 mm) and extruder temperatures of 170 to 185^{o}C. There was no mention on fiber diameters. High speeds in the spinning line with two sets of godets were used. The temperatures of the godets

were 65 and 110°C. The take up speed of the first godet set was 200 m/min and the speed of the second set varied from 800 to 1200 m/min giving a DR from 4 to 6. The high speed spinning of as-spun fibers was also carried out with the same equipment only winding the fiber with speeds of 1000 to 5000 m/min. The thermal degradation decreased the M_w to 180 000 g/mol and i.v. to 0.91 dl/g. For the spin drawn fibers the tensile modulus properties varied from 4.3 (DR 4) to 6.3 (DR 6) GPa and break stress from 211 (DR 4) to 460 (DR 6) MPa. The high speed as-spun fibers had a maximum tensile modulus of 4.2 GPa maximum breaking stress of 328 MPa at the winding speed of 2500 m/min. Schmack et al. (2004) further studied the high speed spinning and different polymer compositions. The maximum properties they achieved with those were a tensile modulus of 6.8 GPa and a breaking stress of 300 MPa.

3.3.4. Sutures

The simplest format for fibers is to use them as monofilaments or bundles of multifilaments that can be twined and/or twisted with themselves or with other fibers to a yarn. For medical purposes the monofilaments can be used as such for suture applications. The suture can also be a braided mono or multifilament. The PLLA and PLA 96 polymers as pure are currently not used as suture materials although studied (Heino et al. 1996, Kangas et al. 2001, Mäkelä et al. 2002), moreover the suture materials include a copolymer of PLLA and PGA (Vicryl®, Vicryl rapide®, and Polysorb™), and of PLLA and PGA/PCL/PTMC (Caprosyn™). The PLA 96 filaments were used to produce triple-stranded bound sutures which were ex vivo studied for suture applications in static and cyclic testing by Viinikainen et al. (2006, 2009). The results showed that the biomechanical properties of the modified Kessler repair performed with PLDLA triple-stranded bound suture exceed the properties of the braided polyester triple-stranded bound suture (Ticron®) repair.

3.4. Textiles

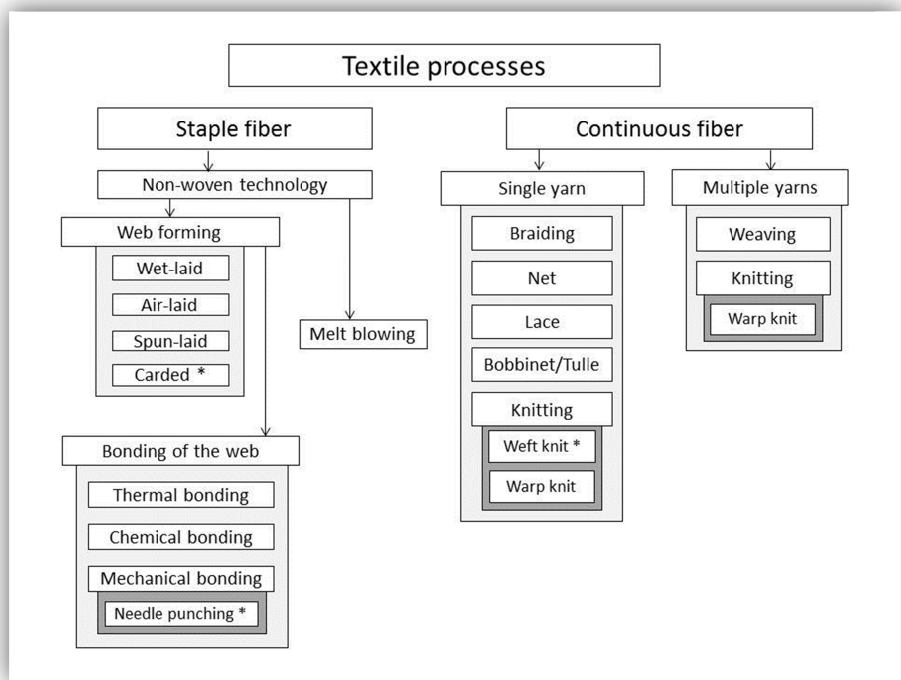

Figure 6. Common methods for continuous and staple fiber fabric manufacturing. The ones used in this thesis are marked with *.

Knitting, braiding, weaving and non-woven manufacturing are the most common methods to form a fabric from fibers (Figure 6). Compared to the weaving which is a fairly simple method, the knitting produces fabrics by inter-looping stitches using knitting needles. The knit forms during the continuous looping process where the fiber is pulled through the previously formed loop to form a new loop. The new forming layer is called course and the length wise running column is called a wale. By altering the needle packs a variety of different knit types can be made (Leong et al. 2000). The braiding is done by intertwining the fibers over and under each other. The fiber spools move in two different opposite running tracks and the braid forms at the top of the spools into an angle determined by parameters. In this technique there are fibers as many as spools used to make it that run lengthwise without forming loops compared to the knit where one continuous fiber makes the fabric. The number of spools, braiding angle, braid type (flat, round), and the dimension can be varied (Ramakrishna & Huang 2003). In the non-woven process the fibers are cut to staple fibers then separated and carded to make a web that is then attach by e.g. needle punching method. There are

other methods for web forming such as wet-laid, spun-laid and air-laid techniques and other attachment methods for the web such as thermal bonding, chemical bonding and mechanical bonding. By melt blowing method it is possible to manufacture non-wovens from the polymer melt. For the TE purposes different properties are needed. The target tissues can be hard, soft, flexible, smooth, or combinations of those since different tissue types exist like bone, soft tissues, tendons, ligaments, and muscles just to mention few. They have a unique 3-D architecture that the support structure, implant, or scaffold should mimic (Hutmacher 2000). By adapting suitable techniques from above mentioned methods the textiles can be used for TE purposes. The fibrous products can possess a variety of 3-D structures and shapes with different permeability parameters that can affect the cell growth and differentiation. It is also possible to manufacture the textiles in a fast and feasible way to produce devices and scaffolds for the TE purposes. The porosity and the interconnectivity of pores that is the most important feature for the TE devices can be taken account when manufacturing the textiles, whereas for some other methods as solvent casting, freeze drying, and supercritical CO_2 that cannot be taken for granted (Wintermantel et al. 1996, Hutmacher 2000, Park & Seo 2011).

3.4.1. Knits for TE

As a result the knitting has been adapted to TE as a manufacturing method and the knitted meshes have been studied for several TE applications. Ligament and tendon studies were performed using silk fibers (Liu et al. 2008) and PLGA 10/90 fibers (3 yarns, 20 filaments/yarn, single filament 25 μm) (Ouyang et al. 2003). Skin studies were performed using knitted PLGA mesh (+ collagen) (Chen et al. 2005) and knitted PLGA-PCL mesh (Ng et al. 2004). Vascular grafts were studied using warp knitted PLA 96 mesh (Koch et al. 2010) and double layered knitted cardiovascular repair patch made of PGA (sheath) and PLLA (core) (Takahashi et al. 2009). Cartilage studies were performed by using PLGA 90/10 knitted mesh with collagen (Dai et al. 2010). Heart valve studies were performed using knitted fibrin-covered PCL (Lieshout et al. 2006). Abdominal wall repair studies from PLLA knit + collagen (Pu et al. 2010). Honkanen et al. (2003) studied the knitted cylindrical PLA 96 scaffolds in vivo for rheumatoid patients to correct the metacarpophalangeal joint. It was reported that a neojoint was formed with these kinds of implants. The longer follow-up study also confirmed the results of the previous study with the knitted circular implants (Honkanen et al. 2010).

The same structure and material was used by Länsman et al. (2006) where they studied the subcutaneously implanted scaffolds in rats. The group noticed that the scaffold was completely filled with connective tissue in three weeks. The pore size differences between the samples had no effect on the tissue ingrowth. The tissue becomes organized into layers of dense connective tissue with thick collagen bundles by the week 48. Waris et al. (2008) reported the 3-year study on the same material and structure in in vivo minipig metacarpophalangeal joint. They also reported the formation of a functional fibrous joint.

3.4.2. Braids for TE

Braiding has been studied for several TE and medical purposes. Incardona et al. (1996) manufactured braids from PLLA fibers supplied by Fambri et al. (1997). They covered the human ligament stiffness range from 0.8 to 6.2 GPa with twisting and braiding. Also for the ligament injury repair purposes Cooper et al. (2005) and Freeman et al. (2007) studied PLGA 90/10 and PLLA as braids, twisted fibers and twisted-braided fibers. The twisted-braided type show good mechanical potential for ACL repair. Similar results were obtained by Lu et al. (2005) as they studied PGA, PLLA and PLGA 82/12 braids. They concluded that when comparing the braids from those fibers the PLLA is the most suitable for ACL repair. For different stenting purposes, braids from biodegradable fibers such as PLLA, PLGA 80/20, and PLA 96 have been studied (Hietala et al. 2001, Nuutinen et al. 2002b, 2003b, Ginsberg et al. 2003, Vaajanen et al. 2003, Laaksovirta et al. 2003, Välimaa & Laaksovirta 2004, Ormiston et al. 2007, Lumiaho et al. 2007).

3.4.3. Non-wovens for TE

The non-wovens were introduced to the science community with a boom when Cao et al. (1997) introduced the “mouse with a human ear on its back”, although the basis for this work started already in 1993 when Langer & Vacanti (1993) studied the PLGA non-wovens scaffolds for cartilage TE. The problem occurring with the non-woven in this study was that the contractive forces were affecting to the implant while healing and this had to be compensated by outer force. Thus the structure itself should be suitable to handle these kinds of forces that occur during the TE healing phase. With the non-wovens this limits the use of the scaffold due to its not so rigid nature. Hutmacher

(2000) stated that non-wovens can only be used for load bearing applications in bioreactor where sufficient support will form when the tissue forms. Sittinger et al. (1994, 1996) studied the PLLA non-woven and came to the results that the homogenous cell distribution was an issue with the non-wovens, since the open structures should be sticky to collect the cells whereas the dense parts cause clotting of the cells. These implications by Hutmacher and Sittinger might have affected the research of the non-wovens. However the PLGA 90/10 fleece was successfully used by the Sittinger group (Rotter et al. 1998) to grow a transplantable chondrocyte–polymer construct in vitro. Perka et al. (2000) studied the PLGA/PDS fleece with fibrin component for bone growth and noticed the cell seeding of pluripotent mesenchymal cells prior to implantation is strongly recommended compared to the fleece without cells. Wu et al. (2007) studied the non-woven for chondrocyte cultivation. They used collagen coated PLGA 90/10 fibers, made from dissembled Vicryl® sutures. Recently the technology and the studies involving traditional non-wovens from synthetic materials have in large extents turned into the side of electrospun non-wovens. The non-wovens manufactured by this method have a submicron to nanometer fiber structure. There are some commercial non-woven products such as from Johnson & Jonhson, The Codman® Ethisorb™ dura patch with a Vicryl fleece and a PDS foil on the other side for dura matter substitution. From the commercial medical non-wovens the Concordia Medical has a product called a Biofelt™ that is produced custom made from PGA, PLLA and PLGA into the shapes of sheets, tubes, and discs. One interesting modern approach using non-woven is reported by Weber et al. (2011) where PGA-P4HB non–woven matrix was used for intracardiac wall defect studies.

3.5. Composites with fibers

The fiber reinforcement of polymer composites is a feasible way to increase the strength, lower the elastic modulus, and increase fatigue resistance. The arrangement of reinforcement fiber and the volume fraction can change the characteristics of the material. The continuous fiber biocomposites can be divided into 2-D and 3-D forms. In 2-D forms the laminates and tape laminates can be found. In the 3-D form the rods, knitted-, braided-, woven-, stitched-, and non-woven composites are the main forms (Ramakrishna et al. 2001, Ramakrishna & Huang 2003, Scholz et al. 2011). Knitted

structures have been studied for manufacturing of composites in various industrial applications. The suitability of knitted reinforcements has been evaluated and it promotes their use in composites (Ramakrishna 1997, Leong et al. 2000, Khondker et al. 2001, Emirhanova & Kavusturan 2008). When comparing the medical fibers in general it can be noticed the biodegradable fibers are weaker compared to the non-degradable fibers. For example the PLLA and PGA 15-25 μm fiber has a tensile strength between the ~ 0.7 to 0.9 GPa whereas for the PTFE (10-12 μm) it is 1.9 GPa for UHMWPE (27 μm) 3.0 GPa, and for Aramid (12 μm) 2.6 GPa (Ramakrishna & Huang 2003). Therefore implants for some applications needing special properties can only be manufactured with non-degradable reinforcement fibers. Yet there are many other applications that benefit from the biodegradable reinforcement which renders the implant completely resorbable.

Kellomäki et al. (2000a, 2000b) used melt-spun 4-ply multifilament yarn from PLA 96 for TE purposes and composite manufacturing. The PLA 70 plate was attached to the knitted mesh tube by compression molding. This composite type showed suitable properties for non-load bearing application in in vitro. P-(ε-CL/L-LA) film was compressed to the sheet to which the knitted mesh tube was spot welded to form a composite. Composite and the knitted mesh were put to in vivo (rabbit paraspinal back muscle). Results showed that the film degraded faster than the mesh. The mesh permitted the tissue ingrowth in to the composite. The group noticed that the composite can be used if guided TE is needed with occlusive film. If only cell ingrowth is needed the mesh is suitable by itself. Ouyang et al. (2005) knitted three 20 filament PLLA yarns (diameter of single filament 25 μm). The knit was the rolled with cultured bone marrow stromal cell sheet. They incubated it for 4 weeks under 4 % strain. No conclusive results were obtained but according to the reports the technique and concept holds a promise.

The PLA was used a reinforcement in the composite implants. The lumbar fusion with a composite implant constructed of PLA 96 knitted fibers + bioglass/PLA 70 matrix + elastic nucleus of 1000PEOT70PBT30 was studied in vivo (mini pigs). After 15 weeks in vivo the ossification occurred (Palmgren et al. 2003). The spinal cage implants by Huttunen et al. (2006) adapted the use of PLA 96 filaments in their composite. They manufactured the fiber reinforcement by braiding the PLA 96 fibers. By using the braid as a fiber reinforcement in the P(L/DL)LA 70/30 + matrix, they increased the impact

strength of the pure polymer by 127 % and of the polymer with 30 % β-TCP filler by 215 %. To the compressive yield strength the fiber reinforcement had no influence. Guarino et al. (2008) used PLLA fibers as reinforcement in a PCL matrix. The composite tube was manufactured by filament winding, phase separation, and salt leaching. Preliminary results were promising after 5-week cell studies.

4. Surface modifications for TE purposes

The purpose of the polymer surface modification is to give the polymer surface a suitable function to meet the target requirements, to alter its behavior, and/or to render the polymer more hydrophilic/hydrophobic. By modifying the surface properties it is possible to make the target cells or proteins more adherent or prevent the adhesion, thus increasing its biocompatibility and bio-functionality.

4.1. Physical treatments

The plasma, gaseous mixture of oppositely charged particles containing neutral atoms and molecules, radicals, and UV photons, can be used as thermal and non-thermal plasma. With thermal plasma, high temperatures are involved and it is not suitable for materials that are sensitive to heat. The non-thermal plasma known as cold plasma contains low temperature ions and is not degrading or damaging the heat sensitive materials, therefore it can be used for medical biodegradable polymers. The cold plasma has a mixture of reactive species that can have an effect on the surface thus it can be used e.g. for plasma treatment and etching. Morent et al. (2011) reviewed the plasma treatments and found that when using cold plasmas from H_2, air, N_2, NH_3, oxygen- and nitrogen containing functionalities similar polar hydrophilic groups are respectively formed on to the polymer surface. The plasma treatments are mainly applied to increase the surface energy but due to the recovery of the surfaces the results obtained are not permanent. Various gases were studied by Wan et al. (2003). They studied the effect of the N_2, O_2, NH_3, and Ar plasma on PLLA film. All the plasma treatments decreased the contact angle thus increasing the hydrophilicity of the surface. The NH_3 plasma treated samples obtained the appropriate hydrophilicity and surface energy with high polar component compared to other gases. The same group continued the studies with the NH_3 plasma for the salt leached freeze dried PLLA scaffolds having a thickness of 4.0 mm. They found that the treatment can modify the surface but it degrades the PLLA. While the degradation was increased in the surface where they noticed a M_w loss of 36 % with the energy of 20 W and 48 % with 50 W, it was not affecting the scaffold inside where only minor M_w changes were occurring at the thicknesses of 1-3 mm. The cell

proliferation to the scaffold was induced and integrity best remained with the energy of 20 W, treatment time of 30 min, and pressure of 30 Pa. Khorasani et al. (2009) studied the CO_2 plasma on solvent cast PLLA sheets and found that it promotes the fibroblast adhesion and growth.

Other methods briefly worth mentioning, that induce bio-functionality into the polymer, are the coating of the biodegradable polymers by another substrate, surface modification by grafting, and mechanical methods to alter the surface topography. The 3,4-dihydroxyphenethylamine (dopamine) coated electro-spun PLLA fibers induced the cell spreading, proliferation, and osteogenic differentiation of the hMSCs (Rim et al. 2012). The hydrophilicity and osteogenic activity was increased with PLLA-poly(ethyl ethylene phosphate) copolymer coated PLLA (Yang et al. 2009). Knitted PLGA 90/10 scaffolds coated with PLCL solution to mimic the cell microenvironment was studied by Vaquette et al. (2010).

4.2. Chemical treatments

The wet chemical treatments have been studied for surface chemistry alteration on polyesters. Although useful, these methods might lead to a faster degradation behavior and loss of mechanical properties. One such chemical used is a NaOH. The fibers from PGA were treated with 1 N NaOH that changes ester groups to carboxylic acid and hydroxyl groups on PGA surfaces. The fiber diameter decreases during the treatment according to the treatment time whereas the molecular weight, crystallinity and thermal properties were not affected. The smooth muscle cell seeding density was doubled compared to the untreated PGA (Gao et al. 1998). The use of chemicals to alter the surface roughness to increase its functionality has been studied. The NaOH treatment on PLGA 50/50 polymer was used to increase porosity and surface area. Compared to the non-treated PLGA it enhanced the smooth muscle cell (Miller et al. 2004) and chondrocyte functions (Park et al. 2005). The KOH was used on PLLA and PLGA 50/50 with neuronal cells, but there was no increase in the cell number for treated PLLA samples. The treatment on the other hand decreased the PLLA contact angle according to the treatment concentration thus increasing the hydrophilicity. For the PLGA there was noticed a biological level cell density, although the cells formed colonies with only few axons and for all concentrations live cells per unite area decreased. In this study the poly-D-lysine used as a control showed the best results (Nisbet et al. 2006).

5. Aims of the study

The aims of the present study were to find answers to the following question.

1. How to melt spin biodegradable P(L/D)LA 96/4 polymers? How the molecular weight and viscosity of the raw material affect the melt spinning parameters and how this is related to the fiber properties and degradation behavior in vitro? (I, III)

2. How the melt spinning parameters affect the thermal degradation and monomer accumulation of P(L/D)LA 96/4 polymer fibers and how the monomer accumulation during melt spinning affects the in vitro degradation? (II, III)

3. How the knitting parameters affect the mechanical properties, degradation, and shelf-life behavior of the P(L/D)LA 96/4 knits? (IV)

4. What is the degradation correlation between the in vitro and in vivo testing and how does the mechanical behavior of scaffolds change due to the tissue ingrowth? (IV)

5. How to manufacture scaffolds for cell culturing purposes, intervertebral disc studies, and temporomandibular joint studies? What is the function of fibers in each application? Do the fiber manufacturing methods enable sufficient mechanical properties for the scaffold/device? (V-VII)

6. How can the surface properties of non-wovens be modified and does this have an influence on the cell distribution and spreading? (V)

6. Materials and methods

6.1. Materials

The following materials were used in this study. For a material a roman number indicates a publication where it was used. Inherent viscosities shown below are measured by the manufacturer.

Polymers:

1. P(L/D)LA 96/4, Poly(L-lactide-co-D-lactide) (96/4), medical grade, PURAC biochem bv, Gorinchem, the Netherlands. Inherent viscosities reported by the manufacturer data sheet.
    a. Inherent viscosity of ~ 1.70 dl/g (VII)
    b. Inherent viscosity of ~ 2.18 dl/g (III)
    c. Inherent viscosity of ~ 4.18 and 4.21 dl/g (VI, unpublished results)
    d. Inherent viscosity of ~ 4.80 dl/g (III,VII)
    e. Inherent viscosity of ~ 5.48 dl/g (II , IV, V, VI, unpublished results)
    f. Inherent viscosity of ~ 6.30 dl/g (III)
2. P(L/DL)LA 70/30, Poly(L-lactide-co-D,L-lactide) (70/30) RESOMER® LR 708, medical grade, inherent viscosity of ~ 6.1 dl/g. Boehringer Ingelheim GmbH, Ingelheim am Rhein, Germany. (IV,VI, VII)
3. Poly-L-lactide (BIOFIX screws / intramedullary nail / pin), Bionx Implants Oy, (currently Conmed Linvatec Biomaterials Oy Ltd.) Tampere, Finland. (VI)
4. 1000PEOT70PBT30 (segmented block copolymer of poly(ethylene oxide terephtalate)/poly(butylene terephtalate) with PEOT/PBT ratio being 70/30), Polyactive®, IsoTis BV, Bilthoven, The Netherlands (currently Integra, New Jersey, USA) Acronym PACT (VI)

Bioceramic:

1. Bioactive glass 13-93 particles (consisting of 6 wt-% Na_2O, 12 wt-% K_2O, 5 wt-% MgO, 20 wt-% CaO, 4 wt-% P_2O_5 and 53 wt-% SiO_2) Vivoxid Oy, Turku, Finland. Acronym BG (VI)

6.2. Processing and manufacturing

6.2.1. Manufacturing of the fibers (I - VII)

Prior the melt spinning all the P(L/D)LA 96/4 polymer batches were dried in the vacuum oven in 100°C (heating gradient of 1°C/min) for 16 hours after which the temperature was gradually lowered to the room temperature. After the drying the polymers were removed from the oven under a N_2 atmosphere and further placed in to the hopper again under a N_2 atmosphere. The fiber manufacturing line was a continuous melt spinning hot-drawing unit with a single screw extruder combined with an orientation line. All the fibers were manufactured using a single screw micro extruder with screw diameter of 12 mm and L/D 24:1 by Gimac (Gimac, Gastronno, Italy). The compression ratio of the screw was 1:1.237. The extruder had six heating zones, the first three for the barrel, two for melt mixing and stabilizing, and one for the spinneret. The polymer melt temperature and the melt pressure was measured from the zone 5. Two methods for orientating the fibers were used. They were either, hot drawn using caterpillars and ovens or drawn by high-speed spinning machine using an induction heated godets. Different spinnerets and orientation parameters were used for fiber manufacturing and the information is gathered in to Appendix 1A and B. The residence time was measured as a minimum time it takes for a polymer pass through the extruder at a chosen screw speed.

6.2.2. Manufacturing of the BG + PACT composite rod (VI)

The crushed and milled bioactive glass 13-93 particles were sieved to the particle distribution of 50-125 μm. Polymer was dried in the vacuum oven in 80°C (heating gradient of 1°C/min) for 48 hours. The 1000PEOT70PBT30 copolymer was mixed in the Gimac microextruder with bioactive glass particles. Both the polymer and the polymer/glass composition were separately extruded through a Ø 3 mm round die. The average diameter of the produced rod was 3.7 mm. The average glass content was calculated on the basis of burning tests by removing the polymer and weighing the

remaining glass. The average glass content of the composite was 23 wt-%. The rods were cut to the lengths of 5 mm.

6.2.3. Manufacturing of the plate preform (VII)

The polymer was dried similarly as for the fiber manufacturing but 80^{o}C was the drying temperature for a poly(L/DL)lactide 70/30 polymer. Gimac microextruder was used for processing. The polymer was extruded through a 30 x 0.5 mm flat die after which it was drawn from the melt using a caterpillar to a continuous strip with dimensions of 10 x 0.16 mm.

6.2.4. Manufacturing of the non-wovens (V, VII)

Melt-spun P(L/D)LA 96/4 fibers were cut to staple fibers length of 60 mm. Staple fibers were separated and a pre-mat was manufactured using a carding machine. The mat was needle punched to non-woven mat. For the publication VII the non-woven was used as such and the thickness of the mat was 1.0 to 2.0 mm. The picture of the non-woven can be found in Appendix 2. For the publication V the non-woven thickness of 3.0 - 4.0 mm was also compressed in 85^{o}C between the 1.0 mm restrictors so that the final thickness of the mat was ~1.0 mm.

6.2.5. Manufacturing of the single jersey knits (IV, VI, VII)

For the publication IV, both P(L/D)LA 96/4 multifilament yarn batches were knitted to a tubular single jersey knit using a circular knitting machine equipped with a ½" needle cylinder (Elha R-1S, Textilmaschinenfabrik Harry Lucas GmbH, Neumünster, Germany). Parameters in the process were the number of the latch needles and the loop size (knit height). Knits were cut to samples of 70 mm in length each and the ends were heat sealed to prevent the loop running. For the publication VI 8-filament fiber was knitted and for or the publication VII The 4-filaments yarn was repeated to make a 12-filament yarn.

6.2.6. Manufacturing of the cylindrical scaffolds (IV)

For the publication IV the cylindrical scaffolds were manufactured from the 4-filament or 8-filament P(L/D)LA 96/4 yarn. The knits were cut to a size according to the requested size of the ready scaffold and rolled to the cylindrical shape. The end of the knit was fixed to the roll with a biodegradable "glue" prepared by dissolving poly(L/DL)lactide 70/30 polymer into acetone. Scaffolds were heat-treated at 70^{o}C / 15 min in a mould for the desired shape. Picture of the cylindrical scaffold can be found in Appendix 2.

6.2.7. Manufacturing of the intervertebral implant (VI)

The intervertebral (IVD) implant was a combination of the following components: rods (PACT /+ BG), P(L/D)LA 96/4 knit and the matrix constituent. The matrix material was a mixture of 15 wt-% of medical grade poly(L/DL)lactide 70/30 and 85 wt-% of bioactive glass 13-93. The polymer was dissolved in acetone (ratio of the polymer/acetone was 2 g / 30 ml) and the bioactive glass was mixed to it to form a paste-like mixture. The paste was thoroughly spread on to the knit. The combination of knit and matrix was rolled around PACT /+ BG composite rods that formed the elastic core of the implant. The implant was heat-treated in a mold at 80^{o}C for 1 h, cooled down to room temperature and removed from the mold. Similarly was manufactured the reference implants, by adding one component at a time for each set. This resulted in nine reference sets. Picture of the cylindrical composite implant can be found in Appendix 2.

6.2.8. Manufacturing of the temporomandibular joint implant (VII)

Two types of temporomandibular joint (TMJ) implant were manufactured. The P(L/DL)LA 70/30 plate + P(L/D)LA 96/4 non-woven implant and P(L/DL)LA 70/30 plate + P(L/D)LA 96/4 knit implant. For the plate + non-woven the continuous strip was cut to 10 x 60 mm pieces as well as the non-woven mat. The mat was placed on the strip and using ultrasonic-welding machine the edges of the two materials were welded/fused together. From this preform, 5 x 7 mm samples were cut. These were the final

dimension of the implant. The picture of the non-woven + plate implant can be found from Appendix 2. For the plate + knit implant the continuous strip was cut to 10 x 60 mm pieces. The knit was cut to 60 mm pieces and compression molded in 80^{o}C and 2 MPa pressure, to give the knit a flat outlook. The compressed knit and the plate were ultrasonically welded together from the edges. After this the 5 x 7 mm samples were cut from the preform.

6.2.9. Surface treatments (V)

To remove any impurities caused by needle punching and carding, ethanol washing of fabrics, mentioned in 6.2.4, was performed prior to other treatments for a period of 2 x 20 min in ultrasound wash. The samples were dried in a vacuum at room temperature. Samples were named as non-woven ethanol washed (NW E), non-woven compressed ethanol washed (NWP E), non-woven compressed KOH treated (NWP KOH) and non-woven compressed plasma treated (NWP Plasma). Plasma treatment was carried on to the plain fibers and the non-woven scaffolds. Low-temperature plasma was applied using Plasma Prep 5 instrumentation (GaLa instrumente, Bad Schmalmach, Germany). The chamber was evacuated three times, adding oxygen between evacuations and finally the atmosphere was allowed to settle at 10 Pa. Frequency of 200 kHz was applied for defined periods of time from 0 to 300 s, with power settings of 50 W, 70 W and 100 W. After plasma treatment, the oxygen atmosphere was held for an additional 5 minutes after which the samples were placed in airtight bags. To modulate the surface properties of the fibers and the non-woven fabrics, the samples were subjected to alkaline hydrolysis at room temperature using 2.5 M KOH in a solution of methanol 50 vol. % / water 50 vol. % for time periods of 5, 20, 60 and 240 minutes. After hydrolysis the samples were dried in a laminar flow hood for 2 days.

6.3. Characterization

6.3.1. Viscosity and molecular weight measurements (II, III, IV, V, VI)

Weight average molecular weight (M_w), number average molecular weight (M_n), and the inherent viscosity (i.v.) of the raw materials and produced fibers were determined by

size exclusion chromatography (SEC) using a gel permeation chromatography device (GPC) (Waters, Milford MA, USA).) The polydispersity (PD) was calculated as the M_w/M_n ratio. Two parallel 150 ml samples with concentration of 0.1 mass-%, diluted in chloroform, were injected at a flow rate of 1.0 ml/min. The columns used for exclusion were a 5-µm PL-gel Guard pre-column and two 5-µm PL-gel mixed-C columns (Polymer Laboratories, Amherst, USA). The detector (Waters 410 RI Differential Refractometer Detector), pump (Waters M515 HPLC-Pump), and auto sampler (Waters 717P plus Auto sampler) were used (Waters, Milford MA, USA). Universal Calibration was obtained for P(L/D)LA 96/4 ($k = 5.45*10^{-4}$ dl/g, $\alpha = 0.73$), and mean values of results were used. The used standards were narrow polystyrene standards. Two measurements were made for each of the data points. Due to the nature of analytical techniques the significant difference between molecular weight values was chosen to be ± 1000 Da. The samples (III) were collected form the screw pitches by halting the process and rapidly exerting the screw on to the air cooling unit.

The viscosities of the three polymers (III) were measured at temperatures of 220-250 ^oC using a rotational rheometer (Physica MCR-301, Anton Paar Ostfilder, Germany). Plate-plate geometry, diameter of 25 mm and a gap size of 1 mm, was used. Three parallel samples were measured.

6.3.2. Thermal characterization (II, IV, V, VI)

Differential scanning calorimeters (DSC) Perkin Elmer Pyris 1(II, IV) (Perkin Elmer, Norwalk, CT, USA), Perkin Elmer DSC7 (VI) (Perkin Elmer, Norwalk, CT, USA) and TA instruments Q1000 (V) (TA instruments, New Castle, DE, USA) were used for thermal characterization. Samples were heated from 20^{o}C to 220^{o}C at a rate of 20^{o}C/min, and after a rapid cooling, the heating procedure was repeated. Glass transition temperatures (T_g) were determined from the second heating cycle. Melting temperatures (T_m) were determined from the melting peak of the first heating cycle, and the crystallinity (X_c) of the samples was determined from the melting enthalpy using 93.7 J/g (Fisher et al. 1973) as the melting endotherm of 100 % Poly(L-lactide). Indium was used as a standard calibration material. Two measurements were made for each of the data points. If the results either in T_g or T_m differed more than 1^{o}C between the

samples a third sample was analyzed. The publication III thermal measurements were done only once.

6.3.3. Lactide monomer characterization (II, III)

The lactide monomer content of fibers was measured using a gas chromatograph (Thermo Finnigan, Trace GC, Autosampler 3000, MA, USA), equipped with a 25m x 0.32 mm i.d WCOT fused filica Cp-Sil 43 CB Varian chrompack capillary column. A Flame Ionisation Detector (FID) was used for detection. Two parallel samples were used.

6.3.4. In vitro characterization (II - VI)

Two different buffer solutions were used to incubate the samples, phosphate buffered saline (PBS, 3.48 g/dm^3 Na_2HPO_4 - 0.755 g/dm^3 NaH_2PO_4 - 5.9 g/dm^3 NaCl) (II, III, IV, V, VI) and simulated body fluid (SBF) (Filgueiras et al. 1993) (IV). The incubation times varied among the sets the maximum being 48 weeks. Temperature during the incubation was held at 36.5^{o}C and the pH at 7.4 ± 0.2. The buffer solution was changed fortnightly and the pH measured at 21^{o}C.

6.3.5. In vivo characterization (IV)

Thirty-two Sprague-Dawley male rats 16-19 weeks old (mean 17), were operated on. The site of incision was shaved and then sterilized with chlorohexidin. In each rat, four Ø15 mm cylindrical P(L/D)LA 96/4 scaffolds were implanted in pockets that were dissected in the dorsal subcutaneous tissue. The implants were fixed in place using two non-absorbable, polyamide stitches (Dermalon® 4-0). The skin was then closed using non-absorbable similar polyamide sutures. The study periods were 3, 12, 24, 48, and 52 weeks. After the sacrifice samples were prepared by removing the external connective tissue formed outside the scaffold. The tissue grown into porous scaffold and the scaffold itself was left untouched. Samples were placed in the saline and tested within 24 hours from sacrifice.

6.3.6. Mechanical characterization (II - VII)

All the tensile tests were run on Instron materials testing machine (Instron 4411 Materials Testing Machine, Instron Ltd., High Wycombe, England). All the tensile properties on fibers were tested with gauge length of 50 mm, 500 N load cell and with a crosshead speed of 30 mm / min. Five or more parallel samples were used for fiber testing. The knits were tested with gauge length of 20 mm. The non-woven (V) tensile test parameters were 100 mm / min testing speed and 40 mm gauge length. For the non-woven testing, tear test samples (70 mm x 40 mm with a cut of 50 mm long in the middle of the shorter edge) were used. All the 0-week samples were tested wet. Three parallel samples were used for non-woven testing.

The compression properties of the cylindrical scaffolds (IV) were tested using a Lloyd LR 30K Materials Testing Machine (Lloyd Instruments Ltd, Fareham, England). Crosshead speed was 1 mm / min. Specimens were compressed between polished stainless steel plated and 5 N preload was applied to minimize the influence of rough surfaces of the scaffolds after which the new zero/starting point was set. The scaffolds were tested until 2 mm extension was reached (50-67 % thickness change). Initial compression results were measured on dry specimens. After hydrolysis the wet specimens were tested. Three to four parallel samples were used. For in vivo the specimens were tested as wet and with the ingrown tissue. Five parallel in vivo samples were used for testing. Cylindrical composite implants (VI) were compressed up to 9.3 kN. Three parallel samples were used.

7. Results

7.1. Polymer processing and melt spinning (II, III, V)

7.1.1. Influence of the initial polymer on fiber molecular properties

All the polymer batches were measured for molecular properties and those will be used instead of the ones reported by the manufacturer. During the melt spinning process the polymer is subjected to thermal degradation due to the heat. The amount of degradation under this heat is also governed by the polymer residence time in the extruder. The amount of heat correlated to fiber quality in such way that the temperatures shown are the lowest possible temperatures that gave a good quality fiber with the used setup. If the raw material has a low molecular weight and i.v. (here 100 kDa and 2.30 dl/g) there is change neither in M_w nor in i.v. after the melt spinning (Figures 7 & 8). By increasing the initial M_w to 220 kDa (with i.v. of 4.14 dl/g), we can observe a clear drop in the molecular properties of the polymer. There is a 36 % drop in the M_w and 28 % drop in the viscosity when the nozzle temperature is 250^{o}C. The increase in nozzle temperature by 7^{o}C results to 45 % and 36 % drop in M_w and i.v. respectively. Further increase to 266^{o}C in temperature results to M_w drop of 48 % but this drop had no effect on the viscosity. When the M_w of the raw polymer is 270 kDa there is a drop of 50 % in M_w and 34 % in i.v. caused by the melt spinning. Further increasing temperature and polymer M_w to 350 kDa (i.v. 5.00 dl/g) results in a 63 % drop in M_w and 43 % drop in i.v. after the spinning. For the other high M_w 350 kDa polymers (i.v 5.47 dl/g) the data shows a decrease from 47 to 62 % in M_w. This data reveals that the actual M_w and i.v. drop is more when the starting values are high. The molecular properties are closer after melt processing. The average M_w and i.v. of all melt-spun fibers was 140 ± 22 kDa and 3.05 ± 0.44 dl/g. This leveling of molecular properties could mean that the polymer thermally brakes down as it needs to achieve the required viscosity level so that good quality fiber can be produced.

When the melt-spun fibers were subjected to 25 kGy gamma irradiation it was noticed that the M_w decreased minimum 71 % and maximum 78%. The i.v. decrease of the polymer fibers after gamma irradiation was lower compared to M_w changes, varying from 62 to 70 %. The irradiation even more leveled the properties since the average M_w and i.v. of all gamma irradiated fibers was 35 ± 5 kDa and 1.03 ± 0.12 dl/g.

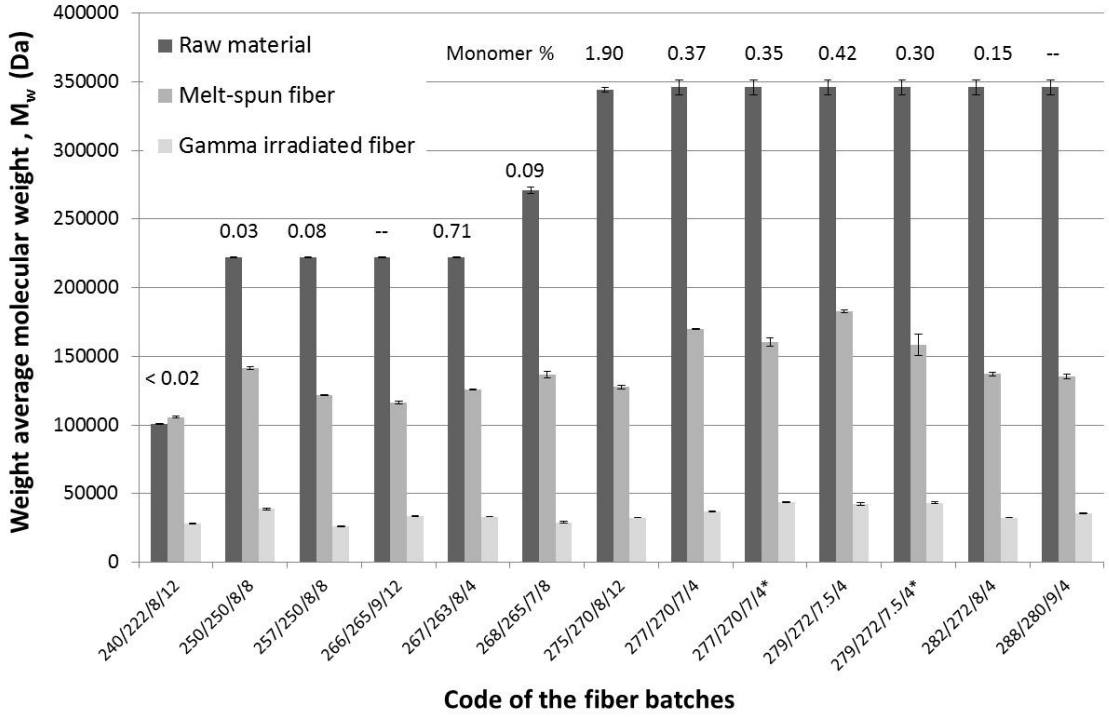

Figure 7. M_w drop and monomer accumulation of P(L/D)LA 96/4 polymer due to the melt spinning and irradiation (average results of n = 2 with standard deviation bars).

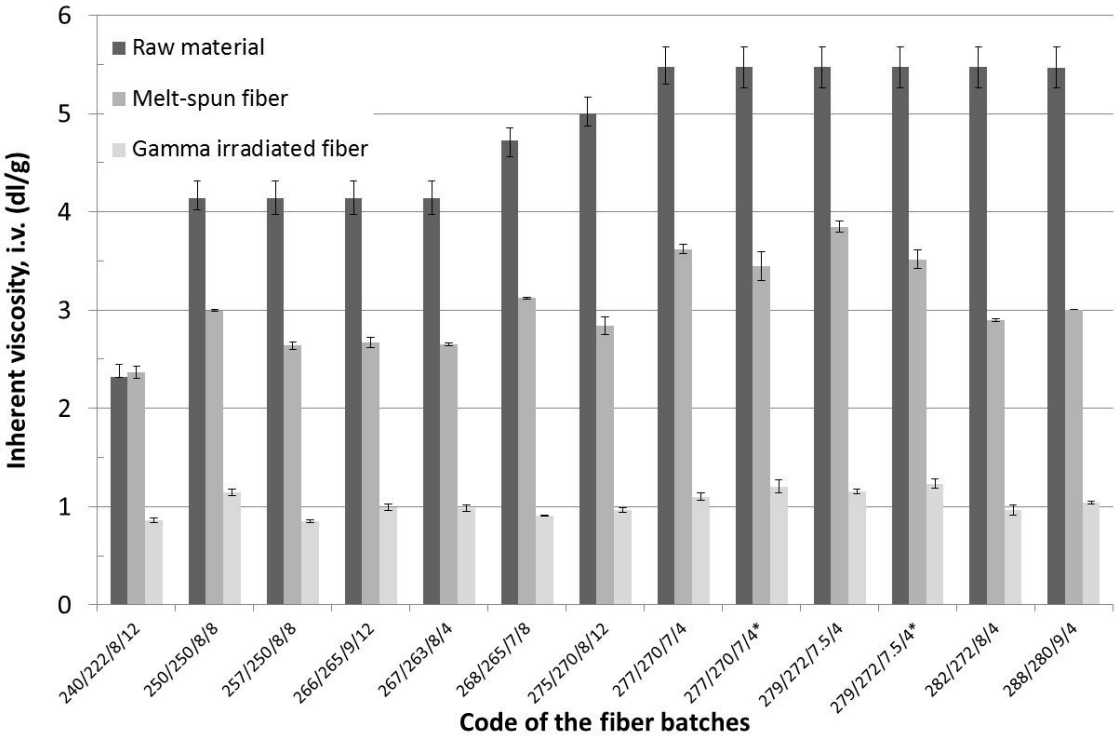

Figure 8. I.v. drop of P(L/D)LA 96/4 polymer due to the melt spinning and irradiation (average results of n = 2 with standard deviation bars).

The highest starting polydispersity (PD) (Figure 9), compared to the other polymers with an exception of 100 kDa polymer, was measured for the 270 kDa (i.v. 4.73 dl/g) polymer batch. The PD showed a minor decrease, after melt spinning, only for the 100 kDa. With a rise in M_w this suggests that there is minor polymerization occurring while processing but the fact that the polymer was purified makes this virtually impossible and the M_w is more or less within error range of GPC. For other batches there was an increase in PD. For most of the samples it was from 5 to 16 % but increases of 23, 27, 20 and 19 % were noticed for polymers processed at nozzle temperatures of 266, 268, 275 and 279^{o}C respectively. Gamma irradiation had no major effect on the PD. Two bigger changes were noticed, an increase of 11 % for the 257^{o}C batch and a decrease of 22 % for the 268^{o}C batch. The increase of the PD was probably due to the polymer degradation that increased the number of shorter polymer chains in the material.

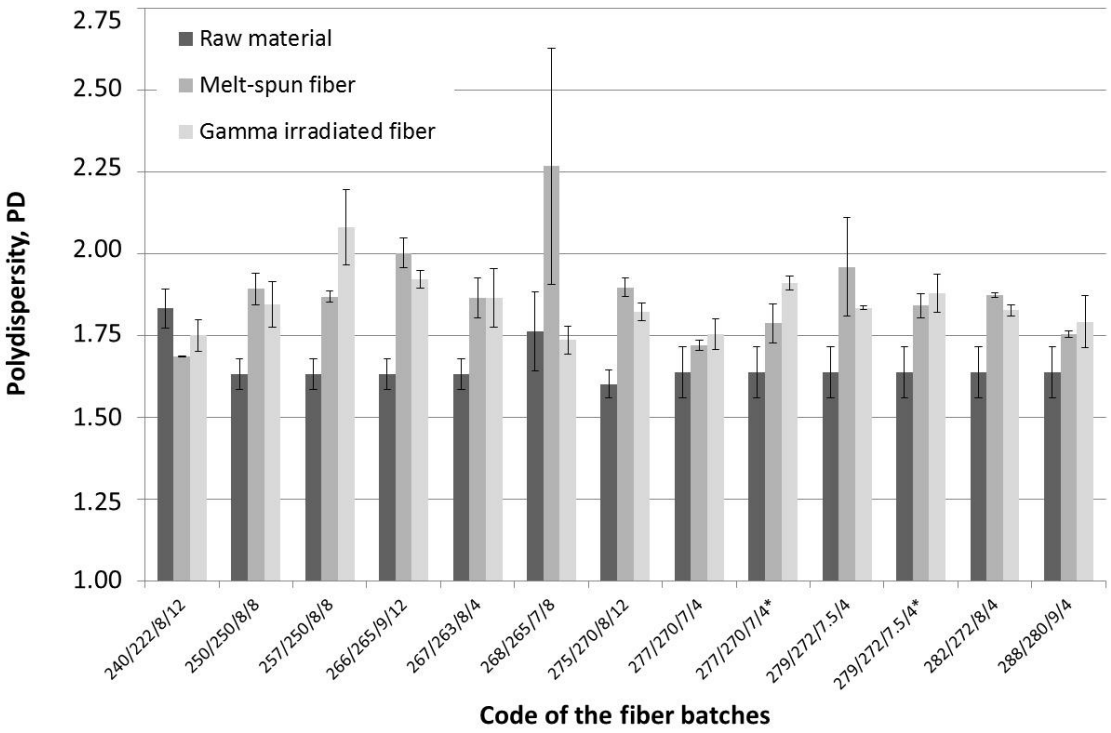

Figure 9. PD of P(L/D)LA 96/4 polymer before and after the melt spinning process and the following irradiation (average results of n = 2 with standard deviation bars).

We tried to determine where the most of the degradation happens during the melt spinning process regarding our equipment. On the basis of the tests we can pinpoint some steps during the process. Considering the extruder barrel and the screw (Figure

10) we found out that a drop in the molecular weight can already be seen in the first part of the screw closer to the transition zone, perhaps in the interphase between the feeding and transition zones. For the higher molecular weight polymer there is a major drop also in the transition zone. But when comparing the results to the final fiber molecular weight we can notice for the 350 kDa polymer the major drop of 55 % happens in the barrel but for the 270 kDa only 27 % drop happens in the barrel. So the following zones, where the melt pressure is measured and in the nozzle zone, the 270 kDa polymer lost 23 % of its molecular weight whereas the 350 kDa polymer lost only 4 % of its original molecular weight, although the melt temperatures were 265 and 270^{o}C respectively. In comparison, the 100 kDa polymer showed no thermal degradation during the process. This implies that for the higher M_w polymers the shear stress induced by the higher viscosity, together with the friction induced temperature rise, increases the degradation.

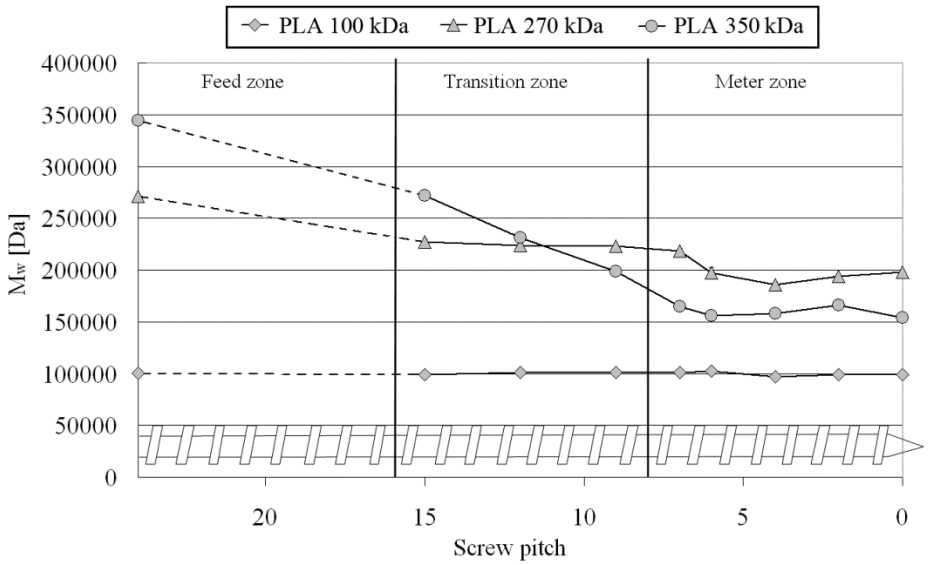

Figure 10. M_w of P(L/D)LA 96/4 polymer during the melt spinning process, a schematic picture of the degradation in the extruder barrel. (Modified from Publication III)

The shear rate in the beginning of the transition zone (pitch 15) was 2.49 1/s (7 rpm) and 2.84 1/s (8 rpm). The shear rate for the metering zone, where the flight depth was constant and smallest, was 3.17 1/s (7 rpm) and 3.63 1/s (8 rpm). The metering zone shear rates were used for rotational rheometer studies (Figure 4-6, Publication III) that suggested that there were high shear stresses for the 270 and 350 kDa polymers in the processing temperatures that probably caused the degradation. The degradation

stabilization in the metering zone is probably due to the reduced viscosity at the transition zone which further reduces the shear stress in the metering zone.

7.1.2. Influence of the initial P(L/D)LA 96/4 on thermal properties

The changes in the thermal properties are shown in Table 4. The peak melting temperature (T_m) increases or decreases due to the melt processing but after the gamma irradiation the T_m always decreases resulting to a value lower than the raw material T_m, with the exception of 240/222 fiber. For this batch the T_m increases from 156 to 159^{o}C after processing but undergoes no change due to the irradiation. For all other batches the gamma irradiated fiber T_m is at the range of 152-155^{o}C.

Table 4. Thermal characterization data of polymers, fibers and gamma irradiated fibers.

	Melt temperature T_m (^{o}C)	**Melting enthalpy** ΔH_f (J/g)	**Glass transition temperature** T_g (^{o}C)	**Recrystallization enthalpy** ΔH_c (J/g)
Raw material	**155.6**	**34.2**	**59.8**	**0**
240/222/8/12				
Extruded fiber	158.5	31.2	60.0	0
Gamma irradiated fiber	159.1	30.4	60.1	6.3
Raw material	**166.2**	**38.8**	**61.9**	**0**
266/265/9/12				
Extruded fiber	154.5	35.1	59.3	0
Gamma irradiated fiber	152.6	41.7	57.9	5.4
267/263/8/4				
Extruded fiber	155.5	33.0	58.9	0
Gamma irradiated fiber	153.1	41.7	57.1	2.7
Raw material	**159.5**	**39.9**	**59.5**	**0**
268/265/7/8				
Extruded fiber	162.8	32.0	60.5	0
Gamma irradiated fiber	154.4	38.6	58.4	5.8
Raw material	**161.2**	**37.7**	**59.3**	
275/270/8/12				
Extruded fiber	154.8	25.0	56.8	0
Gamma irradiated fiber	152.6	35.2	55.0	4.5
Raw material	**165.9**	**42.0**	**61.9**	**0**
277/270/7/4				
Extruded fiber	155.7	31.3	60.3	0
Gamma irradiated fiber	154.8	35.2	59.0	1.9
277/270/7/4*				
Extruded fiber	150.8	27.3	59.9	0
Gamma irradiated fiber	154.7	33.3	57.6	1.3
279/272/7.5/4				
Extruded fiber	152.2	29.9	60.0	0
Gamma irradiated fiber	154.6	30.9	57.8	1.1
279/272/7.5/4*				
Extruded fiber	149.0	29.1	60.0	0
Gamma irradiated fiber	154.9	34.3	58.9	1.2
288/280/9/4				
Extruded fiber	152.8	28.1	60.6	0
Gamma irradiated fiber	155.7	35.8	58.4	2.6

There is a drop in the melting enthalpy (ΔH_f) for all the fiber batches due to the processing. The minimum decrease is 9 % (for 240/222) and the maximum decrease is 35 % (for 277/270*). And for all the fiber batches, with the exception of 240/222, the gamma irradiation increases the melting enthalpy (crystallinity). The glass transition temperature (T_g) is also affected due to the processing, but not that much due to the gamma irradiation. Neither processing nor irradiation has an effect on the T_g of the 240/222 batch. For other fiber batches the T_g decreases to a level of 57 to 59^oC, with the exception of 275/270 batch, that has a T_g of 55^oC after the gamma irradiation. The gamma irradiation also has an effect on the recrystallization capability of the polymer. Only after the irradiation we can observe the recrystallization in the P(L/D)LA 96/4 polymer. This is probably due to recrystallization due to the smaller chains that were produced during the random main chain cleavage.

7.1.3. Influence of the screw speed and residence time on thermal degradation and fiber diameter

During the polymer processing the screw speed determines the residence time the polymer has in the extruder. The more time the material spends in the extruder, the more time it has for the thermal degradation. Although less screw speed also results to lower shear forces and increasing the screw speed increases the shear. In the Figure 11 we can see that the residence time has almost a linear correlation to the molecular weight. As the residence time increases the molecular weight of the P(L/D)LA 96/4 drops. When rpm 9 is compared to the raw material (350 kDa) there is a 47-48 % reduction in M_w, for the rpm 5 there is 55 % and for the rpm 3 there is 64 % decrease in M_w. If the starting temperature values are set to T1 (nozzle 277^oC, measuring zone 270^oC) the influence of the residence time (330 s) to the total molecular weight decrease in this context is 16 %. Similar situation is with the T2 (nozzle 282^oC, measuring zone 275^oC) where the influence of the residence time (330 s) to the total molecular weight decrease is 13 %.

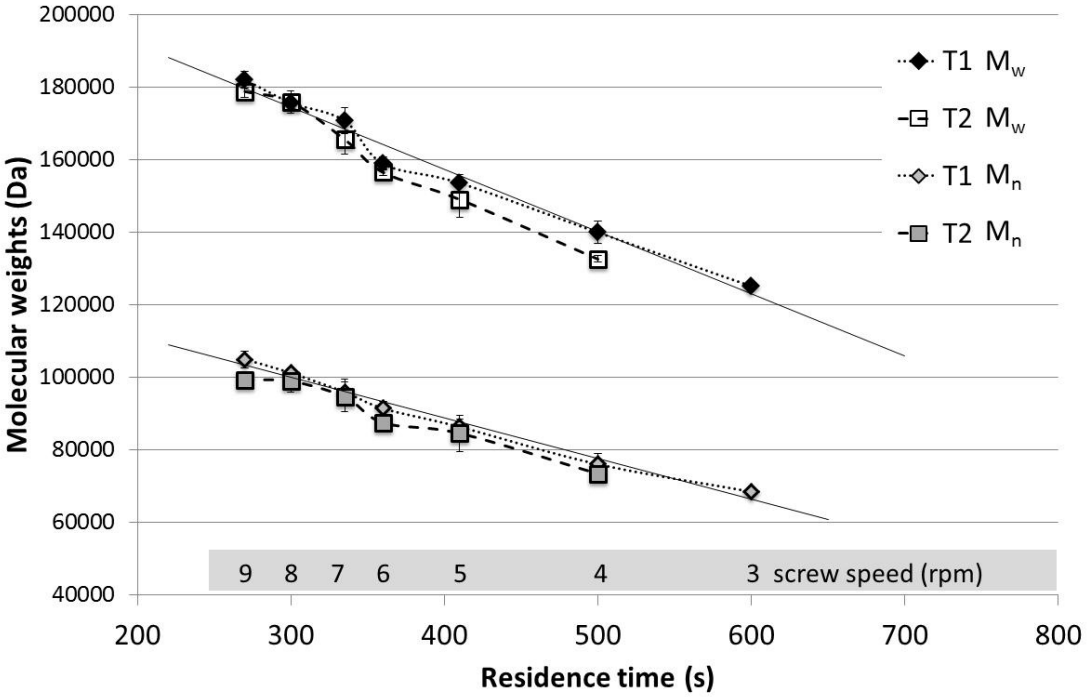

Figure 11. Molecular weight decrease in correlation to the residence time and screw speed of P(L/D)LA 96/4 with raw material M_w of 350 kDa, in temperatures T1 (nozzle 277°C, measuring zone 270°C) and T2 (nozzle 282°C, measuring zone 275°C). (Average results of n = 2 with error bars)

The screw speed has an effect on the final fiber diameter by controlling the material output volume. We can notice a correlation to this as the single fiber diameter decreases when the screw speed decreases (Publication II, Figure 1). Considering the change in the fiber volume for the T1 we can calculate the stepwise volume changes of 11, 18, 9, 17, 23 and 30 % for every screw speed 8, 7, 6, 5, 4 and 3 rpm, respectively, compared after each speed change. There is no correlation between the used temperature profiles and the fiber diameter.

7.1.4. Influence of the screw speed and temperature on monomer accumulation

When studying the process induced monomer, we noticed that in the process the residence time is one variable the other being the temperature (Publication II, Figure 6). When the residence time increases, it has a linear type correlation to the monomer content. As the residence time increases the monomer content increases. When the temperature increases from T1 to T2 the slope of the graph (monomer vs. residence time) increases. We can also see a stepwise increase in the monomer content when the temperature is increased from T1 to T2. As the molecular weight drops the monomer content increases but we can notice that there is no correlation between a particular fiber M_w and fiber monomer content (Publication II, Figure 4). It is noticeable that for chosen monomer content the difference between the T1 and T2 remains at a level of 16 ± 4 kDa. Then again, for a chosen M_w level the difference between the T1 and T2 is gradually increasing. For M_w of 17, 15, and 14 kDa the monomer content differences between the T1 and T2 are 0.18, 0.26 and 0.33 wt-%.

When studying the correlations between the processing parameters and the properties the similar processing conditions, molecular weight, and monomer content has to be evaluated. The 350 kDa (i.v. 5.47 dl/g) materials shown here are chosen since the material is the same that is used in "publication II, Figure 6". By plotting the values from these batches into the graph (publication II, Figure 6) we can study the correlations in question (Figure 12). We found some correlation between the different batches. When the temperatures were the same the single data points gave 0.1 wt-% higher monomer content values and similar or lower M_w values. When the temperatures between the T1 and T2 were studied there was only one good correlative data point regarding the monomer content and this was the 279/272 point. Otherwise similar 0.1 wt-% error regarding the monomer was noticed for the other data points but no correlation when the M_w was compared. For the 282/272 data point there was no correlation and the results were contradictory.

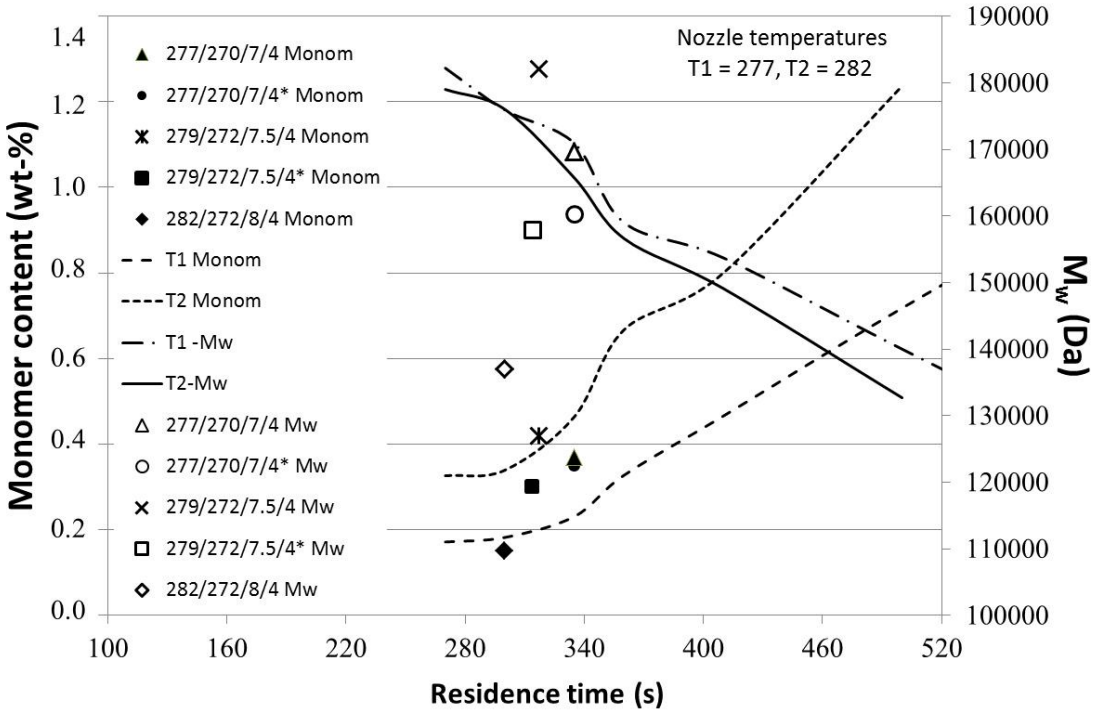

Figure 12. Monomer content and M_w curves plotted from publication II. Points plotted from other tests to find out if there is a correlation between the publication II results and similar other tests. (Modified from Publication II, Figure 6)

7.1.5. Influence of irradiation on fiber strength retention

The strength retention due to the gamma irradiation can be seen in Figure 13. The 25 kGy gamma irradiation caused from 15 to 44 % decrease in the tensile strength compared to the non-irradiated fiber. The higher decrease in strength due to gamma irradiation between the fiber batches did not correlate with a higher decrease or increase of either M_w or M_n during the irradiation. There was no correlation to the PD either when this data was evaluated against the molecular data.

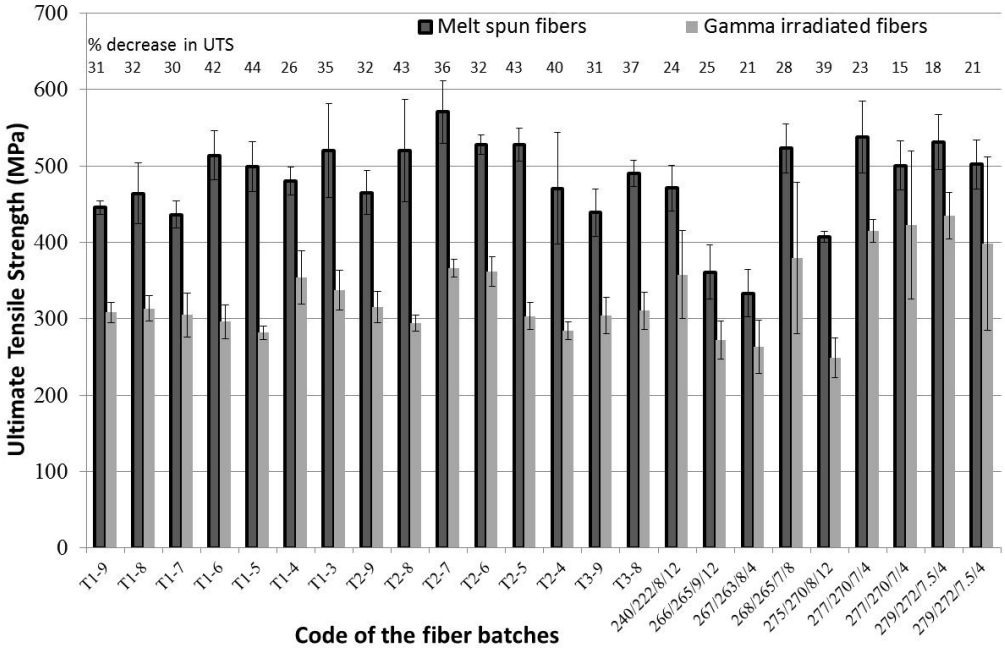

Figure 13. Ultimate tensile strength of the fibers plotted before and after γ-irradiation. (Average results of n = 5 with standard deviation bars) (Modified from Publication II, Figure 2)

7.2. Knit properties (IV, VII)

7.2.6. Influence of the knitting parameters

The knit manufacturing parameters affected the mechanical properties of the tubular single jersey knits (Figure 14 & publication IV, Table 3). The strain properties varied from 33 to 44 %. The loop size has an effect on the strain although the strain for 4-filament knits decreases and for 8-filament knits increases when the loop size decreases. When the number of needles increases, the strain increases. The half loop values were calculated to give a comparison to the similar non-knitted yarn, since half of the loop corresponds to the yarn with the same amount of filaments that were used in the knit. The load per half loop values showed similar results for all the 8-filament knits but for 4-filament small loop knits the values were 24 to 34 % lower than of the knit with big loop. This indicates that the smaller amount of filaments has a greater influence on the knitting properties. This can also be seen as the loop size correlation. The less there are filaments, the greater difference between the small and big loop size. As for the knit break load the same tendency can be seen. The 8-filament knit break loads are similar

whether small or big loops are used whereas the break load for the 4-filament knit is affect by a loop size. The bigger loop correlates to a stronger half loop strength between the similar yarn knits. As expected the break load and strength increases when the amount of fibers are increased and when the amount of needles in increased in the needle bed. The actual fiber break load decreases ~ 66 % after knitting, when compared to the half loop break load.

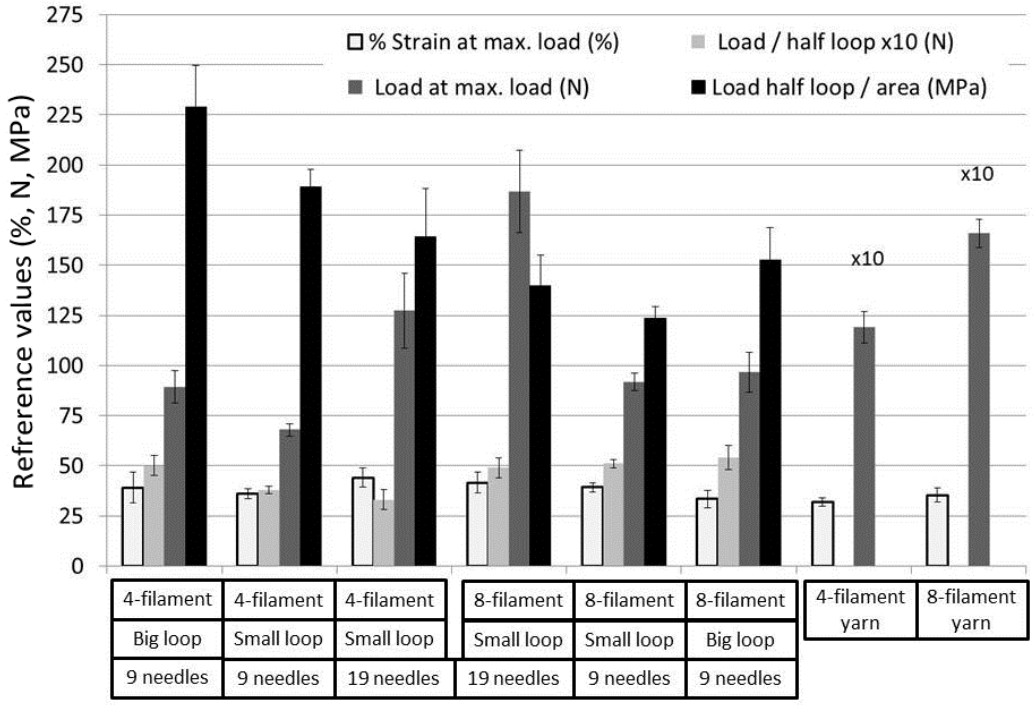

Figure 14. Knit properties for different gamma irradiated knits. (Average results of n=5 with standard deviation bars)

7.2.7. Influence of the welding on mechanical properties

When the P(L/D)LA 96/4 knit and the non-woven is ultrasonically welded to a PLDLA 70/30 plate there is a drop in the properties of the fibers and the non-wovens in the weld joint (Figure 15). In the test situation it was always the fiber or the non-woven that broke, the plate remained unbroken. The reference fiber yield load was 4.4 N as for the fiber-plate weld it was 0.8 N, this was also the maximum tensile load obtained for the fiber-plate weld. For a comparison the maximum break load obtained for the reference fiber was 12.6 N. For a reference non-woven the obtained yield load was 6.3 N as for the non-woven-plate weld it was 2.3 N. The maximum tensile load for the non-woven was 18.6 N and for the weld it was 6.4 N. The non-woven fibers distributed the damage

among the number of filament whereas in the case of 4 filaments there were only 4-filaments to distribute the damage due to the welding.

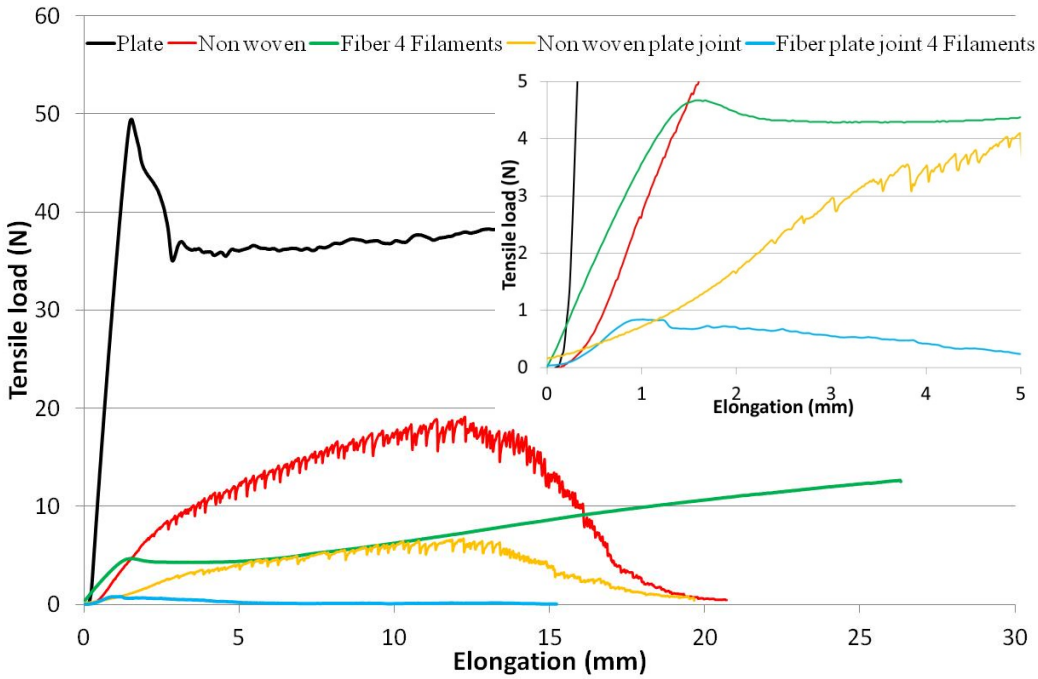

Figure 15. Average tensile plot for materials and their ultrasonic weld seems

The difference between the two different types of weld seams can be observed in Figure 16. The uniform layer, that is the weld seam, is formed in both cases. The welding process pushes up the plate weld sides due to the retractive forces of the fabrics. In the case of the non-woven, the filaments on top of the seam can be recognized although from the plate side they are fused together with the plate. The same structure cannot be noticed when using the knits. The thicker knit filaments needed more energy during the welding to make a proper weld seam. Therefore the knit was totally fused with the plate thus the fibers cannot be observed from the weld seam neither with SEM nor with optical microscope (Figure 16 B). But with the polarized light the fusion zone can clearly be observed since the scattering light (dispersed color scheme Figure 16 C) disappears at the points where the fusion is complete. There is disturbance in the plate matrix due to the welding and mainly due to the filaments pushing into the plate and this can be seen as a zone next to the filament. The heat accumulating in the welding also makes the ends of the filaments swell from the point when exiting the plate.

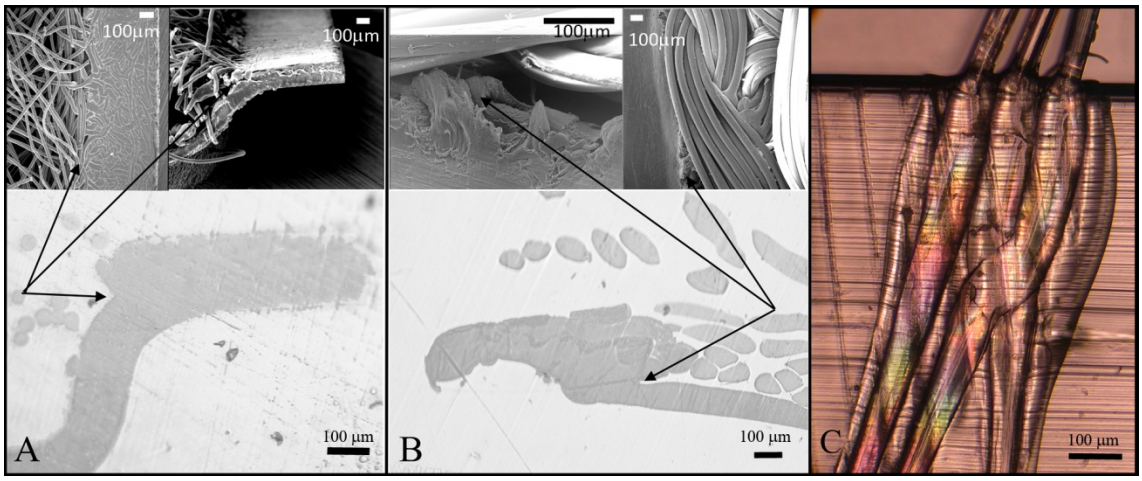

Figure 16. A) Non-woven-plate weld seam, B) knit-plate weld seam and C) polarized microscope picture showing the weld seam for the single filaments used in the tensile testing. Starting point of the weld seam is marked with arrows.

7.3. Scaffold properties (VI)

7.3.8. Cylindrical composite scaffolds for IVD studies

The different compositions of the composite scaffolds were compression tested (Figures 17 & 18). The load/distance curve was plotted since the calculation on the composite area was not feasible. The softness of the P(L/D)LA 96/4 knit alone can be seen as a reduced amount of load required to compress the scaffold. In the case of the knit/polymer scaffold the construct is strong and rigid compared to the other composites. When introducing an inner core to the scaffold the compression load decreases. It makes no difference to the mechanical properties to of those samples, whether there are BG particles embedded in the polymer matrix or not. Then again, the inner core material has an impact. The PACT+BG core seems to increase the mechanical properties. This may result from a better attachment of the rod to the knit by the matrix polymer due to the glass particles.

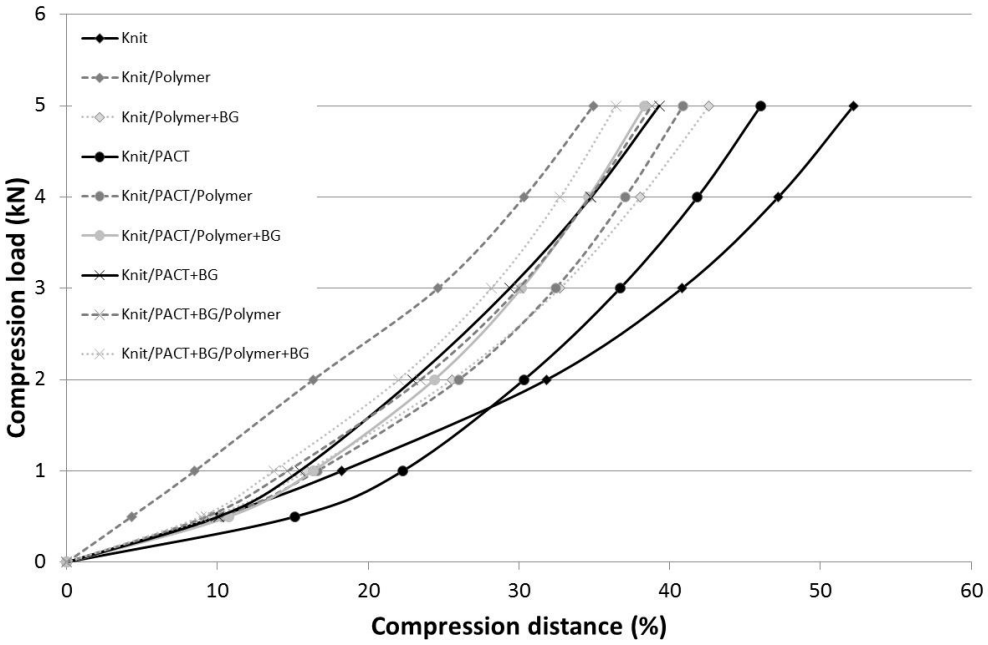

Figure 17. Cylindrical composite scaffolds. Variations between the different composite structures under compression testing (Average of n=3).

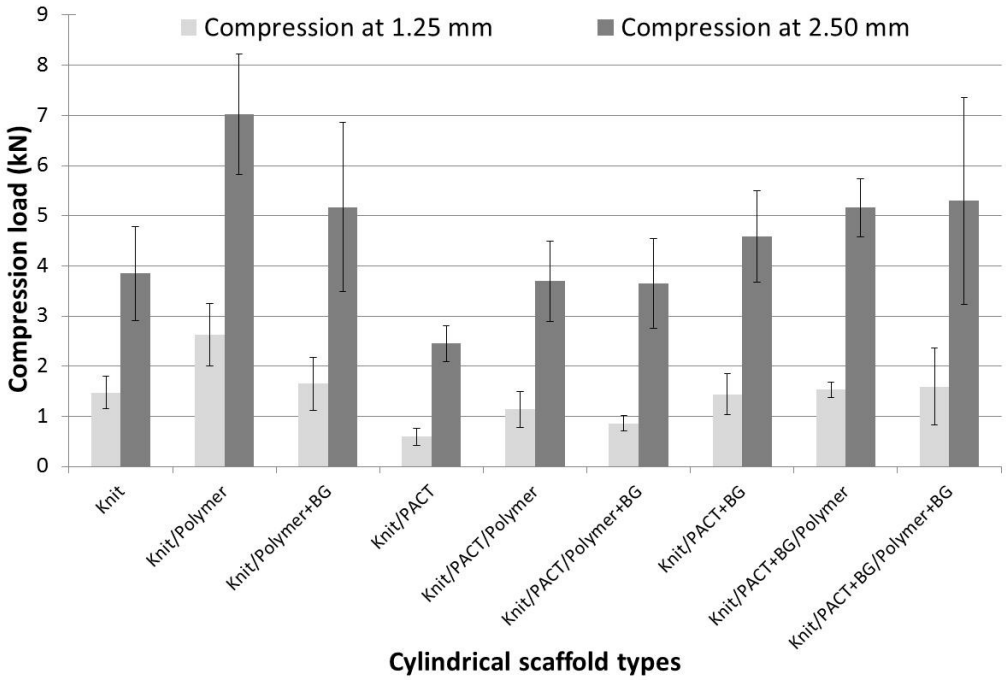

Figure 18. Comparison between the selected compression distances with different composite scaffold. (Average values of n = 3 with standard deviation bars)

7.4. Influence of the surface modifications (V)

7.4.9. Fiber molecular properties and thermal properties

Effect of surface treatment methods on molecular and thermal properties of P(L/D)LA 96/4 fibers were evaluated (Publication V, Table 4). When the fiber is subjected to oxygen plasma treatment there is no considerable change in the M_n, M_w or i.v. properties. In the case of KOH treatment we can see an average drop of 12 % in M_n and 4% M_w in 5 min treatment. Thermal properties of the fibers remained unchanged apart from the crystallinity in the case of KOH treatment. The crystallinity changes according to the treatment time from 26 to 31 to 44 % with 5, 20 and 60 min treatment times. The KOH 60 minute treatment time was the limit since the longer treatment times resulted in higher dissolution of the fiber and it could not be used. The 5 minutes at 50 W and 3 minutes at 70 W were the treatment limits in the case of the oxygen plasma treatment for the fiber. The 70 W power was also the highest that could be used. The effect of the heat can be noticed from the Figure 19.

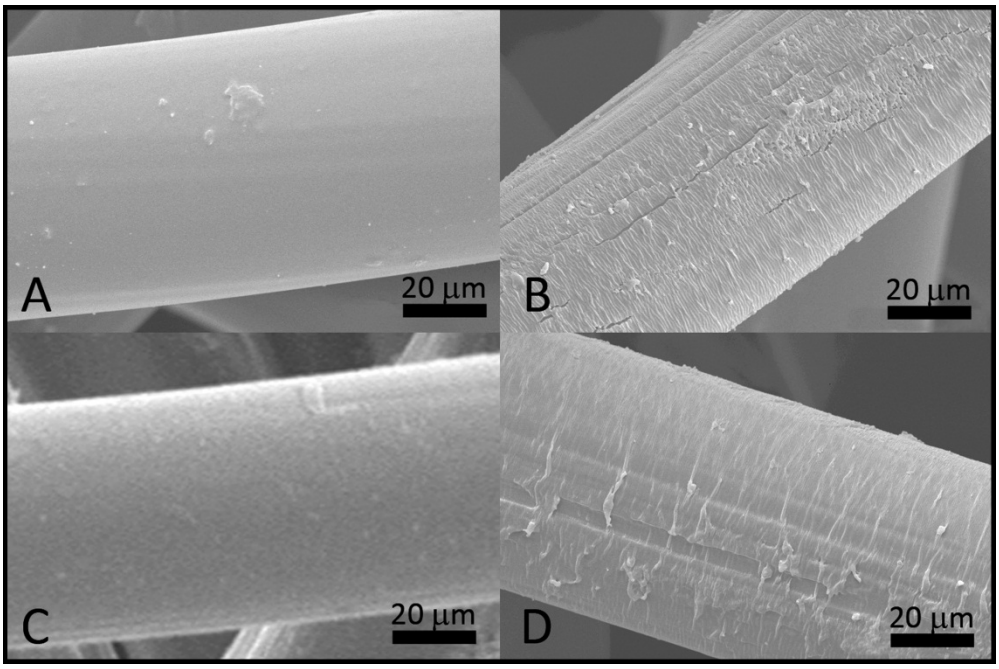

Figure 19. SEM pictures from the P(L/D)LA 96/4 fiber surfaces. Untreated fiber (A), oxygen plasma treated fiber 50 W 5 min (B), KOH treated fiber 5 min (C) and oxygen plasma treated fiber 70 W 2 min (D).

There are folds accumulating into the surface of the fibers due to shrinkage when oxygen plasma is applied. The plasma also causes the cracking of the surface in the fiber direction. With higher energies and prolonged treatment times the heat accumulating into the chamber destroyed the fiber structure.

7.4.10. Mechanical properties

The oxygen plasma treatment affects the mechanical properties of P(L/D)LA 96/4 fibers (Figure 20). The point where the change occurs is for the 50 W the 3 minute mark and for the 70 W the 2 minute mark. The yield point decreases ~0.7-1.0 N and the elongation increases substantially according to the treatment time from that point onwards. For the KOH treated fibers there is no change in tensile properties for 5 minute treatment. The 20 minute treatment lowers the yield load 20 % and break load 10 % as for the 60 minute treatment time the decrease in yield load is 41 % and in break load 35 %. The KOH treatment had no effect on the elongation properties since there was a reduction of volume from the surface that did not affect the fiber properties inside the fiber.

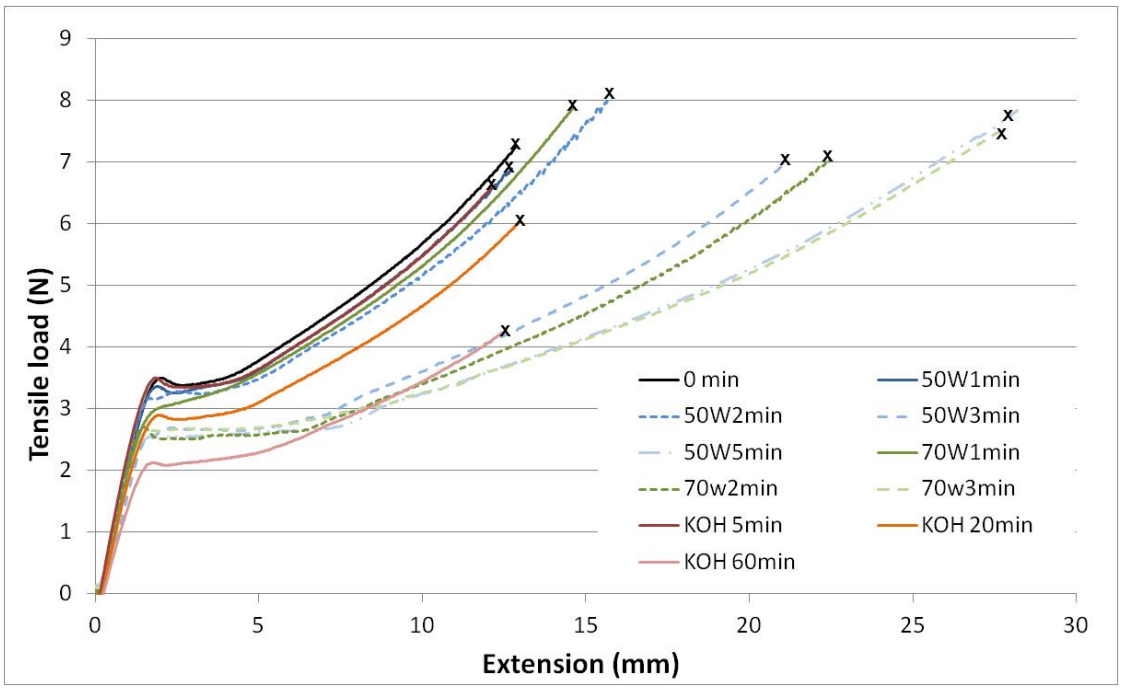

Figure 20. Behavior of modified fibers during tensile testing. (Average plot from n=5)

The surface treatments had an effect on the fiber thickness (Publication V, Figure 4). Due to its chemical nature the KOH treatment dissolved the fiber surface according to the treatment time. In 60 minutes we can observe a ~15 μm decrease in fiber diameter. For the plasma treated fibers the vacuum chamber heats up resulting in an increase in fiber diameter due to the stress relaxation behavior of molecule chains. The 70 W 3 minute treatment increases the diameter by ~11 μm but the 50 W 5 minute treatment increases the diameter only ~4 μm.

7.4.11. Non-woven properties

The different surface treatment methods were investigated for the non-woven samples. It was noticed (Publication V, Figure 5 & Table 6) that the ethanol treatment increases the rapid water intake by factor of three. After vacuum drying of the ethanol treated samples the increase was still 230 % compared to the non-treated non-woven. When vacuum dried ethanol treated samples were compared to the non-vacuumed samples there was a 10 % decrease in rapid water uptake. A different behavior is seen when the non-woven was compressed an average of 70 % from its original thickness, to a thickness of 1 mm. The rapid water intake capability decreased ~ 20 % due to the compression. The ethanol treatment for the compressed non-woven increased the rapid water uptake only 13 %. The vacuum drying after ethanol treatment resulted in 45 % decrease compared to the non-treated. As for the oxygen plasma treated compressed non-woven samples, there was an increase of 115 % and for the KOH treated there was an increase of 70 % in rapid water uptake. The contact angle measurements gave verification to these phenomena since there is no wetting with the control and ethanol treated vacuum dried samples compared to ethanol, plasma and KOH treated samples.

7.5. Hydrolytic degradation: Mechanical properties (II - VI)

7.5.1. Fibers

The tensile strength of the P(L/D)LA 96/4 fiber batches can be seen in Figure 21. The degradation of the 1.90 wt-% monomer fiber batch clearly showed a rapid degradation compared to other batches. For the fibers 277/270, 277/270*, 279/272 and 279/272* there was no cooling unit attached which was seen as higher strength during the first weeks of the hydrolysis. For most of the samples the 28-week time point seemed to be the last time point where the samples could be tested. The only batch that could be tested after 28 weeks was the 240/222 fiber which had monomer content under the detection limit.

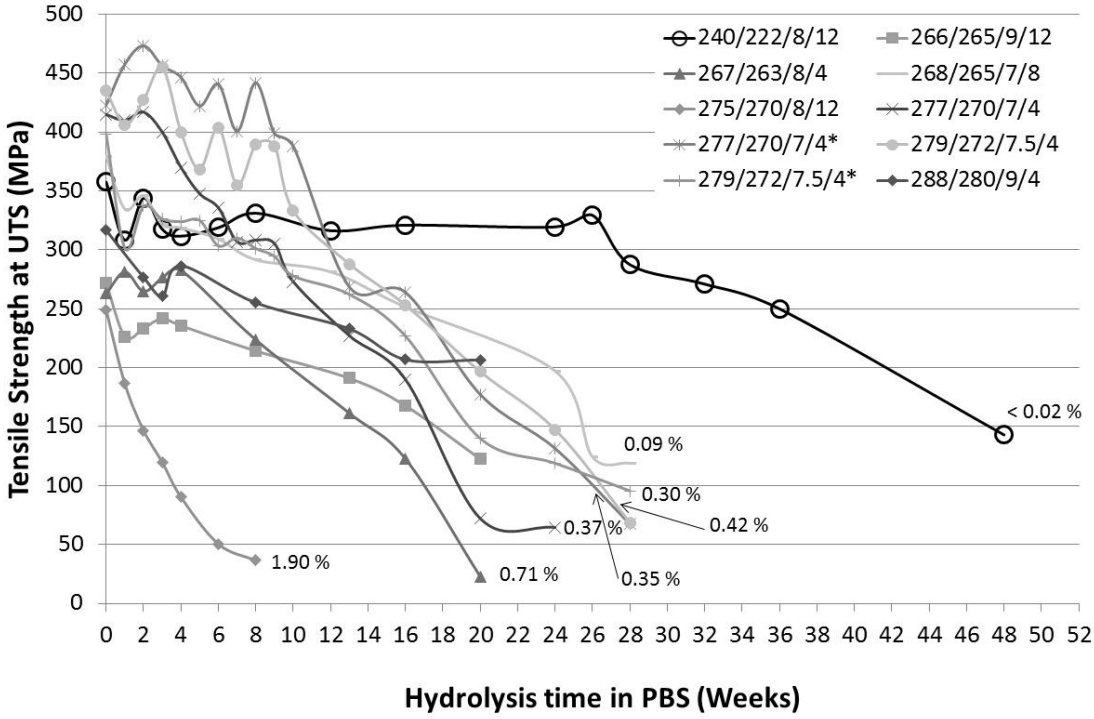

Figure 21. Stress at the point of ultimate tensile strength plotted against incubation time for gamma irradiated fibers (average results of n=5). Monomer wt-% shown after the set where available.

The load needed to break the P(L/D)LA 96/4 fiber bundle can be seen in Figure 22. The three fibers having the greater break load after irradiation are the two 12-filament fiber batches and the 8-filament fiber batch. The third 12-filament fiber batch had less than

50 % lower break load that that of the other two. The 4-filament fibers had average break loads from 6 to 9 N.

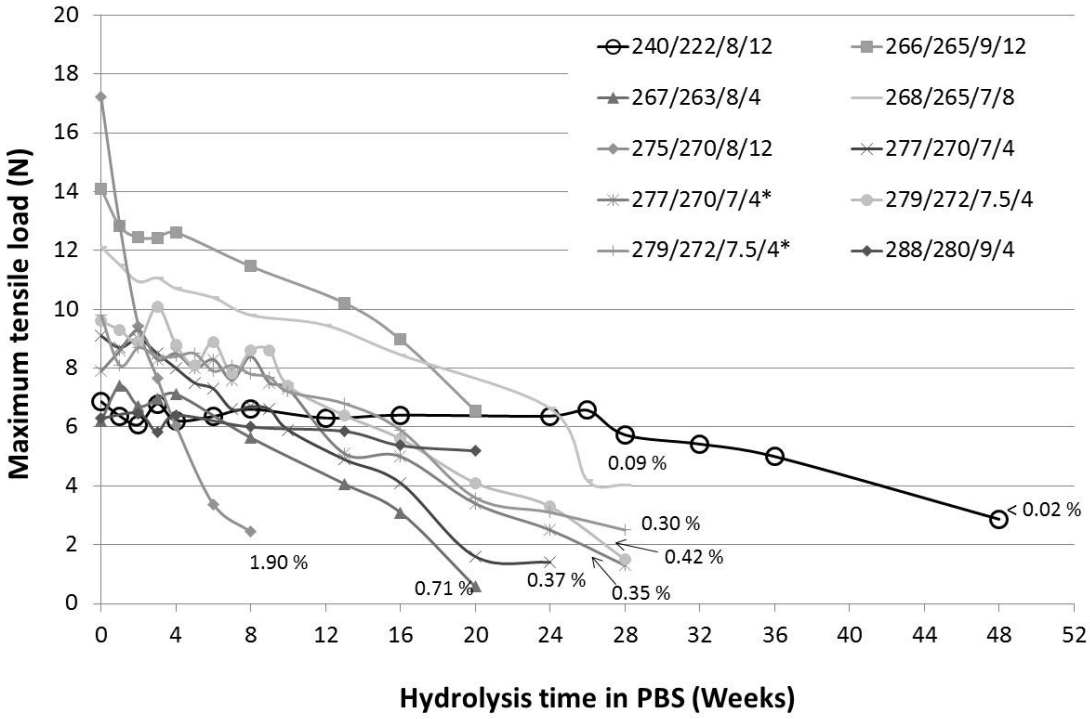

Figure 22. Load at the point of break plotted against incubation time for gamma irradiated fibers (average results of n=5). Monomer wt-% shown after the set where available.

Based on the degradation profile of the fibers with different amount of monomer (Publication II, Figure 7) we can notice that fibers with different monomer contents behaved differently during the 10-week incubation. If the monomer amount was an average of 0.2 wt-% or less there was no specific changes in the degradation profile. When there was an average of 0.3 wt-% monomer we could already see a 10 % drop in the tensile strength. When the monomer amount in the fiber increased to an average of 0.5 wt-% there was a drop from 8 to 40 % from initial tensile strength after 10-week incubation. The most drastic drop was noticed when the amount of process induced monomer was from 0.8 to 1.2 wt-%. Those fibers had a 40 to 60 % decrease in tensile strength after 10-week hydrolysis when compared to the values prior the hydrolysis.

7.5.2. Knits: Hydrolysis studies

The 19-needle 4-filament knits retained their load over the 100 N for 9 weeks and 8-filament knits for 18 weeks. For both fiber types the degradation speeds up as after those time points (Publication IV, Figure 3). For the 9-needle knits the behavior was similar. After 9 weeks the 9-needle 8-filament knits lost 15 % of mechanical properties whereas the 9-needle 4-filament knit lost as much as 30 %. The small and big loop size behaved similarly during the hydrolysis. When studying the strength properties during the hydrolysis of the knits, the fiber showed to be more meaningful parameter than the knitting parameters. The strength decrease profile was different between the fiber batches but rather same for different knitting parameters (Publication IV, Figure 4). The 4-filament knits degrade faster than the 8-filament knits. The 8 filament knits sustained their strength until week 15 or 18 after which it decreased rapidly until week 26. The 4-filament knits sustained their strength until week-9 after which it decreased rapidly until week 22.

7.5.3. Knits: Shelf-life studies

The mechanical properties during the 3-year shelf-life studies were measured and the data can be seen in (Publication IV, Table 4). Little variation can be found from the mechanical data. All the series 3 year data points are within the 0 to 10 % margin compared to the 0 year time point, with only three exceptions. Some results even show an increase in the mechanical values.

7.5.4. Cylindrical knitted scaffolds: Hydrolysis and in vivo

When comparing the 1-week samples the 19 mm scaffold is the most softest having 80 to 84 % less mechanical support when compared to the 12 and 15 mm scaffolds respectively (Publication IV, Figure 7). The 12 and 15 mm samples show similar behavior during the 1-week compression. The hydrolysis results for the cylindrical knitted scaffolds show a decrease in the compression properties already after week 1 for all the sizes. At 12 weeks and onwards, the implanted 15 mm scaffolds tested with ingrown tissue were stiffer than the references incubated in PBS.

7.5.5. Cylindrical composite scaffolds: Hydrolysis

As the samples were tested wet the inner core of PACT swelled up. Approximately 0 to 2 kN compression is only the compression due to the PACT core. The cylindrical composite scaffolds show that during the incubation the compressive strain behavior follows a similar trend throughout the load scheme (Figure 23) and the scaffolds get softer until week 6. Between the weeks 6 and 12 the hardening of the composite scaffold increases thus lowering the compressive strain. The faster degrading core also had an effect on the hardening behavior. The decrease in compressive strain continued until the week 15 (the end of the hydrolysis). Although the data (Publication VI) suggests that the 0 to 2 kN compression is due to the PACT + BG core the change in compressive strain is also seen at higher loads.

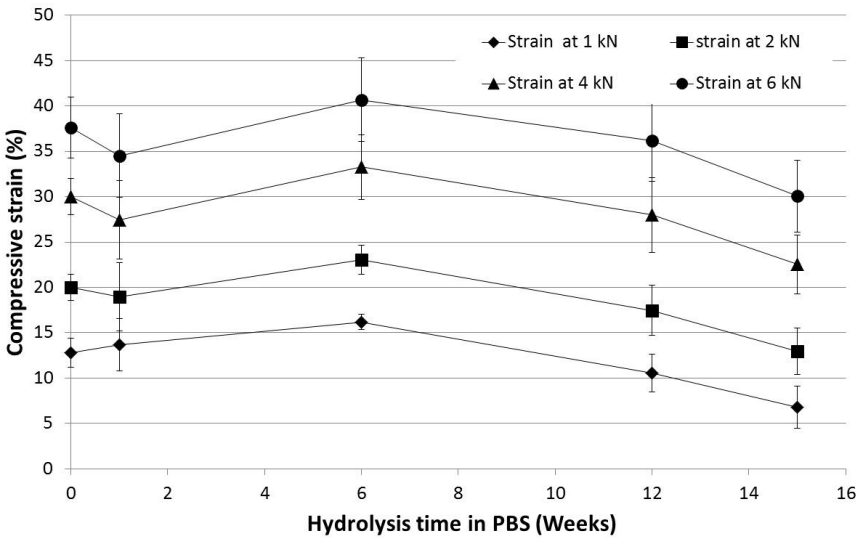

Figure 23. Cylindrical composite scaffold in vitro compressive strain variations due to the incubation. (Average results of n=5 with standard deviation bars)

7.5.6. Non-woven scaffolds

As the non-wovens were incubated in PBS we noticed the effect the water had on the friction between the fibers. The slippage of the fibers, as the non-woven network was loosened due to the water, was seen already during first hydrolysis week (Table 5). The tear force per unit weight decreased 47 % already after one week incubation. The major drop was seen between the weeks 8 and 13 where the decrease was 80 % in tear force

and 87 % when compared to the 0-week data. For all the incubation weeks the strain is close to a 100 % or higher indicating that the fabric is not breaking but rather stretching until entanglements are disconnected.

Table 5. Non-woven properties in hydrolytic testing in PBS.

Hydrolysis time	Max.tear force/weight (N/g)		Strain at max.tear force (%)		Fabrik weight g/m^2 [a, b]
(Weeks)	Mean [a]	StDev	Mean [a]	StDev	
0	78.5	12.1	138	14	261
1	41.4	5.5	134	9	304
8	43.2	13.4	125	24	306
13	8.9	2.5	99	6	276
16	5.3	2.4	96	20	316
20	1.0	0.1	116	70	270

a) n = 3

b) Weight measured from dry samples prior the hydrolysis

7.6. Hydrolytic degradation: Molecular weight and i.v. (II – V)

7.6.1. Fibers

The Figure 24 shows the degradation by means of decreasing M_w against the hydrolysis time. The point where the mechanical testing of the samples was impossible due to the breakage of the fibers is marked with a circle in the Figure 24. The region is situated between the 8 to 10 kDa. The 1.90 wt-% monomer fiber lost all its mechanical properties at the week 8 where the corresponding M_w was also 10 kDa. After 28 weeks the molecular weight drop slows down and a plateau region can be noticed until the end of the testing. If the fibers with 1.90 and < 0.02 wt-% monomer had this plateau region, it cannot be noticed based on these studies. For the first 12 weeks the slope of the curve for the 0.09 wt-% (268/265/7/8) monomer fiber batch is moderate, after which it starts to behave similarly to 0.3 - 0.4 wt-% monomer fiber batches. The week 0 i.v. is between the 0.86 and 1.23 dl/g after sterilization no matter what was the raw material i.v. The i.v. drop during the incubation follows the same pattern than the M_w decrease. It is linearly decreasing for the 0.3 - 0.4 wt-% monomer fiber batches from average 1.0 dl/g to 0.2 dl/g in 36 weeks. There is a difference between the M_w and i.v. and that is the plateau phase. When measuring the i.v. the plateau phase starts 10 weeks later than of the M_w; it starts after 36 weeks of incubation (Table 6). The PD values showed the there is an increase due to the degradation, yet only a moderate one. For the fast degrading

fiber 275/270 with high monomer wt-% of 1.90 the PD decreased below the start value after the initial increase. This decrease took place from 8 to 16 weeks after the loss of mechanical strength.

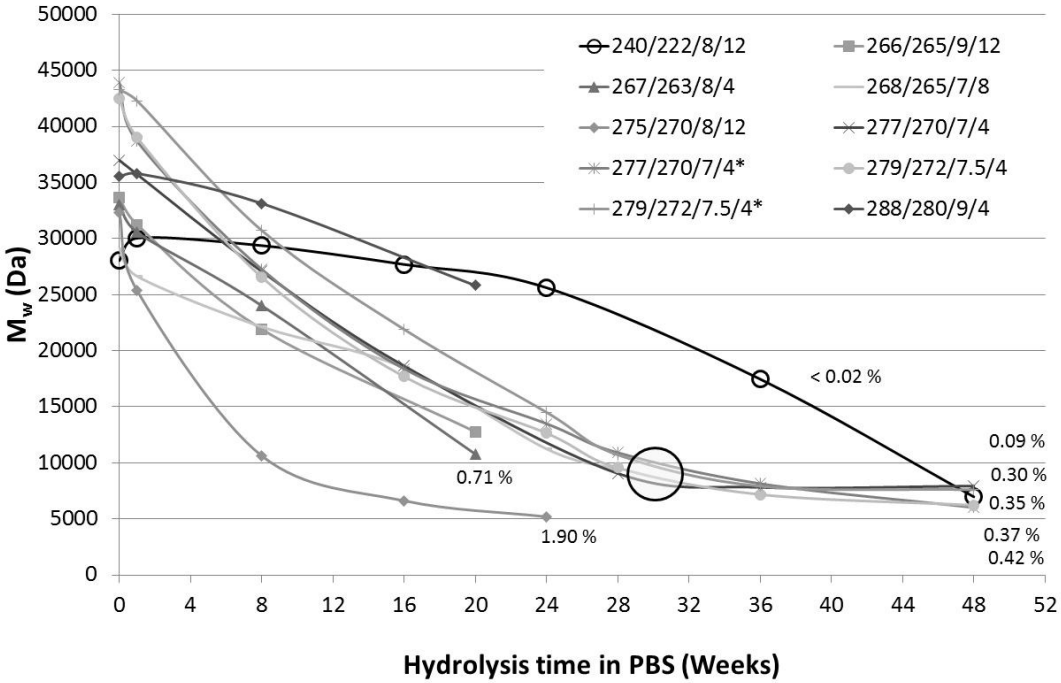

Figure 24. Molecular weight decrease of the fibers during the in vitro incubation. Monomer wt-% shown after the set where available (average results of n = 5). The point after which the mechanical testing failed, is marked with a circle.

Table 6. Inherent viscosity (i.v.) and polydispersity (PD) values for fiber batches during the hydrolysis in PBS (average results of n=2).

i.v. (dl/g) \ Weeks	0	1	8	16	20	24	26	28	36	48
240/222/8/12	0.86 ± 0.02	0.89 ± 0.03	0.90 ± 0.04	0.93 ± 0.01		0.83 ± 0.08	0.64 ± 0.02			0.27 ± 0.02
266/265/9/12	0.99 ± 0.04	0.96 ± 0.02	0.76 ± 0.03		0.51 ± 0.01					
267/263/8/4	0.98 ± 0.03	0.96 ± 0.03	0.81 ± 0.01		0.35 ± 0.01					
268/265/7/8	0.91 ± 0.01	0.86 ± 0.05	0.77 ± 0.01	0.69 ± 0.01		0.49 ± 0.01		0.39 ± 0.01		
275/270/8/12	0.97 ± 0.02	0.85 ± 0.01	0.47 ± 0.02	0.24 ± 0.01		0.22 ± 0.04	0.17 ± 0.04			0.11 ± 0.01
277/270/7/4	1.10 ± 0.04	1.25 ± 0.18	0.90 ± 0.01	0.69 ± 0.03		0.62 ± 0.01		0.31 ± 0.05	0.25 ± 0.01	0.17 ± 0.01
277/270/7/4*	1.21 ± 0.07	1.10 ± 0.01	0.88 ± 0.01	0.67 ± 0.01		0.50 ± 0.02		0.42 ± 0.01	0.27 ± 0.01	0.17 ± 0.01
279/272/7.5/4	1.15 ± 0.03	1.14 ± 0.01	0.85 ± 0.01	0.65 ± 0.01		0.49 ± 0.01		0.40 ± 0.01	0.24 ± 0.01	0.16 ± 0.01
279/272/7.5/4*	1.23 ± 0.05	1.15 ± 0.04	0.98 ± 0.01	0.80 ± 0.02		0.51 ± 0.02		0.44 ± 0.01	0.27 ± 0.02	0.18 ± 0.01
282/272/8/4	0.96 ± 0.05	0.94 ± 0.01	0.91 ± 0.02	0.78 ± 0.01						
288/280/9/4	1.04 ± 0.01	1.06 ± 0.02	1.04 ± 0.01		0.84 ± 0.02					
PD \ Weeks	**0**	**1**	**8**	**16**	**20**	**24**	**26**	**28**	**36**	**48**
240/222/8/12	1.75 ± 0.05	1.91 ± 0.08	1.74 ± 0.01	1.78 ± 0.01		2.02 ± 0.01	2.20 ± 0.08			2.94 ± 0.20
266/265/9/12	1.92 ± 0.03	1.80 ± 0.06	2.00 ± 0.01		2.21 ± 0.02					
267/263/8/4	1.87 ± 0.09	1.80 ± 0.02	1.89 ± 0.06		2.08 ± 0.05					
268/265/7/8	1.74 ± 0.04	1.90 ± 0.15	1.95 ± 0.01	1.77 ± 0.03		2.11 ± 0.02		2.14 ± 0.01		
275/270/8/12	1.82 ± 0.03	2.09 ± 0.11	1.96 ± 0.01	1.96 ± 0.10		1.73 ± 0.01	2.05 ± 0.53			2.24 ± 0.35
277/270/7/4	1.75 ± 0.05	1.71 ± 0.05	1.72 ± 0.07	1.88 ± 0.04		1.89 ± 0.09		1.94 ± 0.05	2.14 ± 0.05	2.29 ± 0.01
277/270/7/4*	1.91 ± 0.02	1.96 ± 0.01	1.74 ± 0.07	1.84 ± 0.05		1.80 ± 0.11		1.98 ± 0.07	2.06 ± 0.07	2.20 ± 0.07
279/272/7.5/4	1.85 ± 0.01	1.91 ± 0.02	1.73 ± 0.13	1.78 ± 0.10		1.84 ± 0.04		1.89 ± 0.02	2.01 ± 0.07	2.19 ± 0.06
279/272/7.5/4*	1.88 ± 0.06	1.89 ± 0.01	1.73 ± 0.12	1.81 ± 0.01		1.88 ± 0.10		1.86 ± 0.04	2.02 ± 0.03	2.29 ± 0.06
282/272/8/4	1.83 ± 0.02	1.74 ± 0.01	1.84 ± 0.04	2.27 ± 0.12						
288/280/9/4	1.79 ± 0.08	1.80 ± 0.10	1.74 ± 0.01		1.69 ± 0.01					

7.6.2. Knits: Shelf-life

As we can see from the Table 7 the molecular properties are not changing during the 2.5 year follow up. The three year data point shows a decrease for M_w and i.v. data and increase in PD for both of the fiber batches. We can notice some changes in the 1.5 year M_w data for both batches suggesting a corrupted data point.

Table 7. Molecular properties of the P(L/D)LA 96/4 knits during a 3 year shelf-life follow-up (average results of n = 2).

	0 years		1/2 year		1 year		1 1/2 years		2 years		2 1/2 years		3 years	
	Mean	StDev	Mean	StDev	Mean	StDev	Mean	StDev	Mean	StDev	Mean	StDev	Mean	StDev
M_w 4F knits	31000	1100	32000	200	31000	100	27000	400	34000	400	33000	200	28000	300
M_w 8F knits	32000	500	31000	300	30000	500	25000	600	30000	100	31000	300	27000	100
i.v. 4F knits	0.99	0.03	1.00	0.01	0.99	0.01	0.90	0.01	1.04	0.03	1.00	0.02	0.88	0.01
i.v. 8F knits	1.01	0.02	0.98	0.01	0.98	0.01	0.86	0.01	0.96	0.03	0.95	0.01	0.89	0.03
PD 4F knits	1.67	0.04	1.75	0.02	1.58	0.01	1.60	0.01	1.47	0.03	1.51	0.04	1.82	0.07
PD 8F knits	1.65	0.11	1.71	0.03	1.59	0.01	1.58	0.02	1.51	0.02	1.52	0.03	1.88	0.05

7.6.3. Cylindrical scaffolds: Hydrolysis and in vivo

The knitted and rolled Ø 15 mm cylindrical scaffolds were tested both in hydrolysis and in animals. In both cases the molecular weight was measured from the core of the scaffold and from the surface of the scaffold to assess if the structure has an effect on the degradation (Table 8, Publication IV, Figures 8 & 9). The results showed that there is no difference in the degradation speed between the core and the surface. Both are degrading at the same speed despite the incubation or implantation time. The major difference can be found from the degradation speed when comparing the methods. In vivo degradation of the scaffolds was slower compared to the hydrolytic degradation. The difference can be first noticed between the weeks 6 and 13. For the incubated scaffolds a continuous degradation takes place. In comparison, the degradation profile of in vivo scaffolds seems to be delayed. Comparing the 48 and 52-week results there was an average of 81 % drop in the M_w for the incubated scaffolds, whereas only 59 % drop in M_w was noticed for the in vivo scaffolds. That difference is noticeable.

Table 8. PBS hydrolysis and in vivo molecular data for the knitted cylindrical scaffolds (average results of n = 2).

Time (Weeks)	0	1	2	3	6	10	13	16	20	24	27	28	32	36	42	48	52
In vivo Mw Core (Da)	**43800**	**40200**	**39300**	**37300**	**43000**		**37900**				**28000**						**17900**
StDev	**1400**	**600**	**4000**	**100**			**100**				**200**						**500**
PBS Mw Core (Da)	43800	41700	38600		38600	33000		23700	22000	18500		16200	13300	10100	9300	8700	
StDev	1400	500	900		200	600		500	300	400		300	700	100	300	200	
In vivo Mw surface (Da)	**44000**	**43700**	**38900**	**38700**	**39200**		**39900**				**29300**						**17900**
StDev	**600**	**200**	**2900**	**700**	**100**		**100**				**200**						**200**
PBS Mw surface (Da)	44000	41600	39100		37100	32500		23100	22800	17700		16300	12700	9700	8800	8000	
StDev	600	200	800		1000	1700		200	100	100		300	300	100	100	100	
In vivo Mn Core (Da)	**26800**	**24200**	**23200**	**22200**	**25500**		**22700**				**16100**						**12100**
StDev	**600**	**200**	**2600**	**400**	**100**		**500**				**200**						**200**
PBS Mn Core (Da)	26800	24100	24000		23200	20700		14800	13800	10600		9000	6500	4800	4100	4200	
StDev	600	1900	900		500	600		800	200	500		200	800	100	100	100	
In vivo Mn surface (Da)	**26500**	**26700**	**23100**	**22900**	**23600**		**24200**				**17100**						**11800**
StDev	**200**	**600**	**1800**	**800**	**400**		**400**				**300**						**200**
PBS Mn surface (Da)	26500	25200	22700		22400	19100		14000	13200	9800		9200	6900	4500	3800	3900	
StDev	200	100	900		100	900		100	100	100		300	300	100	100	100	
In vivo i.v. Core (dl/g)	**1.27**	**1.20**	**1.17**	**1.13**	**1.26**		**1.15**				**0.92**						**0.67**
StDev	**0.03**	**0.01**	**0.09**	**0.01**	**0.01**		**0.01**				**0.06**						**0.01**
PBS i.v. Core (dl/g)	1.27	1.23	1.16		1.16	1.04		0.82	0.77	0.68		0.61	0.53	0.43	0.40	0.38	
StDev	0.03	0.02	0.02		0.01	0.01		0.01	0.01	0.01		0.01	0.02	0.01	0.01	0.01	
In vivo i.v. surface (dl/g)	**1.28**	**1.27**	**1.17**	**1.16**	**1.18**		**1.19**				**0.95**						**0.67**
StDev	**0.01**	**0.03**	**0.06**	**0.02**	**0.01**		**0.01**				**0.01**						**0.01**
PBS i.v. surface (dl/g)	1.28	1.23	1.17		1.13	1.02		0.80	0.79	0.65		0.62	0.51	0.41	0.38	0.36	
StDev	0.01	0.01	0.02		0.02	0.04		0.01	0.01	0.01		0.01	0.01	0.01	0.01	0.01	
In vivo PD Core	**1.63**	**1.66**	**1.70**	**1.68**	**1.69**		**1.67**				**1.74**						**1.47**
StDev	**0.02**	**0.01**	**0.02**	**0.03**	**0.01**		**0.03**				**0.01**						**0.01**
PBS PD Core	1.63	1.74	1.61		1.66	1.59		1.60	1.60	1.74		1.80	2.07	2.12	2.27	2.07	
StDev	0.02	0.12	0.02		0.03	0.07		0.05	0.04	0.05		0.08	0.15	0.01	0.03	0.02	
In vivo PD surface	**1.66**	**1.64**	**1.69**	**1.69**	**1.67**		**1.65**				**1.72**						**1.52**
StDev	**0.01**	**0.03**	**0.01**	**0.03**	**0.03**		**0.03**				**0.02**						**0.01**
PBS PD surface	1.66	1.65	1.72		1.66	1.70		1.64	1.73	1.80		1.78	1.84	2.16	2.3	2.08	
StDev	0.01	0.02	0.03		0.04	0.01		0.01	0.02	0.01		0.02	0.04	0.01	0.05	0.02	

7.7. Hydrolytic degradation: Thermal analysis of the fibers (II, III, V)

During the in vitro incubation the thermal properties of the fiber batches are changing (Table 9). The following phenomena can be seen for all the other fiber batches, except for the 240/222 fiber batch. We can see a behavior where the T_m is the unchanged or increasing for all the fiber batches until the weeks 8 or 16. After those time points the T_m starts to gradually decrease. After the 48-week incubation the T_m is settled between the 147 and 149^{o}C for all the fibers besides the 275/270 fiber, of which T_m decreased to145^{o}C. This 275/270 fiber batch degraded faster than any other batch. For the 240/222 fiber batch the decrease in T_m happens during the first week and T_m remains at the same level during the rest of the 48-week incubation. After this time the T_m is 155^{o}C. The melting enthalpy that is associated with the crystallinity of the polymer increases during the incubation. When calculated using the 100 % crystalline PLLA as reference (93.7 J/g) (Fischer et al. 1973) we get the highest increase from 33.0 to 48.9 % in crystallinity, in 28 weeks for the 279/272 fiber batch. The highest crystallinity 55.9 % was measured for the 266/265 fiber at week 20. Some of the fiber batches incubated for 48 weeks show a minor decrease in crystallinity starting at the week 28.

Such T_g behavior at the weeks 8 or 16, as in the case of T_m, cannot be seen. The behavior that was common for all the fiber batches was that the T_g decreased from the 0-week value when compared to the final 20 or 48 week values after the hydrolysis. The recrystallization enthalpy increases during the incubation until a certain week after which it decreases. The time required, for the fibers, to reach the maximum recrystallization enthalpy is different. As it is only 8 weeks for the 275/270 fiber, for the 240/222 fiber the enthalpy is still increasing at the 48-week time point. This maximum value of recrystallization enthalpy is reached at the similar time points where the mechanical strength can no longer be measured and the M_w is ≤ 10 kDa.

Table 9. Thermal characterization data of the fiber batches from the hydrolysis test.

	Hydrolysis time (Weeks)	**0**	**1**	**8**	**16**	**20**	**24**	**26**	**28**	**36**	**48**
240/222/8/12	Peak T_m (^oC)	159	154.8	155.4	156		155.0	154.8	154.8	154.1	154.5
	Melting enthalpy ΔH_f (J/g)	30.4	39.4	40.7	40.8		40.3	42.9	41.7	41.1	40.1
	T_g (C^o)	60.7	58.4	58.2	58.1		57.0	56.8	56.3	54.5	55.0
	Recryst. enthalpy ΔH_c (J/g)	6.3	7.5	9.3	10.2		10.3	11.8	17.6	28.8	35.4
266/265/9/12	Peak T_m (^oC)	152.6	153	155.9		154.9					
	Melting enthalpy ΔH_f (J/g)	41.8	39.8	38.5		52.4					
	T_g (C^o)	57.9	57.9	57.7		54.2					
	Recryst. enthalpy ΔH_c (J/g)	5.4	4.3	8.1		38.3					
267/263/8/4	Peak T_m (^oC)	153.1	153	153.5		151.9					
	Melting enthalpy ΔH_f (J/g)	41.7	44.9	45.6		46.9					
	T_g (C^o)	57.1	57.2	56.3		50.1					
	Recryst. enthalpy ΔH_c (J/g)	2.7	5.4	13.1		42.8					
268/265/7/8	Peak T_m (^oC)	154.4	155.3	156.6	157		155.0	152.8	153.3	152.5	147.2
	Melting enthalpy ΔH_f (J/g)	38.6	41.1	42.8	41.0		42.3	42.6	41.3	45.8	34.0
	T_g (C^o)	58.4	58.4	58.0	57.3		54.3	49.7	52.2	55.7	56.0
	Recryst. enthalpy ΔH_c (J/g)	5.8	6.1	9.4	15.7		25.7	38.3	33.6	35.0	21
275/270/8/12	Peak T_m (^oC)	152.6	154.6	153.3	154		151.8	151.1	149.7	147.2	144.7
	Melting enthalpy ΔH_f (J/g)	35.2	39.5	44.5	45.3		45.2	46.9	48.5	46.3	45.3
	T_g (C^o)	55.0	53.1	51.3	56.3		56.5	56.3	56.0	55.5	54.4
	Recryst. enthalpy ΔH_c (J/g)	4.5	10.8	39.3	32.0		26.7	23.5	22.5	16.4	7.3
277/270/7/4	Peak T_m (^oC)	154.8	156.7	157.2	156.1		153.4		151.4		146.7
	Melting enthalpy ΔH_f (J/g)	35.2	34.1	42.5	42.8		43.5		45.2		44.9
	T_g (C^o)	59.0	58.8	58.1	55.0		51.4		47.4		54.1
	Recryst. enthalpy ΔH_c (J/g)	1.9	2.5	7	21.8		36.3		29.6		15.6
277/270/7/4*	Peak T_m (^oC)	154.7	155.5	156.8	157		153.2		151.6	153.2	147.3
	Melting enthalpy ΔH_f (J/g)	33.3	36.3	40.4	42.1		45.1		44.6	45.8	44.9
	T_g (C^o)	57.6	58.2	57.2	56.1		52.1		46.4	55.7	54.5
	Recryst. enthalpy ΔH_c (J/g)	1.3	1.3	6.1	19.9		34.9		36.5	33.8	15.9
279/272/7.5/4	Peak T_m (^oC)	154.6	155.9	156.8	156.4		152.4		150.9	153.2	147.0
	Melting enthalpy ΔH_f (J/g)	30.9	37.7	38.9	42.5		44.8		45.8	41.8	38.9
	T_g (C^o)	57.8	58.6	57.8	55.3		50.5		49.6	55.3	53.7
	Recryst. enthalpy ΔH_c (J/g)	1.1	1.7	4.9	18.1		34.1		34.3	22.3	8.8
279/272/7.5/4*	Peak T_m (^oC)	154.9	155.4	156.4	157.1		152.9		152.5	155.1	148.7
	Melting enthalpy ΔH_f (J/g)	34.3	36.8	36.9	40.7		45.6		44.4	40.9	45.5
	T_g (C^o)	58.9	58.6	58.0	57.1		51.5		51.2	56.0	54.5
	Recryst. enthalpy ΔH_c (J/g)	1.2	1.6	3.7	9.9		32.3		33.8	25.5	16.0
288/280/9/4	Peak T_m (^oC)	155.7	156.8	155.7		155.1					
	Melting enthalpy ΔH_f (J/g)	35.8	36.8	38.2		43.9					
	T_g (C^o)	58.4	61.1	58.4		56.9					
	Recryst. enthalpy ΔH_c (J/g)	2.6	1.2	4.6		11.4					

7.8. Visual characterization (II - V)

7.8.1. Melt-spun fibers

During the melt spinning the temperature at the nozzle is crucial for the optimal fiber quality. If the temperature at the nozzle is too low the so called “shark-skin” effect takes place but when the temperature is near the optimum the fiber quality has to be evaluated using microscopy. In Figure 25 A-B the temperature is just below the optimal temperature thus causing grooves onto the fibers. After the fiber exits the nozzle it is subjected to different kinds of abrasive forces during the orientation process. These forces tend to remove the material from the surface of the fiber. The amount of polymer removed and the type of abrasive wear seen in the fibers is affected by the fiber surface temperature and the force which pulls the fiber against the abrasive surfaces (Figure 25 C-D).

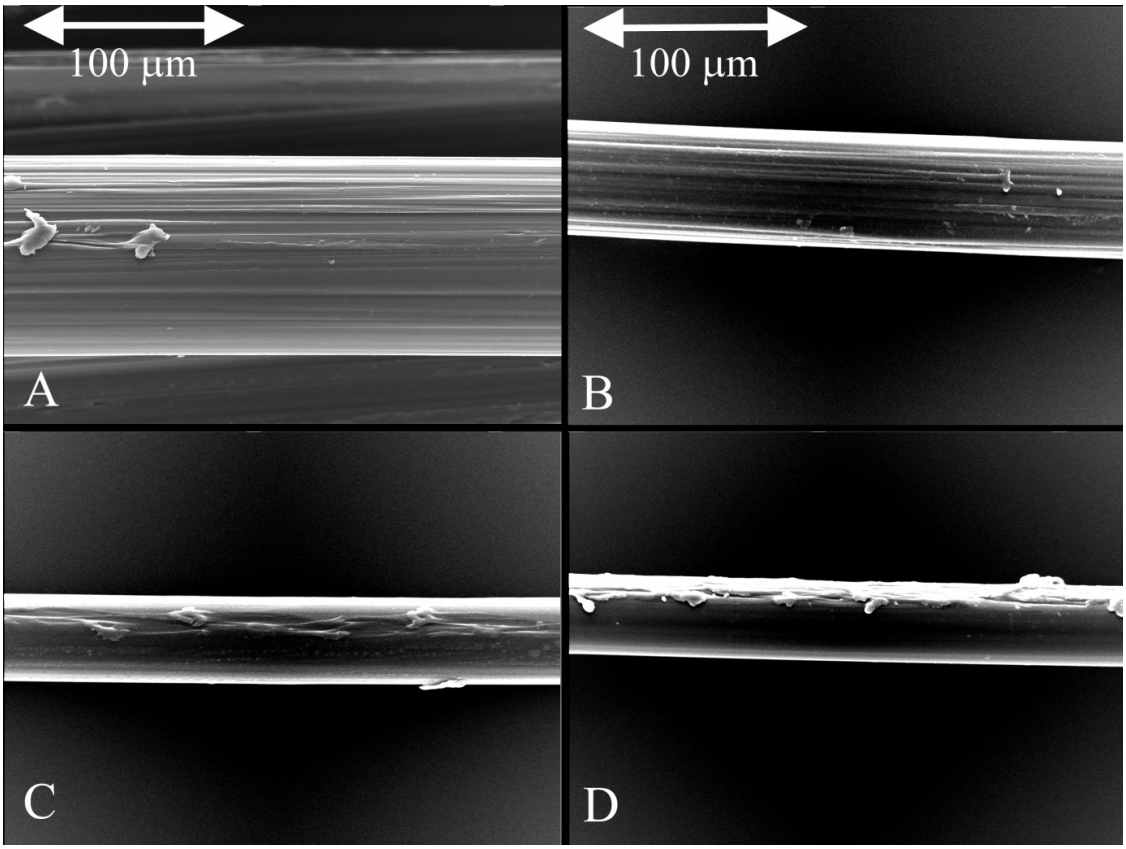

Figure 25. Grooved fiber A) and surface damage, B) grooved fiber, C) scratched fiber and D) scratched and peeled fiber.

7.8.2. Hydrolytic degradation of the fibers

At week zero the orientation direction at the fiber surface is clearly visible and the surface is clear from debris and cracks (Figure 26). There is no change during the first incubation week. At the week 8 into the incubation we can see that for some parts the fiber has lost its orientation caused grooves, although some of them are still visible. There are visible surface changes like cracking to be seen in the surface. After the 24-week incubation there are no longer visible signs of oriented structure throughout the fiber surface. For the 12-ply fibers there are no visible signs of degradation after even 48 or 53 weeks.

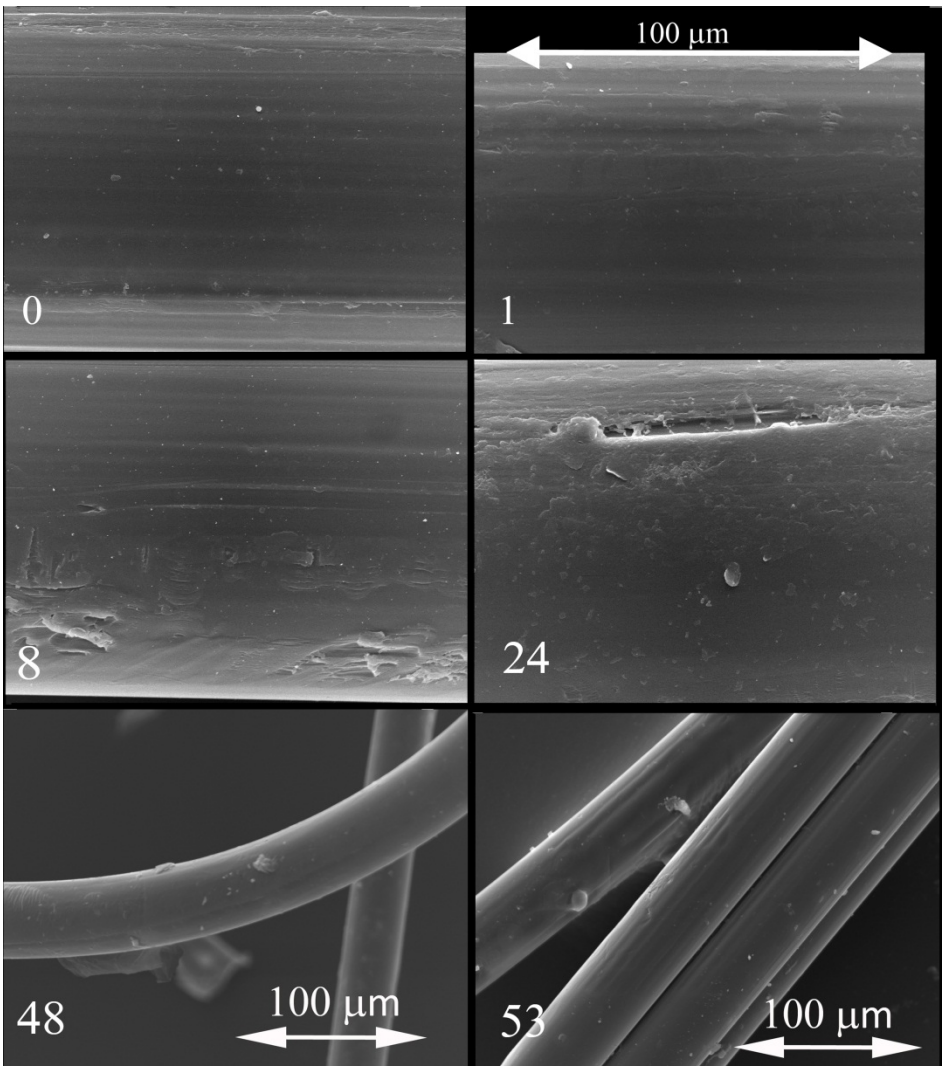

Figure 26. The changes seen on surfaces of the P(L/D)LA 96/4, 4-ply multifilament (288/280/9/4) after 0, 1, 8 and 24 weeks and for 12-ply multifilament (240/222/8/12) after 48 and 53 weeks in incubation in PBS.

7.8.3. Knits and scaffolds

When the fibers were subjected to knitting process there was no fiber damage due to the knitting process. The fibers were intact and undamaged (Figure 27). The carding and the needle punching methods did not affect the fiber quality either. Fibers remained intact in this process also even though the filaments were bended to a small loop sizes (Figure 27 C).

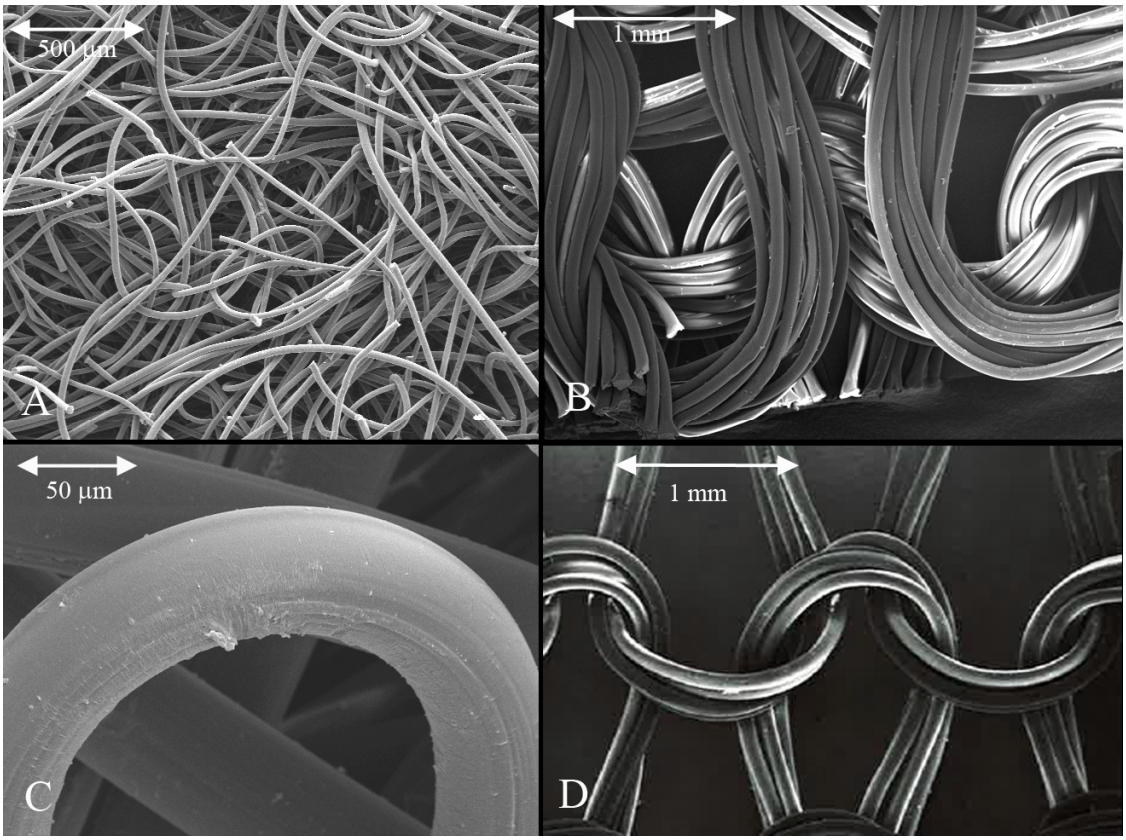

Figure 27. Fabrics made from P(L/D)LA 96/4 fibers; A) the non-woven surface, B) 12-filament weft knit, C) non-woven fiber loop, and D) 4-filament weft knit.

8. Discussion

8.1. Raw material

We found that the molecular properties of the raw medical grade P(L/D)LA 96/4 polymer have an effect onto the processing parameters. The higher the M_w and i.v., the higher is the drop in M_w during the single screw melt spinning with the equipment used. As stated, most of the degradation of high Mw / i.v. polymers occurred in the extruder barrel. The shear stress of the high molecular weight PLAs induced the degradation in the barrel due to their higher viscosity. When working with the viscosity level of ~ 2 dl/g and M_w ~ 100 kDa, there is practically no thermal degradation occurring in our set up. This can result from the stability of this polymer with our equipment size and screw geometry and the low viscosity further induces less shear stress induced degradation. With our melt spinning set up there is a limit viscosity somewhere between 2.2 and 4.1 dl/g which is beneficial to the melt spinning in regards to the polymer degradation in the extruder. This is further due to the processing parameters that can be altered and tuned downward when working with less viscous material. One correlation to these can be found from Nuutinen et al. (2002a-b) as they processed high M_w and i.v. PLA materials. They also used high (295^{o}C) nozzle temperatures while processing. This resulted in a major drop of M_w and i.v. but what is noticeable that the higher M_w 648 000 g/mol and i.v. 9.52 dl/g PLLA resulted in a far greater drop regarding molecular properties than lower M_w 413 000 g/mol and i.v. 6.85 dl/g P(L/D)LA 96/4 in melt spinning. Extrusion parameters were not revealed. Similar Purac PLLA polymers were used by Yuan et al. (2000). They noticed that when extrusion temperatures were not changed and using the same temperature in the nozzle, the higher molecular weight polymers degraded more. If the screw speed was faster this could be then due to the increased shear stress that leads to a viscous dissipation that increases the melt temperature thus increasing the thermal degradation in the extruder. Since the screw speed Yuan et al. used did not change, this implies that higher molecular weight polymer induced higher shear stresses and higher friction that induces higher temperatures as well. So the shear stress and the temperature together degraded the material. Yuan et al. further noticed that when the crystallinity of the high molecular weight polymer is high it also requires higher nozzle temperatures during spinning compared to the high molecular weight polymer with

lower crystallinity. In all we concluded that the processing temperatures must be kept as low as possible if one needs to avoid thermal degradation, point stated also by Taubner & Shishoo (2001). And using low viscosity polymers the shear stress induced degradation can be minimized and even lower screw speeds can be used.

The higher the raw polymer M_w, the higher is the probability for monomer accumulation during the melt extrusion process. Of course, this is dependent on the processing parameters and conditions. The hydrolytical degradation induced by pressure and heat was shown to induce lactic acid formation (Tsuji et al. 2008). In our study we showed a direct dependency between the temperature, residence time, and the monomer accumulation, in a melt spinning process. The temperature has a stepwise increase on monomer accumulation whereas the residence time increased the monomer content more or less linearly. It also seems that the monomer might be developed in the autocatalytic manner in higher temperatures, probably by the oligomers and monomers occurring during the extrusion (Liu et al. 2006).

This thesis states that the raw material properties affect the melt spinning of P(L/D)LA 96/4 polymer. The higher M_w and i.v. require higher temperatures that affect the properties of the polymer along with the shear stress from the screw. The extruder set up must be configured for the lowest possible temperatures, with suitable shear rates, and with the highest possible throughput to obtain the minimum amount of degradation during the melt spinning. Since these parameters cannot all be achieved at the same time, the optimal is a compromise between them. The nozzle geometry, throughput speed, and the viscosity at the nozzle also play a part since they define the pre-oriented structure on the as-spun fiber point made also by Fambri et al. (1997).

8.2. Hot drawing

The factor favoring the continuous melt spinning hot drawing process compared to the two-step as-spun hot drawing is that there is no need for a second processing step which thus saves time, and faster take off speeds can be used (Schmack et al. 2001). The drawing of the fibers in this thesis resulted in 3.3 to 5.1 drawing ratios. It is known that different collection speeds, or take off speeds, result in different properties (Fambri et al. 1997, Fourné 1999), and that the drawing has direct effect on fiber modulus

(Andriano et al. 1994, Ward 1997). In our work (publication II) we used the same take off speed 14.6 m/min and orientation parameters therefore the same draw ratio was obtained for all the fibers in that study. The parameters that were changed were the temperature profile in the extrusion and the screw speed (residence time, material through put). The same draw ratio did not result in similar tensile properties on the basis of material through put. Variations in tensile strength from 420 to 570 MPa were noticed. Only one screw speed (the highest, 9 rpm) showed this phenomena, where all the fibers despite the temperature, obtained equal mechanical properties. We further noticed that for the different temperatures used there was a highest tensile property found, which was never the highest speed applied. The tensile strength obtained was increasing to a certain point when again the properties dropped. This data concludes that there is a tensile maximum that is also affected by the throughput speed (mass flow, Ziabicki 1976) not only the draw ratio. Although the take-off speed is kept the same, the less material coming out results in higher difference in absolute speed of the material at point of exit, at the nozzle. This difference in speed of the flowing polymer affects the crystallinity fraction, morphology and the molecular structure of the amorphous phase. Since the cooling rate is now different, due to different material volume, this results in different crystalline/amorphous structures in semi crystalline polymer systems. As there were only slight changes in crystallinity we assume that the affect is due to the type of crystalline structure that is formed into the as-spun fiber as well as due to the morphology of the amorphous phase, thus both affecting the fiber properties.

When comparing the different hot drawing properties in this thesis we can conclude that the sufficient cooling is necessary at the take-off. There was no drastic difference in crystallinity whereas there was a decrease in the recrystallization enthalpy correlating to the fact that the polymer had less free un-crystallized parts in their molecular network. This resulted into higher tensile properties but at the same time to an uncontrolled degradation behavior during the amorphous phase degradation. This could be seen a faster drop in tensile UTS during the first 12 weeks compared to the similar fibers with a proper cooling. The importance of cooling on biodegradable polymer crystallization on different molecular weight PLLAs was noticed by Migliaresi et al. (1991) and Ahmed et al. (2009). Migliaresi et al. (1991) noticed that the speed of the cooling affects the 31 000 g/mol PLLA and it attained most of the crystallization potential during the cooling. This molecular weight level allows rapid molecular motion within relative non-

viscous medium. They attained crystallinity of 38.5 % when cooling -5°C/min, and 57.6 % when cooling -0.5°C/min. So this rapid molecular motion that causes the crystallization during the cooling resulted in more compact crystallization. The obtained crystallinity in our fibers was similar whether they were cooled or not but the recrystallization enthalpy correlates to the fact that there is difference between the two. The one parameter affecting the results is the fiber variation; the thickness changes of the fiber. The two most important factors governing the variation is the cooling and yarn tension (Fourné 1999). With that in mind, the greater variation results to a different strength results due to the fiber diameter change. This can be seen in tensile strength data from the hydrolysis tests. The non-cooled fibers showed oscillation in the beginning of the hydrolysis.

This thesis states that the take-off speed must be suitable and it must be selected according to the polymer output volume. By adjusting temperatures in the extruder it is possible to affect the flow thus effecting on the fiber quality and strength. Therefore if we change one of the three; speed, temperature, or take-off speed, the others have to be taken into account. The cooling must be suitable during the spinning for optimized and good quality fiber.

8.3. Gamma irradiation

When combining the total degradation from processing and gamma-irradiation of P(L/D)LA 96/4, Daculsi et al. (2001) and Nuutinen et al. (2002b) reported both a combined degradation of ~ 80 %. In our studies of the P(L/D)LA 96/4 fibers, the combined degradation regarding M_w was at the range of 82 to 90 % and regarding i.v. from 72 to 83 %. This difference is attributed to the drop of molecular properties during the melt extrusion since the drop of M_w and i.v. of irradiated fiber compared to non-irradiated fiber was from 71 to 78 % for all the batches, resulting to a level from 28 kDa to 44 kDa depending on the fiber batch. Only material showing a noticeable difference was the i.v. 2.30 dl/g material of which combined degradation regarding M_w was 72 % and of i.v. it was 63 % and this was mainly due to the irradiation. Where Nuutinen et al. (2002a) showed a ~ 32 % increase in crystallinity for high M_w PLLA the same tendency for P(L/D)LA 96/4 was not shown. The raw material affected only the 100 kDa polymer. With this polymer there was a 1 % decrease in crystallinity. With other polymer batches there was an increase from 1 to 11 % in crystallinity. We can observe

an increase in crystalline enthalpy for all the fibers after gamma, the highest measured for the lowest M_w P(L/D)LA 96/4.

The strength retention due to the gamma irradiation varied from 15 to 44 % and tensile modulus varied from -18 to +13 % in the fibers used in this thesis. We found that there was a correlation between the processing conditions and the radiation degradation. When there is no cooling unit used after the nozzle, there was less radiation degradation occurring than with the fibers that were cooled/quenched after the nozzle. This is probably due to the crystalline structure due to the ambient temperature cooling, already discussed in hot drawing paragraph.

8.4. Hydrolytic degradation of the fibers

We showed that the fiber thickness is not affecting the tensile properties of the fiber during the 10-week hydrolytic incubation in PBS for melt-spun fibers if the monomer content is similar. This is in contrast to the study of Pegoretti et al. (1997). There was information and knowledge available about the monomer effect on degradation (Kellomäki et al. 2003) but no relevant journal publications concerning fibers, until our group published results from the processing induced monomer effect on hydrolytic degradation. The amount of monomeric lactic acid needed to induce a difference during 10-week degradation is > 0.2 wt-%. We showed that the increase in monomer content then further increases the degradation rate. For the lower amounts of lactide monomer Paakinaho et al. (2011) showed that the thermally induced lactide monomer affected the degradation of PLGA 85L/15G polymer rods. The 0.03, 0.05, 0.10 and 0.20 wt-% monomer amounts showed no difference in shear strength values until the week 8. After this time it was noticed that the lower the amount of monomer the longer the degradation stability. The mass loss also showed a delayed start regarding the monomer contents where higher monomer contents started to lose their mass earlier.

The molecular weight decrease is somewhat affected by the monomer content during the hydrolysis, although monomer contents at the range of 0.1 to 0.7 wt-% show similar type first order linear degradation behavior. This phenomenon was also noticed by Paakinaho et al. (2011) regarding the viscosities of the low wt-% (< 0.02) monomer rods. Then again in our study the i.v. 2.30 dl/g polymer with > 0.02 % monomer shows no degradation during the first 24 weeks, this does not fit the two-step degradation

behavior reported by other studies (Pohjonen & Törmälä 1994) but more or less fits the profile of the PLLA reported by Tsuji et al. (2000). It is assumed that the monomer increases the water penetration to the material. The water absorption due to oligomers was noticed by Schliecker et al. (2003) but no sudden increase in water absorption could be noticed in our fibers due to monomer increase. Even if not measurable, it does not rule out the possibility of such phenomena due to the inaccuracy of the measuring methods. Yet the increase in water absorption could explain the faster hydrolytic degradation. Added monomer was shown to be diluted out of the polymer in 3 weeks by Hyon et al. (1997). When the monomer was added prior the extrusion it diluted out more or less in 2 weeks (Paakinaho et al. 2011). This diluted part can then be replaced by the water molecules. We can assume that before the monomer was leached out it catalyzed the chain scission that formed acidic end groups. These end groups then enhanced the hydrolysis rate (Tsuji et al. 2000).

Same pattern than above is noticeable with tensile properties. Especially the load properties follow the trend where the monomer amounts do have a more linear relationship with the process induced monomer. On the basis of this thesis we noticed a pattern in behavior thus we can speculate that if the monomer levels are known among the other measurable properties the degradation can be predicted and in the future we can build a model governing this subject. Yet more information about the molecular level data and thorough studies are needed for this. The modeling of hydrolytic degradation has been studied (Pohjonen & Törmälä 1994, Weir et al. 2004b, Wang et al. 2008) and in some publications the monomers forming due to hydrolysis has been taken account. The only model taking into account a process induced monomers was given by the Paakinaho et al. (2011) for the PLGA 85L/15G rods with lactide contents from 0.05 to 0.20 wt-%.

As we have shown, the process induced monomer amounts of > 0.8 wt-%, do play a major role in the degradation at the beginning of the hydrolysis, so this should be also considered in the equations. Now this tensile data in this thesis is measured only for fibers. The effect of monomer on degradation has been shown regarding the PLGA 85L/15G rods (Paakinaho et al. 2011) and SR-PLLA pins (Kellomäki et al. 2003). For the SR-PLLA pins, their volume is ~ 800 times larger compared to our fibers. We see similar trend in the degradation behavior yet different results when compared to our results (Kellomäki et al. 2003). This leads to an assumption that the effect of the

monomer on degradation of different shapes and sizes would have to be studied as well. The fiber volume is very small, therefore the autocatalytic effect phenomena in the core should be non-existent. As the smaller chains are cleaved from the main chain, they can be more easily diffused out from thinner samples (Grizzi et al. 1995). Also the device dependent dimensions influence the degradation phenomena (Burkersroda et al 2002).

The melting temperature first increases, this may be due to thickening of the crystallites by the enhanced chain mobility that is due to the chain scission in the amorphous region. Finally the T_m starts to decrease. This is possibly due to the reduced crystallite thickness (Tsuji & Ikada 2000). The melting enthalpy, thus crystallinity, of the fibers first increases and the T_g decreases as the amorphous regions start to degrade and the smaller chains recrystallize. The presence of the units can also be observed as an increase in recrystallization enthalpy. After this the crystallinity either stays at the high level or after a time starts to decrease. We also see an increase in T_g and a decrease in the recrystallization enthalpy. This transaction takes place near the M_w level < 10 kDa for almost all the fibers. The decrease in the recrystallization enthalpy relates to the start of the degradation of the residue crystalline structure (Tsuji & Ikada 2000). The most rapid degradation occurred with the 1.90 % monomer fiber at the week-8. After that the fiber tensile properties could not be measured and at that time point the M_w was 10 kDa. It was noticed that below this molecular weight all the other fiber batches lost their tensile properties as well. Between the weeks 0 and 8 the T_g of the 1.90 wt-% monomer fiber decreased from 55 to 51^{o}C and the recrystallization enthalpy increased from 4.5 to 39.3 J/g which was also the peak value. The T_g of this fiber then increased to ~ 56^{o}C, and stayed at that level until 48 weeks (end of the study). When other fiber batches were compared the peak values of recrystallization enthalpy they were at similar level from 33.8 to 42.8 J/g. The peak values to certain extent correlate with the 10 kDa limit and the loss of mechanical properties for all the fibers.

When considering the formation of process induced monomer, the processing uniqueness should be considered. With this in mind, if we compare the 0.09 wt-% monomer fiber that was melt-spun in publication (III) with the publication (II) results we see that the fiber in question showed a 25 % drop in UTS after the 10-week incubation. These results are not correlating. The differences between the fibers are the raw material, draw ratio, fiber thickness and the crystallinity. The fiber with 0.09 wt-% monomer has ~5 % higher crystallinity and a higher draw ratio than with the ~ 0.2 wt-%

monomer fibers. The explanation where crystalline polymers has a tendency to degrade slower (Kellomäki et al. 2003), especially in the long run (Vert et al. 1992) is ruled out. This was not confirmed by Tsuji et al. (2000) where they noticed no difference in degradation of PLLA plates with 30 and 45 % crystallinity in 10 weeks. It was further noticed by Tsuji & Ikada (2000) that the increase in initial crystallinity seemed to increase the degradation. This 5 % higher crystallinity might then explain that. Our assumption is that different processing conditions affected the amorphous / crystalline structure. There are three types of amorphous chains locating in between the lamellas (in the restricted amorphous region), tie chains, folding chains, and chains with free end. Then there is the random free amorphous regions locating outside the spherulites (Tsuji & Ikada 2000). We assume that it is the conformation and degradation of the restricted amorphous region that holds together the oriented crystalline structure that is responsible of this difference. Therefore the mechanism leads to a faster decline in the tensile strength of the 0.09 monomer % fiber compared to the ~ 0.2 monomer % fiber.

This thesis states that the monomer affected the degradation. There is clear correlation to the degradation profiles with different monomer amount. We can observe three different types of degradation profiles:

1) Below the detection level monomer content (< 0.02 wt-%) P(L/D)LA 96/4 fibers retained both molecular and mechanical properties for 24 weeks. The properties remained unchanged and a plateau region was noticed until the week-24, after which the properties were gradually decreasing. The possible plateau region at the end was not discovered, although it might be present and starting after the week-48.

2) The second profile detected belongs to the fibers with monomer from 0.1 to 0.7 wt-%. These fibers more or less retained their properties for 8 to 10 weeks and only gradual decrease in tensile properties was noticed. After this the degradation slope increases until it reaches the beginning of the plateau region. The molecular properties for these fibers decrease linearly until the plateau region at 10 kDa. After this point the fibers had no mechanical strength left.

3) The third profile belongs to the high monomer fibers > 0.8 wt-% where a rapid decrease of both mechanical and molecular properties was noticed. The plateau region was unclear although the slope decreased significantly after the loss of all mechanical strength. The M_w limit in this case was also 10 kDa.

The monomer effect regarding the degradation of the P(L/D)LA 96/4 polymer is not yet fully covered. The writer therefore suggests that by carefully controlling the experiments while obtaining more data, this phenomenon could be thoroughly studied.

8.5. Knits and scaffolds

The optimization of the knits for in vivo purposes was carried out. The knit loop size, loop number, and fiber type were the studied variables during the hydrolysis studies as a model for in vivo. The knit degradation studies showed that the degradation stability is solely based on the fiber quality and properties not on the used knitting parameters. The different fiber batches resulted in fairly similar outcome before the degradation when considering the absolute mechanical properties, yet the 4 filament fiber surpassed when strength was measured. Although 8 filament fiber had 4 filaments more, the diameter of the single filament was 10 μm smaller. This leads to an assumption that the 8 filament fiber surface properties were somehow subjected to more wear due to knitting process. The degradation behavior let us assume that the fiber molecular properties played a part during the degradation since 4 filament fiber degraded faster. At the time of experiments the monomer was not measured for these samples, yet it would solely explain the difference in degradation behavior of these knit types, manufactured from two different fiber batches. Our knits did not match the properties of the Gupta & Revagade (2009) but dry-jet-wet spinning of high M_v PLLA ($1.39x10^5$), different parameters in weft knitting, and different fiber size was used compared to our study (Gupta et al. 2006).

As we studied the 3-year storage degradation we found that the samples retained all of their mechanical properties. The reports writer found showed similar behavior for 25 kGy gamma irradiated PLLA after 336 days storage. The molecular weight although decreased slightly in the Birkinsaw et al. (1992) study whereas no change in molecular weight was observed by Pluta et al. (2008) after 1 year storage. The 3-year shelf test shows the good product quality. It also shows that these melt-spun fibers/knits can be used after long periods when appropriately stored.

The knitted cylindrical scaffolds for all sizes showed similar behavior after 1-week hydrolysis. The compression resistance of samples decreased drastically in the small strains. After 2 weeks there was no substantial compression resistance. The in vivo samples, on the other hand, showed steadily increasing compression resistance due to a

block of tissue within the fibrous scaffold. This is an example of how the starting properties of the highly porous scaffolds with interconnected pores are not superior but sufficient to fulfill the task. We noticed that the hydrolytic degradation of the scaffolds was faster than the subcutaneous degradation. After 52 weeks in vivo the M_w was still 18 kDa. From this we can conclude that the degradation behavior of this material in vivo takes a long time, point stated by Waris et al. (2008). This cylindrical implant type from P(L/D)LA 96/4 material was used successfully in the repair of the MCP joints in humans by Honkanen et al. (2003, 2010) and in minipigs by Waris et al. (2008). This scaffold type is first filled in with vascular loose connective tissue and after time the connective tissue matures to dense fibrous tissue. The scaffold is almost completely degraded after 3 years in vivo. In 2011 this scaffold type and material it was made from gained the CE mark by the name RegJoint.

This thesis showed that the rolled knits do not carry mechanical loading for long in hydrolysis without any other support. If such a support is made by making the cylindrical scaffold as a composite with glass polymer substance it retains its properties at least the measured 15 weeks. The problem with the composite scaffolds was the shape recovery. Although implants had a fairly stiff structure the matrix polymer was not elastic enough and it showed further stiffening during the incubation. The good property on this implant is that it just cannot be broken in compression. It retains its oval shape. The deposition of presumably calcium phosphate deposition (Niiranen & Törmälä 1999) during the hydrolytic incubation was noticed with the IVD implants. Kandziora et al. (2004) showed the importance of calcium phosphate compared to autologous bone in interbody fusion cage fusion. The bioactive glass in our implant was to give the same adhesion component to the bone. This ossification was shown by Palmgren et al. (2003) while testing the implant in minipigs. The work by Lazaennec et al. (2006) is promising due to the research with similar P(L/DL)LA 96/4 polymer as a resorbable cage material. They promote the study of this material to be used as an intervertebral fusion cage. Is it possible to manufacture this type of cage by using fibrous structures remains to be seen but the writer promotes the composite idea since many properties can be combined using the composite technology.

The PLA non-woven is hydrophobic and the wetting of the scaffold is an issue what we tried to overcome with plasma and solvent treatment. The only beneficial method that allowed the rapid intake of cells + medium into a fairly tight non-woven matrix was the

oxygen plasma treatment. The plasma was shown to improve cell affinity (Wan et al. 2003, Nagakawa et al. 2006) but the usability in the long run would require a plasma treatment machine close to the end user because it has been shown that the affects diminishes over time, although this might be avoided by restoring the PLA samples in temperature between 0 – 4^{o}C (Yang et al. 2002). The non-woven scaffold reported in this thesis, like stated by Hutmacher (2006), itself is not suitable for load bearing strength requiring applications. But the non-woven should not be undermined as a structure for further development since it can be used in TE as recent studies have shown (Weber et al. 2011).

The scaffolds prepared for the TMJ studies were manufactured using knitted fabrics and non-woven attached to a plate. Good cell seeding capabilities was noticed only with the plate + non-woven type, due to the more porous structure of the cell seeding platform. This was studied by Mauno et al. (2008) and Mäenpää et al. (2010) and they found that adipose stem cells together with this scaffold type can be used in TMJ tissue engineering as a chondrogenic differentiation platform.

Scaffold architecture plays an important role with cells and in differentiation of cells. Kumar et al. (2011) showed that the scaffold structure is more important than previously thought in human bone marrow stromal cell differentiation. By changing the scaffold morphology they suggest that the certain lineage of the cells can be endorsed. Therefore the work with scaffolds, manufactured using fibrous products, is still undergoing by the writer and our research group. The basic phenomena of interactions and especially cell differentiation relation to the different structures and materials are yet to be fully covered and thus needs to be further studied.

9. Conclusions

On the basis of this thesis I have come to following conclusions.

1)

- Different medical grade P(L/D)LA 96/4 polymers require different processing parameters that are governed by the molecular weight and the viscosity of the polymer.
- Different medical grade P(L/D)LA 96/4 polymers have a different degradation profile during the melt spinning, that is governed by the viscosity of the polymers.
- The hydrolytic degradation of the P(L/D)LA 96/4 fibers is not solely governed by the starting level of the molecular weight, nor viscosity. There is also a factor of production induced monomer that needs to be verified and taken in to account.

2)

- Most of the degradation in the single screw extrusion set-up during fiber spinning happens in the extruder barrel due to the heat and shear from the screw.
- The process-induced lactide monomer accumulation is dependent on the temperatures used and residence time of the P(L/D)LA 96/4 polymer. Monomer accumulates in the high temperature regions in the extruder. The used equipment and the raw material properties have an influence on the monomer accumulation.
- In the current work it is shown that the lactide monomer induces a faster hydrolytic degradation on to the fibers. The speed of the hydrolytic degradation is dependent on the monomer amount.
- The effect of the monomer on hydrolytic strength retention of the fiber can be evaluated on the basis of the monomer content, fiber molecular weight and starting mechanical properties. This thesis shows three different kinds of hydrolytic degradation behavior patterns depending on the monomer content.

3)

- Fibers from medical grade P(L/D)LA 96/4 polymers can be produced that enable the textile manufacturing. The fiber properties and textile processes can be adjusted to allow the further manufacturing of different scaffolds for tissue engineering application.

- By altering the knitting parameters it is possible to affect the properties of the scaffolds.
- The fiber quality as a parameter has a stronger influence on hydrolytic degradation properties than the knitting parameters.
- The gamma irradiated knitted P(L/D)LA 96/4 products retain their molecular and mechanical properties at least three years in storage conditions.
- Even when thin fibers with high surface area are used for the knit/implant/scaffolds the degradation time for the P(L/D)LA 96/4 is relatively long. This needs to be taken into account when finding a suitable target tissue.

4)

- The in vitro degradation was faster for the P(L/D)LA 96/4 fibers than the in vivo degradation.
- The knitted and rolled cylindrical P(L/D)LA 96/4 scaffold is a tissue-engineered construct since it can be implanted and it fills in with the connective tissue which then carries the mechanical load better than the scaffold.

5) Different fabrication methods were successfully used to manufacture the scaffolds for cell culturing purposes, intervertebral disc and temporomandibular joint applications with sufficient mechanical properties.

6) The oxygen plasma treatment can be used to increase the hydrophilicity and wetting properties of P(L/D)LA 96/4 fibrous scaffolds. It also promotes the cell attachment and proliferation.

References

Abe, H., Takahashi, N., Kim, K.J., Mochizuki, M. & Doi, Y. 2004, "Thermal Degradation Processes of End-Capped Poly(l-lactide)s in the Presence and Absence of Residual Zinc Catalyst", Biomacromolecules, vol. 5, pp. 1606-1614.

Ahmed, J., Zhang, J.-X., Song, Z. & Varshney, K. 2009, “Thermal Properties of Polylactides. Effect of molecular mass and nature of lactide isomer”, Journal of Thermal Analysis and Calorimetry, vol. 95, no. 3, pp. 957-964.

Andriano, K.P., Pohjonen, T. & Törmälä, P. 1994, "Processing and Characterization of Absorbable Polylactide Polymers for Use in Surgical Implants", Journal of Applied Biomaterials, vol. 5, pp. 133-140.

Babanalbandi, A., Hill, D.J.T., O´Donnel, J.H., Pomery, P.J. & Whittaker, A. 1995, "An electron spin resonance study on y-irradiated poly(L-lactic acid) and poly(D,L-lactic acid) ", Polymer Degradation and Stability, vol. 50, no. 3, pp. 297-304.

Bergsma, J.E., Rozema, F.R., Bos, R.R.M., Rozendaal, A.W.M., Jong, W.H., Teppema, J.S. & Joziasse, C.A.P. 1995, "Biocompatibility and degradation mechanisms of predegraded and non-predegraded poly(lactide) implants: an animal study", Journal of Materials Science: Materials in Medicine, vol. 6, no. 12, pp. 715-724.

Birkinshaw, C., Buggy, M., Henn, G.G. & Jones, E. 1992, "Irradiation of poly-d,l-lactide", Polymer Degradation and Stability, vol. 38, no. 3, pp. 249-253.

Bonnichon, P., Sarfati, P.O., Santoni, P., Jeanty, I., Meatchi, T., Crougneau, S., Pariente, D. & Ming, L.S. 1996, "Absorbable Adams-DeWeese caval clip: an experimental study", Annals of vascular surgery, vol. 6, pp. 517-523.

Böstman, O. & Pihlajamäki, H. 2000, "Clinical biocompatibility of biodegradable orthopaedic implants for internal fixation: a review", Biomaterials, vol. 21, no. 24, pp. 2615-2621.

Burkersroda, F.V., Schedl, L. & Göpferich, A. 2002, "Why degradable polymers undergo surface erosion or bulk erosion", Biomaterials, vol. 23, no. 21, pp. 4221-4231.

Cai, H., Dave, V., Gross, R.A. & McCarthy, S.P. 1996, "Effects of physical aging, crystallinity, and orientation on the enzymatic degradation of poly(lactic acid)", Journal of Polymer Science Part B: Polymer Physics, vol. 34, no. 16, pp. 2701-2708.

Cam, D. & Marucci, M. 1997, "Influence of residual monomers and metals on poly (l-lactide) thermal stability", Polymer, vol. 38, no. 8, pp. 1879-1884.

Cao, Y., Vacanti, J.P., Paige, K.T., Upton, J. & Vacanti, C.A. 1997, "Transplantation of Chondrocytes Utilizing a Polymer-Cell Construct to Produce Tissue-Engineered Cartilage in the Shape of a Human Ear", Plastic and Reconstructive Surgery, vol. 100, no. 2, pp. 297-302.

Carothers, W.H., Dorough, G.L. & van Natta, F.J. 1932, "Studie of the Polymerization and Ring Formation.X. The Reversible Polymerization of Six-Membered Cyclic Esters.",Journal of the American Chemical Society, vol. 54, no. 2, pp. 761-772.

Chabot, F., Vert, M., Chapelle, S. & Granger, P. 1983, "Configurational structures of lactic acid stereocopolymers as determined by 13C□{1H} n.m.r.", Polymer, vol. 24, no. 1, pp. 53-59.

Chen, G., Sato, T., Ohgushi, H., Ushida, T., Tateishi, T. & Tanaka, J. 2005, "Culturing of skin fibroblasts in a thin PLGA–collagen hybrid mesh", Biomaterials, vol. 26, no. 15, pp. 2559-2566.

Cicero, J.A. & Dorgan, J.R. 2001, "Physical Properties and Fiber Morphology of Poly(lactic acid) Obtained from Continuous Two-Step Melt Spinning", Journal of Polymers and the Environment, vol. 9, no. 1, pp. 1-10.

Cicero, J.A., Dorgan, J.R., Garrett, J., Runt, J. & Lin, J.S. 2002a, "Effects of molecular architecture on two-step, melt-spun poly(lactic acid) fibers", Journal of Applied Polymer Science, vol. 86, no. 11, pp. 2839-2846.

Cicero, J.A., Dorgan, J.R., Janzen, J., Garrett, J., Runt, J. & Lin, J.S. 2002b, "Supramolecular morphology of two-step, melt-spun poly(lactic acid) fibers", Journal of Applied Polymer Science, vol. 86, no. 11, pp. 2828-2838.

Cooper, J.A., Lu, H.H., Ko, F.K., Freeman, J.W. & Laurencin, C.T. 2005, "Fiber-based tissue-engineered scaffold for ligament replacement: design considerations and in vitro evaluation", Biomaterials, vol. 26, no. 13, pp. 1523-1532.

Cordewener, F.W., Rozema, F.R., Bos, R.R.M. & Boering, G. 1995, "Material properties and tissue reactions during degradation of poly (96L/4D-Lactide)-a study in vitro and in rats", Journal of Materials Science: Materials in Medicine, vol. 6, pp. 211-217.

Cordewener, F.W., van Geffen, M.F., Joziasse, C.A.P., Schmitz, J.P., Bos, R.R.M., Rozema, F.R. & Pennings, A.J. 2000, "Cytotoxicity of poly(96l/4d-lactide): the influence of degradation and sterilization", Biomaterials, vol. 21, no. 23, pp. 2433-2442.

Cutright, D.E. & Hunsuck, E.E. 1971, "Tissue reaction to the biodegradable polylactic acid suture", Oral Surgery, Oral Medicine, Oral Pathology, vol. 31, no. 1, pp. 134-139.

Dai, W., Kawazoe, N., Lin, X., Dong, J. & Chen, G. 2010, "The influence of structural design of PLGA/collagen hybrid scaffolds in cartilage tissue engineering", Biomaterials, vol. 31, no. 8, pp. 2141-2152.

Dietmar W.H., 2000, "Scaffolds in tissue engineering bone and cartilage", Biomaterials, vol. 21, no. 24, pp. 2529-2543.

Ekevall, E., Golding, C. & Mather, R.R. 2004, " Design of textile scaffolds for tissue engineering: the use of biodegradable yarns", International Journal of Clothing Science and Technology, vol. 16, no. 1/2.

Emirhanova, N. & Kavusturan, Y. 2008, "Effect of knit structure on the dimensional and physical properties of winter outerwear knitted fabrics.", FIBRES & TEXTILES in eastern Europe, vol. 16, no. 2(67), pp. 69-74.

Fambri, L., Pegoretti, A., Fenner, R., Incardona, S.D. & Migliaresi, C. 1997, "Biodegradable fibres of poly(l-lactic acid) produced by melt spinning", Polymer, vol. 38, no. 1, pp. 79-85.

Fambri, L. & Migliaresi, C. 2010, "Crystallization and Thermal Properties" in Poly(lactic acid): Synthesis, structures, properties, and applications., eds. R. Auras, L. Lim, S.E.M. Selke & H. Tsuji, A John Wiley & Sons, Inc, Hoboken, New Jersey, pp. 113-124.

Filgueiras, M.R.T., La Torre, G. & Hench, L.L. 1993, "Solution effects on the surface reactions of three bioactive glass compositions", Journal of Biomedical Materials Research, vol. 27, pp. 445-453.

Fischer, E.W., Sterzel, H.J. & Wegner, G. 1973, "Investigation of the structure of solution grown crystals of lactide copolymers by means of chemical reactions", Kolloid-Zeitschrift und Zeitschrift für Polymere, no. 251, pp. 980-990.

Fourné, F. 1999, Synthetic Fibers: Machines and Equipment, Manufacture, properties, Hanser Publishers, Munich.

Freeman, J.W., Woods, M.D. & Laurencin, C.T. 2007, "Tissue engineering of the anterior cruciate ligament using a braid–twist scaffold design", Journal of Biomechanics, vol. 40, no. 9, pp. 2029-2036.

Gao, J., Niklason, L. & Langer, R. 1998, "Surface hydrolysis of poly(glycolic acid) meshes increases the seeding density of vascular smooth muscle cells", Journal of Biomedical Materials Research, vol. 42, no. 3, pp. 417-424.

Ginsberg, G., Cope, C., Shah, J., Martin, T., Carty, A., Habecker, P., Kaufmann, C., Clerc, C., Nuutinen, J. & Törmälä, P. 2003, "In vivo evaluation of a new bioabsorbable self-expanding biliary stent.", Gastrointestinal Endoscopy, vol. 58, no. 5, pp. 777-784.

Grizzi, I., Garreau, H., Li, S. & Vert, M. 1995, "Hydrolytic degradation of devices based on poly(dl-lactic acid) size-dependence", Biomaterials, vol. 16, no. 4, pp. 305-311.

Groot, W., van Krieken, J., Sliekersl, O. & de Vos, S. 2010, "Production and purification of lactic acid and lactide" in Poly(lactic acid): Synthesis, structures, properties, and applications., eds. R. Auras, L. Lim, S.E.M. Selke & H. Tsuji, A John Wiley & Sons, Inc, Hoboken, New Jersey, pp. 3-18.

Gruber, P., Hall, E. & Kolstad, J. 1992, “Continuous process for manufacture of lactide polymers with controlled optical purity.” U.S.Patent 5258488

Guarino, V., Causa, F., Taddei, P., di Foggia, M., Ciapetti, G., Martini, D., Fagnano, C., Baldini, N. & Ambrosio, L. 2008, "Polylactic acid fibre-reinforced polycaprolactone scaffolds for bone tissue engineering", Biomaterials, vol. 29, no. 27, pp. 3662-3670.

Gupta, B. & Revagade, N. 2009, "Development and structural evaluation of poly(lactic acid) based knitted scaffold for human urinary bladder reconstruction", Indian Journal of Fibre & Textile Research, vol. 34, pp. 115-121.

Gupta, B., Revagade, N., Anjum, N., Atthoff, B. & Hilborn, J. 2006, "Preparation of poly(lactic acid) fiber by dry-jet-wet-spinning. I. Influence of draw ratio on fiber properties", Journal of Applied Polymer Science, vol. 100, no. 2, pp. 1239-1246.

Gupta, M.C. & Deshmukh, V.G. 1982, "Thermal oxidative degradation of poly-lactic acid Part II: Molecular weight and electronic spectra during isothermal heating", Colloid & Polymer Science, vol. 260, no. 5, pp. 514-517.

Hakkarainen, M., Karlsson, S. & Albertsson, A.-C. 2000, ”Influence of the Low Molecular Weight Lactic Acid Derivatives on Degradability of Polylactide”, Journal of Applied Polymer Science, vol.76, pp. 228-239.

Heino, A., Naukkarinen, A., Kulju, T., Törmälä, P., Pohjonen, T. & Mäkelä, E.A. 1996, "Characteristics of poly(L-)lactic acid suture applied to fascial closure in rats", Journal of Biomedical Materials Research, vol. 30, no. 2, pp. 187-192.

Hietala, E., Salminen, U., Ståhls, A., Välimaa, T., Maasilta, P., Törmälä, P., Nieminen, M.S. & Harjula, A.L.J. 2001, "Biodegradation of the copolymeric polylactide stent. Long-term follow-up in a rabbit aorta model", Journal of Vascular Research, vol. 38, pp. 361-369.

Honkanen, P.B., Kellomäki, M., Lehtimäki, M.Y., Törmälä, P., Mäkelä, S. & Lehto, M.U.K. 2003, "Bioreconstructive Joint Scaffold Implant Arthroplasty in Metacarpophalangeal Joints: Short-Term Results of a New Treatment Concept in Rheumatoid Arthritis Patients", Tissue engineering, vol. 9, no. 5, pp. 957-965.

Honkanen, P.B., Tiihonen, R., Skyttä, E.T., Ikävalko, M., Lehto, M.U.K. & Konttinen, Y.T. 2010, "Bioreconstructive poly-L/D-lactide implant compared with Swanson prosthesis in metacarpophalangeal joint arthroplasty in rheumatoid patients: a randomized clinical trial", Journal of Hand Surgery (European Volume), vol. 35, no. 9, pp. 746-753.

Huttunen, M., Ashammakhi, N., Törmälä, P. & Kellomäki, M. 2006, "Fibre reinforced bioresorbable composites for spinal surgery", Acta Biomaterialia, vol. 2, no. 5, pp. 575-587.

Hyon, S.-H., Jamshidi, K. & Ikada, Y. 1998, "Effects of residual monomer on the degradation of DL-lactide polymer", Polymer International, vol. 46, no. 3, pp. 196-202.

Ikada, Y. 2006, "Scope of Tissue Engineering" in Tissue Engineering: Fundamentals and Applications, Elsevier Ltd, Oxford, pp. 1-89.

Incardona, S.D., Fambri, L. & Migliaresi, C. 1996, "Poly-L-lactic acid braided fibres produced by melt spinning: characterization and in vitro degradation", Journal of Materials Science: Materials in Medicine, vol. 7, no. 7, pp. 387-391.

Jamshidi, K., Hyon, S.-H. & Ikada, Y. 1988, "Thermal characterization of polylactides", Polymer, vol. 29, no. 12, pp. 2229-2234.

Jiang, X., Luo, Y., Tian, X., Huang, D., Reddy, N. & Yang, Y. 2010, "Chemical structure of poly(lactic acid)" in Poly(lactic acid): Synthesis, structures, properties, and applications., eds. R. Auras, L. Lim, S.E.M. Selke & H. Tsuji, A John Wiley & Sons, Inc, Hoboken, New Jersey, pp. 69-82.

Kandziora, F., Pflugmacher, R., Scholz, M., Eindorf, T., Schnake, K.J. & Haas, N.P. 2004, "Bioabsorbable Interbody Cages in a Sheep Cervical Spine Fusion Model", Spine, vol. 29, no. 17, pp. 1845-1855.

Kangas, J., Paasimaa, S., Mäkelä, P., Leppilahti, J., Törmälä, P., Waris, T. & Ashammakhi, N. 2001, "Comparison of strength properties of poly-L/D-lactide (PLDLA) 96/4 and polyglyconate (Maxon®) sutures: In vitro, in the subcutis, and in the achilles tendon of rabbits", Journal of Biomedical Materials Research, vol. 58, no. 1, pp. 121-126.

Kellomäki, M., Pohjonen, T. & Törmälä, P. 2003, "Self Reinforced POlylactides: Optimization of Degradation and Mechanical Properties" in Biodegradable Polymers, ed. R. Arshady, Citius Books, London, pp. 211-235.

Kellomäki, M. 2000, “Bioabsorbable and Bioactive Polymers and Composites for Tissue Engineering Applications”, Dissertation, Tampere University of Technology, Tampere, Finland.

Kellomäki, M., Niiranen, H., Puumanen, K., Ashammakhi, N., Waris, T. & Törmälä, P. 2000b, "Bioabsorbable scaffolds for guided bone regeneration and generation", Biomaterials, vol. 21, no. 24, pp. 2495-2505.

Kellomäki, M., Puumanen, K., Waris, T. & Törmälä, P. 2000a, "In Vivo Degradation of Composite Membrane of P(ε-CL/L-LA) 50/50 Film and P(L/D)LA 96/4 Mesh" in Materials for Medical Engineering., eds H. Stallforth & P.A. Revell, Wiley-VCH, Weinheim, pp. 79-85.

Kellomäki, M. & Törmälä, P. 2004, "Processing of Resorbable Poly-α-Hydroxy Acids for Use as Tissue-Engineering Scaffolds" in Biopolymer Methods in Tissue Engineering, eds. A.P. Hollander & P.V. Hatton, Humana Press, New Jersey, pp. 1-10.

Khondker, O.A., Herszberg, I. & Leong, K.H. 2001, "An investigation of the structure-property relationship of knitted composites", Journal of Composite Materials, vol. 35, no. 6, pp. 489-508.

Khorasani, M.T., Mirzadeh, H. & Irani, S. 2009, "Comparison of fibroblast and nerve cells response on plasma treated poly (L-lactide) surface", Journal of Applied Polymer Science, vol. 112, no. 6, pp. 3429-3435.

Koch, S., Flanagan, T.C., Sachweh, J.S., Tanios, F., Schnoering, H., Deichmann, T., Ellä, V., Kellomäki, M., Gronloh, N., Gries, T., Tolba, R., Schmitz-Rode, T. & Jockenhoevel, S. 2010, "Fibrin-polylactide-based tissue-engineered vascular graft in the arterial circulation", Biomaterials, vol. 31, no. 17, pp. 4731-4739.

Kopinke, F.D., Remmler, M., Mackenzie, M., Möder, M. & Wachsen, O. 1996, "Thermal decomposition of biodegradable polyesters-II. Poly(lactic acid)", Polymer Degradation and Stability, vol. 53, pp. 329-342.

Kowalski, J.B. & Morrissey, R.F. 1996, “Sterilization of Implants” in Biomaterials Science: An Introduction to Materials in Medicine., eds. B.D. Ratner, A.S. Hoffman, F.J. Schoen, & J.E. Lemmons. Academic Press, San Diego, pp. 415-420

Kulkarni, R.K., Pani, K.C., Neuman, C. & Leonard, F. 1966, "Polylactic acid for surgical implants", Archives of Surgery, vol. 93, pp. 839-843.

Kumar, G., Tison, C.K., Chatterjee, K., Pine, P.S., McDaniel, J.H., Salit, M.L., Young, M.F. & Simon Jr., C.G. 2011, "The determination of stem cell fate by 3D scaffold structures through the control of cell shape", Biomaterials, vol. 32, no. 35, pp. 9188-9196.

Laaksovirta, S., Välimaa, T., Isotalo, T., Törmälä, P., Talja, M. & Tammela, T.L.J. 2003, "Encrustation and Strength Retention Properties of the Self-expandable, Biodegradable, Self-reinforced L-Lactide-Glycolic Acid Co-polymer 80:20 Spiral Urethral Stent In Vitro", The Journal of urology, vol. 170, no. 2, Part 1, pp. 468-471.

Langer, R. & Vacanti, J.P. 1993, "Tissue engineering ", Science, vol. 260, no. 5110, pp. 920-926.

Länsman, S., Pääkkö, P., Ryhänen, J., Kellomäki, M., Waris, E., Törmälä, P., Waris, T. & Ashammakhi, N. 2006, "Poly-L/D-lactide (PLDLA) 96/4 Fibrous Implants: Histological Evaluation in the Subcutis of Experimental Design", Journal of Craniofacial Surgery, vol. 17, no. 6, pp. 1121-1128.

Lazennec, J., Madi, A., Rousseau, M., Roger, B. & Saillant, G. 2006, "Evaluation of the 96/4 PLDLLA polymer resorbable lumbar interbody cage in a long term animal model", European Spine Journal, vol. 15, no. 10, pp. 1545-1553.

Leong, K.H., Ramakrishna, S., Huang, Z.M. & Bibo, G.A. 2000, "The potential of knitting for engineering composites-a review", Composites: Part A applied science and manufacturing, vol. 31, pp. 197-220.

Li, S.M., Garreau, H. & Vert, M. 1990, "Structure-property relationships in the case of the degradation of massive aliphatic poly-(α-hydroxy acids) in aqueous media", Journal of Materials Science: Materials in Medicine, vol. 1, no. 3, pp. 123-130.

Li, S. 1999, "Hydrolytic degradation characteristics of aliphatic polyesters derived from lactic and glycolic acids", Journal of Biomedical Materials Research, vol. 48, no. 3, pp. 342-353.

Lieshout, M.V., Peters, G., Rutten, M. & Baaijens, F. 2006, "A Knitted, Fibrin-Covered Polycaprolactone Scaffold for Tissue Engineering of the Aortic Valve", Tissue engineering, vol. 12, no. 3, pp. 481-487.

Lindeque, B.G. 2007, "Gynaecological operations" in Clinical Gynaecology, eds. T.F. Kruger & M.H. Botha, 3rd, Juta & Co. Ltd, Cape Town, pp. 553-563.

Liu, H., Fan, H., Wang, Y., Toh, S.L. & Goh, J.C.H. 2008, "The interaction between a combined knitted silk scaffold and microporous silk sponge with human mesenchymal stem cells for ligament tissue engineering", Biomaterials, vol. 29, no. 6, pp. 662-674.

Liu, X., Zou, Y., Li, W., Cao, G. & Chen, W. 2006, "Kinetics of thermo-oxidative and thermal degradation of poly(d,l-lactide) (PDLLA) at processing temperature", Polymer Degradation and Stability, vol. 91, no. 12, pp. 3259-3265.

Lu, H.H., Cooper Jr., J.A., Manuel, S., Freeman, J.W., Attawia, M.A., Ko, F.K. & Laurencin, C.T. 2005, "Anterior cruciate ligament regeneration using braided biodegradable scaffolds: in vitro optimization studies", Biomaterials, vol. 26, no. 23, pp. 4805-4816.

Lumiaho, J., Heino, A., Kauppinen, T., Talja, M., Alhava, E., Välimaa, T. & Törmälä, P. 2007, "Drainage and antireflux characteristics of a biodegradable self-reinforced, self-expanding X-ray positive poly-L-D-lactide spiral partial ureteral sten: an experimental study", Journal of Endourology / Endourological society, vol. 21, no. 12, pp. 1559-1564.

Mäenpää, K., Ellä, V., Mauno, J., Kellomäki, M., Suuronen, R., Ylikomi, T. & Miettinen, S. 2010, "Use of adipose stem cells and polylactide discs for tissue engineering of the temporomandibular joint disc", Journal of the Royal Society Interface, vol. 7, no. 42, pp. 177-188.

Mainil-Varlet, P., Rahn, B. & Gogolewski, S. 1997, "Long-term in vivo degradation and bone reaction to various polylactides: 1. One-year results", Biomaterials, vol. 18, no. 3, pp. 257-266.

Mäkelä, P., Pohjonen, T., Törmälä, P., Waris, T. & Ashammakhi, N. 2002, "Strength retention properties of self-reinforced poly l-lactide (SR-PLLA) sutures compared with polyglyconate (Maxon®) and polydioxanone (PDS) sutures. An in vitro study", Biomaterials, vol. 23, no. 12, pp. 2587-2592.

Mauno, J., Hagström, J., Mäenpää, K., Ellä, V., Miettinen, S., Kellomäki, M., Ylikomi, T., Lindqvist, C. & Suuronen, R. 2008, "The effect of adipose stem cells on tissue engineering of the rabbit temporo-mandibular joint disc: Evaluation with cone beam computed tomography .", Proceedings of the 5th Tampere Tissue Engineering Symposium, ed. J.M.A. Tanskanen, April 23-25.

McNeill, I.C. & Leiper, H.A. 1985, "Degradation studies of some polyesters and polycarbonates—2. Polylactide: Degradation under isothermal conditions, thermal degradation mechanism and photolysis of the polymer", Polymer Degradation and Stability, vol. 11, no. 4, pp. 309-326.

Mezghani, K. & Spruiell, J.E. 1998, "High speed melt spinning of poly(L-lactic acid) filaments", Journal of Polymer Science Part B: Polymer Physics, vol. 36, no. 6, pp. 1005-1012.

Middleton, J.C. & Tipton, A.J. 2000, "Synthetic biodegradable polymers as orthopedic devices", Biomaterials, vol. 21, no. 23, pp. 2335-2346.

Migliaresi, C., De Lollis, A., Fambri, L. & Cohn, D. 1991, "The effect of thermal history on the crystallinity of different molecular weight PLLA biodegradable polymers", Clinical Materials, vol. 8, no. 1-2, pp. 111-118.

Miller, D.C., Thapa, A., Haberstroh, K.M. & Webster, T.J. 2004, "Endothelial and vascular smooth muscle cell function on poly(lactic-co-glycolic acid) with nano-structured surface features", Biomaterials, vol. 25, no. 1, pp. 53-61.

Morent, R., De Geyter, N., Desmet, T., Dubruel, P. & Leys, C. 2011, "Plasma Surface Modification of Biodegradable Polymers: A Review", Plasma Processes and Polymers, vol. 8, no. 3, pp. 171-190.

Nair, L.S. & Laurencin, C.T. 2007, "Biodegradable polymers as biomaterials", Progress in Polymer Science, vol. 32, no. 8-9, pp. 762-798.

Nakagawa, M., Teraoka, F., Fujimoto, S., Hamada, Y., Kibayashi, H. & Takahashi, J. 2006, "Improvement of cell adhesion on poly(L-lactide) by atmospheric plasma treatment", Journal of Biomedical Materials Research Part A, vol. 77A, no. 1, pp. 112-118.

Ng, K.W., Khor, H.L. & Hutmacher, D.W. 2004, "In vitro characterization of natural and synthetic dermal matrices cultured with human dermal fibroblasts", Biomaterials, vol. 25, no. 14, pp. 2807-2818.

Niiranen, H. & Törmälä, P. 1999, "Bioabsorbable polymer plates coated with bioactive glass spheres", Journal of Materials Science: Materials in Medicine, vol. 10, no. 12, pp. 707-710.

Nisbet, D.R., Pattanawong, S., Nunan, J., Shen, W., Horne, M.K., Finkelstein, D.I. & Forsythe, J.S. 2006, "The effect of surface hydrophilicity on the behavior of embryonic cortical neurons", Journal of Colloid and Interface science, vol. 299, no. 2, pp. 647-655.

Nishida, H. 2010, "Thermal degradation" in Poly(lactic acid): Synthesis, structures, properties, and applications., eds. R. Auras, L. Lim, S.E.M. Selke & H. Tsuji, A John Wiley & Sons, Inc, Hoboken, New Jersey, pp. 401-412.

Nuutinen, J., Clerc, C., Reinikainen, R. & Törmälä, P. 2003b, "Mechanical properties and in vitro degradation of bioabsorbable self-expanding braided stents.", Journal of Biomaterials Science Polymer Edition, vol. 14, no. 3, pp. 255-266.

Nuutinen, J., Clerc, C. & Törmälä, P. 2003a, "Mechanical properties and in vitro degradation os self-reinforced radiopaque bioresorbable polylactide fibres.", Journal of Biomaterials Science Polymer Edition, vol. 14, no. 7, pp. 665-676.

Nuutinen, J., Clerc, C., Virta, T. & Törmälä, P. 2002a, "Effect of gamma, ethylen oxide, electron beam and plasma sterilization on the behaviour of SR-PLLA fibres in vitro.", Journal of Biomedical Science Polymer Edition, vol. 13, no. 12, pp. 1325-1336.

Nuutinen, J., Välimaa, T., Clerc, C. & Törmälä, P. 2002b, "Mechanical properties and in vitro degradation of bioresorbable knitted stents", Journal of Biomaterilas Science Polymer Edition, vol. 13, no. 12, pp. 1313-1323.

Ormiston, J.A., Webster, M.W.I. & Armstrong, G. 2007, "First-in-human implantation of a fully bioabsorbable drug-eluting stent: The BVS poly-L-lactic acid everolimus-eluting coronary stent", Catheterization and Cardiovascular Interventions, vol. 69, no. 1, pp. 128-131.

Ouyang, H.W., Goh, J.C.H., Thambyah, A., Teoh, S.H. & Lee, E.H. 2003, "Knitted Poly-lactide-co-glycolide Scaffold Loaded with Bone Marrow Stromal Cells in Repair and Regeneration of Rabbit Achilles Tendon", Tissue Engineering, vol. 9, no. 3, pp. 431-439.

Ouyang, H.W., Toh, S.L., Goh, J., Tay, T.E. & Moe, K. 2005, "Assembly of bone marrow stromal cell sheets with knitted poly (L-lactide) scaffold for engineering ligament analogs", Journal of Biomedical Materials Research Part B: Applied Biomaterials, vol. 75B, no. 2, pp. 264-271.

Paakinaho, K., Heino, H., Väisänen, J., Törmälä, P. & Kellomäki, M. 2011, "Effects of lactide monomer on the hydrolytic degradation of poly(lactide-co-glycolide) 85L/15G", Journal of the Mechanical Behavior of Biomedical Materials, vol. 4, no. 7, pp. 1283-1290.

Palade, L., Lehermeier, H.J. & Dorgan, J.R. 2001, "Melt Rheology of High L-Content Poly(lactic acid)", Macromolecules, vol. 34, no. 5, pp. 1384-1390.

Palmgren, T., Ylinen, P., Tulamo, R., Kellomäki, M., Törmälä, P. & Rokkanen, P. 2003, "Lumbar intervertebral disc replacement using bioabsorbable self-reinforced poly-L-lactide full-threaded screws, or cylindrical implants of polylactide polymers, bioactive glass and polyactive", Veterinary and Comparative Orthopaedics and Traumatology, vol. 16, pp. 138-144.

Park, S. & Seo, M. 2011, "Chapter 3: Basic Technologies Developed for Tissue Engineering" in Interface Science and Technology, Oxford, Elsevier Ltd, pp. 235-421.

Park, G.E., Pattison, M.A., Park, K. & Webster, T.J. 2005, "Accelerated chondrocyte functions on NaOH-treated PLGA scaffolds", Biomaterials, vol. 26, no. 16, pp. 3075-3082.

Pegoretti, A., Fambri, L. & Migliaresi, C. 1997, "In vitro degradation of poly(L-lactic acid) fibers produced by melt spinning", Journal of Applied Polymer Science, vol. 64, no. 2, pp. 213-223.

Perka, C., Schultz, O., Spitzer, R., Lindenhayn, K., Burmester, G. & Sittinger, M. 2000, "Segmental bone repair by tissue-engineered periosteal cell transplants with bioresorbable fleece and fibrin scaffolds in rabbits", Biomaterials, vol. 21, no. 11, pp. 1145-1153.

Pluta, M., Murariu, M., Alexandre, M., Galeski, A. & Dubois, P. 2008, "Polylactide compositions. The influence of ageing on the structure, thermal and viscoelastic properties of PLA/calcium sulfate composites", Polymer Degradation and Stability, vol. 93, no. 5, pp. 925-931.

Pohjonen, T. & Törmälä, P. 1994, "Hydrolytic degradation of ultra-high-strength-reinforced poly-L-lactide. A temperature dependence study." in In Biodegradable Implants in Fracture Fixation, eds. K.S. Leung, L.K. Hung & P.C. Leung, Department of Orthopaedics and Traumatology, The Chinese University of Honk Kong and World Scientific Publishing Co. Pte. Ltd, Singapore, pp. 75-88.

Pu, F., Rhodes, N.P., Bayon, Y., Chen, R., Brans, G., Benne, R. & Hunt, J.A. 2010, "The use of flow perfusion culture and subcutaneous implantation with fibroblast-seeded PLLA-collagen 3D scaffolds for abdominal wall repair", Biomaterials, vol. 31, no. 15, pp. 4330-4340.

Ramakrishna, S. 1997, "Characterization and modeling of the tensile properties of plain weft-knit fabric-reinforced composites." Composites Science and Technology, vol. 57, pp. 1-22.

Ramakrishna, S. & Huang, Z. 2003, "9.06 - Biocomposites" in Comprehensive Structural Integrity, eds. I. Milne, O. Ritchie & B. Karihaloo, Pergamon, Oxford, pp. 215-296.

Ramakrishna, S., Mayer, J., Wintermantel, E. & Leong, K.W. 2001, "Biomedical applications of polymer-composite materials: a review", Composites Science and Technology, vol. 61, no. 9, pp. 1189-1224.

Ramkumar, D.H.S. & Bhattacharya, M. 1998, "Steady shear and dynamic properties of biodegradable polyesters", Polymer Engineering & Science, vol. 38, no. 9, pp. 1426-1435.

Rim, N.G., Kim, S.J., Shin, Y.M., Jun, I., Lim, D.W., Park, J.H. & Shin, H. 2012, "Mussel-inspired surface modification of poly(L-lactide) electrospun fibers for modulation of osteogenic differentiation of human mesenchymal stem cells", Colloids and Surfaces B: Biointerfaces, vol. 91, pp. 189-197.

Rotter, N., Aigner, J., Naumann, A., Planck, H., Hammer, C., Burmester, G. & Sittinger, M. 1998, "Cartilage reconstruction in head and neck surgery: Comparison of resorbable polymer scaffolds for tissue engineering of human septal cartilage", Journal of Biomedical Materials Research, vol. 42, no. 3, pp. 347-356.

Saikku-Bäckström, A., Tulamo, R., Pohjonen, T., Törmälä, P., Räihä, J.E. & Rokkanen, P. 1999, "Material properties of a absorbable self-reinforced fibrillated poly-96L/4D-lactide (SR-PLA96) rods; a study in vitro and in vivo", Journal of Materials Science: Materials in Medicine, vol. 10, no. 1, pp. 1-8.

Saikku-Bäckström, A., Tulamo, R., Räihä, J.E., Pohjonen, T., Toivonen, T., Törmälä, P. & Rokkanen, P. 2004, "Intramedullary fixation of femoral cortical osteotomies with interlocked biodegradable self-reinforced poly-96l/4d-lactide (SR-PLA96) nails", Biomaterials, vol. 25, no. 13, pp. 2669-2677.

Sakai, W. & Tsutsumi, N. 2010, "Photodegradation and radiation degradation" in Poly(lactic acid): Synthesis, structures, properties, and applications., eds. R. Auras, L. Lim, S.E.M. Selke & H. Tsuji, A John Wiley & Sons, Inc, Hoboken, New Jersey, pp. 413-421.

Sarasua, J., Prud'homme, R.E., Wisniewski, M., Le Borgne, A. & Spassky, N. 1998, "Crystallization and melting behavior of polylactides", Macromolecules, vol. 31, no. 12, pp. 3895-3905.

Sarasua, J., López-Rodríguez, N., Zuza, E., Petisco, S., Castro, B., del Olmo, M., Palomares, T. & Alonso-Varona, A. 2011, "Crystallinity assessment and in vitro cytotoxicity of polylactide scaffolds for biomedical applications", Journal of Materials Science: Materials in Medicine, vol. 22, no. 11, pp. 2513-2523.

Schliecker, G., Schmidt, C., Fuchs, S., Wombacher, R. & Kissel, T. 2003, "Hydrolytic degradation of poly(lactide-co-glycolide) films: effect of oligomers on degradation rate and crystallinity", International journal of pharmaceutics, vol. 266, no. 1–2, pp. 39-49.

Schmack, G., Tändler, B., Vogel, R., Beyreuther, R., Jacobsen, S. & Fritz, H. 1999, "Biodegradable Fibers of Poly(L-lactide) Produced by High-Speed Melt Spinning and Spin Drawing", Journal of Applied Polymer Science, vol. 73, no. 14, pp. 2785-2797.

Schmack, G., Jehnichen, D., Vogel, R., Tändler, B., Beyreuther, R., Jacobsen, S. & Fritz, H. 2001, "Biodegradable fibres spun from poly(lactide) generated by reactive extrusion", Journal of Biotechnology, vol. 86, no. 2, pp. 151-160.

Schmack, G., Tändler, B., Optiz, G., Vogel, R., Komber, H., Häußler, L., Voigt, D., Weinmann, S., Heinemann, M. & Fritz, H. 2004, "High-speed melt spinning of various grades of polylactides", Journal of Applied Polymer Science, vol. 91, no. 2, pp. 800-806.

Schmitt, E.E. & Polistina, R.A. 1967, Surcigal sutures. US.Patent 3297033

Scholz, M., Blanchfield, J.P., Bloom, L.D., Coburn, B.H., Elkington, M., Fuller, J.D., Gilbert, M.E., Muflahi, S.A., Pernice, M.F., Rae, S.I., Trevarthen, J.A., White, S.C., Weaver, P.M. & Bond, I.P. 2011, "The use of composite materials in modern orthopaedic medicine and prosthetic devices: A review", Composites Science and Technology, vol. 71, no. 16, pp. 1791-1803.

Sittinger, M., Bujia, J., Minuth, W.W., Hammer, C. & Burmester, G.R. 1994, "Engineering of cartilage tissue using bioresorbable polymer carriers in perfusion culture", Biomaterials, vol. 15, no. 6, pp. 451-456.

Sittinger, M., Reitzel, D., Dauner, M., Hierlemann, H., Hammer, C., Kastenbauer, E., Planck, H., Burmester, G.R. & Bujia, J. 1996, "Resorbable polyesters in cartilage engineering: Affinity and biocompatibility of polymer fiber structures to chondrocytes", Journal of Biomedical Materials Research, vol. 33, no. 2, pp. 57-63.

Södergård, A. & Näsman, J. 1996, “Melt Stability Study of Various Types of Poly(L-lactide)”, Industrial & Engineering Chemistry Research, vol. 35, no. 3, pp. 732-735.

Södergård, A. & Stolt, M. 2002, "Properties of lactic acid based polymers and their correlation with composition", Progress in Polymer Science, vol. 27, no. 6, pp. 1123-1163.

Solarski, S., Ferreira, M. & Devaux, E. 2007, "Thermal and mechanical characteristics of polylactide filaments drawn at different temperatures", Journal of the Textile Institute, vol. 98, no. 3, pp. 227-236.

Suuronen, R., Pohjonen, T., Hietanen, J. & Lindqvist, C. 1998, "A 5-year in vitro and in vivo study of the biodegradation of polylactide plates", Journal of Oral and Maxillofacial Surgery, vol. 56, no. 5, pp. 604-614.

Tadmor, Z. & Gogos, C.G. 2006, Principles of Polymer Processing, 2nd edition, John Wiley & Sons, New York.

Takasaki, M., Ito, H. & Kikutani, T. 2003a, "Structure Development of Polylactides with Various D-Lactide Contents in the High-Speed Melt Spinning Process", Journal of Macromolecular Science, vol. B42, no. 1, pp. 57-73.

Takasaki, M., Ito, H. & Kikutani, T. 2003b, "Structure Development of Polylactides with Various D-Lactide Contents in the High-Speed Melt Spinning Process", Journal of Macromolecular Science, vol. B42, no. 3, pp. 403-420.

Taubner, V. & Shishoo, R. 2001, "Influence of processing parameters on the degradation of poly(L-lactide) during extrusion", Journal of Applied Polymer Science, vol. 79, no. 12, pp. 2128-2135.

Tian, H., Tang, Z., Zhuang, X., Chen, X. & Jing, X. 2012, "Biodegradable synthetic polymers: Preparation, functionalization and biomedical application", Progress in Polymer Science, vol. 37, no. 2, pp. 237-280.

Törmälä, P., Pohjonen, T. & Rokkanen, P. 1998, "Bioabsorbable polymers: Materials technology and surgical applications", Proceedings of the Institution of Mechanical Engineers, Part H: Journal of Engineering in Medicine, vol. 212, pp. 101-111.

Tsuji, H. 2010, "Hydrolytic degradation" in Poly(lactic acid): Synthesis, structures, properties, and applications., eds. R. Auras, L. Lim, S.E.M. Selke & H. Tsuji, A John Wiley & Sons, Inc, Hoboken, New Jersey, pp. 345-381.

Tsuji, H. 2008, Degradation of poly(lactide)-based biodegradable materials, Nova Science Publishers.

Tsuji, H. & Ikada, Y. 2000, "Properties and morphology of poly(l-lactide) 4. Effects of structural parameters on long-term hydrolysis of poly(l-lactide) in phosphate-buffered solution", Polymer Degradation and Stability, vol. 67, no. 1, pp. 179-189.

Tsuji, H., Mizuno, A. & Ikada, Y. 2000, "Properties and morphology of poly(L-lactide). III. Effects of initial crystallinity on long-term in vitro hydrolysis of high molecular weight poly(L-lactide) film in phosphate-buffered solution", Journal of Applied Polymer Science, vol. 77, no. 7, pp. 1452-1464.

Tsuji, H., Saeki, T., Tsukegi, T., Daimon, H. & Fujie, K. 2008, "Comparative study on hydrolytic degradation and monomer recovery of poly(l-lactic acid) in the solid and in the melt", Polymer Degradation and Stability, vol. 93, no. 10, pp. 1956-1963.

Urayama, H., Moon, S. & Kimura, Y. 2003, "Microstructure and Thermal Properties of Polylactides with Different L- and D-Unit Sequences: Importance of the Helical Nature of the L-Sequenced Segments", Macromolecular Materials and Engineering, vol. 288, no. 2, pp. 137-143.

Vaajanen, A., Nuutinen, J., Isotalo, T., Törmälä, P., Tammela, T.L.J. & Talja, M. 2003, "Expansion and fixation properties of a new braided biodegradable urethral stent: An experimental study in the rabbit", The Journal of Urology, vol. 169, pp. 1171-1174.

Välimaa, T. & Laaksovirta, S. 2004, "Degradation behaviour of self-reinforced 80L/20G PLGA devices in vitro", Biomaterials, vol. 25, no. 7–8, pp. 1225-1232.

Vaquette, C., Kahn, C., Frochot, C., Nouvel, C., Six, J., De Isla, N., Luo, L., Cooper-White, J., Rahouadj, R. & Wang, X. 2010, "Aligned poly(L-lactic-co-e-caprolactone) electrospun microfibers and knitted structure: A novel composite scaffold for ligament tissue engineering", Journal of Biomedical Materials Research Part A, vol. 94A, no. 4, pp. 1270-1282.

Vert, M., Li, S. & Garreau, H. 1992, "New Insights on the Degradation of Bioresorable Polymeric Devices Based on Lactic and Glycolic Acids", Clinical materials, vol. 10, pp. 3-8.

Vert, M., Christel, P., Chabot, F. & Leray, J. 1984, "Bioresorbable plastic materials for bone surgery" in Macromolecular materials, eds. G.W. Hastings & P. Ducheyny, CRC press, Inc, Boca Raton, Florida, pp. 119-142.

Vert, M. 2005, "Aliphatic polyesters: great degradable polymers that cannot do everything", Biomacromolecules, vol. 6, no. 2, pp. 538-546.

Viinikainen, A., Göransson, H., Huovinen, K., Kellomäki, M., Törmälä, P. & Rokkanen, P. 2006, "Material and knot properties of braided polyester (Ticron®) and bioabsorbable poly-L/D-lactide (PLDLA) 96/4 sutures", Journal of Materials Science: Materials in Medicine, vol. 17, no. 2, pp. 169-177.

Viinikainen, A., Göransson, H., Huovinen, K., Kellomäki, M., Törmälä, P. & Rokkanen, P. 2009, "Bioabsorbable poly-l/d-lactide (PLDLA) 96/4 triple-stranded bound suture in the modified Kessler repair: an ex vivo static and cyclic tensile testing study in a porcine extensor tendon model", Journal of Materials Science: Materials in Medicine, vol. 20, no. 9, pp. 1963-1969.

von Oepen, R. & Michaeli, W. 1992, "Injection moulding of biodegradable implants", Clinical materials, vol. 10, no. 1-2, pp. 21-28.

Wachsen, O., Platkowski, K. & Reichert, K.H. 1997a, "Thermal degradation of poly-l-lactide—studies on kinetics, modelling and melt stabilisation", Polymer Degradation and Stability, vol. 57, no. 1, pp. 87-94.

Wachsen, O., Reichert, K.H., Krüger, R.P., Much, H. & Schulz, G. 1997b, "Thermal decomposition of biodegradable polyesters- III. Studies on the mechanisms of thermal degradation of oligo-L-la&de using SEC, LACCC and MALDI-TOF-MS", Polymer Degradation and Stability, vol. 55, no. 2, pp. 225-231.

Wan, Y., Tu, C., Yang, J., Bei, J. & Wang, S. 2006, "Influences of ammonia plasma treatment on modifying depth and degradation of poly(l-lactide) scaffolds", Biomaterials, vol. 27, no. 13, pp. 2699-2704.

Wan, Y., Yang, J., Yang, J., Bei, J. & Wang, S. 2003, "Cell adhesion on gaseous plasma modified poly-(l-lactide) surface under shear stress field", Biomaterials, vol. 24, no. 21, pp. 3757-3764.

Wang, Y., Pan, J., Han, X., Sinka, C. & Ding, L. 2008, "A phenomenological model for the degradation of biodegradable polymers", Biomaterials, vol. 29, no. 23, pp. 3393-3401.

Ward, I.M. 1997, Structure and properties of oriented polymers, 2nd edition, Chapman & Hall, London.

Weber, B., Schoenauer, R., Papadopulos, F., Modregger, P., Peter, S., Stampanoni, M., Mauri, A., Mazza, E., Gorelik, J., Agarkova, I., Frese, L., Breymann, C., Kretschmar, O. & Hoerstrup, S.P. 2011, "Engineering of living autologous human umbilical cord cell-based septal occluder membranes using composite PGA-P4HB matrices", Biomaterials, vol. 32, no. 36, pp. 9630-9641.

Weir, N.A., Buchanan, F.J., Orr, J.F., Farrar, D.F. & Boyd, A. 2004a, "Processing, annealing and sterilisation of poly-l-lactide", Biomaterials, vol. 25, no. 18, pp. 3939-3949.

Weir, N.A., Buchanan, F.J., Orr, J.F. & Dickson, G.R. 2004b, "Degradation of poly-L-lactide. Part 1: in vitro and in vivo physiological temperature degradation", Proceedings of the Institution of Mechanical Engineers, Part H: Journal of Engineering in Medicine, vol. 218, no. 5, pp. 307-319.

Wintermantel, E., Mayer, J., Blum, J., Eckert, K.L., Lüscher, P. & Mathey, M. 1996, "Tissue engineering scaffolds using superstructures", Biomaterials, vol. 17, no. 2, pp. 83-91.

Woodruff, M.A. & Hutmacher, D.W. 2010, "The return of a forgotten polymer—Polycaprolactone in the 21st century", Progress in Polymer Science, vol. 35, no. 10, pp. 1217-1256.

Wu, W., Feng, X., Mao, T., Feng, X., Ouyang, H., Zhao, G. & Chen, F. 2007, "Engineering of human tracheal tissue with collagen-enforced poly-lactic-glycolic acid non-woven mesh: A preliminary study in nude mice", British Journal of Oral and Maxillofacial Surgery, vol. 45, no. 4, pp. 272-278.

Yang, X., Sun, T., Dou, S., Wu, J., Wang, Y. & Wang, J. 2009, "Block Copolymer of Polyphosphoester and Poly(l-Lactic Acid) Modified Surface for Enhancing Osteoblast Adhesion, Proliferation, and Function", Biomacromolecules, vol. 10, no. 8, pp. 2213-2220.

Yang, J., Bei, J. & Wang, S. 2002, "Improving cell affinity of poly(D,L-lactide) film modified by anhydrous ammonia plasma treatment", Polymers for Advanced Technologies, vol. 13, no. 3-4, pp. 220-226.

Yuan, X., Mak, A.F.T., Kwok, K.W., Yung, B.K.O. & Yao, K. 2001, "Characterization of poly(L-lactic acid) fibers produced by melt spinning", Journal of Applied Polymer Science, vol. 81, no. 1, pp. 251-260.

Yuan, X., Mak, A.F.T. & Yao, K. 2002, "In vitro degradation of poly(L- lactic acid) fibers in phosphate buffered saline", Journal of Applied Polymer Science, vol. 85, no. 5, pp. 936-943.

Ziabicki, A. 1976, Fundamentals of fiber formation: The science of fiber spinning and drawing, John Wiley & Sons, Ltd., London.

Zou, H., Yi, C., Wang, L., Liu, H. & Xu, W. 2009, "Thermal degradation of poly(lactic acid) measured by thermogravimetry coupled to Fourier transform infrared spectroscopy", Journal of Thermal Ananalysis and Calorimetry, vol. 97, no. 3, pp. 929-935.

Appendix 1A

Processing parameters for the P(L/D)LA 96/4 fibers and P(L/DL) 70/30 plate.

(Orientation temperatures column markings, / = caterpillar, - = joint ovens, -o = winder, G = godet, D = godet pair/duo)

IV (dl/g)	Acronym	Filament count	Screw speed	Set extruder temperatures (°C)	Orientation temperatures (°C)	Draw ratio	Average fil. Ø (µm)	Monomer wt-%	Publication number
Extruded and continuous drawing with caterpillars and ovens									
5.48	T1-9	4	9	200/215/230/235/270/277	/ 105 / 125-125 / 120 -o	3.88	101	0.17	II
5.48	T1-8	4	8	200/215/230/235/270/277	/ 105 / 125-125 / 120 -o	3.88	95	0.18	II
5.48	T1-7	4	7	200/215/230/235/270/277	/ 105 / 125-125 / 120 -o	3.88	86	0.23	II
5.48	T1-6	4	6	200/215/230/235/270/277	/ 105 / 125-125 / 120 -o	3.88	74	0.33	II
5.48	T1-5	4	5	200/215/230/235/270/277	/ 105 / 125-125 / 120 -o	3.88	65	0.47	II
5.48	T1-4	4	4	200/215/230/235/270/277	/ 105 / 125-125 / 120 -o	3.88	54	0.72	II
5.48	T1-3	4	3	200/215/230/235/270/277	/ 105 / 125-125 / 120 -o	3.88	93	0.98	II
5.48	T2-9	4	9	200/215/230/235/275/282	/ 105 / 125-125 / 120 -o	3.88	92	0.33	II
5.48	T2-8	4	8	200/215/230/235/275/282	/ 105 / 125-125 / 120 -o	3.88	84	0.34	II
5.48	T2-7	4	7	200/215/230/235/275/282	/ 105 / 125-125 / 120 -o	3.88	79	0.46	II
5.48	T2-6	4	6	200/215/230/235/275/282	/ 105 / 125-125 / 120 -o	3.88	73	0.67	II
5.48	T2-5	4	5	200/215/230/235/275/282	/ 105 / 125-125 / 120 -o	3.88	63	0.80	II
5.48	T2-4	4	4	200/215/230/235/275/282	/ 105 / 125-125 / 120 -o	3.88	63	1.24	II
5.48	T3-9	4	9	200/215/230/235/280/287	/ 105 / 125-125 / 120 -o	3.88	105	0.36	II
5.48	T3-8	4	8	200/215/230/235/280/287	/ 105 / 125-125 / 120 -o	3.88	90	0.52	II
4.80	268/265/7/8	8	7	200/215/235/253/265/268	/ 90-90 / 140-140 / -o	4.29	73	0.09	III
2.18	240/222/8/12	12	8	170/180/190/205/222/240	/ 90-90 / 140-140 / -o	4.61	45	< 0.02	III

Appendix 1B

Processing parameters for the P(L/D)LA 96/4 fibers and P(L/DL) 70/30 plate.

(Orientation temperatures column markings, / = caterpillar, - = joint ovens, -o = winder, G = godet, D = godet pair/duo)

IV (dl/g)	Acronym	Filament count	Screw speed	Set extruder temperatures (°C)	Orientation temperatures (°C)	Draw ratio	Average fil. Ø (µm)	Monomer wt-%	Publication number
Extrusion and continuous drawing with caterpillars and ovens									
6.26	275/270/8/12	12	8	200/215/230/255/270/275	/ 90-90 / 140-140 / -o	4.44	79	1.90	III
5.48	248/237/6/4	4	6-7	190/200/220/235/254/267	/ 90 / 115-115 / 110 -o	4.58	80	NA	IV
5.48	264/250/8/8	8	8	190/200/220/235/250/264	/ 90 / 115-115 / 110 -o	4.50	70	NA	IV
5.48	288/280/9/4	4	9	200/215/230/235/280/288	/ 90-90 / 145-145 / -o	5.10	84	NA	V fiber
4.18	266/265/9/12	12	9	185/205/228/245/265/266	/ 90-90 / 130-130 / -o	4.26	50	NA	V non-woven
4.21	261/250/10/8	8	10	185/195/215/230/250/261	/ 90 / 115-115 / -o	4.46	80	NA	VI fiber
5.48	273/258/4/4	4	4	200/215/230/235/258/273	/ 110 / 135-135 / 125 -o	4.80	78	0.51	VII fiber
4.18	250/250/8/8	8	8	180/190/200/240/250/250	/ 90-90 / 140-140 / -o	4.68	75	0.03	Unpublished
4.18	267/263/8/4	4	8	187/197/207/245/263/267	/ 90-90 / 140 / 120 -o	4.06	90	0.71	Unpublished
5.48	277/270/7/4	4	7	200/215/230/235/270/277	/ 105 / 125-125 / 120 -o	4.28	80	0.37	Unpublished
5.48	277/270/7/4*	4	7	200/215/230/235/270/277	/ 105 / 130-130 / 125 -o	4.40	80	0.35	Unpublished
5.48	279/272/7.5/4	4	7.5	200/215/230/235/272/279	/ 105 / 125-125 / 120 -o	4.20	85	0.42	Unpublished
5.48	279/272/7.5/4*	4	7.5	200/215/230/235/272/279	/ 105 / 125-125 / 120 -o	3.50	90	0.30	Unpublished
5.48	282/272/8/4	4	8	200/215/230/243/272/282	/ 105-105 / 125-125 / -o	4.25	85	0.15	Unpublished
4.18	257/250/8/8	8	8	185/195/205/240/250/255	/ 90-90 / 140-140 / -o	5.20	84	0.08	Unpublished
Extrusion and continuous drawing with high speed spinning machine									
1.7	High speed F	1	10	170/180/190/220/230/250	G1 70, G2 90, D 90,	4.0	20 - 30	NA	VII non-woven
Extrusion with plate die and continuous drawing with single caterpillar									
6.10	30 mm x 0.5 mm plate die		22	175/185/195/215/228/248			10 x 16 mm plate size		VII

Appendix 2

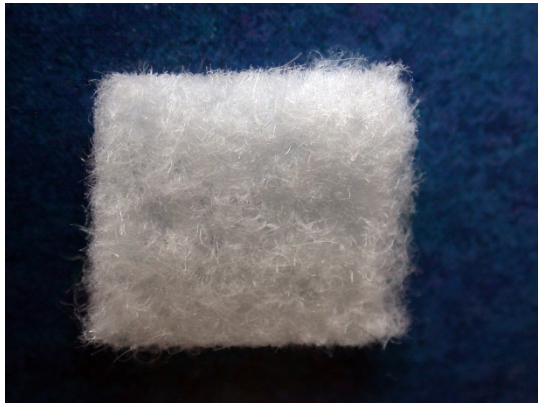

Non-woven felt (V)

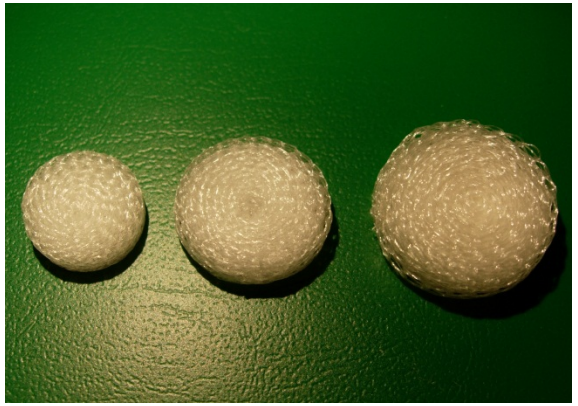

Cylindrical scaffolds sizes Ø 12, 15 and 19 mm (IV)

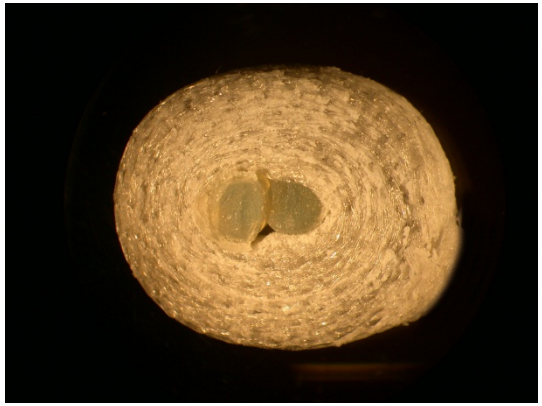

Cylindrical intervertebral disc composite implant (VI)

Temporomandibular non-woven-plate implant (VII)

ORIGINAL PUBLICATIONS

Publication I

Pirhonen, E. & Ellä, V.

Melt spinning

In: Wnek, G.E. & Bowlin, G.L. (eds.). Encyclopedia of Biomaterials and Biomedical Engineering.

New York, NY. Informa Healthcare. 2nd ed., 3, (2008), pp. 1816-1823

Publication II

Ellä, V., Nikkola, L. & Kellomäki, M.

Process-induced monomer on a medical-grade polymer and its effect on short-term hydrolytic degradation

Journal of Applied Polymer Science, vol. 119, no. 5, (2011), pp. 2996-3003

Publication III

Paakinaho, K., Ellä, V., Syrjälä, S. & Kellomäki, M.

Melt spinning of poly(L/D)lactide 96/4: Effects of molecular weight and melt processing on hydrolytic degradation

Polymer Degradation and Stability
vol. 94, no. 3, (2009), pp. 438-442

Polymer Degradation and Stability 94 (2009) 438–442

Contents lists available at ScienceDirect

Polymer Degradation and Stability

journal homepage: www.elsevier.com/locate/polydegstab

Melt spinning of poly(L/D)lactide 96/4: Effects of molecular weight and melt processing on hydrolytic degradation

K. Paakinaho [a,*], V. Ellä [a], S. Syrjälä [b], M. Kellomäki [a]

[a] Department of Biomedical Engineering, Tampere University of Technology, Hermiankatu 12 B, P.O. Box 692, FI-33101 Tampere, Finland
[b] Department of Material Science, Tampere University of Technology, Korkeakoulunkatu 10, P.O. Box 527, FI-33101 Tampere, Finland

ARTICLE INFO

Article history:
Received 7 September 2008
Accepted 3 November 2008
Available online 21 November 2008

Keywords:
Polylactide
Degradation
Molecular weight
Melt spinning
Viscosity
Monomer

ABSTRACT

This study focused on determining the effects of molecular weight on the degradation of polylactide 96L/4D in melt spinning and the effects of melt processing on hydrolytic degradation. Three polylactides with different inherent viscosities were melt spun, and the fibres were studied *in vitro*. Results showed that during melt spinning high-molecular-weight polylactide degraded because polymer chains were subject to high shear stress and high melt temperatures, whereas a low-molecular-weight polylactide with low melt viscosity was not affected by melt processing. Most degradation occurred during the melting phase in the length of the extruder barrel. Lactide monomer, generated as the polymer degraded in the melt, significantly affected *in vitro* degradation such that the degradation rate was directly proportional to the lactide concentration of the polymer.

1. Introduction

Polylactides, which belong to the family of poly-α-hydroxy acids, constitute a biodegradable polymer family commonly used in medical applications. They are thermoplastic polyesters, whose polymer backbone is formed from lactic acid monomer units. The properties of the polymer enable the production of different varieties of the material for various applications such as sutures, bone fixation devices, and tissue engineering scaffolds [1–5].

Polylactide fibres are well-functioning source material for the production of biodegradable implants by means of common textile techniques [4,5] or for reinforcing polymer composites [6]. Different methods of spinning polylactide have been studied [7–9]; the studies have covered poly-L-lactide [10,11] as well as different lactide copolymers [12,13]. The copolymerization of lactide enantiomers affects the polymer's crystal structure, which with increasing crystallinity affects the polymer's melting temperature [12]. Reportedly, semicrystalline and amorphous polylactides also differ in their melt viscosity, the former having a higher melt viscosity than the latter [14].

Polylactides, as well as polyesters in general, are prone to thermal degradation. During melt processing, their molecular weight decreases due to the scission of polymer chains [15–17]. During melt processing, degradation increases because of moisture, residual monomers and oligomers, but especially because of residual catalytic metal components [15]. In a hydrolytic environment, the post-processing molecular weight is significant in light of the polymer's mechanical properties and its degradation time. The above are important factors in designing composite materials for a medical application, in which the initial strength and strength retention during healing are crucial, or for a tissue engineering scaffold to provide adequate support for seeded cells to grow.

Understanding the relationships between the factors affecting molecular degradation during melt processing helps to produce advanced medical devices with suitable strength and degradation characteristics. Our objective was to study the melt spinning of various molecular-weight polylactides and the effects of melt processing on hydrolytic degradation *in vitro* after γ-irradiation.

2. Materials and methods

2.1. Materials

The polymers used in this study were medical grade P(L/D)LA 96/4 copolymers (PURAC Biochem bv) with inherent viscosities reported by the manufacturer of 2.18 dl/g (PLA22), 4.80 dl/g (PLA48), and 6.26 dl/g (PLA63). The residual monomer content of all polymers was <0.05%.

2.2. Material characterization

The molecular weights (M_w, M_n), the calculated related values of polydispersity (PDI), and the intrinsic viscosity (i.v.) of the raw

* Corresponding author. Tel.: +358 40 849 0975; fax: +358 3 3115 2250.
E-mail address: kaarlo.paakinaho@tut.fi (K. Paakinaho).

0141-3910/$ – see front matter © 2008 Elsevier Ltd. All rights reserved.
doi:10.1016/j.polymdegradstab.2008.11.010

materials and produced fibres were determined by size exclusion chromatography (SEC), which was also used to monitor the rate of the fibres' hydrolytic degradation *in vitro*. Two parallel 150 μl samples with concentration of 0.1 wt-%, prepared in chloroform, were injected at a flow rate of 1.0 ml/min. The columns used for exclusion were a PLgel 5-μm Guard precolumn and two PLgel 5-μm mixed-C columns, manufactured by Polymer Laboratories, Amherst, USA. The detector (Waters 410 RI Differential Refractometer Detector), pump (Waters M515 HPLC-Pump), and autosampler (Waters 717P plus Autosampler) were manufactured by Waters Operating Corporation, Milford, USA. Universal Calibration was obtained for P(L/D)LA 96/4 ($k = 5.45 \times 10^{-4}$ dl/g, $a = 0.73$), and mean values of results were used.

Monomer determinations were performed in Lahti Research Laboratory (Lahti, Finland). The L-lactide content was measured using gas chromatography (DC8000, CE Instruments, Rodano, Italy) and an FI-detector after chloroform dilution. The measuring resolution was 0.02%, and mean values of three parallel measurements were used to determine the monomer content of the processed fibres.

A rotational rheometer (Physica MCR-301, Anton Paar Ostfildern, Germany) was used to measure the viscosities of the three raw materials at four different temperatures, selected based on the processing temperatures of 220 °C, 230 °C, 240 °C, and 250 °C. A plate–plate geometry was used with a diameter of 25 mm and a gap size of 1 mm. Three parallel measurements were taken, and the mean values of the results were used.

2.3. Melt spinning

Before extrusion, the materials were dried in a vacuum heated to 100 °C at a rate of 1 °C/min, held there for 16 h, and then allowed to cool to room temperature before use. Fibre spinning was done in a two-step melt spinning/hot-drawing process using a Gimac TR melt extruder with a screw diameter of 12 mm, an L/D of 24:1, and a screw geometry of 1:1.237, B.V.O (Gimac, Castronno, Italy). The extruder comprised six heating zones, the first three for the barrel, two for melt mixing and stabilizing, and one for the die. The extruder zone temperatures used for each material are shown in Table 1. Two different dies, 8-filament (single orifice diameter 0.4 mm) and 12-filament (single orifice diameter 0.2 mm), were used in melt spinning. Melt pressure was monitored during spinning with a melt pressure instrument in zone five (Dynisco pressure sensor, model TPT 484-7.5M-6/18-B379, Dynisco Instruments, USA). Extrusion was carried out in a nitrogen atmosphere and drawing in ambient laboratory conditions.

For information on the effects of heat and shear stress on molecular degradation in the extruder barrel, three melt spinnings were done using the same parameters as in the original melt spinnings but with samples collected from the extracted screw. After the spinning stabilized, the die was removed, the screw was pushed out of the extruder barrel, and samples were collected immediately from screw pitches, that is, from the screw tip and from pitches 2, 4, 6, 7, 9, 12, and 15, as counted from screw tip to screw root. Immediately after harvesting, the samples were cooled in air flow and then analyzed by SEC.

2.4. γ-Irradiation

After melt spinning and hot drawing, all specimens were γ-irradiated for sterility with a radiation dose of 25 kGy by a commercial supplier.

Table 1
Extruder zone temperatures (°C) for melt spinning.

Fiber	Polymer	Barrel 1	Barrel 2	Barrel 3	Nozzle 1	Nozzle 2	Nozzle 3
F22	PLA22	170	180	190	205	222	240
F48	PLA48	200	215	235	253	265	268
F63	PLA63	200	215	230	255	270	275

2.5. In vitro

To study the rate of hydrolytic degradation, fibres were placed in a phosphate buffer solution (PBS, 3.54 g/dm^3 Na_2HPO_4 – 0.755 g/dm^3, NaH_2PO_4 – 5.9 g/dm^3, NaCl buffered saline) at pH 7.40 ± 0.05, and their degradation was monitored with tensile tests and SEC. Samples were incubated for 1, 2, 3, 4, 6, 8, 12, 16, and 24 weeks at 37 °C. The buffer solution was changed fortnightly.

Tensile tests were run on the fibres to measure their tensile strength retention and to monitor indirectly their hydrolytic degradation (Instron 4411 Materials Testing Machine, Instron Ltd., High Wycombe, England). All tensile tests were run at ambient temperature with non-sterile and sterile fibres tested dry and fibres from *in vitro* specimens tested wet. The testing parameters were a grip distance of 50 mm, a load cell of 500 N, and a crosshead speed of 30 mm/min.

3. Results

3.1. Molecular degradation and monomer generation during melt spinning

The effects of melt spinning and gamma irradiation on M_n, M_w and i.v. are shown in Fig. 1. The sample materials had different thermal degradation behavior: PLA22 did not degrade during melt spinning, whereas decreases in M_w and i.v. were 50% and 34% for PLA48 and 63% and 43% for PLA63, respectively. Differences in molecular weight and i.v. after melt spinning were evened out in gamma irradiation, in which the decrease in M_w and i.v. in melt spun fibres was 73% and 64% for F22, 79% and 71% for F48, and 75% and 66% for F63, respectively. The molecular weights and i.v. of all specimens were nearly the same after both melt processing and sterilization despite the molecular weight and i.v. of the raw materials or melt-spun fibres. The L-lactide content of the melt-spun fibres was <0.02 wt-% for F22, 0.09 wt-% for F48, and 1.90 wt-% for F63.

3.2. Effects of shear stress and heat on molecular weight during extrusion

The effects of heat and shear stress on M_w and PDI in the length of the extruder barrel are shown in Figs. 2 and 3. In the experiment, screw pitch 15, which is located immediately after the first heating zone in the extruder barrel, was the first pitch to yield molten polymer for sample harvesting. PLA48 and PLA63, which both

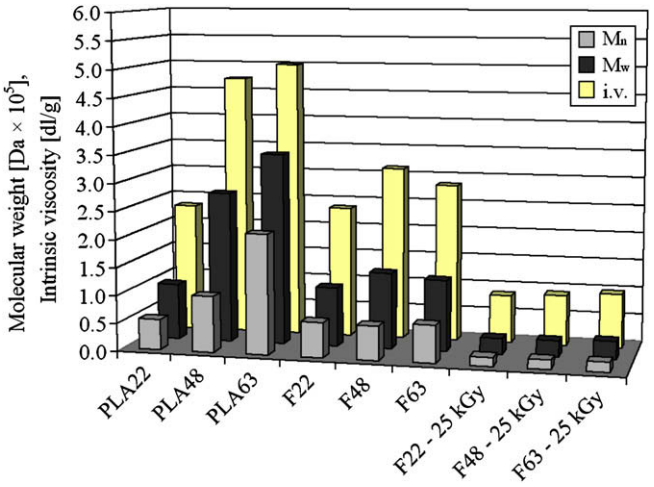

Fig. 1. Effects of processing and sterilization on M_w, M_n and i.v., $n = 2$.

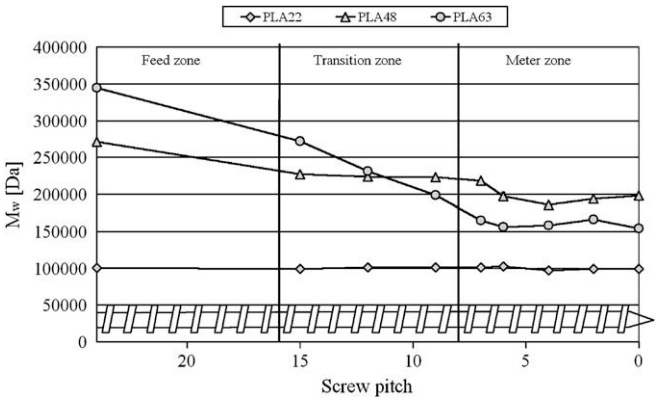

Fig. 2. Schematic view of extruder screw and molecular degradation in extruder barrel during melt spinning, $n = 2$.

degraded markedly during melt spinning, showed a gradual degradation profile in the extruder barrel. The M_w of both materials dropped to the beginning of the metering zone, after which virtually no further degradation took place in the length of the extruder barrel. The decrease in M_w between pitches 24 and 6 was 27% for PLA48 and 55% for PLA63. PLA22 did not show any degradation in the extruder.

3.3. Viscosity and shear stress at extrusion temperatures

Figs. 4–6 show viscosity results measured with a rotational rheometer. The three materials differed significantly in their melt viscosities and melt behaviour. PLA22 showed typical shear-thinning behaviour, and its viscosities corresponded with the test temperatures. PLA48 and PLA63 were also shear thinning; however unlike PLA22, they did not reach their zero viscosity level at shear rates between 0.1 and 10.0 1/s. At 220 °C and 230 °C, their viscosities were so high that the test was interrupted because the rheometer reached its maximum torque. PLA48 and PLA63 showed similar melt viscosities at 240 °C and 250 °C with shear rates between 0.1 and 10.0 1/s. At higher shear rates, the viscosity of PLA48 started dropping more rapidly at 250 °C than at 240 °C, at which the viscosity slope was nearly linear. In rotational rheometric analysis with plate–plate or cone–plate geometries, polymer melts undergo various instabilities when shear velocity is increased, the so-called edge fracture being the most common [18]. It was thus impossible to gain reliable measurement data at high shear velocities (>10.0 1/s).

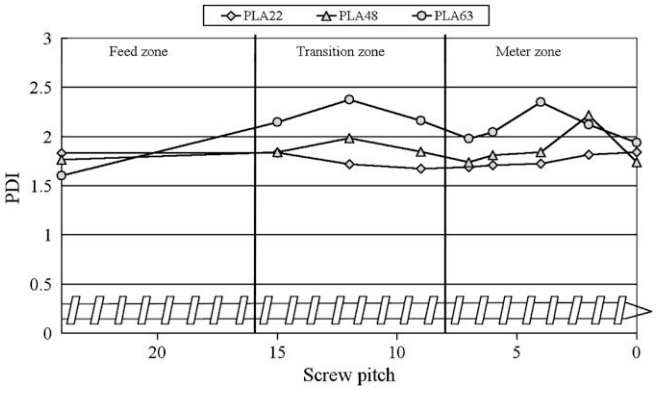

Fig. 3. Schematic view of extruder screw and PDI changes in length of extruder barrel, $n = 2$.

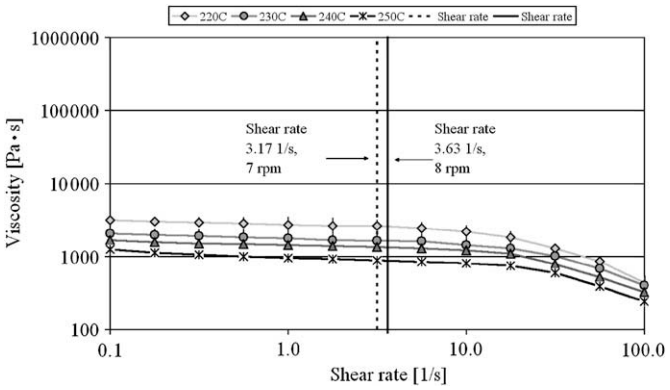

Fig. 4. Viscosity at different temperatures of PLA22 on logarithmic scale, $n = 3$.

With the flat plate approximation and assuming pure drag flow, the shear rate in the screw channel can be approximated by [19],

$$\gamma = \frac{\pi DN}{h \times 60}$$

where γ = shear rate, N = screw revolution speed (rpm), D = outer screw diameter, h = flight depth.

The screw used in this study had the following dimensions: $D = 11.9$ mm, $h = 1.375$ mm (in the metering zone). With the screw revolutions (rpm) used in this study, it was possible to approximate shear rates: 3.17 1/s when $N = 7$ (rpm) and 3.63 1/s when $N = 8$ (rpm). Though the shear rate equation gives a mean, not an exact value, shear rates for melt spinning all specimens can be used to approximate viscosities at test temperatures. Because the shear rate changes depending on the extruder screw section, it is reasonable to apply the equation in the metering zone of the screw. At the beginning of the screw, the non-molten material creates a much more complex situation, to which the equation does not apply.

3.4. Effects of hydrolytic degradation on molecular weight and strength retention

The effects of hydrolytic degradation on M_n and M_w are shown in Fig. 7. The γ-irradiation levelled the differences between the molecular weights of melt-spun samples such that sample fibres had similar molecular weights at the beginning of the *in vitro* test series. Despite this similarity, the fibres differed significantly in their degradation behaviour. The most affected by the hydrolytic environment was F63, which degraded the most during melt spinning. During 24 weeks *in vitro*, the M_w loss of F63 was 84% whereas that of F48 was 61% and that of F22 only 10%. F63 lost most of its molecular weight (67%) in the first third of the *in vitro* period.

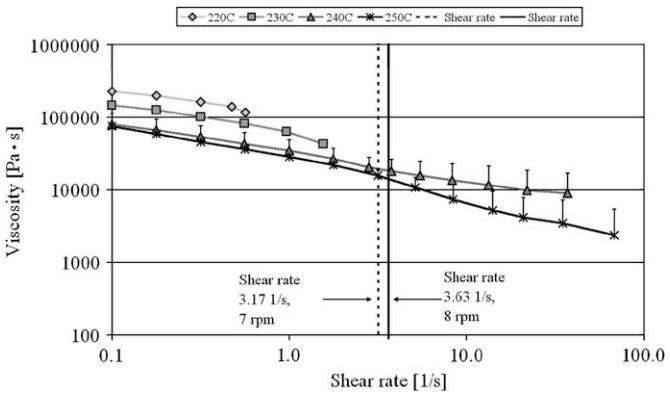

Fig. 5. Viscosity at different temperatures of PLA48 on logarithmic scale, $n = 3$.

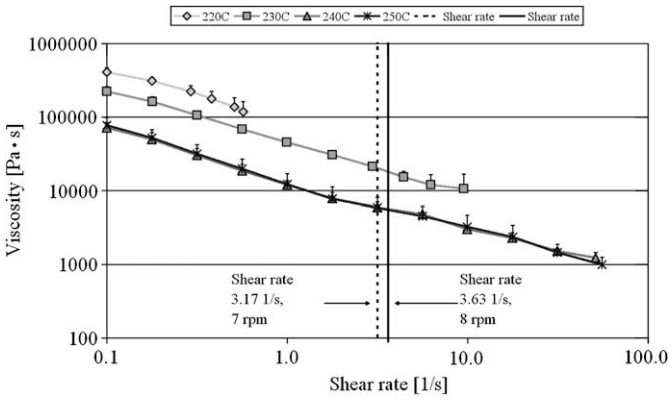

Fig. 6. Viscosity at different temperatures of PLA63 on logarithmic scale, $n = 3$.

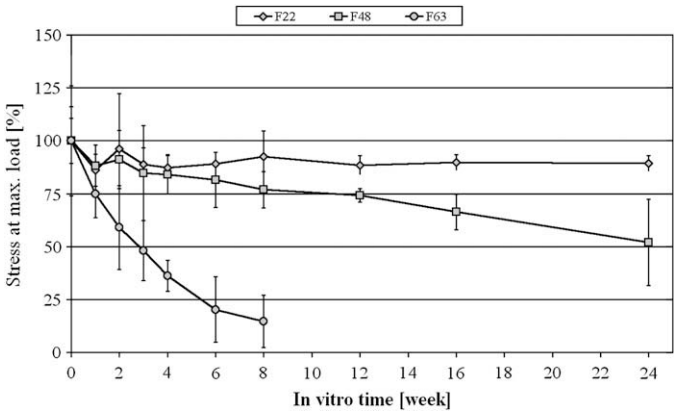

Fig. 8. Effects of hydrolytic degradation on ultimate tensile strength, $n = 5$.

Loss of tensile properties correlates well with loss of molecular weight (results of the tensile test are given in Fig. 8). F22 was the most stable, losing only 11% of its tensile strength over 24 weeks *in vitro*. F63 lost its tensile strength quite fast in the early weeks *in vitro*, and after 8 weeks the fibres could no more to be tested for tensile strength because they had lost all their mechanical properties.

4. Discussion

The P(L/D)LA 96/4 copolymers with different initial molecular weights showed different degradation characteristics during melt spinning so that the higher the initial molecular weight, the stronger the molecular degradation, with most degradation occurring in the length of the extruder barrel. In the extruder barrel, polymer chain degradation of PLA48 and PLA63 continued to the beginning of the meter zone, probably because of high shear stresses until the molecular weight was low enough to withstand the shearing of the screw. PLA22, which initially had a lower melt viscosity than PLA48 and PLA63, could withstand the shear stress and could also be melt spun at lower temperatures than PLA48 and PLA63, and thus did not degrade in melt spinning. Earlier studies have reported a 50% decrease in the i.v. of P(L/D)LA 96/4 with an i.v. of 4.21 dl/g in melt spinning [20], a 31% decrease in the M_w of P(L/DL)LA 92/8 with an M_w of 16,400 Da [11], and a 68% decrease in the viscometric molecular weight (M_v) of PLLA with an M_v of 330,000 Da [10].

Measurements made with the rotational rheometer testify an interdependency between molecular weight and melt viscosity. Viscosities measured at shear rates used in the melt spinning of PLA48 and PLA63 were high compared to PLA22. Viscosities measured at shear rates used in the melt spinning of PLA48 PLA63 were high compared to PLA22 and decreased nearly linearly, whereas PLA22 with significantly lower viscosity had typical shear thinning behavior, similar to that in Ref. [7]. The decrease of viscosity during the rotational rheometric analysis of PLA48 and PLA63 may have resulted from molecular chain degradation caused by interaction of high temperatures (240–250 °C) and shear stress or from an edge fracture in the polymer melt during measurements inflicting an error into the analysis [21].

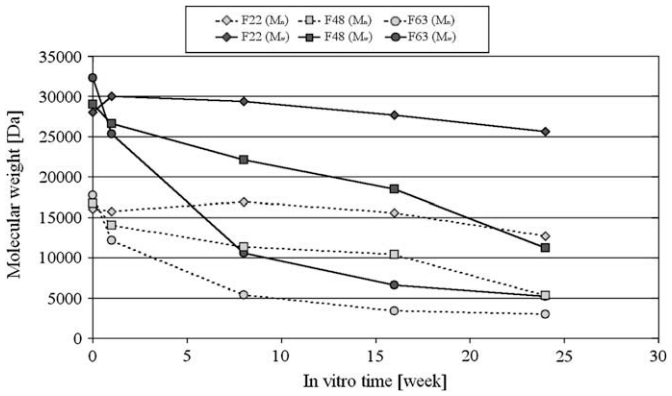

Fig. 7. Effects of hydrolytic degradation on molecular weight, $n = 2$.

With the used melt-spinning parameters, the shear stress affecting the polymer in the first third of the extruder barrel length caused significant molecular degradation in PLA48 and PLA63. These polymers continued degrading molecularly until their molecular weights dropped so that the melt viscosity was probably low enough to halt the degradation caused by the shearing action of the screw in the extruder barrel. The melt spinning of high-molecular-weight polylactides (PLA48 and PLA63) required significantly higher extruder temperatures than that of the low-molecular-weight polylactide (PLA22) to reach a low enough viscosity for melt spinning to proceed. However, high extruder temperatures combined with high shear stress generated more lactide monomer on PLA48 (0.09%) and PLA63 (1.9%).

The varying effects of γ-irradiation on the fibres evened out the differences in their molecular weight after melt spinning. The radiation caused more molecular degradation in F48 and F63, which had higher molecular weights after melt spinning, than in F22. In Ref. [5], the decrease in the M_w of P(L/D)LA 96/4 in γ-irradiation (25 kGy) was reported as 73%, and in Ref. [22] the decrease in the intrinsic viscosity of PLLA was 62%. In both melt spinning and γ-irradiation (25 kGy), molecular degradation was reportedly 70% in Ref. [20] and the decrease in i.v. ~80% in Ref. [23] and 81% in Ref. [24]. The variation between fibres used in this study and in Refs. [5,22] could be explained by the inaccuracy of the γ-irradiation process.

Melt-spun fibres showed different hydrolytic degradation behaviours *in vitro*, though tested fibres had nearly the same M_w and PDI before the *in vitro* test; the difference between the maximum and minimum in the M_w of melt-spun and γ-irradiated fibres was 1.7% of that of the raw material. Similar behaviour has also been reported in Ref. [25], where the degradation rate of fibres melt spun with different extruders showed significantly different degradation profiles regardless of their similar molecular weight and PDI before *in vitro* testing. Noteworthy in this study was that the lactide monomer content of the melt-spun fibres differed significantly with the monomer content ranging from <0.02% to 1.9%. In the 24-week *in vitro* study, the monomer content had a markedly increasing effect on the hydrolytic degradation rate, the drop in molecular weight (M_w) being 84% for F63 (monomer

content 1.9%), 61% for F48 (monomer content 0.09%), and only 9% for F22 (monomer content <0.02%). The angle of the molecular weight slope is apparently linked with the lactide monomer content of the polymer so that the higher the monomer content, the steeper the slope of degradation. Earlier studies [26,27] have reported the effects of residual monomer content on polylactide degradation but focused on demonstrating the importance of polymer purity on the performance of the material. However, in this study, lactide monomer was generated into purified polymer via thermal degradation in melt processing.

The 12-week *in vitro* strength retentions of the melt spun and γ-irradiated fibres were 88% for F22 and 74% for F48, which are better than or similar to those in Ref. [5] or Ref. [24], in which P(L/D)LA 96/4 fibres and yarns maintained 75% and ~50%, respectively, of their initial ultimate tensile strength during hydrolysation over 13 weeks. In this study, the molecular degradation rate of F48 was closest to the fibres in Ref. [5] despite its lower initial molecular weight (M_w). Results similar to those for F22 and F63 on mechanical properties *in vitro* were achieved in [25], where fibres maintained ~80% of their initial strength while their M_w dropped ~30% during a 24-week *in vitro* period, or the fibres lost their mechanical properties after 8 weeks after their M_w had dropped ~75%.

As generally understood, mechanical properties are related to the molecular weight of the polymer. Thus the strength retention in vitro can be controlled by controlling the degradation rate, which is likely to be related to the lactide monomer content of melt-processed polylactide. The higher the monomer content, the more rapidly molecular weight and mechanical properties decline.

5. Conclusions

The rheological properties of polylactide significantly affect its degradation in melt processing in terms of molecular weight and monomer generation, which markedly affect material properties *in vitro*. By studying the relationships between melt temperature and shear stress, we can better understand the degradation behaviour of a polymer in melt processing. In addition, the thermally generated lactide monomer may offer interesting possibilities to control the hydrolytic degradation rate of polylactide.

Acknowledgements

The authors appreciate the research funding received from the European Commission (Biosys: Intelligent Biomaterial Systems for Cardiovascular Tissue Repair, STRP 013633). We would also like to thank Eira Lehtinen and Sanna Siljander for their help during this work.

References

[1] Mäkelä P, Pohjonen T, Törmälä P, Waris T, Ashammakhi N. Strength retention properties of self-reinforced poly-L-lactide (SR-PLLA) sutures compared with polyglyconate (Maxon®) and polydioxanone (PDS) sutures. An in vitro study. Biomaterials 2002;23:2587–92.
[2] Saikku-Bäckström A, Tulamo R, Räihä JE, Kellomäki M, Toivonen T, Törmälä P, et al. Intramedullary fixation of cortical bone osteotomies with absorbable self-reinforced fibrillated poly-96/4-lactide (SR-PLA96) rods in rabbits. Biomaterials 2001;22:33–43.
[3] Rokkanen PU, Böstman O, Hirvensalo E, Mäkelä EA, Partio EK, Pätiälä H, et al. Bioabsorbable fixation in orthopaedic surgery and traumatology. Biomaterials 2000;21:2607–13.
[4] Kellomäki M, Niiranen H, Puumanen K, Ashammakhi N, Waris T, Törmälä P. Bioabsorbable scaffolds for guided bone regeneration and generation. Biomaterials 2000;21:2495–505.
[5] Ellä V, Gomes M, Reis R, Törmälä P, Kellomäki M. Studies of p(L/D)LA 96/4 non-woven scaffolds and fibres; properties, wettability and cell spreading before and after intrusive treatment methods. Journal of Materials Science Materials in Medicine 2007;18:1253–61.
[6] Huttunen M, Ashammakhi N, Törmälä P, Kellomäki M. Fibre reinforced bioresorbable composites for spinal surgery. Acta Biomaterialia 2006;2:575–87.
[7] Schmack G, Tändler B, Optiz G, Vogel R, Komber H, Häußler L, et al. High-speed melt spinning of various grades of polylactides. Journal of Applied Polymer Science 2004;91:800–6.
[8] Schmack G, Jehnichen D, Vogel R, Tändler B, Beyreuther R, Jacobsen S, et al. Biodegradable fibres spun from poly(lactide) generated by reactive extrusion. Journal of Biotechnology 2001;86:151–60.
[9] Gupta B, Revagade N, Anjum N, Atthoff B, Hilborn J. Preparation of poly(lactic acid) fiber by dry-jet-wet spinning. II. Effect of process parameters on fiber properties. Journal of Applied Polymer Science 2006;101:3774–80.
[10] Fambri L, Pegoretti A, Fenner R, Incardona SD, Migliaresi C. Biodegradable fibres of poly(L-lactic acid) produced by melt spinning. Polymer 1997;38:79–85.
[11] Schmack G, Tändler B, Vogel R, Beyreuther R, Jacobsen S, Fritz H. Biodegradable fibers of poly(L-lactide) produced by high-speed melt spinning and spin drawing. Journal of Applied Polymer Science 1999;73:2785–97.
[12] Andriano KP, Pohjonen T, Törmälä P. Processing and characterization of absorbable polylactide polymers for use in surgical implants. Journal of Applied Biomaterials 1994;5:133–40.
[13] Penning JP, Dijkstra H, Pennings AJ. Preparation and properties of absorbable fibres from L-lactide copolymers. Polymer 1993;34:942–51.
[14] Fang Q, Hanna MA. Rheological properties of amorphous and semicrystalline polylactic acid polymers. Industrial Crops and Products 1999;10:47–53.
[15] Cam D, Marucci M. Influence of residual monomers and metals on poly (L-lactide) thermal stability. Polymer 1997;38:1879–84.
[16] Kopinke F-D, Remmler M, Mackenzie K, Möder M, Wachsen O. Thermal decomposition of biodegradable polyesters – II. Poly(lactic acid). Polymer Degradation and Stability 1996;53:329–42.
[17] Wachsen O, Platkowski K, Reichert K-H. Thermal degradation of poly-L-lactide – studies on kinetics, modelling and melt stabilisation. Polymer Degradation and Stability 1997;57:87–94.
[18] Mall-Gleissle SE, Gleissle W, McKinley GH, Buggisch H. The normal stress behaviour of suspensions with viscoelastic matrix fluids. Rheologica Acta 2002;41:61–76.
[19] Giles Jr Harold F, Wagner Jr John R, Mount EM. Extrusion – the definitive processing guide and handbook. William Andrew; 2005. p. 79–81.
[20] Kellomäki M, Puumanen K, Waris T, Törmälä P. *In vivo* degradation of composite membrane of P(ε-CL/L-LA) 50/50 film and P(L/D)LA 96/4 mesh. Materials for Medical Engineering 2000:79–85.
[21] Dealy JM. Melt rheology and its role in plastics processing theory and applications. Dordrecht: Kluwer Academic Publishers; 1999.
[22] Nuutinen J, Clerc C, Virta T, Törmälä P. Effect of gamma, ethylene oxide, electron beam, and plasma sterilization on the behaviour of SR-PLLA fibres in vitro. Journal of Biomaterials Science Polymer Edition 2002;13:1325–36.
[23] Kellomäki M, Paasimaa S, Törmälä P. Pliable polylactide plates for guided bone regeneration: manufacturing and in vitro. Proceedings of the Institution of Mechanical Engineers – Part H: Journal of Engineering in Medicine 2000;214:615–29.
[24] Honkanen PB, Kellomäki M, Lehtimäki MY, Törmälä P, Mäkelä S, Lehto MUK. Bioreconstructive joint scaffold implant arthroplasty in metacarpophalangeal joints: short-term results of a new treatment concept in rheumatoid arthritis patients. Tissue Engineering 2003;9:957–65.
[25] Kellomäki M. Bioabsorbable and bioactive polymers and composites for tissue engineering applications. Tampere: TUT; 2000. p. 68–69.
[26] Kellomäki M, Pohjonen T, Törmälä P. Self reinforced polylactides. In: Arshady R, editor. Biodegradable polymers. London: Citus Books; 2003. p. 212.
[27] Hyon S-H, Jamshidi K, Ikada Y. Effects of residual monomer on the degradation of DL-lactide polymer. Polymer International 1998;46:196–202.

Publication IV

Ellä, V., Annala, T., Länsman, S., Nurminen, M., Kellomäki, M.

Knitted polylactide 96/4 L/D structures and scaffolds for tissue engineering: Shelf life, in vitro and in vivo studies

Biomatter, vol. 1, no.1, (2011), pp. 102-113

Biomatter 1:1, 102-113; July/August/September 2011; © 2011 Landes Bioscience

Knitted polylactide 96/4 L/D structures and scaffolds for tissue engineering

Shelf life, in vitro and in vivo studies

Ville Ellä,[1,*] Tuija Annala,[2] Satu Länsman,[3] Manu Nurminen[1] and Minna Kellomäki[1]

[1]Department of Biomedical Engineering; Tampere University of Technology; Tampere, Finland; [2]Scaffdex Ltd.; Tampere, Finland; [3]Department of Ophthalmology; Oulu University Hospital; Oulu, Finland

Key words: polylactic acid, fibrous implant, knitting, scaffold, in vitro, in vivo, tissue engineering, degradation, shelf life

This study covers the whole production cycle, from biodegradable polymer processing to an in vivo tissue engineered construct. Six different biodegradable polylactide 96/4 L/D single jersey knits were manufactured using either four or eight multifilament fiber batches. The properties of those were studied in vitro for 42 weeks and in 0- to 3-year shelf life studies. Three types (Ø 12, 15 and 19 mm) of cylindrical scaffolds were manufactured from the knit, and the properties of those were studied in vitro for 48 weeks. For the Ø 15 mm scaffold type, mechanical properties were also studied in a one-year in vivo experiment. The scaffolds were implanted in the rat subcutis. All the scaffolds were γ-irradiated prior to the studies. In vitro, all the knits lost 99% of their mechanical strength in 30 weeks. In the three-year follow up of shelf life properties, there was no decrease in the mechanical properties due to the storage time and only a 12% decrease in molecular weight. The in vitro and in vivo scaffolds lost their mechanical properties after 1 week. In the case of the in vivo samples, the mechanical properties were restored again, stepwise, by the presence of growing/maturing tissue between weeks 3 and 12. Faster degradation was observed with in vitro scaffolds compared to in vivo scaffolds during the one-year follow up.

Introduction

Polylactides (PLA), purified and medical-grade forms of polymers have been used for tissue repair and reconstruction applications for decades. Due to their good processability, suitable properties and biodegradability as well as non-toxic degradation products, it is still an interesting polymer family for biomedical and TE purposes.[1] An important factor when considering commercial products is that several products made of PLAs exist that already have FDA approval or an equivalent permit.

Monofilaments and multifilament fibers have been produced from PLA polymers with varying properties, depending on the processing parameters.[2-4] PLA fibers can be used as such, e.g., as sutures to close soft tissue wounds,[5] but they are also versatile preforms from a manufacturing perspective. Methods familiar from the textile industry can be used to produce various kinds of textile structures using continuous fibers as well as stapled ones, but fibers as well as textile structures can be used as elements in composites too.

The applicable techniques include, for example, non-woven methods[6-8] and knitting[9-14] to produce porous structures for guided tissue ingrowth and tissue engineering purposes. Though textiles can be used as such, they can also be used as preforms to prepare three-dimensional structures, like scaffolds, e.g., for bone reconstruction[15] and for small joint reconstructions.[16-19]

It is well known that for tissue engineering scaffolds, specific pore size is needed to enable cell ingrowth, =tissue formation and maturation,[20] and interconnective pores are essential for constructing a viable 3D tissue engineered construct.[20,21] It is also easy to modify the parameters of the textile production and monitor the influences of the production to the finished product,[22] and thus, by varying the parameters, several products with very different properties can result.

In this paper, we covered the process from raw material to TE product. We studied the mechanical and molecular properties of manufactured fibers made of poly(L/D)lactide 96/4, tubular single jersey knits made of fibers and cylindrical scaffolds prepared from the knits. We studied the differences of the manufacturing parameters of the knits, and we assessed their long-term stability in hydrolysis in buffer solution at 37°C. For the knits, we also studied the long-term storage stability, so called shelf life, for up to 3 years. We were also in position to study both in vitro and in vivo degradation for up to 1 year for the cylindrical scaffolds and to compare their mechanical behavior under compression. The importance and relationship between the tissue ingrowth and the mechanical properties were assessed.

*Correspondence to: Ville Ellä; Email: ville.ella@tut.fi
Submitted: 04/12/11; Revised: 07/02/11; Accepted: 07/22/11
DOI: 10.4161/biom.1.1.17447

Table 1. Knitting parameters for six knit types

Sample	Filament Count	Barrel Size	Needles in the Barrel	Loop Size	Course/cm	Wales/cm	Loop Length (mm)
4F	4						
8F	8						
8F-9Ns	8	½"	9	Small	8.1	6.6	6
8F-9Nb	8	½"	9	Big	4.1	4.2	11
4F-9Nb	4	½"	9	Big	4.1	4.2	11
4F-9Ns	4	½"	9	Small	8.1	6.6	6
4F-19Ns	4	½"	19	Small	8.1	6.6	6
8F-19Ns	8	½"	19	Small	8.1	6.6	6

Results

Initial properties of the fibers and knits. Measured single fiber diameters for 4-ply fibers were 78–82 μm and for the 8-ply fibers, 68–70 μm. The initial mechanical properties of the non-irradiated 4- and 8-ply multifilament fibers after extrusion and hot drawing were measured (**Table 3**). The higher number of filaments had a statistically significant increase in tensile load, but the cross-sectional area-related properties (strength and modulus) were statistically significantly higher for the 4-ply yarn bundle. The ultimate break load per yarn was an average 57% higher with the 4-ply fiber and 75% higher with the 8-ply fiber when compared to the yarns in the knits. Due to the structure type of the knits, there was a drastic (> 99.3%) decrease in modulus when comparing the knits and the fibers. For the strain properties, there was an average increase of 17% in the 4-filament 9-needle group and a 38% increase in the 4-filament 19-needle group. For the 8-filament 9-needle group, there was no change in average values, but for the 19-needle knit, there was a 17% increase in strain properties.

The loop size statistically significantly affected the maximum load of 4F-knit, but differences between small and big loop size were not statistically significant in 8F-knit. Similar behavior was noticed for the modulus values, where the modulus is statistically significantly increased by the bigger loop size—68% for 8F-knit and 63% for the 4F-knit. The loop size against strain showed an increase in 4F-knit when the loop size was bigger, but this difference was not statistically significant. However, decrease of strain in the 8F-knit was statistically significant with smaller loop size. Increase of number of needles from 9 to 19 also had a statistically significant effect on the properties of the knits.

In vitro results of the knits. When the load values were plotted against the incubation time (**Fig. 3**), the influence of the number of yarns on the absolute load properties is clearly seen, giving the 19 needle and 8F knits higher load values. When the strength values were plotted against the incubation time (**Fig. 4**), we noticed that the batches with 4-ply knits will start to lose their strength after 9 weeks and 8-ply knits after 15 weeks. At the beginning, the 4-ply knit is stronger until week-12, after which it will lose strength more rapidly. The difference between 12 and 15 weeks is statistically significant.

The average starting (**Table 1**) strain levels (32–44%) of the knits decreased along the load values and dropped down to ~10% between the weeks 9 and 21. The deepest drop can be noticed with 4F-19Ns, which dropped from 41% to 12.6% between weeks 9 and 15. All mechanical properties of the tested knits were statistically significantly decreased after 12 weeks in vitro.

The initial M_w of the raw material was 280 kDa, and after the extrusion and γ-irradiation, the M_w dropped statistically significantly down to 32 kDa for both of the fiber batches. There was a constant decrease in molecular weights and in viscosity during the incubation (**Fig. 5 and 6**), which achieved statistically significant levels in 9 weeks. A steady increase in polydispersity can be seen for both 4F and 8F between the weeks 30 and 42. However, the only statistically significant change in polydispersity was measured in 42 weeks for 4F.

Results of the shelf life tests. In the shelf life tests, all the specimens retained their mechanical properties during the studied 3-year period (**Table 4**). No statistically significant differences were indicated by Student t-test ($p > 0.05$) in comparison with mechanical properties of 0 weeks and 3 years. All the mechanical values showed a similar behavior. There was no difference in standard deviations for 0- or 3-year samples.

The combination of storage time and storing conditions slightly influenced the molecular properties of the stored γ-irradiated knits. We noticed that there was a statistically significant decrease when comparing the 0-week knits M_w ~ 32 kDa and M_n ~ 18 kDa to 3-year ones M_w ~ 28 kDa and M_n ~ 15 kDa (**Fig. 5**). There was an average 12% drop in the molecular weights during the 3-year study. The 2.5 year samples still retained similar molecular properties to those in the beginning. This time point is clearly seen on the PD curves (**Fig. 6**), which all show a definitive increase after 2.5 years. PD at 2.5 years was ~1.55, whereas at the 3-year point it was ~1.85. Otherwise steady measurements were disturbed at the 1.5 year study point for all the studied groups. This is, very likely the result of an error with the GPC equipment, or the 1.5-year samples were somehow corrupted in the analysis. Unfortunately, it was not possible to re-perform measurements afterwards.

In vitro results of the cylindrical scaffolds. The average porosity of the scaffolds (measured dry from un-incubated samples) is from ~81 to 87% (**Table 2**). The pore size distribution was calculated using the CT data. For a 15 mm scaffold, it was calculated that there were 42% < 100 μm pores, 35% 100–200 μm pores, 19% 200–300 μm pores and 4% of >300 μm pores.

For all the scaffold sizes (ϕ 12, 15 and 19 mm), the compression tests (**Fig. 7**) showed similar stiffness behavior. At week 1,

Table 2. Manufacturing details for 12, 15 and 19 mm scaffolds

Scaffold	Average Scaffold Diameter (mm)	Average Scaffold Height (mm)	Length of Knit (mm)	Average Weight (g)	Average Porosity %
12	12.3 ± 0.2	3.3 ± 0.2	120	0.135 ± 0.004	86.8 ± 2.6
15	14.8 ± 0.2	3.6 ± 0.3	200	0.22 ± 0.04	83.7 ± 1.0
19	19.3 ± 0.3	4.7 ± 0.3	350	0.36 ± 0.04	80.9 ± 8.7

Table 3. Preliminary mechanical properties for the yarns and the knits

YARNS	Load at Max Load (N)	Stress at Max Load (MPa)	% Strain at Max Load (%)	Modulus (GPa)	Yield Stress (MPa)	% Strain at Yield (%)
4-ply (n = 10)*	11.9 ± 0.8	581.2 ± 44.1	31.9 ± 2.2	8.0 ± 0.8	191.0 ± 9.9	2.8 ± 0.1
8-ply (n = 5)*	16.6 ± 0.7	561.6 ± 19.5	35.4 ± 3.6	7.1 ± 0.2	148.1 ± 2.8	2.6 ± 0.1
KNITS	**Load at Max Load (N)**	**Load/$_{1/2}$ loop (N)**	**% Strain at Max Load (%)**	**Modulus (MPa)**		
8F-9Ns (n = 8)	91.7 ± 4.3	5.1 ± 0.2	39.2 ± 2.3	23.9 ± 1.5		
8F-9Nb (n = 8)	96.6 ± 10.1	5.4 ± 0.6	33.4 ± 4.3	40.3 ± 4.3		
8F-19Ns (n = 8)	186.8 ± 20.6	4.9 ± 0.5	41.6 ± 5.1	16.5 ± 0.9		
4F-9Nb (n = 8)	89.3 ± 8.2	5.0 ± 0.5	39.1 ± 7.7	30.0 ± 4.3		
4F-9Ns (n = 8)	67.8 ± 3.1	3.8 ± 0.2	35.9 ± 2.5	18.4 ± 1.0		
4F-19Ns (n = 8)	127.2 ± 18.6	3.3 ± 0.5	44.1 ± 4.7	11.4 ± 0.6		

*Non γ-irradiated.

the 19 mm scaffold had lower compression values compared to the other two scaffolds. For all the scaffolds, after one week in vitro, there was a major reduction in compression stiffness, and the specimens lost their initial rigidity for the rest of the incubation period. The similar stiffness behavior referred to here was the minimal capability of the scaffolds retaining the compression load after 1-week incubation during a 1.5 mm compression.

GPC results show (**Figs. 8 and 9**) that the degradation rate of the PLA96 fibers in scaffolds in vitro is similar to the degradation behavior of the fibers 4F and 8F. After 42 weeks, the measured molecular weights were the same, M_w ~ 8 kDa and M_n ~ 4 kDa. As for the PD, we can see a definite rise starting from the week 20 PD ~1.6 and rising up to 2.3 at week 42. There is a higher PD rise in the scaffold series compared to the plain fibers (4F and 8F). The molecular properties between the surface and the core of in vitro scaffolds showed no statistically significant differences during the in vitro incubation.

The weight loss of the three scaffold sizes was noticed to begin around the week 28. At week 48, there was a 10% mass loss observed for all the scaffold sizes. When the 15 mm sample weight loss data is plotted against the GPC results (**Fig. 10**), we can observe that the weight loss starts when the molar mass is less than 20 kDa, and it increases more rapidly when the molecular weight is less than 10 kDa.

In vivo results of the cylindrical scaffolds. We can see from the compression test curves (**Fig. 7A–D**) that the scaffold loses its stiffness in vivo before the week-2 test point. After 12 weeks, we can see a rise in stiffness, and it is further increased until week 48.

The degradation rate of the PLA96 fibers in scaffold format in vivo is statistically significantly different after 6 weeks when compared with the degradation rate in vitro. Implanted scaffolds after of 52 weeks had M_w 18 kDa and M_n 12 kDa, whereas it was only 8 kDa after 48 weeks in vitro. However, both of the degradation profiles follow the same trend for the first 4 weeks, after which we can see a delay in the in vivo degradation that eventually leads to a slower degradation compared to the in vitro degradation. The viscosity is also statistically significantly different compared to in vitro samples. There is a clear lag in the viscosity drop in vivo, and in the case of PD, we cannot notice any statistically significant changes.

The 52-week specimens were visually examined (**Fig. 11**), and we can see that the scaffold is still present, visible, maintaining its form and tightly packed in dense connective tissue.

Discussion

The tensile strength of the yarn in the knit is lower than that of the yarn tested prior the knitting. This is due to damage done to the fibers during the knitting as well as due to the non-unidirectional forces inflicted on the yarn due to the loops. For our specimens, the behavior of the 0-week knits was as expected. Similar break forces for 4-ply knits with equal knitting properties were reported earlier by Kellomäki,[9] although the strain property of our knit was ~17% higher. The higher strain values are influenced by the knit density, which was lower in our study.

Increasing the number of needles in the tubular weft knit statistically significantly increased the measured tensile load. Increasing the number of single filaments in fibers in the tubular weft knit has a statistically significant effect on tensile load of certain structures; the only statistically insignificant difference was indicated between 8F-9Nb and 4F-9Nb knits. Higher numbers of filaments in fibers also affect the knitting properties. For a chosen needle and needle bed type, there is a maximum number

Table 4. Shelf life data of the mechanical tests for all knitted samples

		Maximum Load (N)		Load/$_{1/2}$ Loop (N)		Strain at Max Load (%)		Youngs Modulus (MPa)	
	Months	Mean	StDev	Mean	StDev	Mean	StDev	Mean	StDev
8F-9Ns	0	91.7	4.3	5.1	0.2	39.2	2.3	23.9	1.5
	6	101.3	6.8	5.6	0.4	41.7	4.8	17.7	0.9
	12	100.7	6.6	5.6	0.4	40.7	3.9	19.5	2.1
	18	100.2	2.9	5.6	0.2	41.4	3.0	19.8	1.1
	24	96.7	4.1	5.4	0.2	43.3	3.6	20.1	1.5
	30	97.0	5.8	5.4	0.3	41.0	6.4	21.6	2.3
	36	103.7	2.6	5.8	0.1	44.4	2.5	21.2	1.3
8F-9Nb	0	96.6	10.1	5.4	0.6	33.4	4.3	40.3	4.3
	6	95.3	7.1	5.3	0.4	31.7	5.4	24.2	5.3
	12	96.7	6.4	5.4	0.4	35.2	5.9	26.1	0.7
	18	96.9	11.5	5.4	0.6	37.7	3.0	25.8	2.7
	24	96.9	4.5	5.4	0.2	40.0	4.2	23.1	0.4
	30	99.4	4.9	5.5	0.3	37.2	2.2	31.3	2.2
	36	91.5	7.0	5.1	0.4	37.2	6.7	29.6	1.6
4F-9Ns	0	89.3	8.2	5.0	0.5	39.1	7.7	24.3	1.3
	6	94.2	6.9	5.2	0.4	37.4	5.0	22.0	2.1
	12	80.3	8.6	4.5	0.5	28.5	5.9	22.6	1.0
	18	86.2	8.2	4.8	0.5	31.7	3.1	22.7	3.7
	24	81.1	6.4	4.5	0.4	29.6	4.7	22.2	4.5
	30	85.4	3.5	4.7	0.2	31.1	2.9	24.4	1.6
	36	81.2	4.8	4.5	0.3	31.3	4.5	23.4	4.5
4F-9Ns	0	67.8	3.1	3.8	0.2	35.9	2.5	18.4	1.0
	6	73.7	6.6	4.1	0.4	36.0	3.6	15.7	1.5
	12	71.9	2.8	4.0	0.2	37.6	5.5	14.7	3.1
	18	70.8	8.5	3.9	0.5	34.7	6.1	15.7	1.7
	24	73.0	4.2	4.1	0.2	38.5	4.9	15.2	2.8
	30	71.8	3.9	4.0	0.2	34.8	2.0	17.2	1.7
	36	70.8	3.8	3.9	0.2	36.1	3.9	17.6	0.6
4F-19Ns	0	127.2	18.6	3.3	0.5	44.1	4.7	11.4	0.6
	6	138.7	21.9	3.7	0.6	44.5	6.8	9.9	0.5
	12	131.7	4.6	3.5	0.1	45.4	4.0	9.4	0.9
	18	141.4	11.4	3.7	0.3	44.1	3.8	9.7	0.6
	24	119.0	12.6	3.1	0.3	41.5	4.5	8.5	0.8
	30	127.4	4.8	3.4	0.1	44.1	1.8	9.9	0.7
	36	125.7	14.0	3.3	0.4	45.9	3.2	10.3	0.4
8F-19Ns	0	186.8	20.6	4.9	0.5	41.6	5.1	16.5	0.9
	6	204.6	16.0	5.4	0.4	51.3	6.7	13.1	0.7
	12	194.6	12.6	5.1	0.3	46.7	3.9	13.4	0.8
	18	195.8	7.1	5.2	0.2	48.9	4.7	12.9	1.4
	24	195.8	10.2	5.2	0.3	52.2	7.4	11.4	0.9
	30	204.0	11.7	5.4	0.3	49.5	5.7	13.8	0.9
	36	190.1	14.9	5.0	0.4	45.3	6.1	14.2	0.9

n = 5 for all the data points.

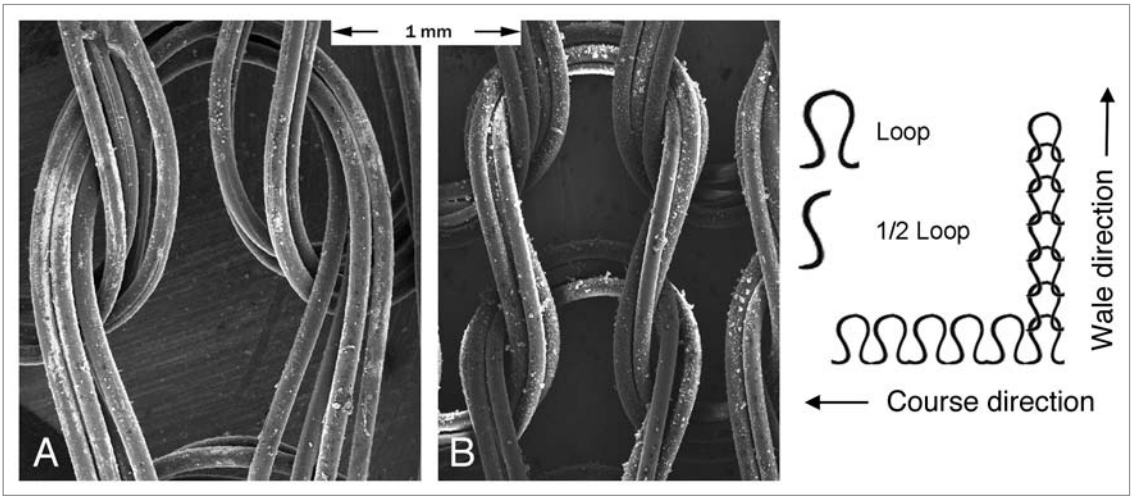

Figure 1. Knit info and SEM pictures of 4-filament knit of (A) 4F-9Nb (big loop size) and (B) 4F-9Ns (small loop size) after 1 week of incubation.

of filaments that can be used where the knitting procedure is optimal for a good quality knit.[23] The mechanical properties of weft knit fabrics are different when the wale and course directions are compared.[24-26] For our purposes, the wale direction is more important, since, in the tubular form, if used as such, the tensile forces are mainly induced in the wale direction. The tensile strength is higher and the extension to break lower in the wale direction. When the stretching is to the wale direction, there is a higher deformation to the wale spacing than to the course spacing.[22] Statistically significant loop size correlation to the tensile strength was noticed more clearly with the 4-ply knit; the longer the loop length, the higher the tensile strength. Similar behavior was noticed when using the knits as reinforcement in the composite structures.[27] The physical properties of the weft knit fabrics differ when the wale and/or course dimensions change, and the elastic recovery, in particular, in the wale direction is higher compared to the course direction.[24] By altering loop size, wale and course properties, it is possible to affect the porosity of the single jersey tubular knit, thus altering the penetration ability of liquids and gases.

The 8-ply fiber lost 15–16% of its mechanical properties (load/$_{½}$ loop) during the 9-week hydrolysis, whereas 4-ply fiber lost 4–30%. Although they underwent similar processing conditions, the retention time was longer for the 4-ply fiber. So, in the process, there is most likely a higher monomer content in the 4-ply fiber. Based on our earlier studies in reference 28, we can predict a 0.2–0.3 wt% of lactide monomer accumulation in the fiber on the basis of the degradation behavior of this medical-grade, high i.v. PLA96. The 8-ply fiber knit retains its strength at a starting level for a longer time compared to the 4-ply knit, supporting this assumption. On the other hand, on the basis of the molecular weight studies, the 8-ply fiber lost its molecular weight faster until week 20, yet we did not observe a critical incline in the behavior compared to the 4-ply fiber. After week 20, the M_w was equalized. The monomer content differences between the fiber batches, therefore, cannot be considerable based on the behavior of M_w during the hydrolysis.[29] The same degradation behavior as a function of M_w reduction for 4-ply fiber was reported by our group[6] for the 20-week period. It could be noticed that, when comparing the molecular weight data, the knit and the scaffold degraded similarly in vitro, so the form of the scaffold had no influence on the degradation speed. Although the knits were incubated in SBF and the scaffolds in PBS, there was no difference noticed between SBF and PBS PLLA backbone degradation, water uptake or mass loss during the first 27 weeks.[30] When material properties are considered, none of the structures could be preferred over the other, as the maximum load level can be achieved by increasing the amount of material and considering that knits would be used as such in suitable applications under tensile forces. If considering that minimal material usage is preferable, then the 4F-9N knits should be used, of the studied ones, when the mechanical properties are suitable for the purpose of use.

The shelf life studies showed a good uniform quality with respect to tensile properties during the whole 3-year period. As for the molecular weight properties, there is a reduction in molecular weights and viscosity and an increase in polydispersity, but there was no change in the mechanical properties and standard deviations when comparing the different knits. This only confirms that changes in molecular level that occurred during storage had no effect on the mechanical properties. It is known that the mechanical properties are not simultaneously affected, even though the molecular weight drops in the beginning of the degradation and considering that the original molecular weight is high enough, since the properties are strongly affected by the actual molecular weight, not only the original molecular weight. So, in the case of bulk PLA 96, the drastic drop in strength is also accompanied by the mass loss,[31] whereas in fiber form, the strength properties are more easily affected due to the subtle changes in morphology caused by the drop in molecular weight[9,29] prior to the loss of mass, as seen in this study, where the mass loss starts at week 24, when fiber tensile properties are already low. Only some shelf life data exists where PLA96 was studied. In a study by Pluta et al., melt-processed material was tested after aging the material for

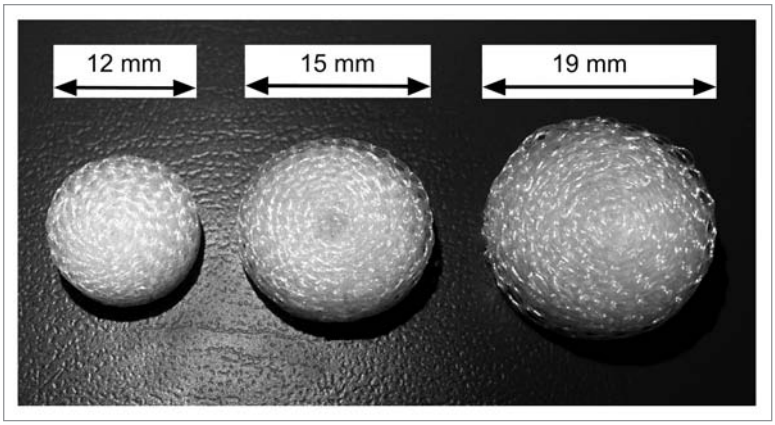

Figure 2. The outlook of the 12, 15 and 19 mm scaffolds after heat treatment.

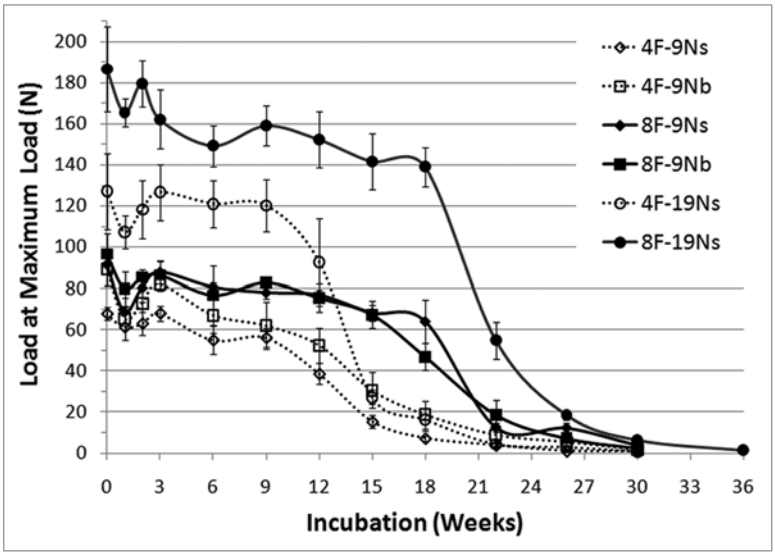

Figure 3. Load properties for all knitted samples (n = 5 for all the data points).

1 year. Results showed no change in molecular weight properties or in polydispersity during the follow up.

It is generally known that pure PLLA loses its properties in vivo in a reasonable amount of time;[33,34] still, it is considered a slow in vivo degrading material due to the presence of material years after the implantation, mainly due to its high crystallinity.[35,36] So, the use of P(L/D)LA with 4 wt% of D-lactide in the structure has been shown to degrade faster while still retaining its properties for a long enough time to be used in operations where longer strength retention or presence is needed.[17] When the speed of the degradation is considered, some previous results suggest a similar[30] or faster[9,33] in vivo degradation compared to in vitro degradation for PLA polymers and PLA-based devices in the subcutaneous space of rats or rabbits. For example, the 56–99% decrease in M_w reported for PLA materials at 27 weeks in the subcutaneous mouse and rat models[35,37] seems to favor faster in vivo degradation when compared with the P(L/D)LA 96/4 fiber degradation behavior in vitro, where a 30–50% drop in M_w occurred during the 27-week period.[9,18] For a slower in vivo degradation, there are indications of delayed degradation, e.g., in the case of PLLA meniscal screw, where after 3 years, the screw had 64.7% of its molecular weight left,[38] a result that does not correspond to animal subcutaneous models or in vitro models. Since many properties (e.g., material origin, processing conditions, in vivo environment) influence the degradation of PLA materials, there is a lot of variation in the results. The P(L/D)LA 96/4 used in our study shows similar molecular weight loss in PBS compared to other studies.[6,18,31] But in this study, we can show a delayed degradation in the in vivo compared to the in vitro model. The reason for this could be the increase of dense connective tissue layers. It was shown by Länsman et al. that the tissue ingrowth reaches the innermost part of the scaffold implant by 3 weeks.[16] Thereafter, the formation of dense connective tissue around each single filament begins, and it gets more compact after 6 weeks, with a clear increase of dense connective tissue by 12 weeks. The layers of connective tissue become denser and thicker over time, forming septae of mature dense connective tissue. The amount of vascularity decreases markedly during maturation of connective tissue. The increasing amount of mature dense connective tissue forms thickening layers around each PLDLA filament. Therefore, the layer of dense connective tissue locates in between the PLDLA filaments and vascularized looser connective tissue. These indications go together with the delayed degradation that was observed in our study, since the difference in degradation rates of in vivo and in vitro samples begins at those weeks. It is also possible that this dense connective tissue might allow the decrease of pH inside the capsule, which might slow down the degradation at the beginning of the pH decrease as suggested by Schlieker et al.[39]

When comparing the different scaffold types, there are no clear differences between the 12 and 15 mm scaffolds. In vitro 1-week compression properties of the 19 mm scaffold are lower due to the dimensions of the sample. The greater height of the sample renders the scaffold softer at the beginning compared to the other two scaffolds, since the knit structure they were made from is the same for all, and the preload of 5 N equalized the starting point for all the samples. So, the scaffolds were somewhat similar from the in vitro perspective. The knitted fabrics produced here are mainly intended for manufacturing a vessel to guide fibrous tissue proliferation in human body. Therefore, they have to have sufficient properties for supporting, for example, the finger joint for rheumatoid patients.[17] As the degradation of the material occurs and the mechanical properties vanish, it is important that the forming tissue takes up the structural forces. For this purpose, it is essential that mature, dense connective tissue can form into the sample before the sample collapses. In the rat studies,[16] this time has proven to be somewhere between the weeks 24–48, and we can clearly show that the effect of the maturing tissue on the compression stiffness is already seen at week 12. Although we can see a clear degradation of the material

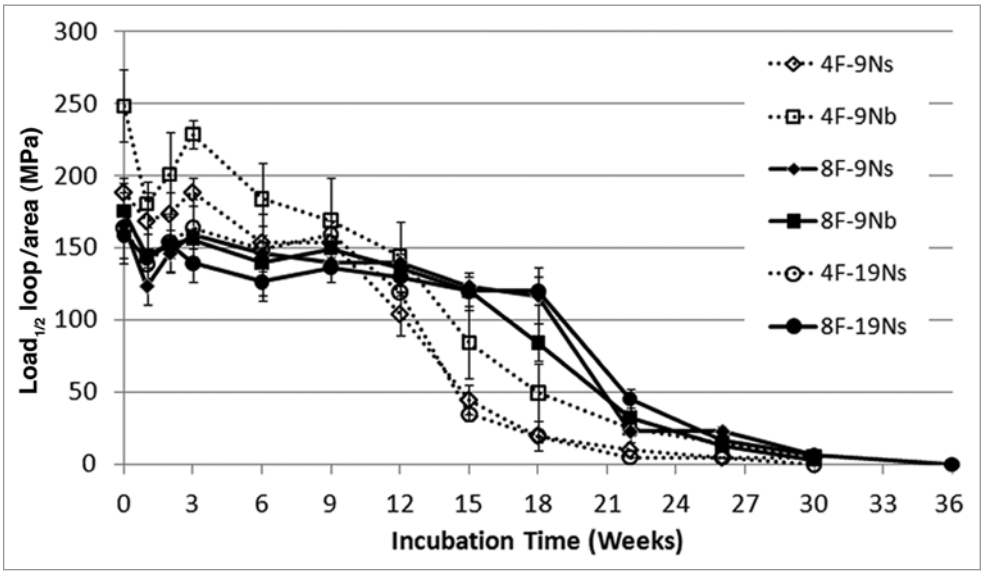

Figure 4. Strength properties for all knitted samples (n = 5 for all the data points).

regarding the knit tensile properties, the properties in compression and post-operative in vivo show that the fiber network is still functional at week 36 and still clearly present in the tissue at week 52.[16,18,19] It has been shown that the same P(L/D)LA 96/4 knitted tube used here is suitable when used as a cylindrical 3D scaffold for gaining a functional metacarpophalangeal or other small joints.[17,19]

What it is essential to notice here is that we have shown that the fiber is not drastically affected by the knitting procedure, and the tubular knit still obtains suitable properties for a favorable time to be used for TE purposes. With parameter setting, it is possible to affect the properties of the knitted samples, although for MCP purposes, the subtle porosity differences seems to play no major part for the connective tissue forming.[16] Therefore, it is vital that the polymer properties and the fiber properties (amount and thickness of the filaments) are considered for even better outcome of the required tissue forming.

Materials and Methods

Multifilament fibers. Two highly purified, medical-grade poly(L/D)lactide 96/4 polymers with intrinsic viscosities of (1) 5.47 dl/g (PLA96A) and (2) 5.70 dl/g (PLA96B) (Purac Biochem, Goringhem, The Netherlands) were used for fiber manufacturing. PLA96A was melt-spun into multifilament fibers (4- and 8-ply), and PLA96B was processed to 4-ply fibers (similar to PLA96A), and these fibers were only used to produce scaffolds. In all cases, Gimac microextruder (Gimac, Gastronno, Italy) with a screw diameter of 12 mm was used. The single orifice diameter in the nozzles was 0.4 mm. The nozzle temperature was 267°C for both batches. The extruder retention time for the 4-ply fiber was 360 s, and for the 8-ply fiber, 300 s. The fibers were hot drawn using three caterpillars (draw ratio 4.5) and three IR ovens (oven temperatures 95/115/120°C). Fibers were further used for knitting and scaffold manufacturing.

Single jersey knits. Both multifilament fiber batches of PLA96A were knitted to a tubular single jersey knit using a circular knitting machine equipped with a ½" needle cylinder (Elha R-1S, Textilmaschinenfabrik Harry Lucas GmbH, Neumünster, Germany). Parameters in the process were the number of the latch needles and the loop size (length of the one continuous loop) that sets the values to wales (vertical columns) and courses (horizontal rows) (**Fig. 1**). The samples, their knitting parameters and properties are shown in **Table 1**. Knits were cut to samples of 70 mm in length each, and the ends were heat sealed to prevent the loop running.

Porous 3D cylindrical scaffolds. The cylindrical scaffolds were manufactured from the 4F-9Ns knit made of PLA96B 4-ply multifilament fibers. The knits were cut to size according to the requested size of the ready scaffold (**Table 2**) and rolled into the cylindrical shape. The end of the knit was fixed to the roll with a biodegradable "glue" prepared by dissolving poly(L/DL)lactide 70/30 polymer into acetone. Scaffolds were heat treated at 70°C/15 min in a mold to obtain the desired shape (**Fig. 2**). The final average porosity of the scaffolds was measured using cone-beam computed tomography (ProMax 3D s, Planmeca, Helsinki, Finland).

In vitro and in vivo. Prior to in vitro incubation or in vivo implantation, the fibers, knits and cylindrical scaffolds were washed with 95% ethanol for 3 minutes in a laboratory-scale ultrasonic washer, dried in vacuum for 24 hours, then packed in vacuum sealed bags (inner layer bag PE, outer layer bag Aluminum/PE for UV-protection) and sterilized by γ-irradiation using a commercial procedure, where the minimum dose was set to 25 kGy. The fibers were incubated for periods of 0, 1, 2, 3, 6, 9, 12, 15, 18, 22, 26, 30, 36 and 42 weeks at 36.5°C in simulated

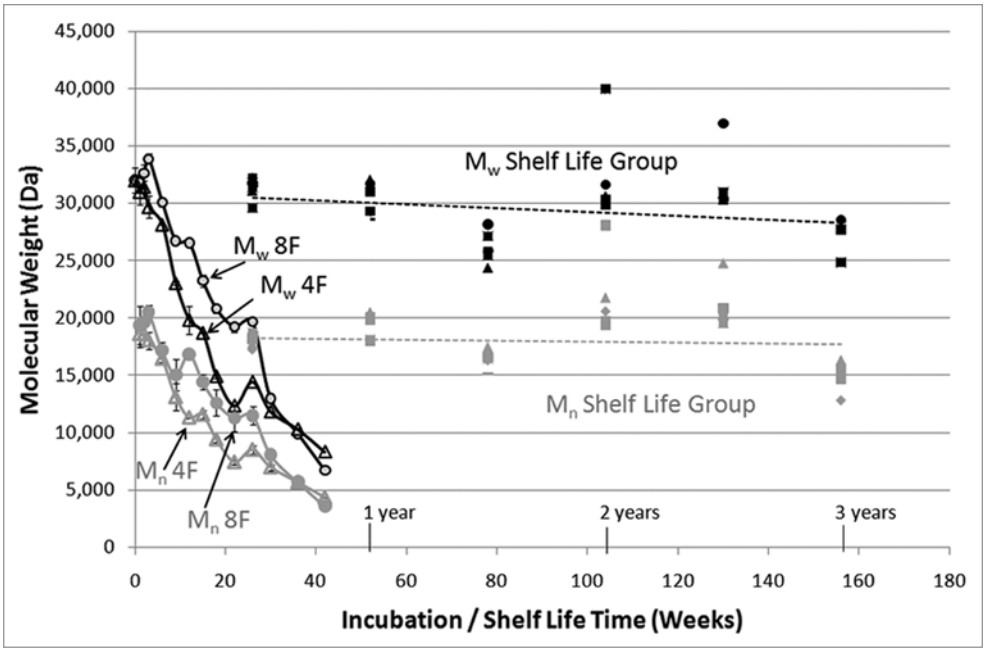

Figure 5. Molecular weight properties of the yarns and shelf life samples.

body fluid[40] (SBF) at pH 7.25. The buffer solution was changed and the pH measured at 21°C fortnightly.

The cylindrical samples were incubated for periods of 0, 1, 2, 6, 10, 16, 15, 18, 20, 24, 28, 32, 36, 42 and 48 weeks at 36.5°C at phosphate buffered saline (PBS) pH 7.25. The specimen mass/buffer solution ratio was, on average, 7.4 g/100 ml. The buffer solution was changed and the pH measured at 21°C fortnightly.

The 15 x 3.5 mm scaffolds were implanted subcutaneously into rats for periods of 3, 12, 24, 48 and 52 weeks. These samples were a part of the study by Länsman et al., and the procedure is previously explained in detail in reference 16.

Shelf life. PLA96 knits were cut to size, washed, dried, packed and γ-irradiated (as described above). Sample packages were placed on the laboratory shelf in ambient room temperature and under normal (atmospheric) pressure to ensure the storage time. Samples were periodically tested (tensile test, molecular weight characterization) after 0.5, 1, 1.5, 2, 2.5 and 3 years.

Material characterization. Number of average molecular weight (M_n), weight average molecular weight (M_w), intrinsic viscosity (i.v.) and polydispersity (PD) were measured by gel permeation chromatography (GPC) relative to narrow polystyrene standards. GPC consisted of Waters 410 RI differential refractometer detector and Waters 515 HPLC pump (Waters, Milford, MA USA). The GPC columns were PL gel 5 μm Guard and 2 PL gel 5 μm mixed-C. Injection volume was 150 μl, and the flow rate of eluent was 1 ml/min. Calibration was performed using monodisperse polystyrene standards, applying Mark-Houwink parameters for PS ($K = 1.12 \times 10^{-4}$ and $a = 0.73$). The samples were dissolved in 0.1% w/v solutions in chloroform at room temperature.

Tensile properties of the fibers and knits samples were tested using Instron 4411 Materials Testing Machine (Instron Ltd., High Wycombe, England). Crosshead speed was 30 mm/min and gauge length was 20 mm. The half loop force was calculated as:

$$\text{Load}_{\text{½ loop}} = \text{Maximum load}/(2 \times \text{needle count})$$

$\text{Load}_{\text{½ loop}}$ refers to the load in the half loop, i.e., in the 4-ply or 8-ply fiber used in the knitting.

Compression properties of the cylindrical scaffolds were tested using a Lloyd LR 30K Materials Testing Machine (Lloyd Instruments Ltd., Fareham, England). Crosshead speed was 1 mm/min. Specimens were compressed between polished stainless steel, plated, and 5 N preload was applied to minimize the influence of the rough surfaces of the scaffolds, after which the new zero/starting point was set. The scaffolds were tested until 2 mm extension was reached (50–67% thickness change). Initial compression results were measured on dry specimens, and after in vitro hydrolysis, wet specimens were tested.

After the sacrifice, samples were prepared by removing the external connective tissue formed outside the scaffold. The tissue grown into the porous scaffold and the scaffold itself were left untouched. Samples were placed in the saline and tested within 24 hours from sacrifice. The above testing procedure was also used for the in vivo scaffolds.

Conclusions

The entirety of the production cycle, from raw material to an in vivo scaffold, was covered. From biodegradable PLA96 polymer

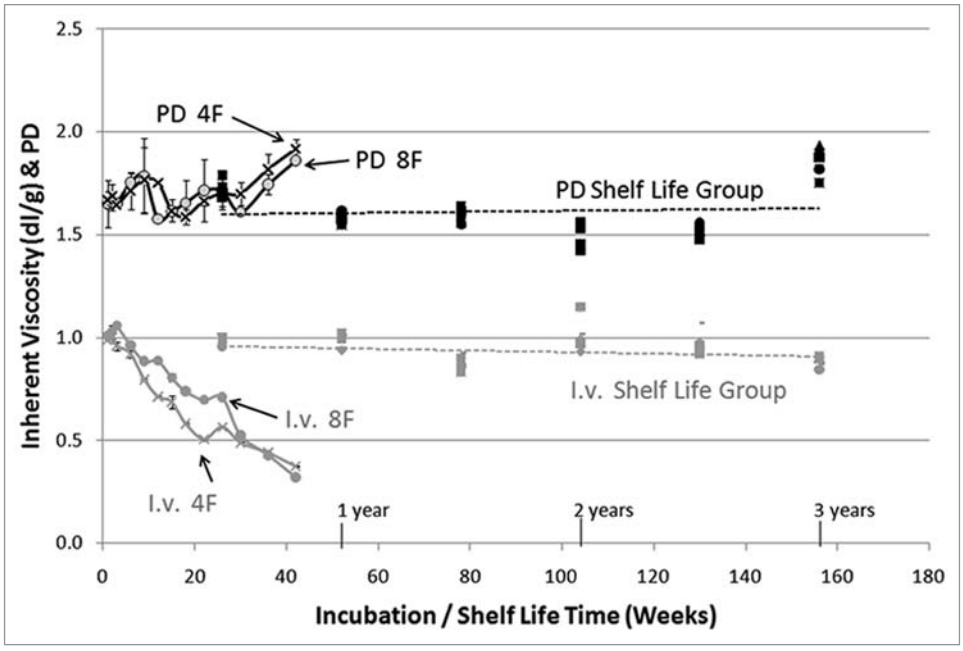

Figure 6. Viscosity and polydispersity data of the yarns and shelf life samples (n = 2 for all data points).

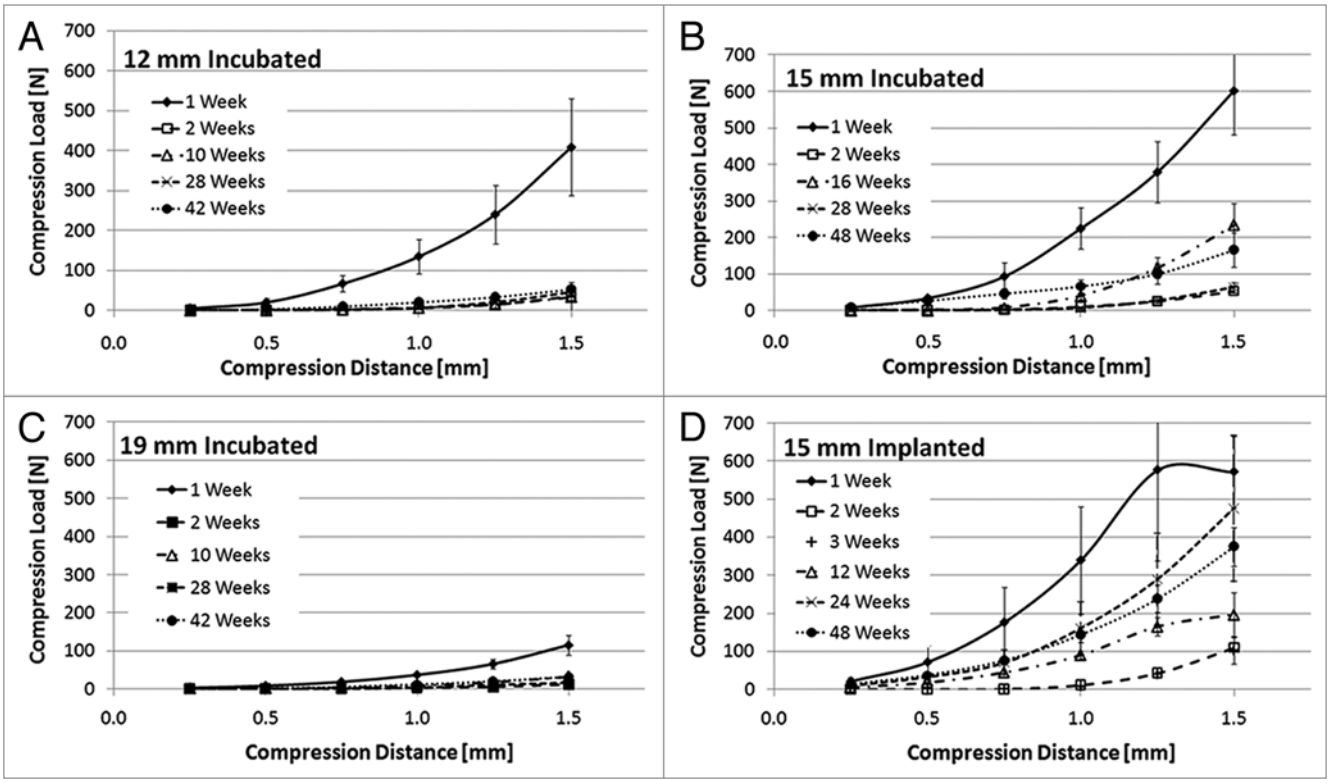

Figure 7. In vitro mechanical data for (A) 12, (B) 15 and (C) 19 mm scaffolds and (D) in vivo data for 15 mm scaffold (n = 3 for all in vitro data points, n = 5 for all in vivo data points except for 1 and 2 week data points n = 4).

fibers, different knit types were prepared. Since these constructions are interesting for further applications, the properties of those knitted samples were tested in vitro as well as in 3-year shelf life (storage time, aging) tests. We confirmed that the mechanical integrity is valid even after 3-year restoration in a controlled atmosphere and at an ambient temperature for the γ-irradiated samples when they were properly packed for storage. The polymer morphology slightly changed during the final

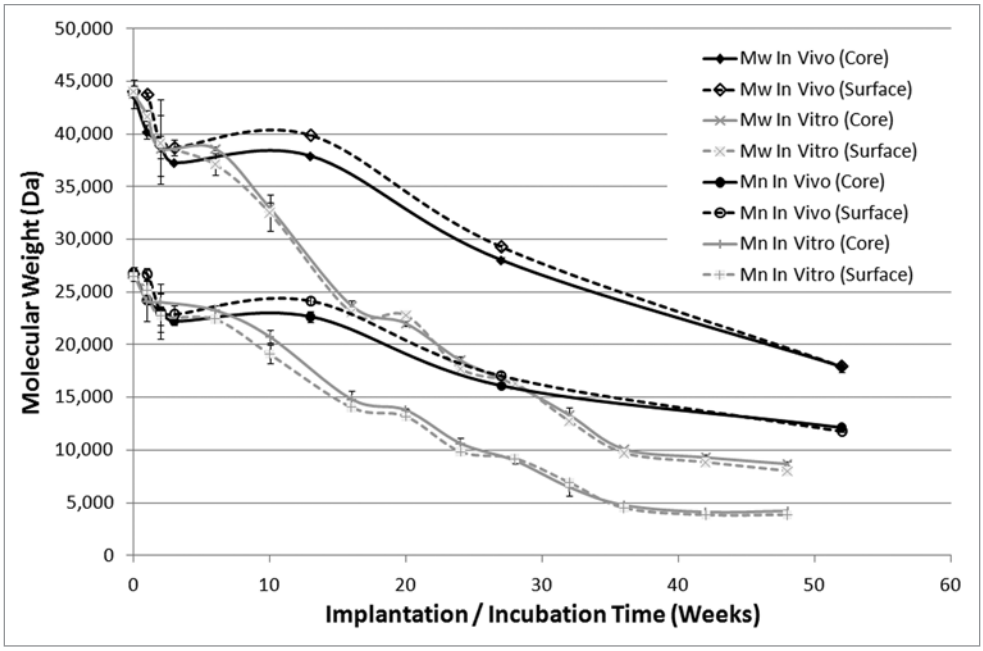

Figure 8. Molecular weight data of the 15 mm scaffold in vivo and in vitro series (n = 2 for all data points).

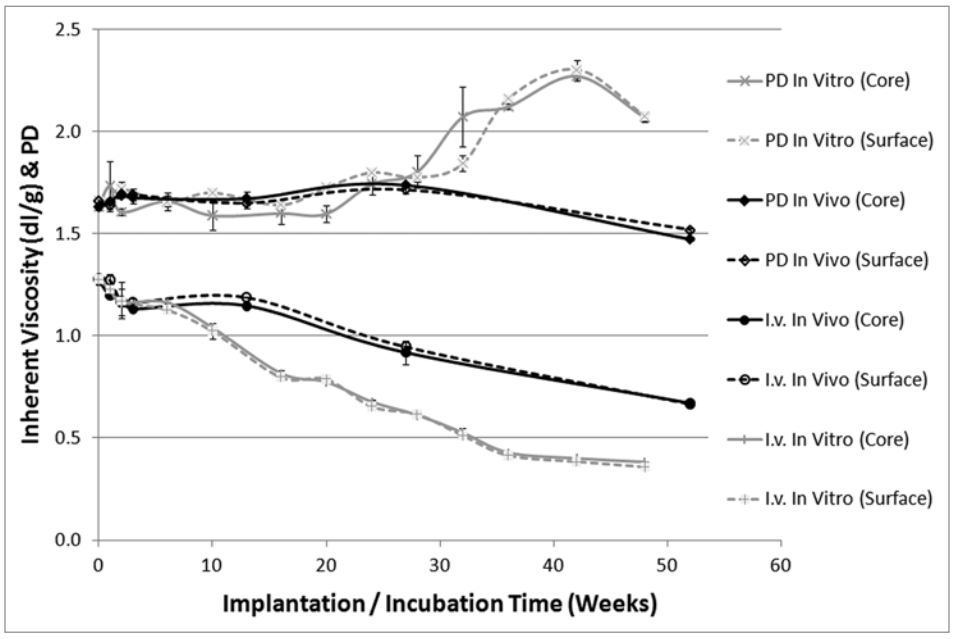

Figure 9. Polydispersity and viscosity data of the 15 mm scaffold in vivo and in vitro series (n = 2 for all data points).

6 months of this storage period, although it had no influence on the mechanical properties. We showed that the degradation characteristics are similar when comparing the knits and the scaffolds. Furthermore, we showed that the weakened mechanical properties resulting from the immersion/implantation of the scaffolds prepared from these knits are enhanced by the ingrown tissue, which actually renders mechanical strength to the scaffold in vivo, thus making the structure a truly tissue-engineered composite. These indications are important when commercializing the structures and planning the use of such scaffolds.

Disclosure of Potential Conflicts of Interest

No potential conflicts of interest were disclosed.

Acknowledgments

The authors would like to thank Ms. Terhi Kulmala, Ms. Anna Sjölund, Ms. Eira Lehtinen and Mr. Fatih Cengiz for their help in testing and analyzing the data. Researcher funds from the Graduate School of the Processing of Polymers and Polymer-Based Multimaterials, financed by Finland's Ministry of Education, is greatly appreciated.

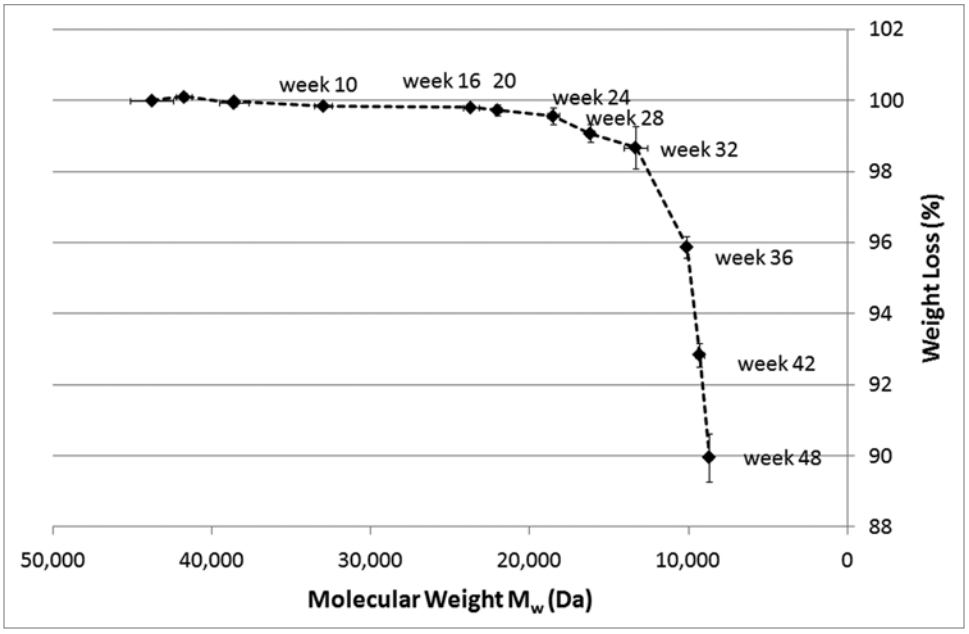

Figure 10. Weight loss data (n = 3) plotted against the M_w (n = 2) during the 15 mm scaffold in vitro incubation.

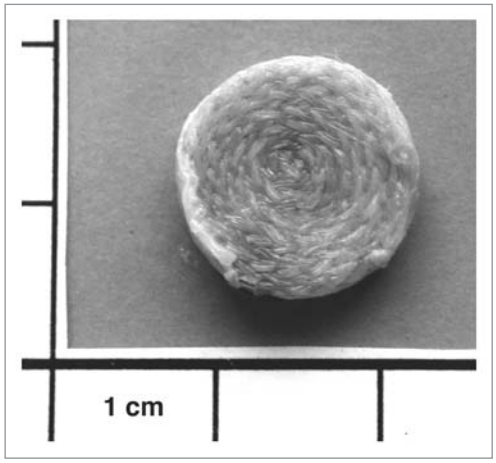

Figure 11. The scaffold after 52 weeks of implantation.

References

1. Gupta B, Revagade N, Hilborn J. Poly(lactic acid) fiber: An overview. Prog Polym Sci 2007; 32:455-82; DOI:10.1016/j.progpolymsci.2007.01.005.
2. Cicero JA, Dorgan JR. Physical properties and fiber morphology of poly(lactic acid) obtained from continuous two-step melt spinning. J Polym Environ 2001; 9:1-10; DOI:10.1023/A:1016012818800.
3. Schmack G, Tändler B, Vogel R, Beyreuther R, Jacobsen S, Fritz HG. Biodegradable fibers of poly(L-lactide) produced by high-speed melt spinning and spin drawing. J Appl Polym Sci 1999; 73:2785-97; DOI:10.1002/(SICI)1097-4628(19990929)73:14<2785::AID-APP1>3.0.CO;2-L.
4. Pegoretti A, Fambri L, Migliaresi C. In vitro degradation of poly(L-lactic acid) fibers produced by melt spinning. J Appl Polym Sci 1997; 64:213-23; DOI:10.1002/(SICI)1097-4628(19970411)64:2<213::AID-APP2>3.0.CO;2-U.
5. Viinikainen AK, Göransson H, Huovinen K, Kellomäki M, Törmälä P, Rokkanen P. Bioabsorbable poly-l/d-lactide (PLDLA) 96/4 triple-stranded bound suture in the modified Kessler repair: an ex vivo static and cyclic tensile testing study in a porcine extensor tendon model. J Mater Sci: Mater Med 2009; 20:1963-9; DOI:10.1007/s10856-009-3747-8.
6. Ellä V, Gomes ME, Reis RL, Törmälä P, Kellomäki M. Studies of P(L/D)LA 96/4 non-woven scaffolds and fibres; properties, wettability and cell spreading before and after intrusive treatment methods. J Mater Sci: Mater Med 2007; 18:1253-61; DOI:10.1007/s10856-007-0144-z.
7. Wu W, Feng X, Mao T, Feng X, Ouyang HW, Zhao G, Chen F. Engineering of human tracheal tissue with collagen-enforced poly-lactic-glycolic acid nonwoven mesh: A preliminary study in nude mice. Brit J Oral Max Surg 2007; 45:272-8; DOI:10.1016/j.bjoms.2006.09.004.
8. Sittinger M, Reitzel D, Dauner M, Hierlemann H, Hammer C, Kastenbauer E, et al. Resorbable polyesters in cartilage engineering: Affinity and biocompatibility of polymer fiber structures to chondrocytes. J Biomed Mater Res 1996; 33:57-63; DOI:10.1002/(SICI)1097-4636(199622)33:2<57::AID-JBM1>3.0.CO;2-K.
9. Kellomäki M. In Bioabsorbable and Bioactive Polymers and Composites for Tissue Engineering. Tampere: Tampere University of Technology Publications 311, Tampere 2000; 246.
10. Koch S, Flanagan TC, Sachweh JS, Tanios F, Schnoering H, Deichmann T, et al. Fibrin-polylactide-based tissue-engineered vascular graft in the arterial circulation. Biomaterials 2010; 31:4731-9; DOI:10.1016/j.biomaterials.2010.02.051.
11. Gundy S, Manning G, O'Connell E, Ellä V, Sri Harwoko M, Rochev Y, et al. Human coronary artery smooth muscle cell response to a novel PLA textile/fibrin gel composite scaffold. Acta Biomater 2008; 4:1734-44; DOI:10.1016/j.actbio.2008.05.025.
12. Tiitu V, Pulkkinen HJ, Valonen P, Pulliainen O, Kellomäki M, Lammi MJ, Kiviranta I. Bioreactor improves the growth and viability of chondrocytes in the knitted poly-L,D-lactide scaffold. Biorheology 2008; 45:539-46; DOI:10.3233/BIR-2008-0492.
13. Tschoeke B, Flanagan TC, Koch S, Harwoko MS, Deichmann T, Ellä V, et al. Tissue-engineered small-caliber vascular graft based on a novel biodegradable composite fibrin-polylactide scaffold. Tissue Eng Part A 2009; 15:1909-18; DOI:10.1089/ten.tea.2008.0499.
14. Guo Z, Chen JJ, Zhang PH. A knitted scaffold for tendon engineering using poly (lactic acid) fibers. Adv Mat Res 2011; 197:164-7; DOI:10.4028/www.scientific.net/AMR.197-8.164.
15. Potier E, Oudina K, Arnaud E, Ellä V, Kellomäki M, Ashammakhi N, et al. Mesenchymal stem cells loaded onto PLDLA scaffolds differentiated towards an osteogenic potential influence of fluid flow. J Biomech 2006; 39:215.
16. Länsman S, Pääkkö P, Ryhänen J, Kellomäki M, Waris E, Törmälä P, et al. Poly-L/D-lactide (PLDLA) 96/4 fibrous implants: Histological evaluation in the subcutis of experimental design. J Craniofac Surg 2006; 17:1121-8; DOI:10.1097/01.scs.0000231627.33382.85.

17. Honkanen PB, Kellomäki M, Lehtimäki MY, Törmälä P, Mäkelä S, Lehto MUK. Bioreconstructive joint scaffold implant arthroplasty in metacarpophalangeal joints: short-term results of a new treatment concept in rheumatoid arthritis patients. Tissue Eng 2003; 9:957-66; PMID:14633380; DOI:10.1089/107632703322495600.
18. Talvitie E, Mutanen M, Kellomäki M. Studies of bioreconstructive P(L/D)LA 96/4 joint scaffolds. In: Tanskanen JMA, et al. (Eds.). Proceedings of the 5th Tampere Tissue Engineering Symposium, Tampere, Finland April 23–25. 2008.
19. Waris E, Ashammakhi N, Lehtimäki M, Tulamo RM, Kellomäki M, Törmälä P, et al. The use of biodegradable scaffold as an alternative to silicone implant arthroplasty for small joint reconstruction: An experimental study in minipigs. Biomaterials 2008; 29:683-91; DOI:10.1016/j.biomaterials.2007.10.037.
20. Hutmacher DW. Scaffolds in tissue engineering bone and cartilage. Biomaterials 2000; 21:2529-43; DOI:10.1016/S0142-9612(00)00121-6.
21. Hutmacher DW. Polymers for Medical Applications, In: Buschow KHJ, Cahn RW, Flemings MC, Ilschner B, Kramer EJ, Mahajan S, et al. Eds. Encyclopedia of Materials: Science and Technology. Oxford: Elsevier Science 2001; 7664-73; DOI:10.1016/B0-08-043152-6/01371-1.
22. Mikucione D, Ciukas R, Mickeviciene A. The Influence of Knitting Structure on Mechanical Properties of Weft Knitted Fabrics. MATERIALS SCIENCE (MEDŽIAGOTYRA) 2010; 16:221-5.
23. Xu W, Zhou F, Ouyang C, Ye W, Yao M, Xu B. Mechanical properties of small-diameter polyurethane vascular grafts reinforced by weft-knitted tubular fabric, J Biomed Mater Res Part A 2010; 92:1-8; DOI:10.1002/jbm.a.32333.
24. Zurek W, Cislo R, Bialek U, Dziewiecka M. Physical Properties of Weft Knitted Fabrics. Text Res J 1986; 56:241-8; DOI:10.1177/004051758605600403.
25. Ramakrishna S. Characterization and modeling of the tensile properties of plain weft-knit fabric-reinforced composites. Compos Sci Technol 1997; 57:1-22; DOI:10.1016/S0266-3538(96)00098-X.
26. De Araújo M, Fangueiro R, Hong H. Modelling and simulation of the mechanical behaviour of weft-knitted fabrics for technical applications, Part I: General considerations and experimental analyses. AUTEX Research Journal 2003; 3; In press.
27. Khondker OA, Herszberg I, Leong KH. An Investigation of the structure-property relationship of knitted composites. J Compos Mater 2001; 35:489-508; DOI:10.1177/002199801772662127.
28. Ellä V, Nikkola L, Kellomäki M. Process-induced monomer on a medical-grade polymer and its effect on short-term hydrolytic degradation. J Appl Polym Sci 2011; 119:2996-3003; DOI:10.1002/app.33027.
29. Paakinaho K, Ellä V, Syrjälä S, Kellomäki M. Melt spinning of poly(l/d)lactide 96/4: Effects of molecular weight and melt processing on hydrolytic degradation. Polym Degrad Stabil 2009; 94:438-42; DOI:10.1016/j.polymdegradstab.2008.11.010.
30. Hooper KA, Macon ND, Kohn J. Comparative histological evaluation of new tyrosine-derived polymers and poly (L-lactic acid) as a function of polymer degradation. J Biomed Mater Res 1998; 41:443-54; PMID:9659614.
31. Niemelä T. Effect of β-tricalcium phosphate addition on the in vitro degradation of self-reinforced poly-l,d-lactide. Polym Degrad Stab 2005; 89:492-500; DOI:10.1016/j.polymdegradstab.2005.02.003.
32. Pluta M, Murariu M, Alexandre M, Galeski A, Dubois P. Polylactide compositions. The influence of ageing on the structure, thermal and viscoelastic properties of PLA/calcium sulfate composites. Polym Degrad Stab 2008; 93:925-31; DOI:10.1016/j.polymdegradstab.2008.02.001.
33. Laitinen O, Törmälä P, Taurio R, Skutnabb K, Saarelainen K, Iivonen T, et al. Mechanical properties of biodegradable ligament augmentation device of poly(L-lactide) in vitro and in vivo. Biomaterials 1992; 13:1012-6; PMID:1472587; DOI:10.1016/0142-9612(92)90152-E.
34. Pistner H, Stallforth H, Gutwald R, Mühling J, Reuther J, Michel C. Poly(L-lactide): a long-term degradation study in vivo. Part II: Physico-mechanical behaviour of implants. Biomaterials 1994; 15:439-50; DOI:10.1016/0142-9612(94)90223-2.
35. Pistner H, Bendix DR, Mühling J, Reuther JF. Poly(L-lactide): a long-term degradation study in vivo. Part III. Analytical characterization. Biomaterials 1993; 14:291-8; DOI:10.1016/0142-9612(93)90121-H.
36. Suuronen R, Pohjonen T, Hietanen J, Lindqvist C. A 5-Year in vitro and in vivo study of biodegradation of polylactide plates. J Oral Maxil Surg 1998; 56:604-14; DOI:10.1016/S0278-2391(98)90461-X.
37. Gogolewski S, Jovanovic M, Perren SM, Dillon JG, Hughes MK. Tissue response and in vivo degradation of selected polyhydroxyacids: Polylactides (PLA), poly(3-hydroxybutyrate) (PHB), and poly(3-hydroxybutyrate-co-3-hydroxyvalerate) (PHB/VA). J Biomed Mater Res 1993; 27:1135-48; PMID:8126012.
38. Willcox N, Roberts S. Delayed biodegradation of a meniscal screw. Arthroscopy 2004; 20:20-2; PMID:15243418; DOI:10.1016/j.arthro.2004.04.018.
39. Schliecker G, Schmidt C, Fuchs S, Kissel T. Characterization of a homologous series of D,L-lactic acid oligomers; a mechanistic study on the degradation kinetics in vitro. Biomaterials 2003; 24:3835-44; PMID:12818556; DOI:10.1016/S0142-9612(03)00243-6.
40. Filgueiras MR, La Torre G, Hench LL. Solution effects on the surface reactions of a bioactive glass. J Biomed Mater Res 1993; 27:445-53; PMID:8385143.

Publication V

Ellä, V., Gomes, M.E., Reis, R.L., Törmälä, P. & Kellomäki, M.

Studies of P(L/D)LA 96/4 non-woven scaffolds and fibres; properties, wettability and cell spreading before and after intrusive treatment methods

Journal of Materials Science: Materials in Medicine
vol. 18, (2007), pp. 1253-1261

J Mater Sci: Mater Med (2007) 18:1253–1261
DOI 10.1007/s10856-007-0144-z

Studies of P(L/D)LA 96/4 non-woven scaffolds and fibres; properties, wettability and cell spreading before and after intrusive treatment methods

Ville Ellä · Manuela E. Gomes · Rui L. Reis · Pertti Törmälä · Minna Kellomäki

Received: 8 November 2005 / Accepted: 29 March 2006 / Published online: 3 February 2007

Abstract Poly(L/D)lactide 96/4 fibres with diameters of 50 and 80 μm were produced. The smaller diameter fibres were carded and needle punched to form a non-woven mat. Fibres and non-woven mats were hydrolysed for a period of 20 weeks. Fibres and pressed non-woven discs were treated with low-temperature oxygen plasma and alkaline KOH hydrolysis and ethanol washing was used as a reference treatment. The non-wovens lost 50% of their tear strength after 8 weeks in vitro while the fibres still retained 65% tensile strength after 20 weeks. Hydrolysation time in KOH, treatment time and power settings of the oxygen plasma were all directly proportional to the mechanical properties of the fibres. Increasing time (and power) resulted in lower tensile properties. Rapid wetting of the scaffolds was achieved by oxygen plasma, KOH hydrolysation and ethanol washing. Cell culturing using fibroblast cell line was carried out for the treated and non-treated non-woven scaffolds. In terms of adhesion and the spreading of the cells into the scaffold, best results after 3-day culturing were obtained for the oxygen plasma treated scaffolds.

V. Ellä (✉) · P. Törmälä · M. Kellomäki
Institute of Biomaterials,
Tampere University of Technology,
P. O. Box 589, Tampere 33101, Finland
e-mail: ville.ella@tut.fi

M. E. Gomes · R. L. Reis
3Bs Research Group – Biomaterials,
Biodegradables and Biomimetics,
University of Minho, Campus de Gualtar,
Braga 4710-057, Portugal

M. E. Gomes · R. L. Reis
Department of Polymer Engineering,
University of Minho, Campus de Azurém,
Guimaraes 4800-058, Portugal

Introduction

Tissue engineering (TE) is one of the most challenging fields in biomaterial science as is the material technical means needed to achieve the foundation into which the cells can grow and form tissue of the desired shape and dynamics. Fibres produced from poly(L-lactic acid) (PLLA), its copolymers (PLDLA), polyglycolide (PGA), and their copolymer (PLGA) have been used as a matrix material for constructing various fabrics such as scaffolds for TE [1–4]. Scaffolds produced from the fibres should be highly porous, with a large surface area, suitable pore size and a highly interconnected network of pores [5]. Scaffold properties should also lead to a homogenous seeding density not only on the surface but also inside the scaffold [6]. The advantage in using fibre-based scaffolds such as non-woven mats over salt-leached or solvent-cast scaffolds is their high porosity and a porous network without additional chemicals; the downside is the uneven distribution of pores. Since polylactide based materials were first used as biomaterials, hydrofobicity has been an important issue. Several techniques have been used to overcome this problem and some of them, such as glow discharge gas plasma treatment [7–9] and alkaline hydrolysis [10], have shown promising results for the bulk and the 3D scaffold surfaces.

Our main objective was to manufacture non-woven scaffolds and to achieve good wettability to the scaffolds without the use of chemicals during the manufacturing process. These fabrics could be used for cell culturing purposes and also as preform for manufacturing more complex scaffold shapes. Post-treatment of the scaffolds requires deep penetration of the reacting agent, hence two methods were chosen for comparison: chemical aging that has previously shown good results when used with PHB/HV [11] and a physical low-temperature plasma treatment method. The effects of the two different surface treatment methods on the properties of highly oriented P(L/D)LA 96/4 fibres and 3D non-woven scaffolds manufactured from these fibres were studied. The influence of increased wettability and porosity of the 3D scaffolds to the adhesion of the seeded fibroblasts was examined.

Materials and methods

Fibre and scaffold manufacturing

Medical grade polymer poly(L/D)lactide 96/4 with intrinsic viscosity of 5.48 dl/g (Purac Biochem, Goringhem, The Netherlands) was used for fibre manufacturing. Polymer was melt-spun into multi-filament fibres (4- and 12-ply), using Gimac microextruder (Gimac, Gastronno, Italy) with screw diameter 12 mm. The fibres were drawn using caterpillars and ovens. The fibres were cut to staple fibres, carded and needle punched into non-woven (NW) mats. NW was compressed at a temperature of 85°C with restrictors of 1.0 mm to produce scaffolds (NWP) of ~1.0 mm thickness. The thickness of the NW prior to compression was 3–4 mm. The various compositions are shown in Table 1 and the treatments performed on the samples are presented in Table 2.

Plasma treatment

The plain fibres and the NWP Plasma scaffolds were plasma treated. Low-temperature plasma was applied using Plasma Prep 5 instrumentation (GaLa instrumente, Bad Schmalmach, Germany). The chamber was evacuated three times, adding oxygen between evacuations and finally the atmosphere was allowed to settle at 10 Pa. Frequency of 200 kHz was applied for defined periods of time from 0 to 300 s, with power settings of 50, 70 and 100 W. After plasma treatment, the oxygen atmosphere was held for an additional 5 min after which the samples were placed in airtight bags.

Table 1 Manufacturing characteristics of the fibres and non-wovens

Ultimate form	i.v. (dl/g)	Filaments per die	Porosity (%)	Single fibre diameter (μm)	Draw ratio
Fibre	5.48	4	–	80	4.6
NW	5.48	12	76–90	48–50	5
NWP	5.48	12	61–80	48–50	5

NW, non-woven; NWP, non-woven compressed to –1.0 mm thickness

Table 2 Treatments for the different samples

	Treatment times/(power)			
	Plasma	KOH	Ethanol washed	In vitro
Fibre	–	–	–	In vitro-hydrolyzation
Fibre	1–5 min/50 W	–	–	–
Fibre	1–3 min/70 W	–	–	–
Fibre	1 min/100 W	–	–	–
Fibre	–	5–240 min	–	–
NW	–	–	–	–
NW E	–	–	2 × 20 min	In vitro-hydrolyzation
NW E	–	–	2 × 20 min	In vitro-fibroblasts
NWP	–	–		–
NWP E	–	–	2 × 20 min	In vitro-fibroblasts
NWP Plasma	All used times	–	–	–
NWP Plasma	2 min/50 W	–	2 × 20 min	In vitro-fibroblasts
NWP KOH	–	All used times	–	–
NWP KOH	–	20 min	2 × 20 min	In vitro-fibroblasts

Chemical treatments

To remove any impurities caused by needle punching and carding, ethanol washing for NW E, NWP E, NWP KOH and NWP Plasma fabrics was performed prior to other treatments for a period of 2×20 min in ultrasound wash. The samples were dried in a vacuum at room temperature.

To modulate the surface properties of the fibres and the NWP KOH fabrics, the samples were subjected to alkaline hydrolysis at room temperature using 2.5 M KOH in a solution of methanol 50 vol.%/water 50 vol.% for time periods of 5, 20, 60 and 240 min. After hydrolysis the samples were dried in a laminar flow hood for 2 days.

In vitro

Prior to incubation the fibres and NW E were sterilised by gamma irradiation 25 kGy (Willy Rüsch AG, Germany). No other treatment was made to the set of in vitro fibres. The fibres were incubated for periods of 0, 1, 2, 3, 4, 8, 13, 16, and 20 weeks at 37°C in phosphate buffer solution (PBS, 3.48 g/dm^3 Na_2HPO_4–0.755 g/dm^3 NaH_2PO_4–5.9 g/dm^3 NaCl buffered saline) at pH 7.4. NW E mats were also incubated in PBS for 0, 2, 8, 16 and 20 weeks. The buffer solution was changed fortnightly.

Material characterisation

Molecular weights (M_n and M_w) and polydispersity (PD) were measured by gel permeation chromatography (GPC) relative to narrow polystyrene standards. GPC consisted of Waters 410 RI differential refractometer detector and Waters 515 HPLC pump (Waters, Milford, MA, USA). The GPC columns were PLgel 5 μm Guard and 2 PL gel 5 μm mixed-C. Injection volume was 150 μl and the flow rate of eluent was 1 ml/min. Calibration was performed using monodisperse polystyrene standards applying Mark-Houwink parameters for PS ($K = 1.12 \times 10^{-4}$ and $a = 0.73$). The samples were dissolved in 0.1% w/v solutions in chloroform at room temperature.

The differential scanning calorimeter (DSC) TAinstruments Q1000 (TAinstruments, New Castle, DE, USA) was used for thermal characterisation. The samples were heated from 20°C to 200°C at a rate of 20°C/min and after rapid cooling the heating procedure was repeated. Melting temperatures (T_m) were determined from the melting peak of the second heating; glass transition temperatures (T_g) were determined from the second heating and the crystallinity (X_c) of the samples was determined from the melting enthalpy using 93.7 J/g as the melting endotherm of 100% PLLA [12]. Indium was used for standard calibration.

Tensile properties of the fibres and tear strength of the NW E were tested using Instron 4411 Materials Testing Machine (Instron Ltd, High Wycombe, England). The fibre testing crosshead speed was 30 mm/min and gauge length was 50 mm, for NW E 100 mm/min and 40 mm. For the NW E testing, tear test samples (70 mm × 40 mm with a cut of 50 mm long in the middle of the shorter edge) were used. To enable comparison between the samples, tear force was divided by mass of the sample to compensate for differences in porosity.

Surface characterisation

XPS analysis was performed using an ESCALAB 200A (VG Scientific, West Sussex, UK) with PISCES software for data acquisition and analysis. For analysis, an achromatic Al (Kα) X-ray source operating at 15 kV (300 W) was used. The spectrometer, calibrated with reference to Ag 3d5/2 (368.27 eV), was operated in CAE mode with 20 eV pass energy. The take-off angle used was 90°. Data acquisition was performed at a pressure lower than 10^{-6} Pa. The value of 285.0 eV of the hydrocarbon C1s core level was used as a calibration for the absolute energy scale. Overlapping peaks were resolved into their individual components using XPSPEAK 4.1 software.

Rapid water uptake data was obtained by measuring the weight of the dry scaffold, then inserting it into a distilled water bath for a period of 5 s. After removal it was again weighed. Water uptake was calculated as a percentage of the increase in weight over the dry scaffold.

Cell culturing

Cell culturing was performed to assess the influence of the several surface modification treatments on the cells' adhesion to the treated scaffolds. The samples used were NW E, NWP E, NWP Plasma and NWP KOH scaffolds. NW E and NWP E were used as references. The scaffolds were round disks with a diameter of 10 mm. The NW E scaffolds were gamma irradiated while the rest of the scaffolds were EtO sterilised. The scaffolds were seeded with a cell suspension of mouse fibroblasts (cell line L929) and observed under light microscope (LM) and scanning electron microscope (SEM), after seeding (2 h) and after 3 days of culture.

The adherent cells were enzymatically released using 0.25% Trypsin-EDTA solution (T4049, Sigma, St.Louis, USA), concentrated by centrifugation at 1,200 rpm for 5 min and re-suspended in Dulbecco's Modified Eagle Medium (DMEM, D5523, Sigma, St.Louis, USA) supplemented with 10% fetal bovine serum (S0115, Biochrome AG, Berlin, Germany) and 1% of antibiotics solution (A5955, Sigma, St.Louis, USA). The scaffolds ($n = 3$ for each culturing period) were subsequently placed in non-adherent 12-well plates and each scaffold was seeded with 100 µl of a cell suspension at a concentration of 300×10^4 cells/ml and incubated (in a humidified atmosphere with 5% CO_2 at 37°C) for 2 h. Tissue culture polystyrene wells were used as controls. After this period, a group of scaffolds was retrieved for analysis and another one was transferred to new adherent 12-well plates and cultured up to day 3. At the end of each culture period (2 h and 3 days), the cell/scaffold constructs were rinsed with phosphate-buffered saline (PBS-P4417, Sigma , St.Louis, USA) and fixed in a solution of 2.5% gluteraldehyde for SEM and LM analysis. For observation under the LM (Axioplan 2, Zeiss, Germany), the seeded scaffolds were stained with a 0.4% methylene blue solution. For SEM analysis the scaffolds were subsequently dehydrated in a gradient series of ethanol solutions and sputter coated with gold (Jeol JFC 1100, Jeol, USA). The scaffolds were then observed using SEM (Leica Cambridge S360, Leica, Cambridge, UK).

Results

In vitro hydrolysation of the fibres and the NW E

The results can be seen in Table 3 and Fig. 1. Results for the oriented multifilament fibres showed that for the gamma irradiated fibres the ultimate tensile strength was 75% of initial value after 13 weeks of hydrolysation and for a period of 20 weeks the strength remained above 66% of the initial value. Elastic modulus remained above 75% throughout the study. The strain increased slightly until week 3 at the beginning of hydrolysation and remained at that level until week 20 where a slight increase was noted. Fibre diameter increased 12% during the 20 weeks of hydrolysation.

Results of the tear tests performed on the NW E in vitro samples showed that there was a drop of 50% from original strength within 8–10 weeks. After 15 weeks only 10% of original strength of NW E remained. High strain was obtained for all the NW E samples throughout the in vitro. At week 20 some of the samples retained only 1% of initial strength and there were very large differences in strain between the samples. As a reference, the measured maximum tear force of compressed samples NW P was 122 ± 43 N/g and the strain at maximum tear force was

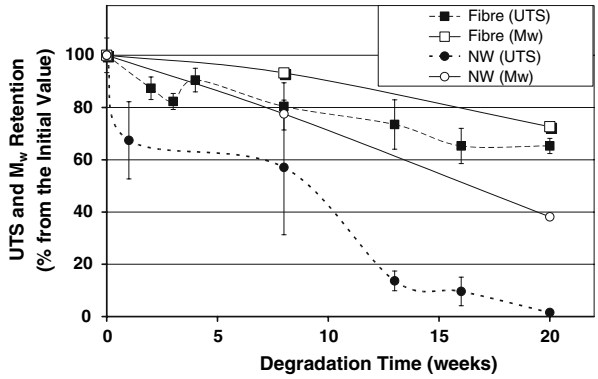

Fig. 1 Overall degradation of fibre and NW

Table 3 In vitro mechanical properties of fibre and NW

In vitro (weeks)	Fibre (multifilament fibre)			NW (non-woven)[a]	
	UTS (MPa)	Strain at Yield (%)	Elastic Modulus (GPa)	Max.Tear Force/ Weight (N/g)	Strain at Max. Tear Force (%)
0 unster.	336 ± 25	25 ± 4	7.1 ± 0.2		
0	317 ± 21	26 ± 1	7.1 ± 0.2	78 ± 12	138 ± 14
2	277 ± 12	34 ± 1	6.6 ± 0.2	41 ± 6[b]	134 ± 9[b]
3	261 ± 8	39 ± 2	5.3 ± 0.2		
4	287 ± 13	32 ± 2	6.7 ± 0.2		
8	255 ± 23	32 ± 2	6.1 ± 0.2	43 ± 13	125 ± 24
13	233 ± 22	31 ± 2	5.9 ± 0.2	9 ± 2	99 ± 6
16	207 ± 14	29 ± 1	5.7 ± 0.2	5 ± 2	96 ± 20
20	207 ± 6	36 ± 1	5.3 ± 0.2	1 ± 0	116 ± 70

$n = 5$

[a] $n = 3$

[b] 1 week

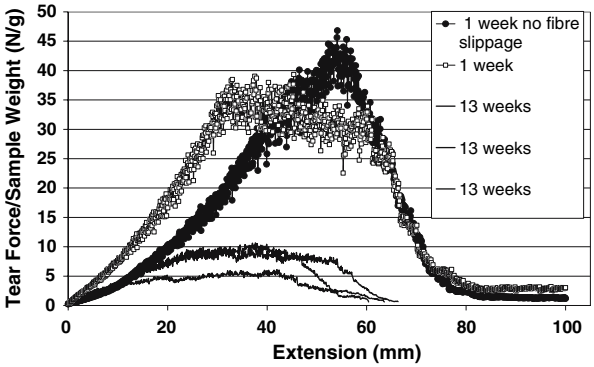

Fig. 2 Fibre slippage of NW in in vitro samples

43.8 ± 23.0%. The specific weight of the NW and NWP fabrics varied from 261 to 316 g/m^2.

Fibre slippage (needle punched entangled fibres come loose) was already seen in the first week and as hydrolysation time increased, fibre slippage in the NW E samples increased. A breaking point was observed in the 1st week samples but none was seen in the 13-week samples (Fig. 2).

Results of the molecular weight and thermal characterisation studies are presented in Table 4. A Viscosity of the polymer dropped by half during the melt processing and for the in vitro series viscosity was decreased due to gamma irradiation by a further ~70%. There was a faster reduction in molecular weight in the case of NW E compared to the fibres. A definitive increase in PD was observed at week 20 in the case of NW E, whereas there was no such increase with the fibres.

The crystallinity of the fibres was increased by gamma irradiation from 29 to 37%, it was further increased during hydrolysation to 45% after 20 weeks. In the case of NW E, crystallinity remained constant between 8 and 20 weeks. During the 20-week hydrolysation, the fibres showed a drop in T_g from 58.6°C to 54.8°C whereas T_g of NW E at 20 weeks was 50.8°C. No change in T_m was detected with the fibres during the hydrolysation (only the initial drop caused by irradiation) whereas a drop of 2°C was observed in the case of NW E from 8 to 20 weeks.

Effect of surface treatments on fibres

Oxygen plasma treatment of the oriented P(L/D)LA 96/4 fibres revealed that with power settings of 50 W the 5 min treatment time was the longest that could be carried out without significant fibre shrinkage. With 70 W the maximum treatment time was 3 min. With 100 W any treatment time resulted in significant changes and damaged the fibre. For power settings of 50 W, treatment times of 1 and 2 min showed no changes in strength or strain properties compared to untreated fibres (Fig. 3), whereas 3 min treatment time increased the strain and 5 min treatment time further increased the strain while the strength decreased. The results of the 70 W treatment showed similar behaviour at shorter time periods, which correlates with the applied power. Fibre diameter (and shrinkage) in all plasma treated samples showed plasma power and treatment dependent behaviour (Fig. 4).

Table 4 Results of the molecular and thermal studies of fibre and NW

	M_W (Da)	I.v. (dl/g)	Polydispersity (PD)	Peak T_m (°C)	Onset T_g (°C)	X_C (%)
Fibre control	130,200 ± 900	2.85 ± 0.03	1.85 ± 0.02	152.8	58.6	29
Fibre 0 week[a]	35,500 ± 500	1.04 ± 0.01	1.79 ± 0.08	155.7	56.4	37
Fibre 8 weeks[a]	33,100 ± 100	1.04 ± 0.01	1.74 ± 0.01	155.7	56.7	39
Fibre 20 weeks[a]	25,800 ± 100	0.84 ± 0.02	1.69 ± 0.01	155.1	54.8	45
Fibre plasma 50 W 1 min	132,900 ± 800	2.83 ± 0.07	1.76 ± 0.05	154.8	57.4	26
Fibre plasma 50 W 2 min	129,800 ± 1800	2.75 ± 0.04	1.82 ± 0.05	153.1	57.3	31
Fibre plasma 50 W 3 min	130,600 ± 600	2.77 ± 0.04	1.83 ± 0.06	153.6	57.7	34
Fibre plasma 50 W 5 min	126,500 ± 2400	2.76 ± 0.06	1.82 ± 0.08	153.6	58.0	32
Fibre plasma 70 W 1 min	132,900 ± 800	2.78 ± 0.08	1.77 ± 0.03	154.1	57.4	32
Fibre plasma 70 W 2 min	132,600 ± 200	2.74 ± 0.04	1.78 ± 0.01	153.1	57.8	30
Fibre plasma 70 W 3 min	128,500 ± 900	2.71 ± 0.05	1.87 ± 0.01	154.2	57.5	30
Fibre KOH 5 min	125,000 ± 1500	2.80 ± 0.01	1.03 ± 0.13	153.7	55.3	26
Fibre KOH 20 min	127,300 ± 2000	2.81 ± 0.10	1.88 ± 0.07	152.8	57.1	31
Fibre KOH 60 min	129,800 ± 400	2.85 ± 0.07	1.94 ± 0.03	152.3	56.6	44
NW 0 week[a]	26,700 ± 600	0.87 ± 0.01	1.87 ± 0.02	NA	NA	NA
NW 8 weeks[a]	20,700 ± 100	0.73 ± 0.03	1.71 ± 0.04	155.4	55.5	40
NW 20 weeks[a]	10,200 ± 100	0.41 ± 0.01	2.16 ± 0.03	153.7	50.8	41

[a] Gamma sterilised

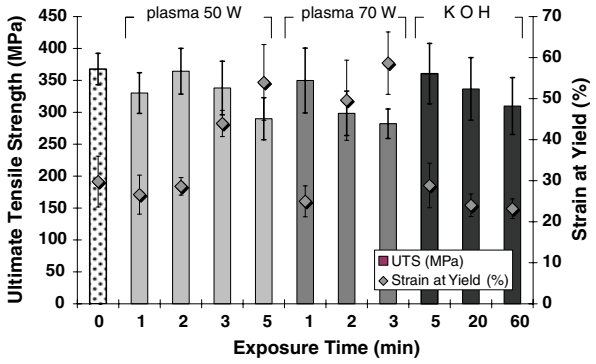

Fig. 3 Mechanical results of the treated fibres

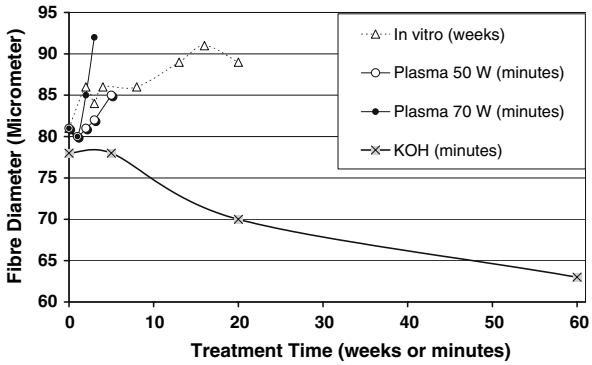

Fig. 4 Fibre dimension versus treatment and in vitro times

Treatment time of 5 min with KOH had no effect on the fibre properties or dimensions whereas both the 20 and 60 min treatment times had an effect on the strength and dimensions due to fibre dissolution. There was no difference in strain properties between the 20 or 60 min treatment times. Treatment time of 60 min showed a decrease of 38% in fibre volume and a decrease of 14% in UTS. Treatment time of 240 min resulted in dissolution of almost all the fibres and their properties could not be measured. There was no change in molecular or thermal properties among the plasma treated groups whereas in the KOH treated groups crystallinity increased along with treatment time.

Effect of surface treatments on NW

On the basis of the fibre studies, a plasma treatment power of 50 W and a time of 2 min were chosen for NWP Plasma. For NWP KOH, a 20 min treatment time was chosen. Rapid water uptake tests (Fig. 5) showed a significant decrease in water uptake when NW and NWP samples were compared. Between the compressed samples, the surface treated NWP Plasma samples doubled and the NWP KOH had 40% increase

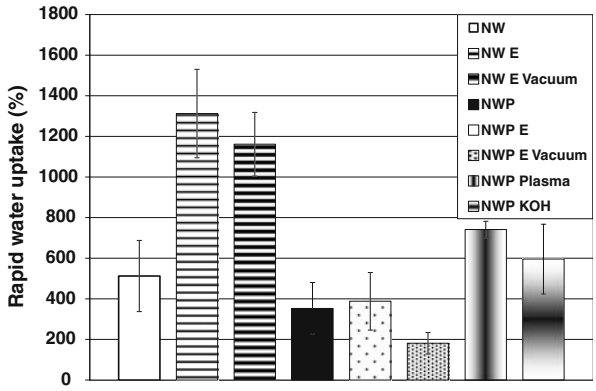

Fig. 5 Rapid water uptake results of NW and treated NWs

Table 5 XPS data of C1s envelope and atomic relation

	C1s (Area/Tot. Peak Area [%])			Atomic % relation
	C–C	C–O	C=O	O/C
NWP	56.8	24.6	19.6	0.49
NWP Plasma	63.4	25.8	13.8	0.51
NWP KOH	79.2	11.2	12.4	0.55

in the amount of water uptake compared to the NWP samples. Most of the water absorbed by the NWP samples was attached to the surface as opposed to the inside of the scaffold. The NW E and NWP E samples showed an increase in water uptake after drying in a flow cabinet. However, after vacuum drying no improvement was obtained with ethanol washing with NWP E Vacuum compared to NWP.

Surface treatments showed only a slight increase in total oxygen content (Table 5). There was a discernable decrease in content of C=O bonds with the NWP Plasma samples. Surface energy could not be calculated using the sessile drop method due to the roughness and protruding fibres on the surface of all the non-woven samples. On the untreated surfaces it was observed that fibres penetrating the contact angle drop did not break the drop. When it did occur (Table 6), total adsorption of the contact angle drop (wetting of the sample) was very fast, ranging from 80 to 300 ms.

Cell seeding

When concentrated cell medium was applied to the NWP Plasma (50 W, 2 min) and the NWP KOH (20 min) scaffolds the medium was adsorbed immediately. When seeding the NW E and NWP E (Fig. 6) scaffolds, the concentrated medium droplet remained on the surface until rest of the medium was added 2 h later.

Table 6 Contact angle testing results

	Wetting
NW & NW (gamma ster.)	No wetting
NWP	No wetting
NWP E	Total wetting[b]
NWP E (vacuum dried)	No wetting
NWP E (EtO)	No wetting
NWP Plasma[a]	Total wetting[b]
NWP Plasma (EtO)	Total wetting[b]
NWP KOH[a]	Total wetting[b]
NWP KOH (EtO)	Total wetting[b]

$n = 6$

[a] All treatment times

[b] Total adsorbtion of the drop in <260 ms

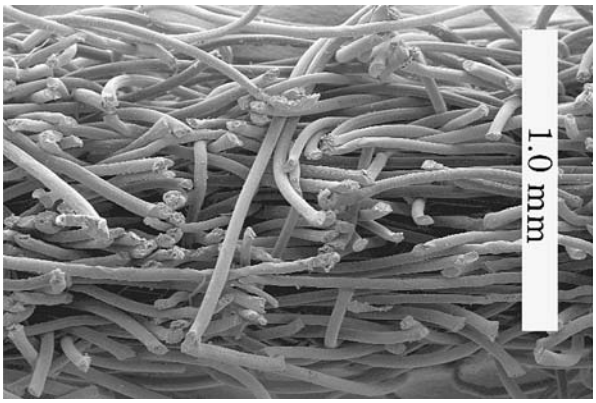

Fig. 6 SEM Picture of NWP sample from the vertical cut surface of the scaffold

After 3 days incubation (Fig. 7) it was confirmed from the SEM pictures that both the untreated NWP and ethanol washed NWP E had cells present in the confluent layer on the surface of the fibres. The cells had not penetrated very deep into the NW E and NWP E scaffolds, continuous layers of cells were found only on the uppermost part of the scaffolds. Cells were detected only on the surface area which was the same size as the incubation droplet and situated directly under the droplet. Only a few individual cells were found outside of this area. In the NWP Plasma scaffolds phenotypically viable and growing cells were found all over the scaffolds, although thicker layers of cells were to be found only in the uppermost layers of the scaffolds. In NWP KOH only a few cells, many of them dead, were found in the scaffolds after three day's incubation.

Discussion

The multifilament fibres in our study retained their UTS for 20 weeks better than the gamma irradiated PLLA monofilament fibres, poly(L/D)lactide 96/4 sutures or yarns, reported earlier [13, 14, 2]. Similar in vitro results were documented with thicker gamma irradiated 500 μm PLLA sutures for strength and strain behaviour [15]. The strength retention behaviour of PLLA multifilament fibres tested as braids [16] was similar to our multifilament fibres that were thicker; their study also showed that thicker monofilament fibres lost their strength faster than thinner multifilament fibres due to a lower orientation degree and crystallinity. Compared to the reported study [13], the fibres in our study retained strength for longer having lower crystallinity, lower intrinsic viscosity after irradiation and D-lactide in the polymer. We believe,

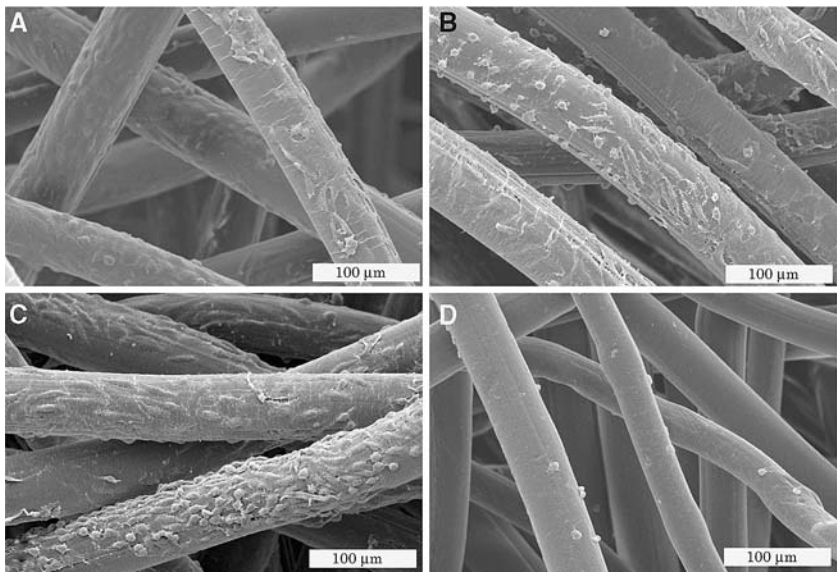

Fig. 7 SEM pictures of samples seeded with cells (fibroblast adhesion and spreading) after 3-day culturing from (**a**) NW E, (**b**) NWP E, (**c**) NWP Plasma and (**d**) NWP KOH scaffolds

therefore, that a higher degree of orientation itself is the key factor as well as monomer content [17, 18] that affects the speed of degradation in fibres. While higher crystallinity increases the strength it does not, however, decrease the strength retention speed of the fibres. When comparing our multifilament fibres to the NW fibres, processing conditions caused a greater drop in both molecular weight and viscosity that could have increased monomer content in the NW fibres thus causing faster degradation. For semi-crystalline poly (L/D)lactide 96/4,crystallinity increased, and molecular weight decreased during gamma irradiation and was further increased during the in vitro. This is consistent with other studies [13, 16, 19]. A similar decrease of ~60% in viscosity was also noticed in earlier studies of PLLA fibres [13].

A very small increase in molecular weight with oxygen plasma treated P(L/DL)LA pins has been reported [20], though this behaviour was not observed in the present study where treatment times and the used power settings were lower. A temperature increase was noticed in the chamber during the treatment and this caused a certain degree of relaxation to the fibres that was manifested as increased diameter and strain. The increase in fibre diameter caused by relaxation was proportional to the used treatment time and power. Previous studies have found no change in bending properties [20] whereas a change in tensile properties was observed in our study due to a temperature increase that has a greater effect over a shorter period of time on the thin oriented fibres than on the thicker, less oriented objects.

Tear strength test does not distinguish between the slippage of the fibres and the breakage of the entangled fibres. The slippage of the fibres can be seen in the data as a prolonged yield point in maximum break force. Slippage is an indication of asymmetrical looping and weak re-looping where the bonding fibre is forming more than one loop through the non-woven structure. This slippage can also be an advantage when considering the dynamical model. This model may have the advantage of making the non-woven adapt more easily to the in situ without loosing its maximum strength. For prolonged periods, where strength is required to last more than 10 weeks for in vitro/in vivo purposes, this non-woven may not be suitable; heavier needle punching parameters should be considered to obtain a more durable fabric. Variation in fabric weight was mainly due to pre-fabric variations caused by static electricity during carding. This variation made the fabric uneven and changed local porosity.

An increase in O/C content in XPS measurements for the plasma treated samples was previously reported for PLLA and PLGA [7, 9]. An increase of such magnitude was not observed in our studies where shorter treatment times were used. Varying results are also reported for PLLA O/C content, ranging from 0.23 to 0.55 [21, 22]. The different results show that the accuracy of the surface bound XPS analysis is dependent on surface topography. We did not detect an increase in –C–O– that could lead to hydroxyl, ether or peroxyl group incorporation, although the plasma treated scaffold itself was very hydrophilic. This was probably due to an increase in polar component on the scaffold fibres which needs to be determined.

Even with a large volume change during KOH aging, the diluted fibres had more strength left when comparing strength over the fibre cross-section area. This result is probably due to the re-crystallization of the dissolved polymer on the surface layers of the fibre. It could also be that the inner part of the fibre actually holds more crystalline structure than the surface. We believe the latter explanation to be correct because during quenching in processing, the surface cools faster thus possibly giving it a less crystalline structure.

It has been noted that the rapid attachment of cells to open network fibre structures is needed, although it was suggested that homogenous cell distribution is the problem with non-woven products [4]. In the case of our NWP Plasma treated scaffolds, fairly even distribution was achieved due to fast wetting and scaffold parameters. Variable density and an uneven distribution of fibres in some parts did not prevent the overall distribution of the cells. The authors recognise, however, that more studies are needed to verify the actual minimum density of the fibres that could act as a clot.

The NWP KOH scaffolds worked poorly in this study. It was noticed that the lowest –C–O– fraction had weaker cell adhesion [9] in the case of PLGA. This was also the case in our study, and fibre thickness was also lower in the case of NWP KOH compared to other scaffolds. It is also possible that residue potassium leads to an alkaline environment and affected cell properties and cell viability.

As seen earlier, the oxygen plasma treatment decreased the hydrophobicity of the poly(L/D)lactide 96/4 non-woven scaffolds. This enhanced the culture medium penetration to the scaffolds and may lead to an easier incubation of different types of cell into non-woven scaffolds made from poly(L/D)lactide 96/4 fibres. The influence of porosity could not be confirmed since no total wetting of the highly porous NW was achieved. Fibre diameter plays a more important role in actual attachment to the fibre. Further study is needed to determine which is the better option for tissue engineering: scaffold porosity with very thin

fibres where cells are entrapped between the fibres or a scaffold with thicker fibres where cells attach directly to the fibres.

A biodegradable non-woven structure combined with a suitable surface modification method is an interesting and feasible way to make scaffolds for tissue engineering purposes. Lactide non-woven scaffolds treated with physical low-temperature oxygen plasma could be used as potential scaffolds in further TE studies.

Acknowledgements Research funds from the European Union Project ''Spare Parts'' (QLRT-2000-00487) and National Technology Agency (TeKes) for the Center of Excellence of Biomaterials are greatly appreciated. This work was also partially supported by the European Union funded STREP Project HIPPOCRATES (NMP3-CT-2003-505758) and was carried out under the scope of the European NoE EXPERTISSUES (NMP3-CT-2004-500283). The authors would like to thank Eira Lehtinen, Milla Törmälä and Iva Pashkuleva for their help during this work.

References

1. M. KELLOMÄKI, T. KULMALA, V. ELLÄ, S. LÄNSMAN, N. ASHAMMAKHI, T. WARIS, P. TÖRMÄLÄ, Abstract presented at the Symposium on Tissue engineering Science, Myconos, Greece, May 19–23, 2002. Abstract no. 25, p 49
2. P. B. HONKANEN, M. KELLOMÄKI, M. Y. LEHTIMÄKI, P. TÖRMÄLÄ, S. MÄKELÄ and M. U. K. LEHTO, *Tissue Eng.* **9**(12) (2003) 957
3. L. E. FREED, G. VUNJAK-NOVAKOVIC, R. J. BIRON, D. B. EAGLES, D. C. LESNOY, S. K. BARLOW and R. LANGER, *Biotechnology* **12**(7) (1994) 689
4. M. SITTINGER, D. REITZEL, M. DAUNER, H. HIERLEMANN, C. HAMMER, E. KASTENBAUER, H. PLACK, G. R. BURMESTER and J. BUJIA, *J. Biomed. Mater. Res. Part B: Appl. Biomater*. **33** (1996) 57
5. A. G. MIKOS, Y. BAO, L. G. CIMA, D. E. INGBER, J. P. VACANTI and R. LANGER, *J. Biomed. Mater. Res*. **27** (1993) 83
6. W. D. HUTMACHER, K. W. NG, C. KAPS, M. SITTINGER and S. KLÄRING, *Biomaterials* **24** (2003) 4445
7. Y. WAN, J. YANG, J. BEI and S. WANG, *Biomaterials* **24** (2004) 3757
8. H. CHIM, J. L. ONG, J.-T. SCHANTZ, D. W. HUTMACHER and M. AGRAWAL, *J. Biomed. Mater. Res*. **65A** (2003) 327
9. Y. WAN, X. QU, J. LU, C. ZHU, L. WAN, J. YANG, J. BEI and S. WANG, *Biomaterials* **25** (2004) 4777
10. J. YANG, Y. WAN, C. TU, Q. CAI, J. BEI and S. WANG, *Polym. Int*. **52** (2003) 1892
11. L. ROUXHET, F. DUHOUX, O. BORECKY, R. LEGRAS and Y.-J. SCHNEIDER, *J. Biomater. Sci., Polym. Ed*. **9**(12) (1998) 1279
12. E. W. FISCHER, H. J. STERZEL and G. WEGNER, *Kolloid-ZuZ Polymere*. **251** (1973) 980
13. J.-P. NUUTINEN, C. CLERC, T. VIRTA and P. TÖRMÄLÄ, *J. Biomater. Sci. Polym. Ed*. **13**(12) (2002) 1325
14. J. KANGAS, S. PAASIMAA, P. MÄKELÄ, J. LEPPILAHTI, P. TÖRMÄLÄ, T. WARIS and N. ASHAMMAKHI, *J. Biomed. Mater. Res. Part B: Appl. Biomater*. **58** (2001) 121
15. P. MÄKELÄ, T. POHJONEN, P. TÖRMÄLÄ, T. WARIS and N. ASHAMMAKHI, *Biomaterials*. **23** (2002) 2587
16. L. DÜRSELEN, M. DAUNER, H. HIERLEMANN, H. PLANCK, L. E. CLAES and A. IGNATIUS, *J. Biomed. Mater. Res. Part B: Appl. Biomater*. **58** (2001) 666
17. M. KELLOMÄKI, T. POHJONEN and P.TÖRMÄLÄ, In ''Biodegradable Polymers'' (Citius Books, London, 2003), PBM series, vol. 2, p. 211
18. T. NAKAMURA, S. HITOMI, S. WATANABE, Y. SHIMIZU, K. JAMSHIDI, S. H. HYON and Y. IKADA, *J. Biomed. Mater. Res*. **23**(10) (1989) 1115
19. P. Mainil-Varlet, R. Curtis and S. Gogolewski, *J. Biomed. Mater. Res*. **36**(3) (1997) 360
20. S. GOGOLEWSKI, P. MAINIL-VARLET and J. G. DILLON, *J. Biomed. Mater. Res*. **32** (1996) 227
21. S.-H. HSU and W.-C. CHEN, *Biomaterials*. **21** (2000) 359
22. Z. GUGALA and S. GOGOLEWSKI, *Biomaterials*. **25** (2004) 2341

Publication VI

Ellä, V., Kellomäki, M. & Törmälä, P.

In vitro properties of PLLA screws and novel bioabsorbable implant with elastic nucleus to replace intervertebral disc

Journal of Materials Science: Materials in Medicine
vol. 16, (2005), pp. 655-662

JOURNAL OF MATERIALS SCIENCE: MATERIALS IN MEDICINE **16** (2005) 655–662

In vitro properties of PLLA screws and novel bioabsorbable implant with elastic nucleus to replace intervertebral disc

V. ELLÄ, M. KELLOMÄKI, P. TÖRMÄLÄ
Institute of Biomaterials, Tampere University of Technology, P.O. Box 589, FIN-33101 Tampere, Finland
E-mail: ville.ella@tut.fi

The suitability of two different implant types for the replacement of the intervertebral disc was studied *in vitro*. Self-reinforced poly-L-lactide (SR-PLLA) screws Ø 4.5 mm were studied 24 weeks *in vitro* and cylindrical implants with elastic nucleus made of poly(L/D)lactide 96/4, poly(L/DL)lactide 70/30, Bioactive Glass n:o 13–93 and Polyactive® 1000PEOT70PBT30 were studied 15 weeks *in vitro*. The cylindrical implant mimics the size and shape of the intervertebral disc. During the *in vitro,* there were no changes in compression properties with either implant types. The screws had sufficient modulus for intervertebral ossification in the canine model and the cylindrical implant showed also sufficient mechanical properties. These results suggest that both implant types could be used in clinical testing.

1. Introduction

The human spine has 26 vertebrae: cervical (neck) 7 vertebrae C1-C7, thoracic (chest) 12 vertebrae T1-T12, lumbar (back) 5 vertebrae, sacral 1 (5 fused) vertebrae and coccygeal 1 (3 to 5 fused) vertebrae. Vertebrae are separated with intervertebral discs which are cushion-like pads acting as shock absorbers. The discs have strong outer ring of fibrocartilage (annulus fibrosus) and inner semi-fluid (nucleus pulposus). The annulus fibrosus also holds together the adjacent vertebrae [1].

Heavy loads subjected to the spine are transformed to the intervertebral discs possibly causing prominence, neural compression and/or rupture of the disc. Also degenerative diseases and aging may damage the intervertebral discs [2]. A frequently used method for repairing a ruptured disc is called spinal fusion. The damaged disc is removed and replaced with a bone graft, or a fusion devise, that fuses the adjacent vertebrae together [3]. The system or adjacent vertebrae is usually stabilized with metal plates and screws. Undesirable effects in long term use and graft-related construct failures have been reported [4, 5]. Different implant types such as total artificial disc replacement implants and nucleus substitute implants have been studied. Only few bioabsorbable implants are commercially available and usually metal implants or bone-grafts are being used [6, 7]. Composite hydrogels, hydroxyapatite, calcium phosphate grafts and composites and other artificial discs have been studied for spinal fusion due to their bone bonding abilities [6, 8–10]. The surface-treated bioactive glass has been shown to serve as surface that nucleus pulposus cells can attach, proliferate and maintain their phenotype [11]. The modern approach would be focused on retaining the motion of the spine instead of fusing the vertebrae together by replacing the intervertebral disc and still maintain the stability and flexibility of the spine.

The ruptured intervertebral disc can be removed and replaced using two surgical approaches, the posterior and the anterior approach. The benefit of the posterior instrumentation is that it is very strong and rigid. The main disadvantage is that it often requires the detachment of the spinal muscles and some complications may occur as the surgeon has to disrupt the facet joints. In the anterior approach the procedure is done entirely from the front. Complications associated with posterior approach may be avoided. Yet some complications such as vascular injury may occur [12].

In clinical findings the anterior interbody fusion has better outcome than the posteolateral fusion with internal fixation, but there is higher rate of fusion in the posteolateral group [12, 13].

The aim of the current work was to estimate the suitability of two different types of spinal implants. Bioabsorbable Self-Reinforced Poly-L-lactide (SR-PLLA) screws and novel bioabsorbable intervertebral disc implants with elastic core were put to *in vitro* and tested for mechanical properties, weight changes, molecular weight changes and thermal properties. The SR-PLLA screws have been successfully used in orthopaedic surgery [14]. For this study the new type of disc implant with elastic core is considered as a fusion device but in the future we hope it could, with minor modifications such as nucleus pulposus cell cultivation, be used to replace the function of the original intervertebral disc. Clinically two screws are intended to be screwed

parallel between two vertebrae in anterior-posterior direction and the screw heads then removed. Two screws are placed side by side so that they support each other in bending, flexion and torsion thus making the system stable. The cavity between the screws will be filled with crushed bone. Both implant types are considered to be placed using anterior fixation approach.

2. Materials and methods

2.1. Implants and screws

2.1.1. Cylindrical composite implants

The implant was a composite with elastic core surrounded by matrix and reinforcement material as seen in Fig. 1.

Core polymer was Polyactive® 1000PEOT70PBT30 (segmented block copolymer of poly(ethylene oxide terephtalate)/poly(butylene terephtalate) with PEOT/PBT ratio being 70/30). The molecular weight of the copolymer was 80,000–125,000 dl g^{-1} (copolymer was supplied by IsoTis BV, Bilthoven, The Netherlands). The copolymer was mixed in the Gimac Ø 12 mm single screw microextruder (Gimac, Gastronno, Italy) with bioactive glass 13-93 particles (consisting of 6 wt% Na_2O, 12 wt% K_2O, 5 wt% MgO, 20 wt% CaO, 4 wt% P_2O_5 and 53 wt% SiO_2, Abmin Technologies Ltd., Turku, Finland). The crushed and milled bioactive glass particles were sieved to particle distribution 50–125 μm. Both the raw polymer and the polymer/glass composition was then separately extruded through a round die, average diameter of the produced rod being 3.7 mm and average content of glass in the composite being 23 wt%. The rods were cut to the lengths of 5 mm.

Matrix material was a mixture of 15 wt% of medical grade poly(L/DL)lactide 70/30 (RESOMER® LR 708, Boehringer Ingelheim, Germany, inherent viscosity 6.1 dl g^{-1}) and 85 wt% of bioactive glass 13–93 (same as above). The polymer was dissolved in acetone (ratio of the polymer/acetone was 2 g/30 ml) and the bioactive glass was mixed to it to form a paste-like mixture.

Matrix reinforcement material was medical grade poly(L/D)lactide 96/4 (PURAC biochem bv, Gorinchem, The Netherlands, inherent viscosity of 5.47 dl g^{-1}) that was melt-spun (Gimac microextruder, Gimac, Gastronno, Italy) to fibres using nozzle with 8 orifices (single orifice diameter 0.4 mm) and oriented using laboratory scale orientation line to the draw ratio 4.2. The multifilament fibre was knitted to a tubular single jersey knit and 300 mm long pieces of the knit was used in each implant.

When combining the components the matrix paste was thoroughly spread on to the PLA96-knit. The combination of knit and matrix was rolled around Polyactive + bioactive glass composite rods that formed the elastic core of the implant. The implant was heat-treated in a mould at 80 °C for 1 h, cooled down to room temperature and removed from the mould. The cylindrical implants were packed and gamma irradiated for sterilization (25 kGy).

Nine reference series ($n = 3$) were made (Table I). All the reference series samples were gamma-sterilised.

TABLE I Compositions of the 9 reference series

	Core material	Matrix material	Matrix reinforcement knit
Set 1	–	[c]	poly(L/D)lactide 96/4
Set 2	–	poly(L/DL)lactide 70/30	poly(L/D)lactide 96/4
Set 3	–	poly(L/DL)lactide 70/30 + BG 13-93	poly(L/D)lactide 96/4
Set 4	Polyactive[a]	[c]	poly(L/D)lactide 96/4
Set 5	Polyactive	poly(L/DL)lactide 70/30	poly(L/D)lactide 96/4
Set 6	Polyactive	poly(L/DL)lactide 70/30 + BG 13-93	poly(L/D)lactide 96/4
Set 7	Polyactive + BG 13–93	[c]	poly(L/D)lactide 96/4
Set 8	Polyactive + BG 13–93	poly(L/DL)lactide 70/30	poly(L/D)lactide 96/4
Set 9[b]	Polyactive + BG 13–93	poly(L/DL)lactide 70/30 + BG 13-93	poly(L/D)lactide 96/4

[a]Extruded Polyactive rod.
[b]*In vitro* composition.
[c]When matrix material was not used the end of the knit was attached to the knit roll with poly(L/DL)lactide 70/30 dissolved in acetone.

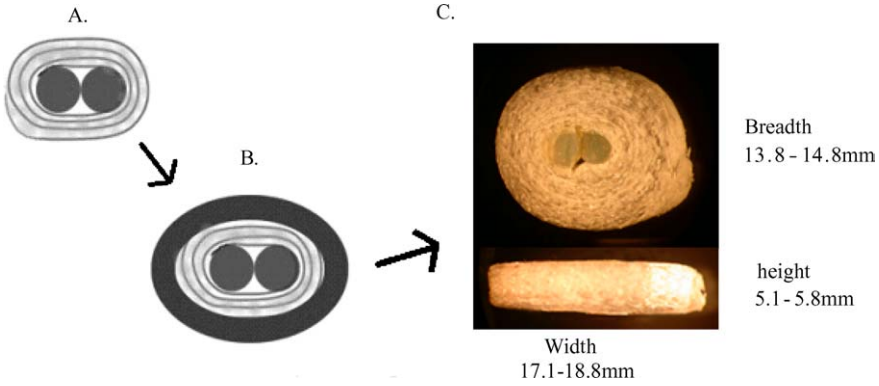

Figure 1 (A) The reinforcement was rolled over the core rods and (B) placed in to the mould. The composite was heat-treated and the mould was (C) removed to form the implant.

2.1.2. Screws

Three different types of gamma-sterilised screws with diameter of 4.5 mm were used (BIOFIX, Bionx Implants Ltd., Tampere, Finland):

(1) Self-reinforced poly-L-lactide, SR-PLLA, screws,
(2) SR-PLLA cannulated screws,
(3) SR-PLLA cannulated screw with intramedullary rod filling in the cannula of the screw.

12 mm pieces from the threaded part of the screws were cut from them and used for mechanical testing. Cut-offs from the screws were used for other studies.

2.2. Mechanical testing

All the tested samples were compressed at a rate of 1 mm min^{-1} between parallel polished steel plates using LLOYD LR 30 K mechanical testing machine (Lloyd Instruments Ltd., Fareham, England). All tested sets had three parallel samples and results are given as averages with standard deviations.

Cylindrical implants were intended for separate use and thus they were tested one at a time. The implants were compressed up to 9.3 kN between the compression plates. The compression modulus (E_c) of the implants was calculated using the formula

$$E_c = \delta/\varepsilon = (\Delta F/A)/(\Delta h/h) \quad (1)$$

where ΔF was the change in load, A was the area of the implant, Δh was the change in extension with corresponding load ΔF, and h was the height of the implant. Because the implants were hand made they were not symmetric ellipses. The area calculated for the ellipse would have been smaller than the actual area, therefore the area was calculated as an average circular area,

$$A = \pi((\text{width} + \text{breadth})/4)^2 \quad (2)$$

this was better estimation of the area. Also the porosity of the implant was not taken into account. The same area was used to calculate the compression stress in different points in the axis. The stiffness was calculated by linear regression from the load-compression curve.

$$\text{Stiffness} = \Delta F/\Delta h \quad (3)$$

Compression test of the screws was performed by testing two parallel 12 mm pieces of screws simultaneously in order to simulate the implantation situation. The screws were compressed to 9.5 kN and the modulus was calculated from the linear part of the curve using the Equation 1. The area used for Equation 1 is in Equation 4

$$A = \{A_2(\text{area at } h_2) + A_1(\text{area at } h_1\}/2 \quad (4)$$

While pressing the screws the area is changing from 0 to 108 mm^2 (hypothetic area if the screws are compressed flat without a change in diameter). To simplify the calculations two extension points ($h_1 = 0.35$ mm and $h_2 = 0.61$ mm) were chosen at linear part of the curves. Thus the average area that was used in the modulus calculus was 48 mm^2. The actual area is significantly smaller because only the threads of the screws are compressed at first thus the actual modulus of the threads is higher than the calculated modulus.

Both the cylindrical implants (set 9) and solid SR-PLLA (type 1) screws were tested wet at indicated periods *in vitro* in a similar manner, except the 0-week cylindrical implants and the reference series were immersed in purified water for 1 h prior testing whereas the 0-week screws were tested dry. The Polyactive + BG rods swelled up during the *in vitro*, this affected the compression curve so that the pressure from 0 to 2 kN was only the compression of the rods, this was also visibly noted. To measure the modulus and stiffness for the whole implant the Δh in compression modulus and the stiffness was measured between 2 and 3 kN from the curve, ΔF being 1 kN.

2.3. *In vitro* procedure

The gamma-sterilized cylindrical implants were immersed in a phosphate buffer solution (PBS, pH 7.4 ± 0.2) and held at 37 °C for periods of 1, 6, 12 and 15 weeks. The samples were individually incubated in buffer solution, solution to mass ratio being ~70 ml g^{-1}. Every 2 weeks the buffer solutions were changed and the pH was measured to ensure the adequate pH level.

Gamma-sterilized type 1 SR-PLLA screw bodies were cut to 12 mm long pieces before *in vitro*. Those together with a shorter left-over piece were immersed in a phosphate buffer solution (PBS, pH 7.4 ± 0.2) and held at 37 °C for periods of 1, 6, 9, 12, 15, 18, 21, 24 weeks. Each incubation set consisted of six samples (three compression tests per incubation period) and the samples for each incubation period were all placed in the same container. The samples were incubated in buffer solution, solution to mass ratio being ~100 ml g^{-1}. Every 3 weeks the buffer solutions were changed and the pH checked.

2.4. Weight measurements of cylindrical implants

All the cylindrical implants were weighed (accuracy of 0.1 mg) before and after the incubation period to calculate the water absorption to the composite structure. Before weighing the wet surface was quickly dried with a tissue paper to remove excess water from the surface of the implant. The weight change was calculated as % against the original sample weight and the actual weight change % was the average of three samples.

2.5. Thermal characterisation

The small left-over piece (screws type 1) was used for DSC (Differential Scanning Calorimetry) and GPC (Gel Permeation Chromatography) studies.

The DSC samples (6 ± 0.2 mg per sample) were heated from 30 to 250 °C at a rate of 20 °C min^{-1} and

after rapid cooling the samples were re-heated from 30 to 250 °C, at a rate of 20 °C min^{-1}. The melting temperature (T_m) was determined from the melting peak of the second heating and the melting enthalpy of the peak was determined. The equipment used was Perkin Elmer DSC7 (Perkin Elmer, Norwalk, CT, USA). The crystallinity was determined from the melting enthalpy using 93.7 J g^{-1} as the melting endotherm of 100% PLLA [15]. Thermal characterisation studies were not done for the cylindrical implants, because the constituents could not be extracted safely.

2.6. Molecular weight measurements

From the GPC (GPC, Waters, Milford, MA, USA) measurements the weight average molecular weight (M_w) and intrinsic viscosity (i.v.) were calculated with narrow polystyrene standards. Chloroform was used as a solvent and eluent. The equipment consisted of differential refractometer detector (Waters 410 RI) and HPLC-pump (Waters 515). The concentration of the sample was 0.1 mass%, injection volume was 150 μl, and the flow rate was 1 ml min^{-1}. Two high-resolution columns together with a guard column (PL-gel 5 μm mixed-C and PL-gel Guard) were used. Temperatures of the columns and the detector were 35 and 40 °C. Two repeat injections per sample were made and the data is the means of those two. Molecular weight measurements were not done for the cylindrical implants, because the constituents could not be extracted safely.

2.7. SEM (Scanning Electron Microscopy) studies

The scanning electron microscope Jeol T 100 (Jeol Ltd. Tokyo, Japan) was used to study the micro-scale changes in the surface of the cylindrical implants during the *in vitro*. The samples were gold sputtered before analysis.

3. Results and discussion

3.1. Composition of the cylindrical implants

The weight% ratios of the components in the composite implants were calculated and are presented in Table II. With this implant production method the obtained bioactive glass content in the *in vitro* samples was from 19 to 35 wt%. Large variation in the glass content is due to the production method where the matrix paste is hand-pasted to the knit. Previous results show that increasing the bioactive glass content in the composite increases the bioactivity [16], and thus the highest possible glass content was the goal.

3.2. Structural changes of the cylindrical implants and screws during hydrolysis

The Polyactive+BG rods started to crack after 1 week *in vitro* due to swelling of the rods causing the pressure against the shell and biodegradation. Because the implants were immersed in PBS free of compression pressure, the Polyactive + BG rods swelled and some expanded 1–3 mm vertically either up or down. This exposed the heads so that between 1 and 6 weeks the heads that were above the implant plane were cut off. At 15 weeks the shell layer of the implant was still firmly rolled around the Polyactive + BG core and no loosening or detachment of that material was noticed. When implanted, the core rods would stay between the adjacent vertebrae and expanding would actually improve the position. Swelling and fragmentation of the Polyactive + BG and the gaps between the glass particles and Polyactive *in vitro* was also noticed in [17].

The screws showed no structural changes during the hydrolysis.

TABLE II Weight contents of the components in the cylindrical implants

	Bioactive glass 13-93 (wt%)	Polyactive 70/30 (wt%)	P(L/D)LA 96/4 (wt%)	P(L/DL)LA 70/30 (wt%)
In vitro set	27.0 ± 8.4	10.8 ± 1.9	58.0 ± 8.1	4.2 ± 1.6
Set 1			99.8 ± 0.0	0.1 ± 0.0
Set 2			88.7 ± 2.1	11.3 ± 2.1
Set 3	20.8 ± 1.2		75.5 ± 1.5	3.7 ± 0.2
Set 4		14.2 ± 0.8	85.3 ± 0.7	0.4 ± 0.1
Set 5		13.7 ± 0.2	77.7 ± 1.8	8.6 ± 2.0
Set 6	23.7 ± 1.5	9.5 ± 0.2	62.6 ± 1.6	4.2 ± 0.3
Set 7	3.6 ± 0.0	12.3 ± 0.1	83.4 ± 0.0	0.6 ± 0.1
Set 8	3.4 ± 0.1	11.3 ± 0.3	76.6 ± 0.1	8.7 ± 0.3
Set 9	23.2 ± 3.8	9.4 ± 1.0	63.7 ± 3.5	3.6 ± 0.7

In vitro set ($n = 15$); Set 1–9 ($n = 3$).

3.3. Weight change of the cylindrical implants

The implants gained weight approximately 5 wt% after 1 h in de-ionised water. After 1 week *in vitro* the implants weight had increased roughly 20 wt% and it remained at the same level until 15 weeks *in vitro*. The weight increase of ~5% in 1 h is due to the water absorption of the Polyactive + BG rods [17], after 1 h the weight gain is due to the swelling of the Polyactive + BG rods and water absorption into the matrix through the pores that are on the surface of the implant. The fragmented Polyactive + BG debris from 1 to 6 weeks were weighed as well and thus did not affect the weight measurements of the implant.

3.4. SEM analysis of the cylindrical implants

The images in Fig. 2 show the changes in cylindrical implant surface during 12 weeks in hydrolysis. In Fig. 2(A) and (C) the bioactive glass particles are clearly visible. There are no visible structural changes after 12 weeks in the surface topography. By comparing the high magnifications Fig. 2(B) and (D), it is noticed that after 12 weeks the surface is covered with white agglomerates presumably calcium phosphate particles. Calcium phosphate deposition with bioactive glass type 13–93 in PBS solution on the surface of poly(L/DL)lactide 70/30 has been noted and studied [18, 19].

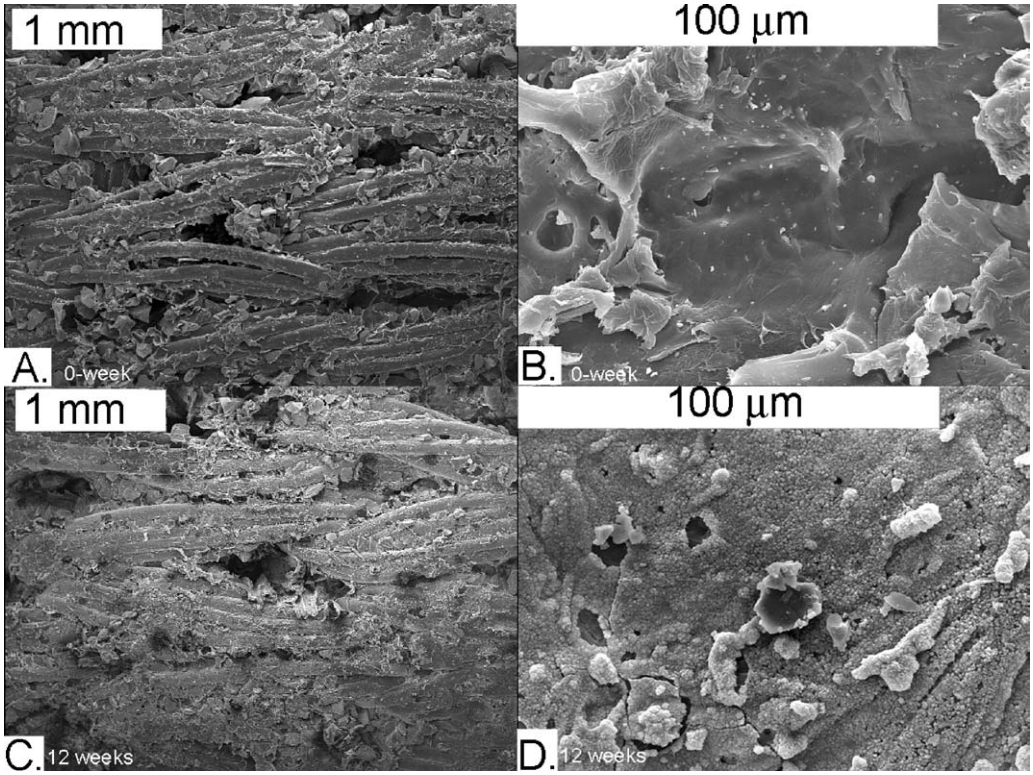

Figure 2 Scanning electron microscopy images from cylindrical implant surface, (A) 35× (B) 1000× magnification 0-week in vitro and (C) 35× (D) 1000 × magnification 12 weeks *in vitro*.

3.5. Mechanical properties

3.5.1. Initial mechanical properties of the cylindrical implants

The reference series (Tables I and II) were mechanically tested and the results are shown in Fig. 3. The influence of the core material and reinforcement matrix was studied in the reference series.

The influence of the core: The core (sets 4 & 7) had a 26–30% increase in modulus with both core types and 14% increase in stiffness with Polyactive + BG core, when compared to the implant without the core (set 1). The Polyactive core (set 5) had an 18% and Polyactive + BG core (set 8) had a 10% increase in modulus when compared to the implant with reinforcement matrix polymer and no core (set 2). The core had no significant change in stiffness values while the reinforcement polymer was filled (sets 3, 6 & 9) or unfilled (sets 2, 5 & 8) with BG. When reinforcement polymer with BG filler was used there was a 19% increase with Polyactive core (set 6) and 10% increase with Polyactive + BG core (set 9) compared to the samples without the core. The slightly higher modulus values with Polyactive core compared to the Polyactive + BG core could be due to the BG particles in Polyactive, BG filler in the Polyactive rod allows the crack development with lower loads and acts as a crack initiators in the Polyactive rods. The lower modulus of the Polyactive rods with bioactive glass filler was also noticed earlier [17].

The influence of reinforcement matrix: The reinforcement matrix polymer increases both stiffness and the modulus of the samples. When the BG filler is added to the reinforcement polymer the stiffness and modulus increases yet again. This trend is clearly seen in Fig. 3. From the sets 1–9 the set 9 was chosen for the *in vitro* studies because it had best strength and modulus combination, when compared to other sets, and it had the highest BG content to improve osteoconductivity.

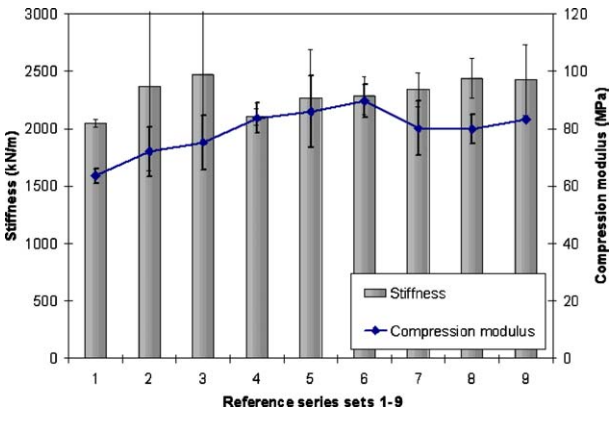

Figure 3 Compression modulus and stiffness of the cylindrical implants.

3.5.2. Mechanical properties of the cylindrical implants in vitro

No significant changes in mechanical properties were noticed during the 15-week hydrolysis (Fig. 4). The modulus of the hydrolysis samples stayed between the error margins through out the hydrolysis and the modulus was 100 ± 10 MPa with stiffness of 3400 ± 250 kN m^{-1} at 15 weeks *in vitro.* Typical stress—compressive strain curve (Fig. 5) shows that the 15-week hydrolysis samples have the highest stress (30 MPa) and lowest compressive strain (0.3 mm mm^{-1}) values. The compression of cylindrical implants in the regions 0–2, 2–4

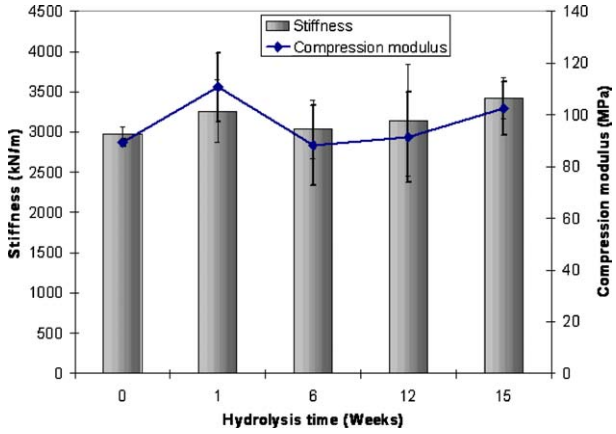

Figure 4 In vitro behavior of the cylindrical implant.

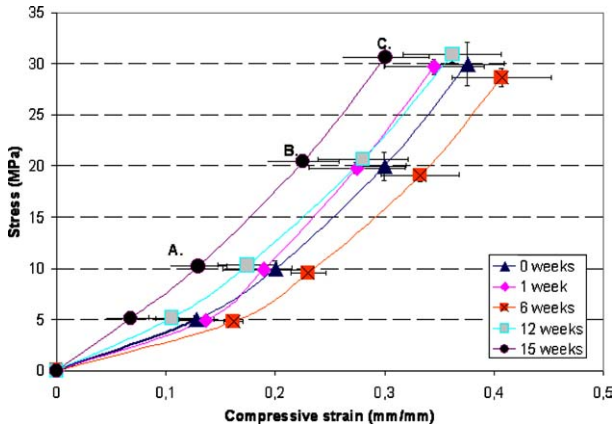

Figure 5 Stress-compressive strain curve of the cylindrical implants (A) 2 kN, (B) 4 kN, and (C) 6 kN.

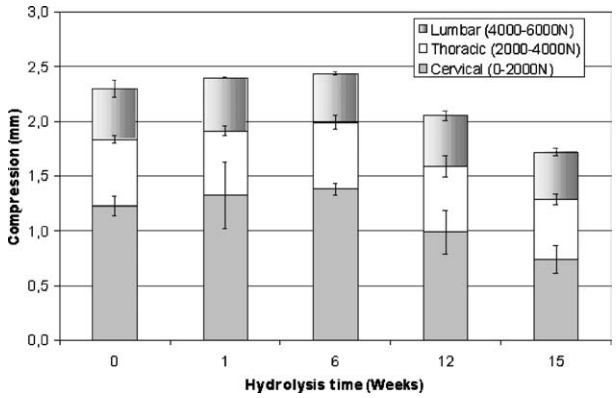

Figure 6 Compression of the cylindrical implants in compression.

and 4–6 kN are in Fig. 6. The compression of the cylindrical implant was 0.7 ± 0.1 mm at 2 kN and 1.3 ± 0.2 mm at 4 kN with 15-week samples. The highest compression properties were noticed with the 15-week samples and this is mainly due to the absence of Polyactive + BG rod ends reaching above the plain of the implant. The Polyactive + BG above plain compression is part of the 0 to 2 kN compression and this has changed with the 12 and 15-week samples, whereas the compression distance from 2 to 6 kN remains the same throughout the hydrolysis.

The average 100 MPa modulus would be adequate modulus for lumbar, thoracic and cervical regions for the canine spine model of the spine, the current stress 30 MPa at compressive strain 0.3 mm mm^{-1} is 50% higher than with the composite semi- IPNs [20]. Each human cervical vertebra stands ∼2 kN, thoracic 2–4 kN and lumbar 4.5–8.3 kN force before breaking [21], and no breakage was observed with cylindrical implants in any of the compressions. Compression tests performed for cadaver region Th_{11}-L_3 samples (4 intervertebral discs present) compression shortening in 2 kN was from 3 to 5.8 mm, in 4 kN from 4.8 to 7.7 mm and in 6 kN from 6.5 to 8.3 mm (some samples already failed at before 6 kN) [22]. The compression of the cylindrical implants in those regions can be seen in Fig. 6 and compared these to the shortening of the sample with four intervertebral discs [22] we see that the cylindrical implant shortening in 0–2 kN and 2–4 kN is comparable to human intervertebral disc behaviour. The cylindrical implants showed higher stiffness when compared to the TFM (titanium fiber mesh) implants and tricortical bone grafts studied by Hoshijima *et al*. [6] and to canine composite disc spacers studied by Vuono-Hawkins *et al.* [23].

3.5.3. Mechanical results of the screws

The compression modulus of the solid screws was three times greater than those of the cannulated screws or the cannulated screws with rod inserted inside of cannula. The cannulated screws failed at forces below 400 N and had compression strength at yield between 7.3–7.6 MPa. The cannulated screws with rods inserted into the cannula had maximum break force of 420 N and compression strength at yield point 8.1–8.8 MPa. These two screw types used this way were not strong enough for the canine spine intervertebral disc purposes. Although the modulus values would have been adequate the compression strength was not sufficient [20]. During the 24-week hydrolysis no critical changes in the modulus were noticed (Fig. 7). The solid screws had modulus of 390 ± 30 MPa after 24-week hydrolysis. This modulus is sufficient for canine spine for cervical, thoracic and lumbar regions [20]. The increase in compression distance of the 4 to 6 kN region can be seen from the Fig. 8. The compression distance values when compared to human spine [22] were sufficient for the cervical spine 0 to 2 kN but slightly low for human thoracic and lumbar area purposes. From the curves it was noted that all the screws in the hydrolysis series had their yield point after 0.61 mm compression. The

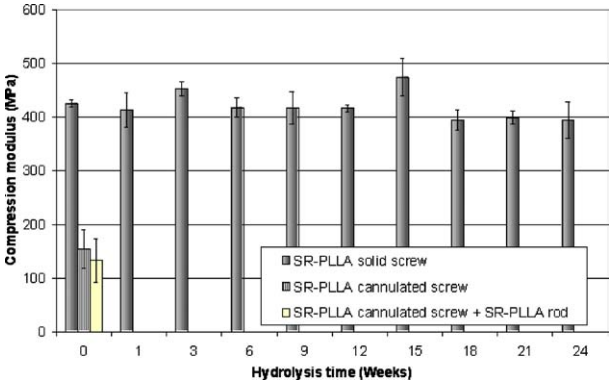

Figure 7 Compression modulus of the screws in hydrolysis.

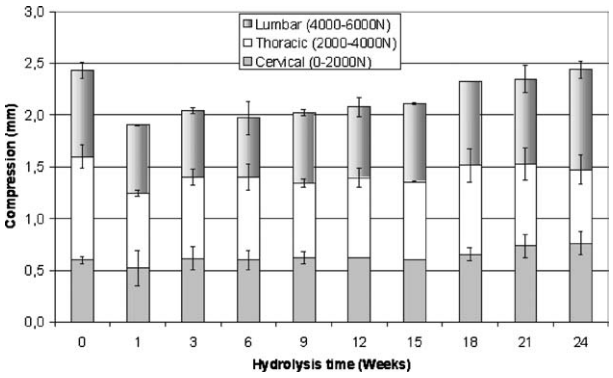

Figure 8 Compression of the screws in hydrolysis.

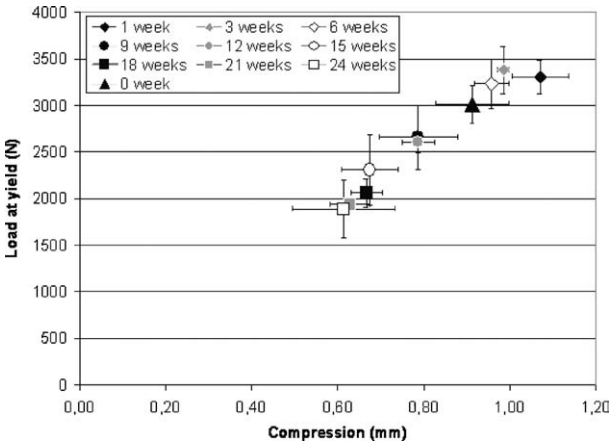

Figure 9 Yield point of the threads in hydrolysis.

yield point decrease due to the softening and failure of the screw threads can be seen during the hydrolysis (Fig. 9). If the implantation to the spine is done so that the threads are embedded in bone, the dynamics of the screws changes and there would not be a visible yield point of the threads. Now this yield point exists in this data due to the compression between the steel plates and is a good indicator of minor degradation behaviour.

3.6. Molecular weight analysis of the screws

The weight average molecular weight (M_w) and the intrinsic viscosity (i.v.) data from the 24-week hydrolysis is in Table III. The M_w of the screws decreased by 45% and the i.v. by 37% during the hydrolysis. Pohjonen *et al*. studied the SR-PLLA Ø 4.5 mm screws and they noticed 43% decrease in viscosity average molecular weight (M_v) after 15-week hydrolysis which corresponds with the results of this study [24].

TABLE III Molecular weight and crystallinity of the solid SR-PLLA screws

In vitro weeks	M_w (g mol^{-1})	i.v. (dl g^{-1})	*In vitro* weeks	T_m (°C)	Crystallinity (%)
0	56400	1.47	0	177	55
1	57000	1.48	1	176	56
3	59100	1.53	3	176	57
6	50100	1.34	6	176	58
9	46800	1.27	9	176	61
12	43600	1.21	12	176	62
15	39700	1.13	15	176	67
18	40500	1.33	18	176	64
21	39500	1.28	21	178	57
24	30700	0.93	24	176	62

M_w = Weight average molecular weight ($n = 2$).
i.v. = Intrinsic viscosity ($n = 2$).

3.7. Thermal properties of the screws

The crystallinity of the SR-PLLA solid screws increased from 55 to 62% in 24-week hydrolysis. Reported increase from 63 to 70% in 15-weeks of hydrolysis [24] and 60 to 65% increase in crystallinity in 24 weeks *in vitro* [25] are slightly higher than the initial and post *in vitro* crystallinity of the studied screws. There was no dramatic change in T_m from 177 °C during 24 weeks *in vitro* which corresponds well with previous study [25].

4. Conclusions

In this study the screws and the cylindrical implant were planned as intervertebral disc replacement devices to ossify the adjacent vertebrae together. The screws and the cylindrical implants are both mechanically suitable for canine intervertebral studies and the cylindrical implant, with present design, also has good mechanical properties for human thoracic and cervical intervertebral disc replacement purposes. Degradation rate of the screws is sufficient but the strength in the transverse direction to the screw axis is not yet adequate for human intervertebral purposes.

The cylindrical implant is a new concept and some detailed design enhancements must be taken to ensure the perfect fit of the implant to the target site. This is relatively easy because the manufacturing procedure of the implant allows easy changes in design of different size intervertebral disc implants. The implant surface has a lot of bioactive glass, the surface topography is not polished and there is porosity on the surface, all this could lead to higher activity on the surface compared to smooth and polished surface without bioactive components. Because the cylindrical implants are reasonably stiff we do not expect the implant to fully recover (to return to its original height post testing). Therefore if these implants are used, the stresses in the operated area should not be high during the fusion period to avoid the permanent compression and the loosening of the implant. But if there should be higher stresses in the operated joint the implant remains unbroken.

Preliminary tests using cylindrical implants and screws on pigs have been performed (L3-L4 and L4-L5 lumbar discs were operated) and the results have shown ossification with both types of implants in 15-week follow up. Cylindrical implants showed better anatomical results compared to screws when the disc spaces were compared [26].

Acknowledgment

The grants of Academy of Finland and of the National Technology Agency (TEKES) for the Center of Excellence of Biomaterials are greatly appreciated.

References

1. E. N. MARIEB, "Human Anatomy and Physiology," 2nd ed. (Benjamin/Cummings, California, 1992) p. 194.
2. C. A. FAGER, "Atlas of Spine Surgery" (Lea & Febiger, London, 1989) p. 3.
3. R. B. CLOWARD, *J. Neurosurg.* **15** (1958) 602.
4. T. R. LEHMANN, K. F. SPRATT, J. E. TOZZI, J. N. WEISTSTEIN, S. J. REINARZ, G. Y. EL-KHY and H. COLBY, *Spine* **12** (1987) 97.
5. J. F. ZUCHERMAN, D. SELBY and W. B. DELONG, in "Lumbar Spine Surgery: Techniques and Complications" edited by A. H. White, R. H. Rothman, C. D. Ray, (C. V. Mosby Company, St. Louis, Missouri, 1987) p. 296.
6. K. HOSHIJIMA, R. W. NIGHTINGALE, J. R. YU., W. J. RICHARDSON, K. D. HARPER, H. YAMAMOTO and B. S. MYERS, *Spine* **22** (1997) 1181.
7. E. O. MARTZ, V. J. GOEL, M. H. POPE and J. B. PARK, *J. Biomed. Mater. Res. (Appl Biomater*) **38** (1997) 267.
8. M. BRUNEAU, J.-F. NISOLLE, C. GILLIARD and T. GUSTIN, *Neurosurg Focus* **10**(4) (2001) Article 8.
9. L. GUO, X. GUO, Y. LENG, J. C. Y. CHENG and X. ZHANG, *J. Biomed. Mater. Res*. **54**(4) (2001) 554.
10. Q.-B. BAO, G. M. MCCULLEN, P. A. HIGHAM, J. H. DUMBLETON and H. A. YUAN, *Biomaterials* **17**(12) (1996), 1157.
11. J. C. GAN, P. DUCHEYNE, E. VRESILOVIC and I. M. SHAPIRO, *J. Biomed. Mater. Res*. **51** (2000) 596.
12. R. D. FRASER, *Spine* **20**(24) (1995) 1675.
13. T. LUND, T. R. OXLAND, B. JOST, P. CRIPTON, S. GRASSMANN, C. ETTER and L. P. NOLTE, *J. Bone Joint. Surg. (Br)* **80**(2) (1998) 351.
14. P. ROKKANEN, O. BÖSTMAN, E. HIRVENSALO, E. MÄKELÄ, E. PARTIO, H. PÄTIÄLÄ, S. VAINIONPÄÄ, K. VIHTONEN and P. TÖRMÄLÄ, *Biomaterials* **21** (2000) 2607.
15. E. W. FISCHER, H. J. STERZEL and G. WEGNER, *Kolloid- ZuZ Polymere* **251** (1973) 980.
16. T. PAATOLA, H. NIIRANEN and P. TÖRMÄLÄ, in Proceedings of the European Society of Biomaterials 2001 Conference, 12th–14th Sept., 2001, p. T114.
17. M. KELLOMÄKI, "Bioabsorbable and Bioactive Polymers and Composites for Tissue Engineering Applications," PhD. Thesis, Tampere University of Technology, Finland, 2000.
18. H. NIIRANEN and P. TÖRMÄLÄ, *J. Mater. Sci. Mater. Med.* **10** (1999) 707.
19. H. NIIRANEN and P.TÖRMÄLÄ, Poster presentation in Proceedings of the 15th European Society of Biomaterials 1999 Conference, 8th–12th, France, Sept., 1999.
20. L. AMBROSIO, P. A. NETTI, S. IANNACE, S. J. HUANG and L. NICOLAIS, *J. Mater. Sci. Mater. Med.* **7** (1996) 251.
21. A. A. WHITE and M. PANJABI, "Clinical Biomechanics of the Spine" (Toronto, 1978).
22. R. BEDZINSKI, "Biomechanica Inzynierska" (Oficyna Wydawnicza Politechniki Wroclawskiej, Wroclaw, Poland, 1997) p. 100.
23. M. VUONO-HAWKINS, M. C. ZIMMERMANN, C. K. LEE, F. M. CARTER, J. R. PARSONS and N. A. LANGRANA, *J. Orthop. Res.* **12**(1) (1994) 119.
24. T. POHJONEN, P. HELEVIRTA, P. TÖRMÄLÄ, K. KOSKIKARE , H. PÄTIÄLÄ and P. ROKKANEN, *J. Mater. Sci. Mater. Med.* **8** (1997) 311.
25. P. MAINIL-VARLET, R. CURTIS and S. GOGOLEWSKI, *J. Biomed. Mater. Res.* **36** (1997) 360.
26. T. PALMGREN, P. YLINEN, R.-M. TULAMO, M. KELLOMÄKI, P. TÖRMÄLÄ and P. ROKKANEN, *Vet. Comp. Orthop. Traumatol.* **16** (2003) 138.

Received 2 February 2004
and accepted 19 October 2004

Publication VII

Ellä, V., Sjölund, A., Kellomäki, M. & Mauno, J.

Manufacturing of temporomandibular joint scaffolds

In: Salonen, R. (ed.). FiberMed06, Fibrous Products in Medical and Health Care, Proceedings, June7-9, 2006 Tampere Hall, Finland 6 p.

MANUFACTURING OF TEMPOROMANDIBULAR JOINT SCAFFOLDS

V. Ellä , A. Sjölund, M. Kellomäki
Tampere University of Technology,
Institute of Biomaterials, P.O Box 589, 33101 Tampere, Finland

J. Mauno
Department of Oral and Maxillofacial Surgery, Helsinki University Central Hospital, Helsinki, Finland

Abstract

Poly(L/D)lactide 96/4 polymer was melt-spun into multi-filament fiber and monofilament fiber. The monofilament fiber was cut to staple fibers, carded and needle punched into non-woven mats. The multifilament fiber was knitted to a tubular single jersey knit. Poly(L/DL)lactide 70/30 polymer plate was extruded. Ultrasonic welding was studied using fiber + plate combination as tear test samples to find out proper settings for welding. Testing was carried out on materials testing machine. Ultrasonic welding was used to attach the knit + plate and non-woven mat + plate. Welding of the samples was studied by means of scanning electron microscopy and light microscopy.
Highest studies parameters resulted in breakage or tearing of the fiber. There was a ten-fold decrease in force needed to break the fiber in tear test after ultrasonic welding. Different ultrasonic parameters showed only small alterations to this break force. Microscopical study revealed non-uniform attachment with non-woven fabrics on the top surface compared to knit fabrics to the plate. Ultrasonic welding is a feasible method in manufacturing of fibrous scaffolds for TE purposes where no greater pulling or distraction forces are directed to the weld joint of the fibers.

1. Introduction

Products and materials for tissue engineering (TE) purposes for temporomandibular joint (TMJ) disorder are studied. A tissue engineered composite TMJ disc could, in future, replace the damaged tissue and a potential scaffold of non-woven polyglycolic acid (PGA) mesh as well as polylactide P(L/D)LA 96/4 composite discs have already been studied. [1,2]
In this study TMJ rabbit model composite discs were manufactured and studied. Rabbit TMJ differ from human joint, so the movement of the rabbit temporomandibularis when chewing was the key issue. The composite disc included a low friction side and a cell attachment side. Low friction side enabled the movement of the jaw against the scaffold plate whereas the cell carrier/attachment side enabled the attachment of the scaffolds before the resorbtion of the implant.

2. Materials and Methods

Rabbit TMJ model composite discs were manufactured. Two compositions of disc were manufactured. The discs were composed of a plate, size of 5 x 7 x 0.16 mm and a non-woven mat or knit. Design of the disc can be seen in Figure 1.

Plate: Medical grade Poly(L/DL)lactide 70/30 (LR 708, Boehringer Ingelheim, Germany) polymer plate was extruded through a 30 x 0.5 mm die and drawn using caterpillars to a continuous strip with dimensions of 10 x 0.16 mm.

Non-woven mat: Medical grade Poly(L/D)lactide 96/4 (Intrinsic viscosity of 1.7 dl/g, Purac Biochem, The Netherlands) polymer was melt-spun into monofilament fiber. Die of 0.5 mm diameter was used along laboratory size extruder. The filament was drawn, using Fournée high-speed spinning machine, to a thickness of 0.02-0.03 mm. The fibers where cut to staple fibers, carded and needle punched to form a non-woven mat.

Knitted fabric: Medical grade Poly(L/D)lactide 96/4 (Intrinsic viscosity of 4.8 dl/g, Purac Biochem, The Netherlands) polymer was melt-spun into multi-filament fiber. A nozzle with 4 orifices (single orifice diameter 0.4 mm) was used along laboratory scale extruder. Filaments were hot drawn using caterpillars and ovens to diameter of 0.08-0.09 mm (for single filament). Filaments were repeated to make a 12-filament yarn. Circular knitting machine was used for manufacturing a tubular single jersey knit.

Plate + non-woven: The strip was cut to 10 x 60 mm pieces as well as the non-woven mat. The mat was placed on the strip and using ultrasonic-welding machine the edges of the two materials were welded/fused together. From this preform, 5 x 7 mm samples were cut.

Plate + knit: The strip was cut to 10 x 60 mm pieces. The knit cut to 60 mm pieces and compression molded in 80 ^{o}C and 2 MPa pressure, to give the knit a flat outlook. The compressed knit and the plate were welded together from the edges. After this the samples were cut from the preform.

Parameters of the welded fiber-plate combinations were tested using a tear test method on a materials testing machine (Instron, England) The ultrasonic

Prior the in vivo testing, all the samples were washed twice in ultrasonic bath using ethanol after which the samples were gamma irradiated with the dose of 15 kGy. Welding of the samples were studied using scanning electron microscopy (JEOL, Japan) and light microscopy.

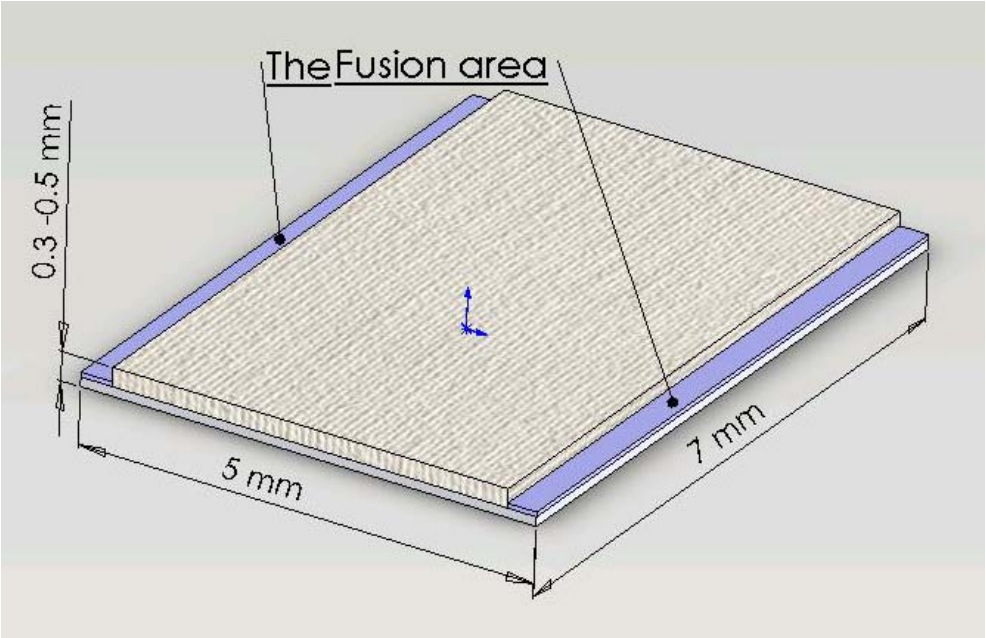

Figure 1. The design of the TMJ scaffold.

3. Results and Discussion

Due to the risk of implant failure (detachment of the fabric from the plate) the weld joints were studied. With correct welding parameters the welding area was totally fused without breaking the adjacent fibers near the fusion area (Figure 2 & 3).

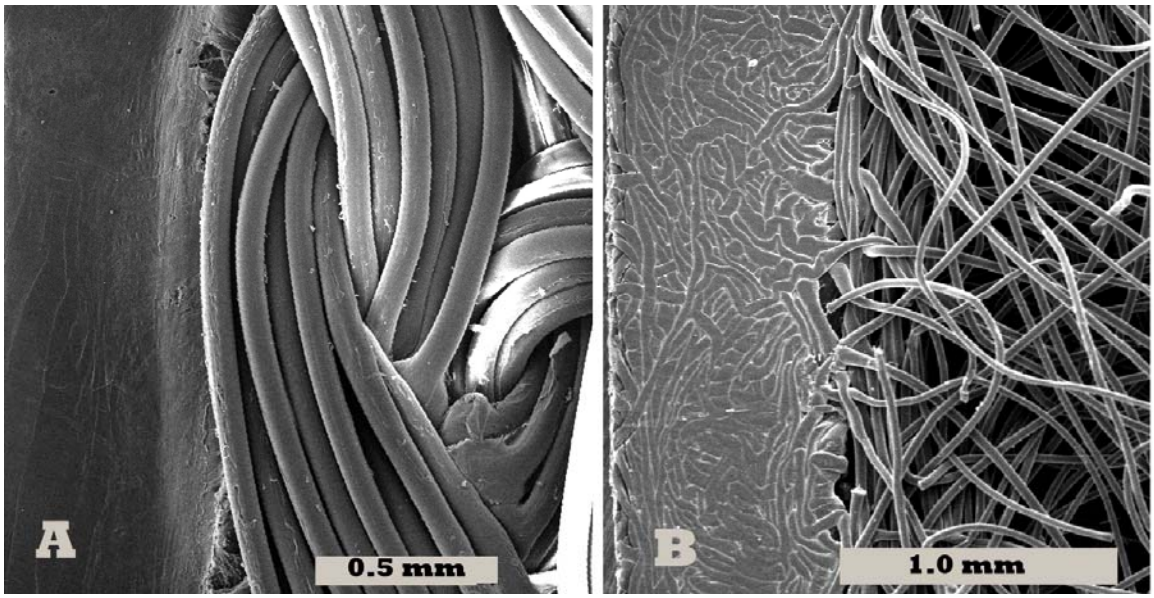

Figure 2. A) weld joint of the knit and plate, B) weld joint of the non-woven and the plate.

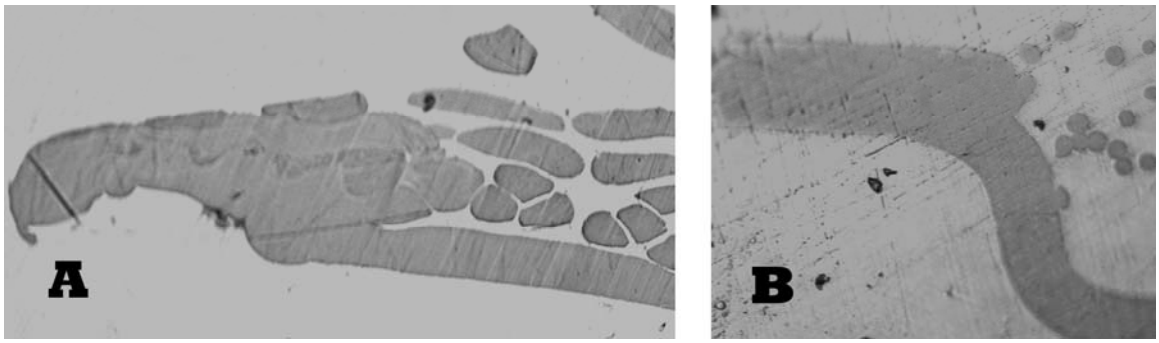

Figure 3. Cross-section of the A) weld joint of the knit and plate and B) weld joint of the non-woven and the plate.

It can be seen that the weld joint of the knit-plate disc uniform in SEM pictures as well as in the light microscopy cross-section pictures. With the non-woven mat- plate the top surface of the fibers at the weld joint are still visible but from the cross section the welding is uniform under the surface. This may result from the dense packing of the numerous fibers in non-woven compared to the knit. Although it was seen during the welding that the thicker fibers of the knit either had uniform welding or the knit broke immediately from the weld joint. There were a lot unusable samples whereas with the non-woven this did not happen.

The ultrasonic welding did affect the plate itself. The welding distorted the plate adjacent the weld joint (figure 3B & 4). This was due to the thicker fabric. The plate had a plastic deformation due to the force afflicted to it by the knit or the non-woven mat. The plate material was also more ductile during the welding due to its amorphous nature, compared to the semi-crystalline fibers. The relaxation behavior can be ruled out since the drawing direction of the plate was parallel to the weld joint. It was noted that there were no problems for the end user due to this distortion of the plate.

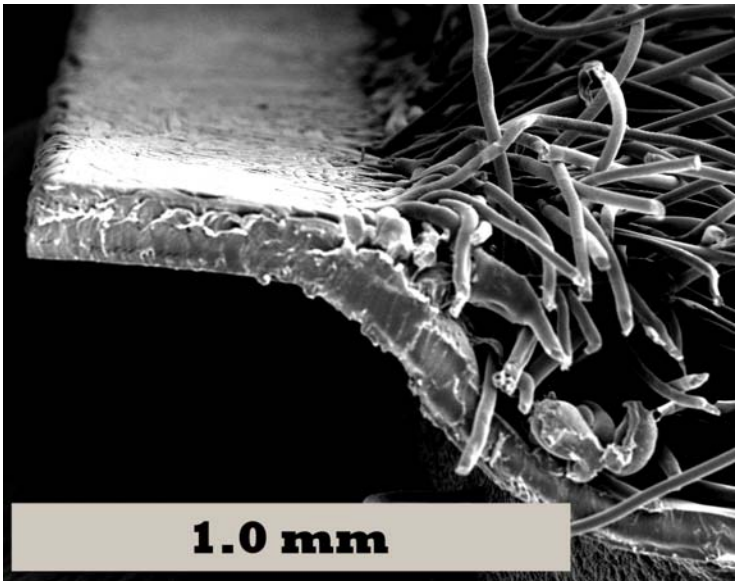

Figure 4. The distortion of the plate due to the ultrasonic welding

Tensile tests were performed on 4 filament fiber – plate combination on different parameters. Comparing the tensile test of the plain fibers vs. the tear test with the best ultrasonic welding parameters, we can see that there is a ten fold decrease in break load (figure 5&6). This magnitude of difference did not chance with the parameter changes. Therefore we can state that the welding joint weakens the fibers.

But when studying the tear test of the non-woven mat-plate, it resulted in low force continuous tear of the non-woven. Therefore we can also state that the weld joint is not the weakest link of the disc in case of non-woven mat-plate and by increasing the amount of fibers at the weld joint we can make the weld joint stronger. The weld joint of the knit-plate could not be tested reliably due to the orientation of the knit and the plate.

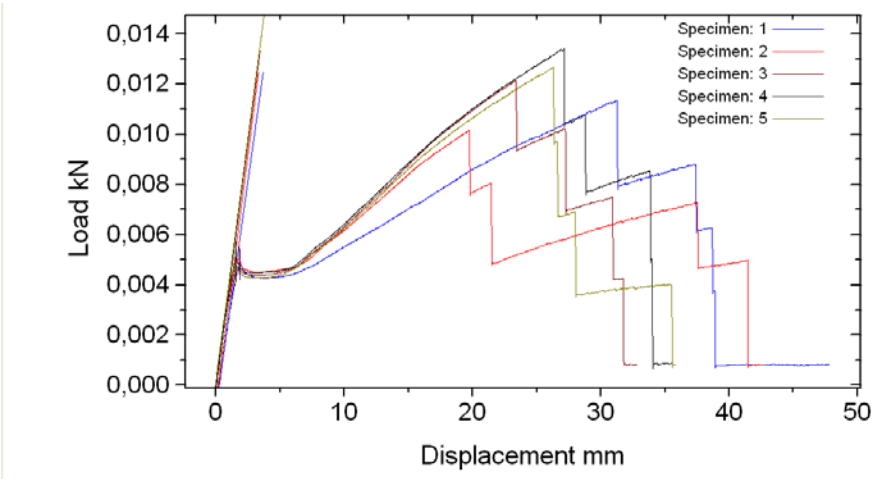

Figure 5. The tensile test of the multifilament knit fibers

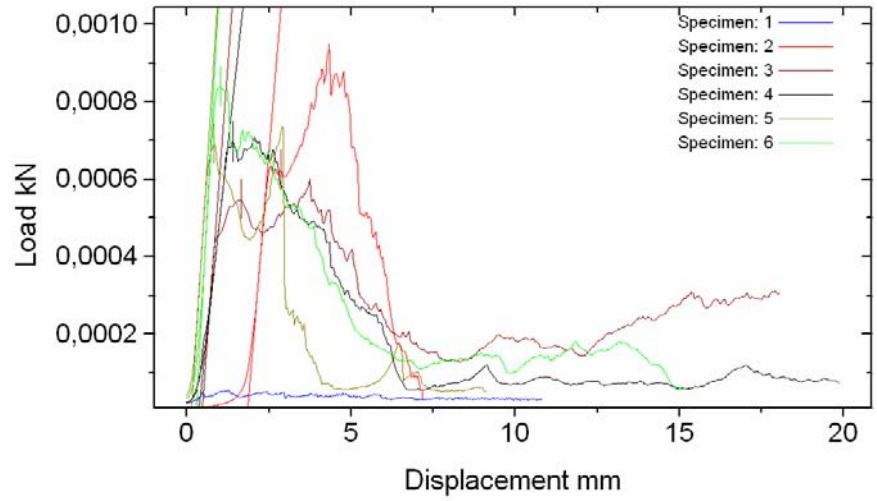

Figure 6. Tensile tear test of the multifilament fiber and plate

4. Conclusions

Ultrasonic welding is fast and feasible method in manufacturing of fibrous scaffolds for TE purposes where no greater pulling or distraction forces are directed to the weld joint of the fibers.

Acknowledgements

Authors would like to thank European NoE EXPERTISSUES (NMP3-CT-2004-500283) and for Center of Excellence, Finnish Funding Agency for Technology and Innovation (TEKES) and Academy of Finland.

References

[1] Almarza, A.J., Athanasiou, K.A., Seeding techniques and scaffolding choice for the tissue engineering of the temporomandibular joint disc, Tissue Eng 10 (2004), pp. 1787–1795.

[2] Mauno, J., Robinson, S., Ellä, V., Laitinen, O., Mäki, T., Kellomäki, M., Lindqvist, C., Suuronen, R., MRI imaging of tissue engineered implants replacing temporomandibular joint disc in rabbits, Congress of the European Association for Craniomaxillofacial Surgery, September 14-18, 2004, Tours, France, p.328

Tampereen teknillinen yliopisto
PL 527
33101 Tampere

Tampere University of Technology
P.O.B. 527
FI-33101 Tampere, Finland

ISBN 978-952-15-2811-8
ISSN 1459-2045